FINAL REPORT

Assessment of geothermal resources in onshore Nova Scotia

Setting the stage, demonstrating value, and identifying next steps

Félix-Antoine Comeau[1]

Stephan Séjourné[2]

Jasmin Raymond[1]

[1]Institut national de la recherche scientifique (INRS), Centre Eau Terre Environnement

[2]Enki GeoSolutions inc.

Rapport de recherche R2002

Prepared for the account of:

Offshore Energy Research Association (OERA)

December 1st, 2020

ISBN : 978-2-89146-939-5 (version électronique)

Dépôt légal - Bibliothèque et Archives nationales du Québec, 2020
Dépôt légal - Bibliothèque et Archives Canada, 2020

Table of Contents

List of figures

List of tables

ACKNOWLEDGEMENTS

This report was written and prepared by the Institut national de la recherche scientifique (INRS) and Enki GeoSolutions. It was developed with support from the Offshore Energy Research Association of Nova Scotia (OERA; Russell Dmytriw), the Nova Scotia Department of Energy and Mines (Fraser Keppie, Gavin Kennedy, Helen Cen and Krista Phillips), and the Nova Scotia Department of Agriculture (Julie Bailey). We would like to give a special mention to Scott Weldon (Department of Energy and Mines of Nova Scotia) for his unstinting dedication to our many requests during data compilation.

FOREWORD

New emerging technologies in the geothermal sector can be a game changer for the profitable exploitation of renewable energy resources currently unused in Nova Scotia. In the short term, direct heat use can be developed to improve energy efficiency, while electricity generation is a long-term objective for the strategic development of renewable energy in the province. Nova Scotia's businesses and energy consumers, showing a high demand for electricity and heat, can benefit from the development of such geothermal resources. More specifically, there is a growing interest in exploring the viability of using geothermal resources to support greenhouse operations and improve the food supply chain sustainability.

In the context of a collaborative program with Nova Scotia's Department of Agriculture (NSDA) and Nova Scotia's Department of Energy and Mines (NSDEM), the Offshore Energy Research Association of Nova Scotia (OERA) held a request for proposals to assess the geothermal resources in onshore Nova Scotia. The team of INRS and Enki GeoSolutions was selected for a study to provide:

1) A review of the general types of geothermal resources in Nova Scotia with reference to key regional, national and global examples;
2) A preliminary evaluation of the potential/favorability of Nova Scotia's geothermal resources (direct use of heat, electricity generation, and heating and cooling from abandoned mines);
3) Recommendations for next steps to further de-risk targeted areas;
4) A discussion about the economic case for potential geothermal resource exploration and development in the province.

EXECUTIVE SUMMARY

The study describes three distinct types of geothermal resource (**Section 1**) available in Nova Scotia:

- Electricity generation (> 80°C, > 3 km)
- Direct-use of heat (< 80 °C, < 4 km)
- Heating and cooling from abandoned mines

For this purpose, the province was divided into 11 regional zones according to the general geological framework of Nova Scotia (**Section 3**), namely nine sub-basins of the Maritimes sedimentary basin, the Meguma terrane and the Devonian intrusives.

Electricity generation and direct-use of heat
119 temperature measurements recorded at depths ranging from 52 to 4,536 m were compiled, analyzed and filtered, mostly from old petroleum and mining exploration wells (**Section 4**). About one third of these data points (44) have been ultimately retained for the evaluation, based on the quality of the input data. Available data on the porosity and permeability of deep aquifers and seismic data were also used. A methodology was then established (**Section 5**) in order to identify and rank the geothermal potential for electricity generation and for direct-use of heat across Nova Scotia (**Section 6**). Five criteria were considered, with different weight factors according to their relative importance:

- Temperature of potential reservoirs (× 3)
- Depth of potential reservoirs (× 3)
- Lithology of potential reservoirs (× 2)
- Temperature uncertainty in the zone (× 1)
- Geological uncertainty in the zone (× 1)

The resulting evaluation of Nova Scotia's geothermal resources is shown below on **Figure A** as a function of economic opportunities (**Section 7**) based on examples of operational geothermal power plants and experimental projects around the world for which electricity generation and direct-use of heat were developed (**Section 2**).

Heating and cooling from abandoned mines
A methodology was developed to estimate the amount of energy available from the mine system for space heating and cooling with the help of geothermal heat pumps, considering a 25-year use (**Section 5**). This evaluation is based on the volume of ore extracted for 287 abandoned mines (coal: 206, metals: 55, industrial minerals: 26; **Figure B**), both underground (85%) and open-pit (15%).

Knowledge gaps and recommendations
Knowledge gaps were addressed for each of the major geological units (Maritimes sedimentary basin, the Meguma terrane and the Devonian intrusives) to better lead future investments and development of geothermal resources in Nova Scotia (**Section 8**). Finally, recommendations for future work were also proposed for the short, medium and long term in order to refine the understanding of the province's geothermal potential (**Section 8**).

Overall geothermal potential of Nova Scotia

Using the methodology outlined above and the information presently available (**Figures A and B**), the following points highlight the geothermal potential of the Province:

- Areas in Hants and Cumberland counties were identified as having a relatively high geothermal potential for electricity generation.
- Most of the province's sedimentary basins had geothermal potential for direct-use of heat.
- New and emerging technologies show promise for expanding the extent of the areas of Nova Scotia that may be considered for direct-use and electricity geothermal development.
- The Province's legacy of coal mining offers interesting opportunities to use abandoned mines for space heating and cooling.

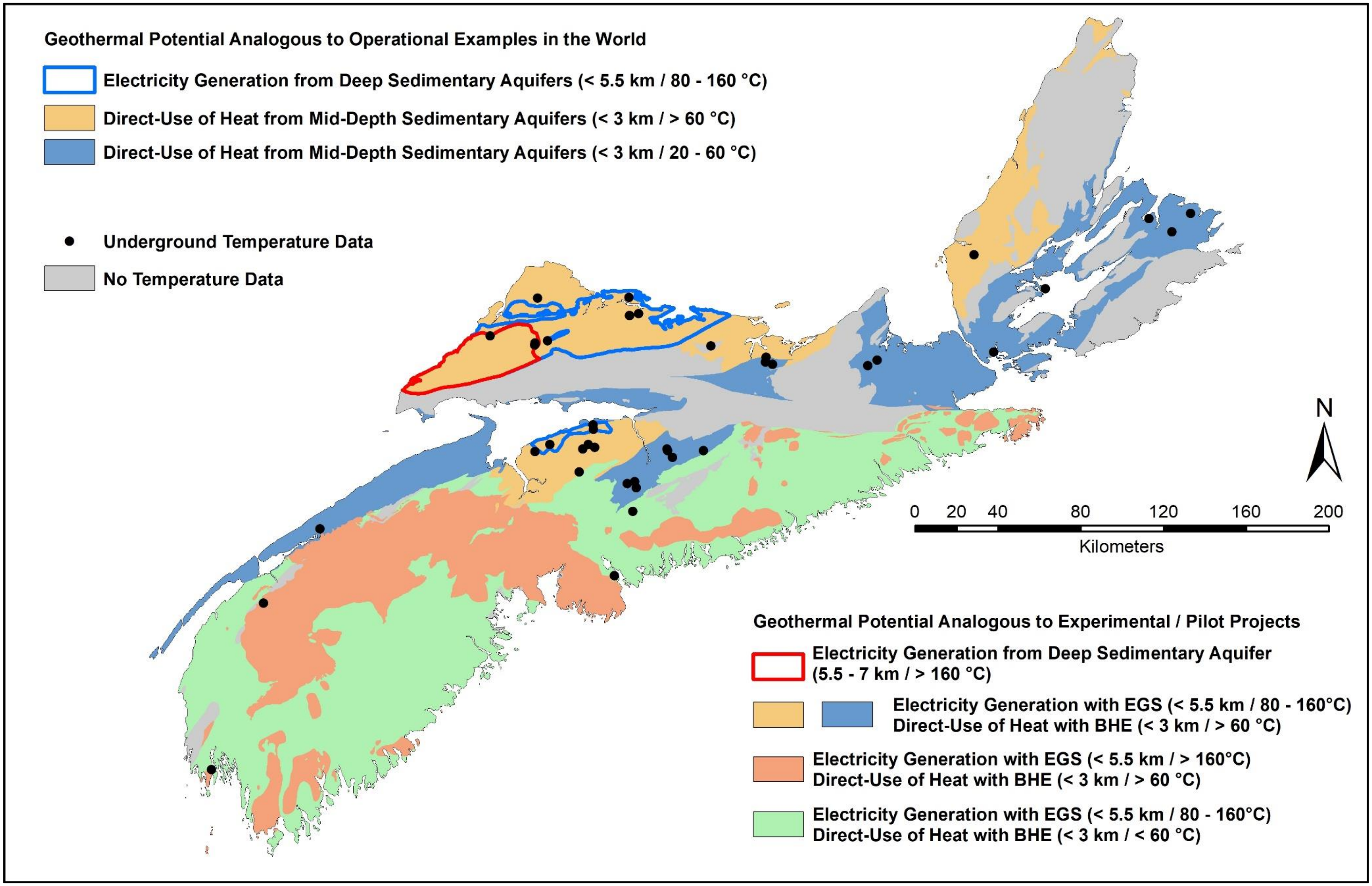

Figure A. Geothermal potential in Nova Scotia for electricity generation and direct-use of heat, based on similar operational examples around the World. Geothermal potential in Nova Scotia for electricity generation, with or without stimulation (enhanced geothermal systems: EGS), and direct-use of heat with or without borehole heat exchanger technology (BHE), based on similar operational examples around the World.

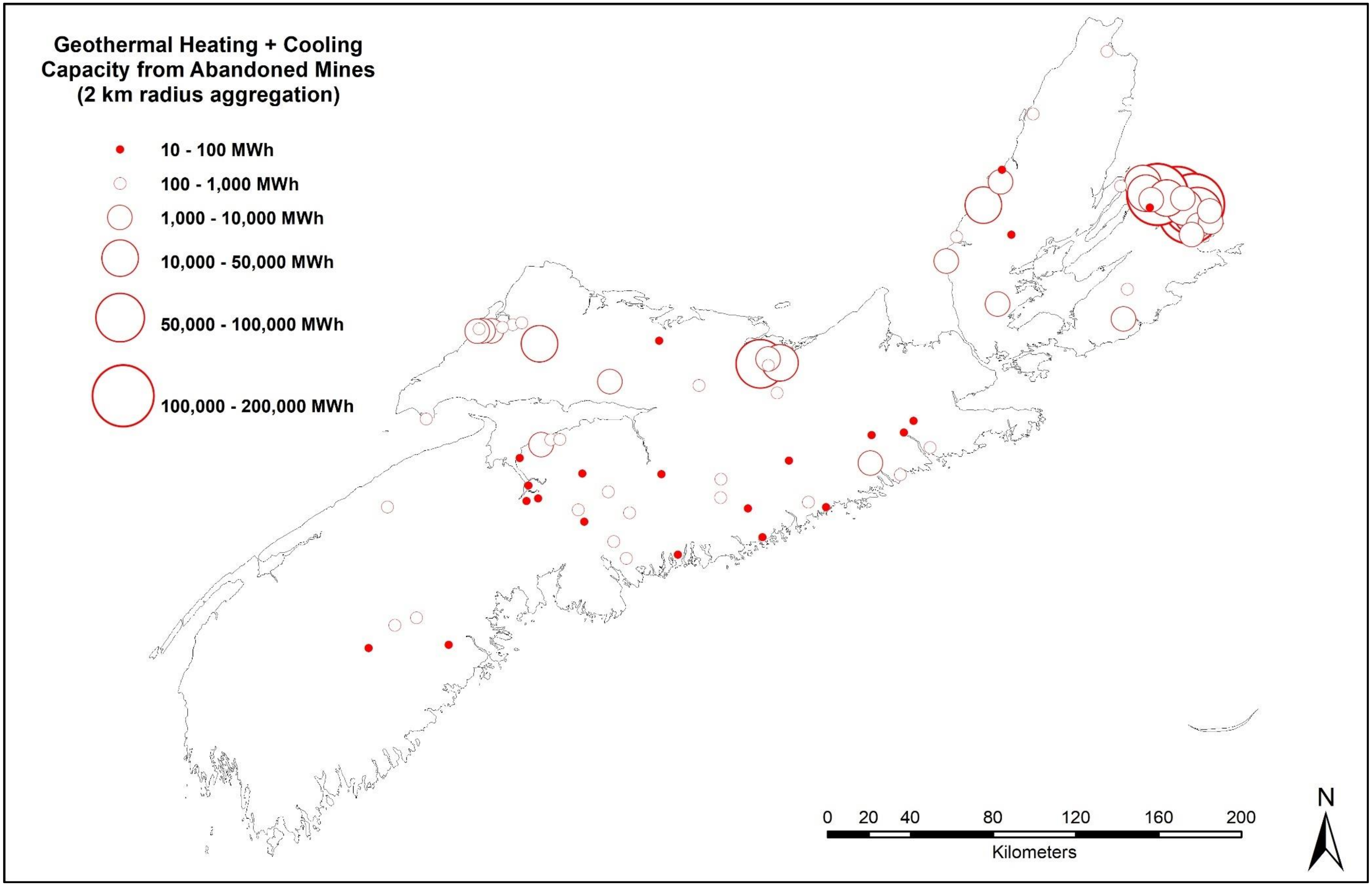

Figure B. Total geothermal energy production capacity in Nova Scotia from abandoned mines for heating and cooling combined purposes. Total geothermal energy production capacity in Nova Scotia from abandoned mines for heating and cooling combined purposes. Mines within a radius of 2 km from each other have been aggregated for clarity purposes.

1. OVERVIEW OF THE GEOTHERMAL RESOURCE TYPES

Geothermal energy is the heat contained within the Earth that generates geological phenomena on a planetary scale. The main sources of this energy are the heat flow originating from the Earth's accretion and the radioactive decay of potassium, thorium, and uranium in the crust. It may be characterized by surface expression of fumaroles, hot springs, geysers and volcanic eruption. Geothermal energy in this report refers to that part of the Earth's heat that can be recovered and exploited by humankind.

The resource is large, is renewable in a broad sense, and is available almost everywhere in the world, depending upon the depth of the resource and the economics associated with its production. Recovery of geothermal energy utilizes only a portion of the stored thermal energy due to limitations in rock permeability that restrict heat extraction through fluid circulation and the minimum temperatures needed at a given site. The total estimated thermal energy above surface temperature to a depth of 10 km under the continents, reachable with current drilling technology, and with a recovery factor of 0.5%, is about three times the annual world consumption for all types of energy (Lund, 2015).

The temperature of the rock increases continuously with depth in a phenomenon called the geothermal gradient, where the temperature increase depends on local geological conditions. The magnitude of geothermal resources in a region or site is a function of the Earth's heat flow, which is proportional to the geothermal gradient measured in deep boreholes and the underground thermal conductivity. Most geothermal exploration and use occur where the geothermal gradient is higher and thus where drilling is shallower and less expensive. An extensive analysis of geological data is needed to identify those shallower geothermal resources, as their occurrence can be due to a combination of factors, for example: (1) a concentration of radiogenic elements; (2) a high surface heat flow, due to a thin continental crust; (3) thermal blanketing or insulation by thick formations of low thermal conductivity rocks such as shale or basement rock with a high feldspar content; and (4) anomalous release of heat of shallow rocks by decay of radioactive elements, perhaps augmented by thermal blanketing. Technical enhancements can be further achieved (Tester et al., 2006), such as hydraulic and chemical stimulation, to create an artificial permeable network when the minimum reservoir qualities are not met, resulting in "Enhanced or Engineered Geothermal Systems (EGSs)".

Throughout the world, major efforts are being made to develop geothermal energy for the production of electricity and/or the direct use of heat (Huttrer, 2020; Lund and Toth, 2020). But more than just a thermal anomaly is needed to profitably exploit geothermal resources. To be exploited, geothermal energy requires the presence of three essential elements: heat, water (steam or hot water) and a permeable geological environment. The resource must be accessible, i.e. a fluid hot enough to generate electricity and close enough to the surface to be reached by technically and economically feasible drilling. On the other hand, the resource must be extractable, i.e., there must be an adequate amount of fluid and the formations must be sufficiently permeable to allow the fluid to flow through the rocks and capture the stored thermal energy.

1.1 Geothermal systems

Plate tectonic settings have a fundamental influence on the characteristics of a geothermal system. The thermal regime and heat flow, hydrogeologic regime, fluid dynamics, fluid chemistry, faults and fractures, stress regime and lithological sequence are all controlled by the plate tectonic framework and are critical for understanding the geothermal system (Moeck, 2014). The thermal state of the active crustal plate boundaries is distinct from that in other large-scale geological provinces, such as tectonically quiescent settings (e.g. cratons), major fault zones (active or inactive), or deep, sedimentary basins (intracontinental or in front of orogenic zones).

In general, geothermal plays are dominated either by a convection or conduction heat transfer regime (**Figure 1.1; Table 1.1**). Convection-dominated geothermal systems host high enthalpy resources and occur at plate tectonic margins, or settings of active tectonism or volcanism. In contrast, conduction-dominated geothermal systems host low to medium enthalpy resources, which can also be called passive geothermal systems due to the absence of convective flow of fluids and short-term fluid dynamics. These systems are located predominately at passive tectonic plate settings, such as the margin of eastern North America, where no significant recent tectonism or volcanism occurs. Here, the geothermal gradient is average, thus this type of geothermal play is located at greater depth than convection-dominated geothermal systems. Conduction-dominated geothermal plays in low permeability domains such as tight sandstones, carbonates or crystalline rock require EGS technology to be utilized on an economic level. Faults can still play an important role in these systems as a fluid conduit or barrier during production and may induce compartmentalization of the system into separate fault blocks. Lithofacies, diagenesis, dissolution processes including karstification and fractures play a major role for reservoir quality evaluation comparable to oil and gas plays.

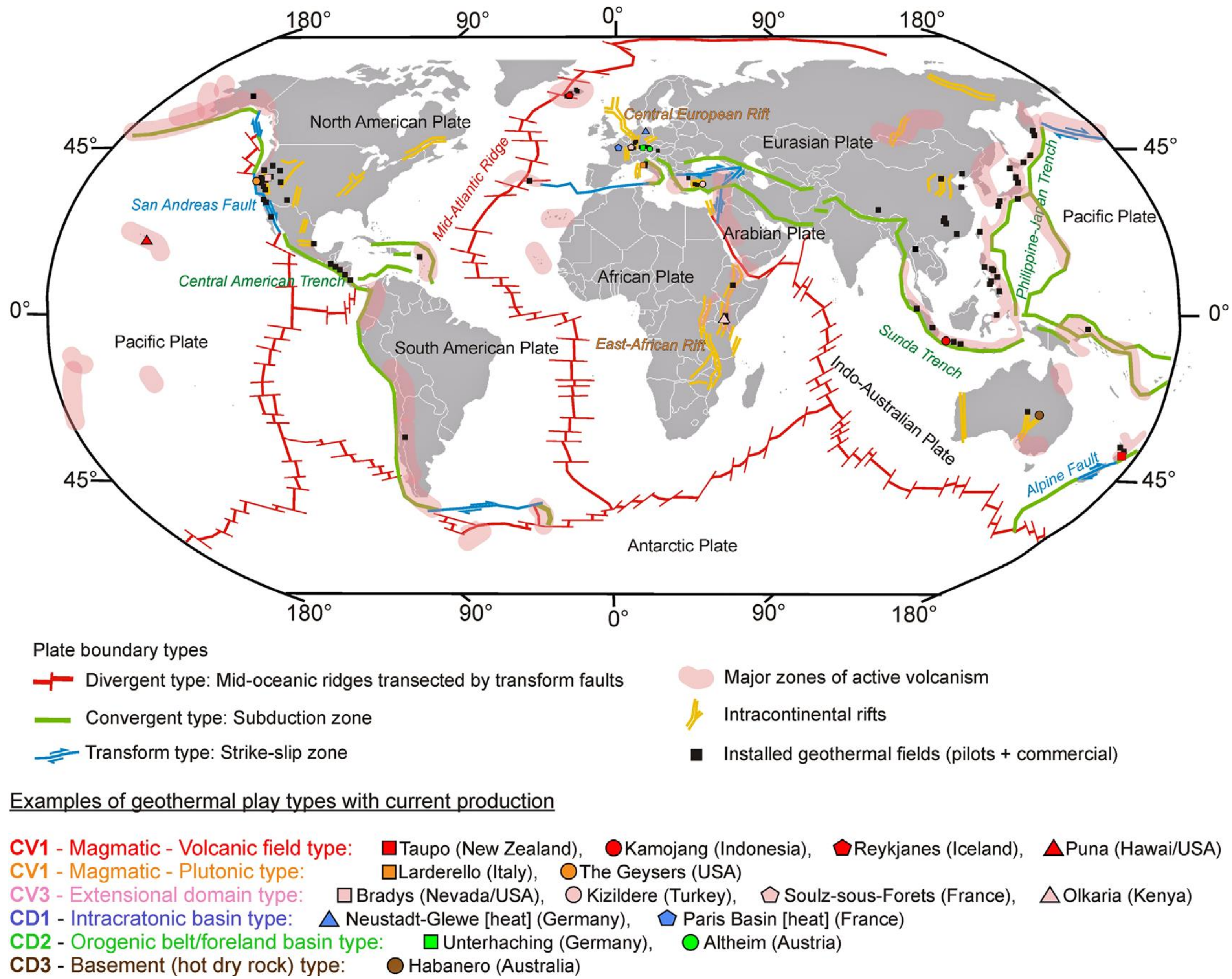

Figure 1.1. Geothermal fields installed worldwide in a plate tectonic setting. Geothermal systems with example fields: CV - Convection dominated heat transfer, CD – Conduction dominated heat transfer (from Moeck, 2014).

Table 1.1. Geothermal examples representing typical geologic systems in which geothermal reservoirs are already discovered and developed.

Geothermal type		Geologic controls	Geological setting	Examples	Host rock	Temperature (°C)
MAGMATIC	**Volcanic**	Magma chambers in active volcanic fields	Volcanic arc regions at subduction zone	Kamojang (Indonesia) Taupo (New Zealand)	Andesites	70 - 320
			Mid oceanic Ridges (MOR) Mantle plumes (hot spots)	Reykjanes (Iceland) Hawaii (USA)	Rhyolithes	
	Plutonic	Crystallizing magma, intrusions and active faulting	Decrescent volcanism in steep terrain at young orogenic belts	Larderello (Italy) The Geysers (USA)	Sediments Granite Gabbro	100-350
	Extensional domain	Active faulting (natural seismicity)	Metamorphic core complexes	Great Basin (Basin and Range, USA) Western Turkey Soultz-sous-Forêts (France)	Volcanic sedimentary rock	150-240
SEDIMENTARY BASIN	**Intracratonic basin (hydrothermal)**	Lithofacies (grain size, mineralogy) Biofacies (fossil content)	Intracontinental rift basins Passive margin basins	North German Basin (Germany)	High-low permeability fluvial sediments	< 150
	Orogenic Belt (hydrothermal)	Litho-/biofacies Faults/fractures	Fold and thrust belts Foreland basin	Southern Cordillera (Canada) Molasse Basin (Switzerland, Germany, Austria)	High–low permeability marine sediments	< 150
EGS	**Basement (petrothermal)**	Faults/fractures	Intracontinental intrusion in flat terrain	Cooper Basin (Australia) Fenton Hill (USA)	Granite rock with high radiogenic heat production	150-320

1.1.1 Magmatic

The main source of geothermal energy around the World is currently magmatic intrusions limited to tectonically active areas or regions with active volcanism. It may be characterized by surface expression of fumaroles, hot springs, geysers, volcanic eruption, and lava flows. The geothermal reservoir is where hot steam or water is trapped under high pressure beneath a tight, non-permeable layer of rocks and is heated by the magmatic intrusion below (**Figure 1.2**). The geothermal wells tap into the geothermal reservoir and access the hot steam or fluid, then transfer it through pipelines to the power plant, after which the fluids are usually returned into the reservoir. Fresh water or precipitation comes from recharge areas such as mountain highs and provides cold meteoric waters which slowly seep through the ground to lower layers through cracks and faults in the rocks.

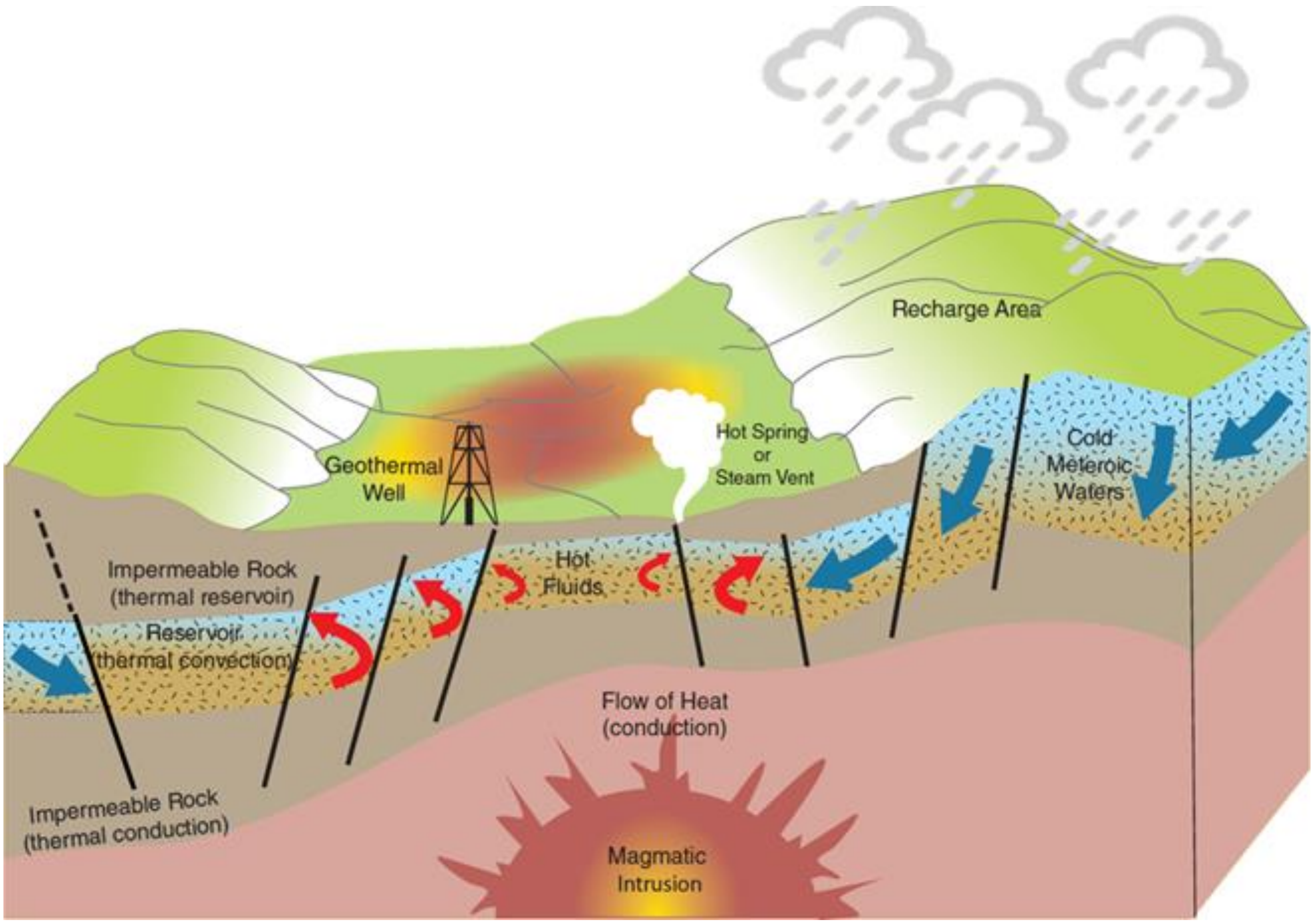

Figure 1.2. Schematic representation of magmatic geothermal system from Dickson and Fanelli, 2003).

1.1.2 Sedimentary basins

This geothermal system can have higher temperature resources compared to the surrounding cratonic bedrock due to the low thermal conductivity of fine-grained sedimentary rocks (**Figure 1.3A**). Specific basin geometry can lead to areas with above average geothermal gradients (> 30 °C km^{-1}). Then, large volume of hot fluids can be contained in porous and permeable geological layers below caprocks. Radiogenic heat can also create resources where granitic intrusions are located near the base of sedimentary basins heating up the local groundwater through the decay of radioactive elements. This localized heating increases the normal geothermal gradient providing hot water at economical drilling depths inside sedimentary basins (**Figure 1.3B**).

Resources can be exploited through a hydrothermal doublet or a deep heat exchangers (500-2,000 m) that can be installed for circulating water inside the ground when the host rock has a low permeability. In a more innovative way, heat exchangers can play an important role in the reuse of abandoned oil and gas wells by circulating a fluid in a closed-loop system for extracting heat by conduction.

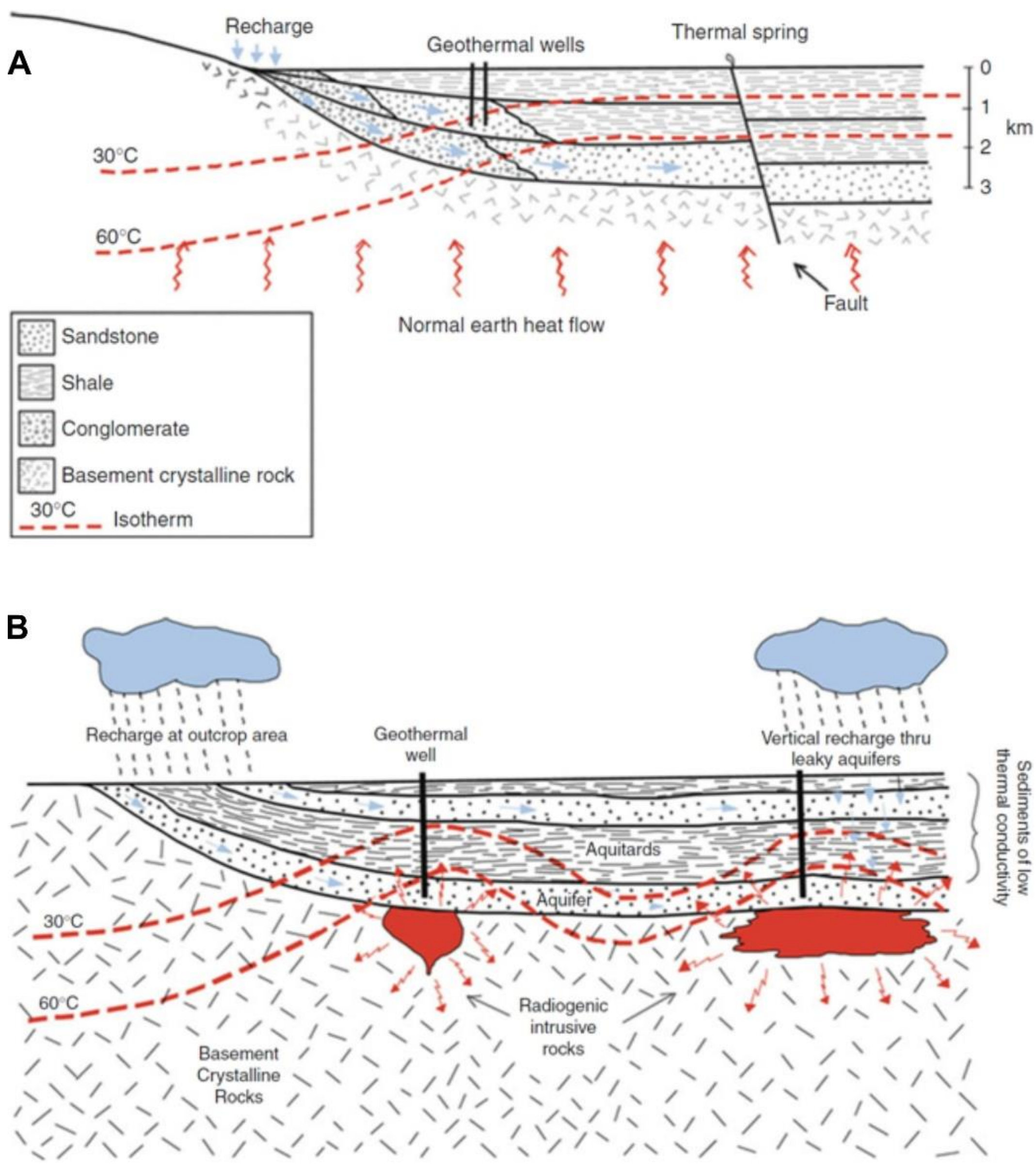

Figure 1.3. Sedimentary basin geothermal resources (from Lund, 2015).

1.1.3 Enhanced geothermal systems (EGS) and deep Borehole heat exchanger (BHE)

Geothermal heat has been traditionally extracted at locations characterized by hydrogeological anomalies, but recent advances in engineering have enabled development of alternative approaches such as Enhanced geothermal systems (EGS) and deep Borehole heat exchanger (BHE). Both EGS and deep BHE technologies harvest Earth's heat without the location constraints of hydrothermal systems.

EGS produce electrical energy by enhancing in-situ permeability and harvesting heat from hot rock geo-reservoirs. The concept of Enhanced Geothermal Systems (EGS), which includes the earlier concept of Hot Dry Rock (HDR), originated in 1974 at the Los Alamos National Laboratory (LANL) in the USA. EGS resources are defined as volumes of rock that have abnormally high heat flow but that have low permeability and thus cannot be exploited in a conventional way. These hot rocks have few pore space or fractures and so contain little water and little or no interconnected permeability. In order to extract the heat, experimental projects have used hydro-fracturing, also known as "fracking", to create artificial reservoirs in such systems, or to enhance existing fracture networks (Breede et al., 2013; Lu, 2017). Once the potential reservoir has been hydraulically fractured to increase its permeability, cold water is injected down one well to extract the heat from the rocks and returned to the surface through a second well in a closed system (**Figure 1.4**). The most important factors which influence the viability of an EGS are fluid flow rate and temperature, where higher flow rates and temperatures support power generation and lower values support direct hot water use (Olasolo et al., 2016). EGS flow rates can be increased via georeservoir permeability stimulation, but temperatures can only be increased by drilling deeper into the Earth's crust.

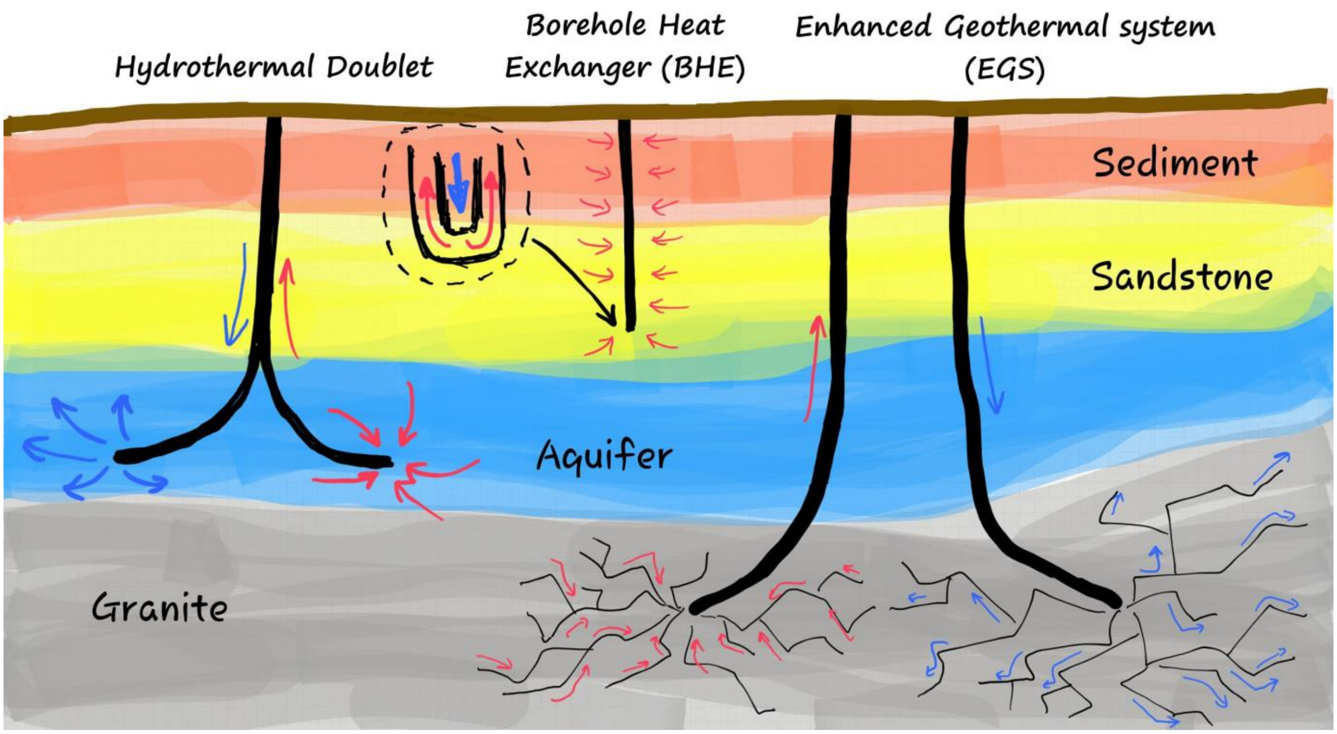

Figure 1.4. Geothermal heat extraction methods (modified from Oberdorfer, 2014).

Different from EGS, BHEs harvest geothermal energy without allowing working fluid to contact soil or rock. Instead, BHEs use various closed loop configurations for circulating working fluid through pipes buried in the subsurface, while exchanging thermal energy with the soil. Shallow BHEs extend 50-200 m depth and are usually coupled with Ground Source Heat Pumps (GSHP) to exploit the subsurface as a thermal source/sink during winter/summer for residential and commercial heating and cooling (Lund and Boyd, 2016). Deep BHEs invoke the same principles as shallow BHEs but they reach depths of 1000-3000 m (Sapinska-Sliwa et al., 2015). Similar to EGS, the production fluid temperature of a deep BHE strongly depends on crustal heat flow. Different from EGS, the efficiency of deep BHEs depends on heat exchanger configuration and the host rock thermal properties instead of hydraulic properties such as porosity and permeability (Dijkshoorn et al., 2013).

1.2 Geothermal resource types

Geothermal energy can be used over a range of temperatures to supply electricity, provide heat and in some cases feed cooling systems. Temperatures above 175 °C are traditionally used to produce electricity; however, with improvements in the organic Rankine cycle or through the use of binary power plants, the usable temperature range has been reduced to around 80-100 °C. Lower temperatures are used for direct heating, generally in the range of 40-100 °C (**Figure 1.5**). Finally, the lowest temperatures from 5 °C to 30 °C, available anywhere in the world at shallow depth (up to 300 m), can be used by heat pumps for heating and cooling. For this study, the potential of shallow geothermal energy extracted by heat pumps is restricted to the use of abandoned mines, and deep geothermal resource types are classified into two different types (electricity generation and direct-use of heat), which are found at different depths according to the geothermal gradient.

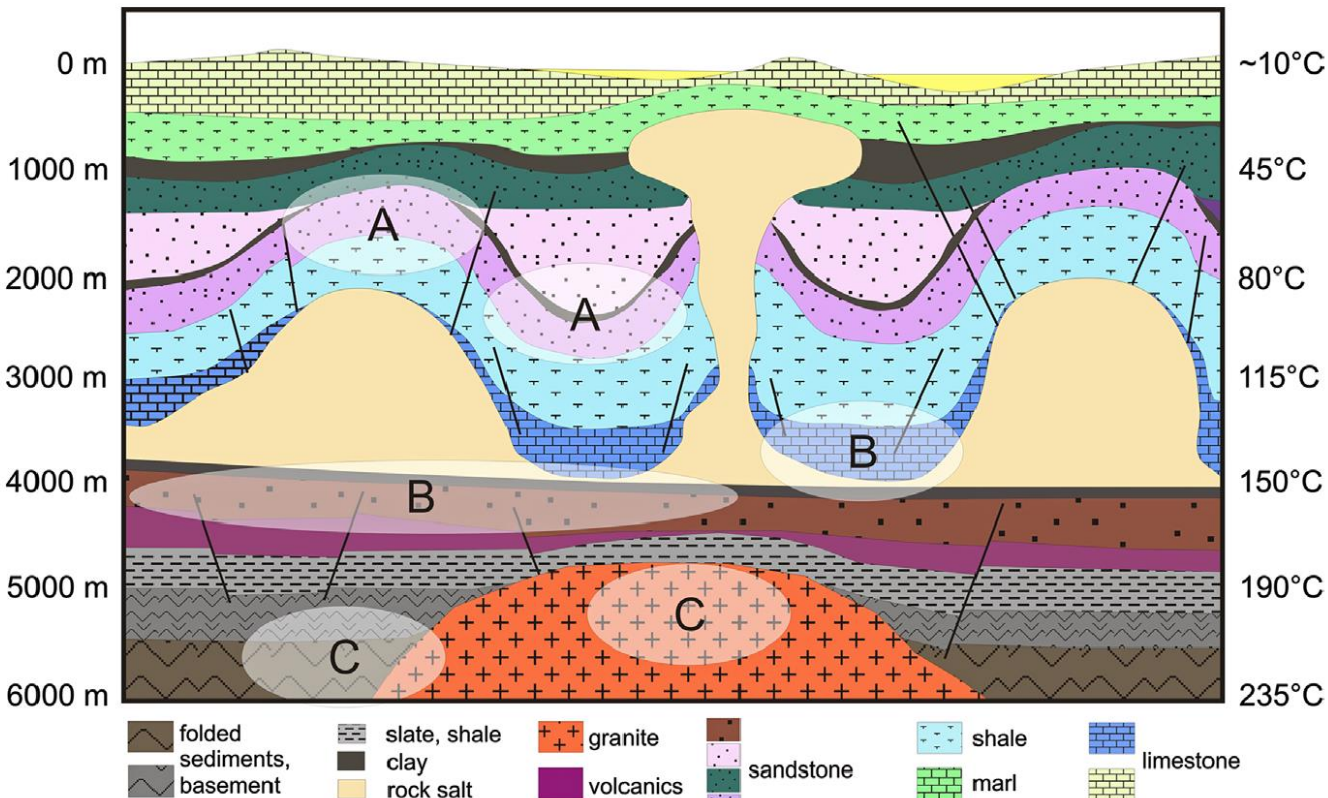

Figure 1.5. Schematic cross-section of a sedimentary basin and various geothermal play types at different depth and temperature ranges. Temperature is an average assuming a geothermal gradient of 32 ºC km^{-1}. A: Geothermal plays above 3 km depth with temperature suitable for direct-use of heat; B: Deep geothermal plays below 3 km depth suitable for both direct-use of heat and electricity generation; C: Very deep geothermal plays below 4km depth as potential EGS (from Moeck, 2014).

1.2.1 Electricity generation (> 80 °C, > 3 km)

Geothermal energy development has traditionally focused on electricity generation (DiPippo, 2015) which can be generated by means of a binary cycle plant if the temperature of the geothermal reservoir is above 80 °C. In 2006, a 200 kW binary power plant was constructed at Chena Hot Springs Resort in Alaska using geothermal fluids at 74 °C, the lowest temperature for electric power generation recorded to date (Lund, 2006).

To generate electricity, heat is recovered from an underground reservoir and used to generate steam which activates a turbine. Geothermal electricity projects are typically associated with large reserves of hydrothermal resources. The first step is to locate a reservoir (van der Meer et al., 2014) and extract the fluid contained in it, so that the geothermal energy in that fluid can then be converted to electricity. Geothermal reserves are similar to oil reserves: they must first be located, then examined to determine whether they contain sufficient fluid for their operation to be viable.

Power plant viability depends on the suitability of an area for geothermal energy production, which is a complex combination of many environmental factors. Geothermal suitability assessments require require time, invasive inspections with drilling probes, high costs, and legal permissions. It is with this in mind that Coro and Trumpy (2020) published a global suitability map of geothermal sites as reference (**Figure 1.6**) based on several parameters such as carbon dioxide emissions, global heat flow, sediment thickness and depth, surface air temperature, precipitation, groundwater resources, earthquake depth, etc.

Although most of the potential lies at the edge of tectonic plates (**Figure 1.7**), several favourable areas are located far from tectonic activity. This is the case for eastern Canada and Nova Scotia, as shown in **Figure 1.6**.

1.2.2 Direct-use of heat from mid-depth aquifers (< 80 °C, < 4 km)

Given that only limited areas in the world have both sufficiently high geothermal gradients and suitable reservoirs to allow for geothermal electricity production, there has been increasing interest in recent years for low-enthalpy geothermal projects focusing on direct heating applications (**Figure 1.8**). More recent developments involve large-scale direct-use of heat projects (Lund and Boyd, 2016), such as district heating (Iceland and France), greenhouse complexes (Netherlands, Hungary and Russia), and major industrial use (New Zealand, Iceland and the USA).

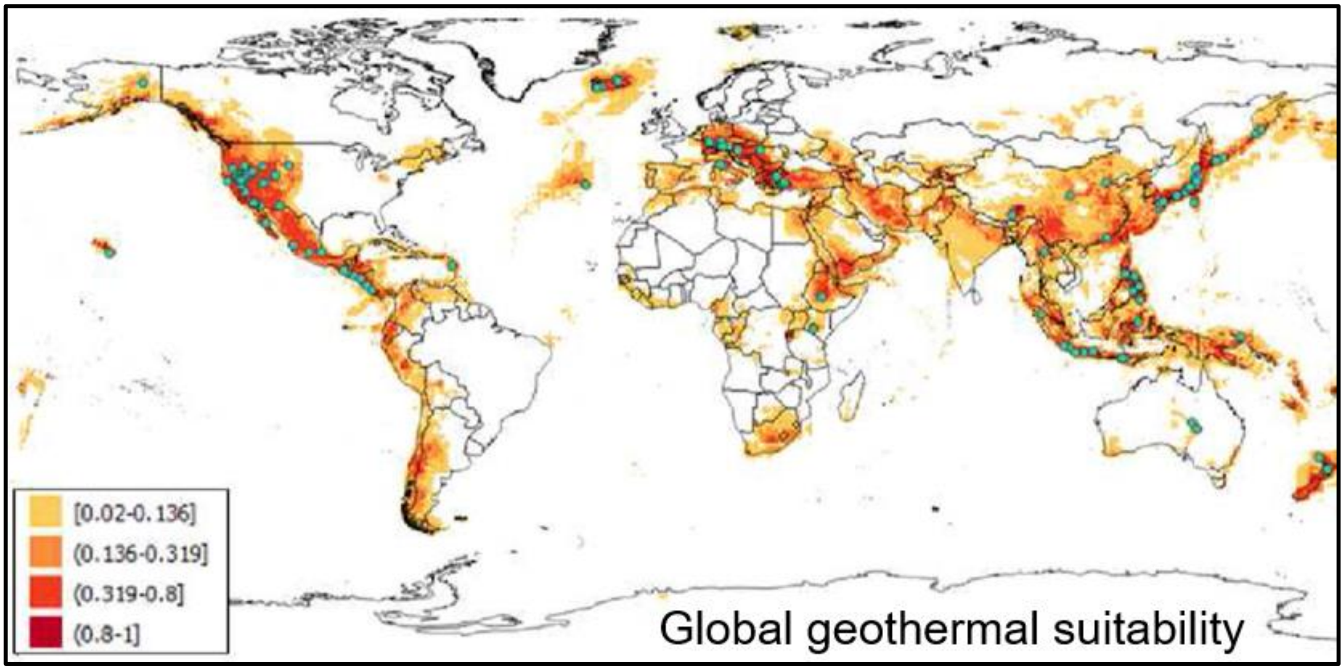

Figure 1.6. Global suitability distribution map of geothermal power plants (from Coro and Trumpy, 2020). Green dots indicate location of operational geothermal power plants.

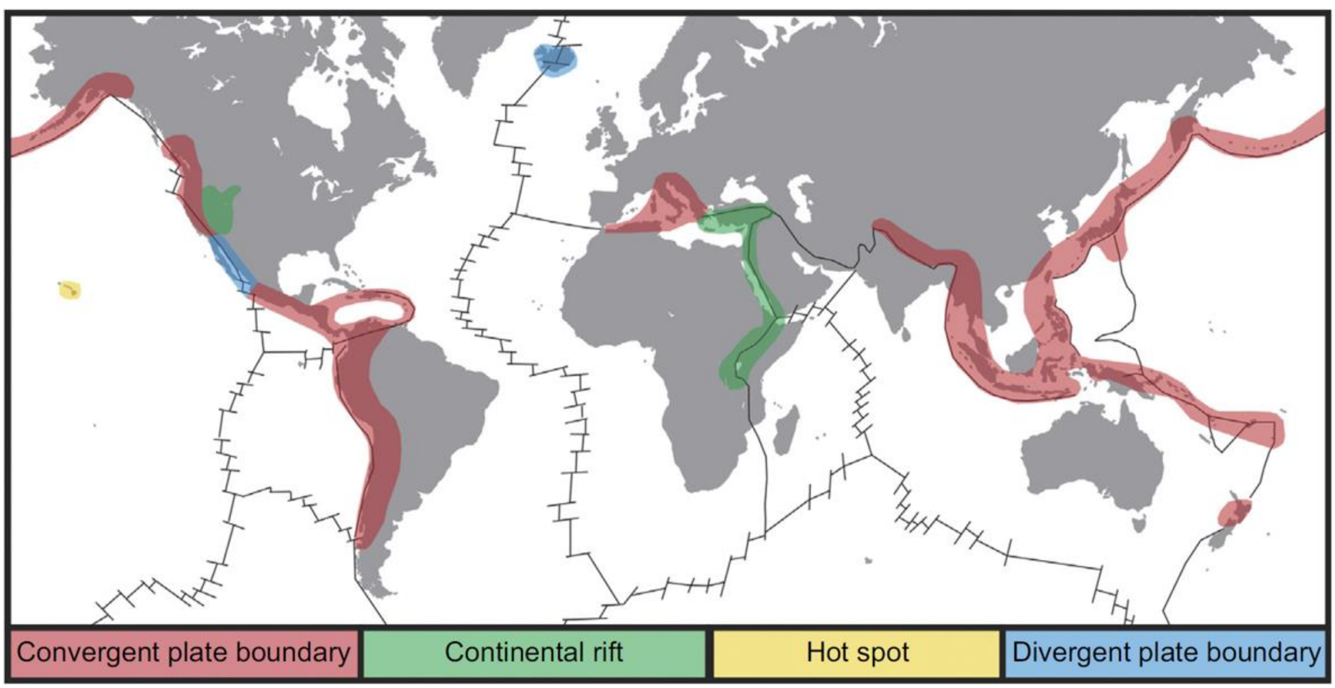

Figure 1.7. Regions of high heat flow and geothermal activity (from DiPippo, 2016).

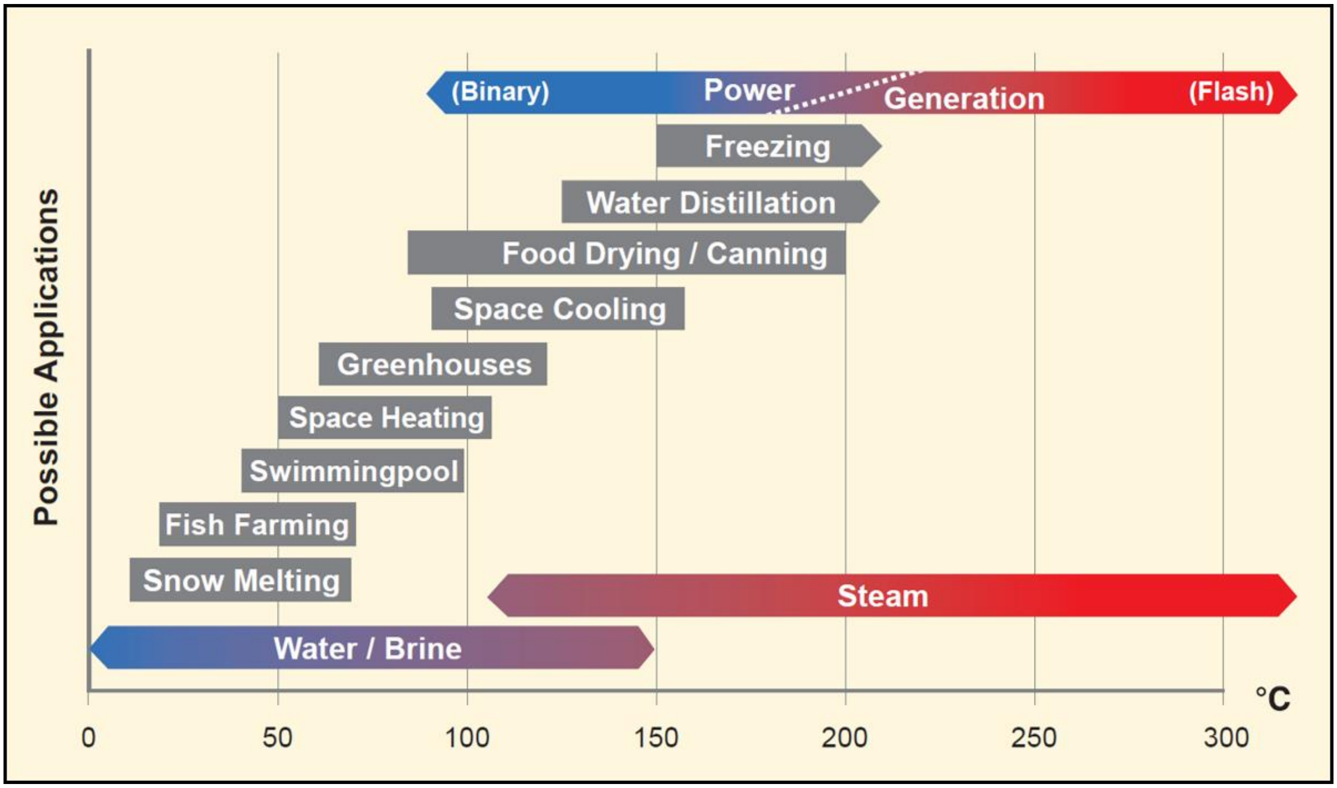

Figure 1.8. Modified Lindal Diagram showing applications for geothermal fluids (from Gehringer and Loksha, 2012).

The primary forms of direct-use include heating swimming pools, space heating (with district heating), agriculture (mainly greenhouse heating, crop drying, and animal husbandry), aquaculture (heating fishponds and raceways), and providing heat for industrial processes. The low-temperature geothermal fluid generally required for direct heat use is available throughout sedimentary basins.

Typical geothermal systems for direct heat consist of two or more wells: hot water is produced by production wells, while injection wells are used to reinject the water after heat has been extracted. Re-injection is mostly applied to preserve aquifer pressure allowing sustainable production, but also to avoid environmental contamination at the surface from geothermal fluids (Kaya et al., 2011; Diaz et al., 2016).

The well layout of most systems is designed to produce energy efficiently for a period of at least 25 years. Geothermal systems have been producing from the Dogger limestone aquifers in the Paris basin in France since the 1970s, which proves that lifetimes of 25 years or more are feasible (Lopez et al., 2010). Axelsson (2010) lists other examples of sustained geothermal production, including a low-enthalpy system in Iceland that has been operational since the 1930s.

The amount of thermal energy stored within aquifers depends on the Earth's heat flow, aquifer volume, and thermal properties. Limberger et al. (2018) present results of a global resource assessment for geothermal energy within deep aquifers up to a depth of three kilometres for direct heat utilization, where greenhouse heating, spatial heating, and spatial cooling are considered. They estimate the global geothermal resource base for direct heat applications by deriving underground temperatures from geophysical data and applying a volumetric heat-in-place method. The distribution of geothermal resources is displayed in a series of maps and the depth of the minimum production temperature is used as an indicator of performance (**Figure 1.9**) and technical feasibility.

Suitable aquifers underlay 16% of the Earth's land surface and store an estimated 4×10^5 to 5×10^6 EJ that can theoretically be used for direct heat applications. Even with a conservative recovery factor of 1% and an assumed lifetime of 30 years, the annual recoverable geothermal energy is in the same order as the world final energy consumption of 363.5 EJ yr^{-1}. Although the amount of geothermal energy stored in aquifers is vast, geothermal direct heat applications are currently underdeveloped with less than one thousandth of their technical potential used.

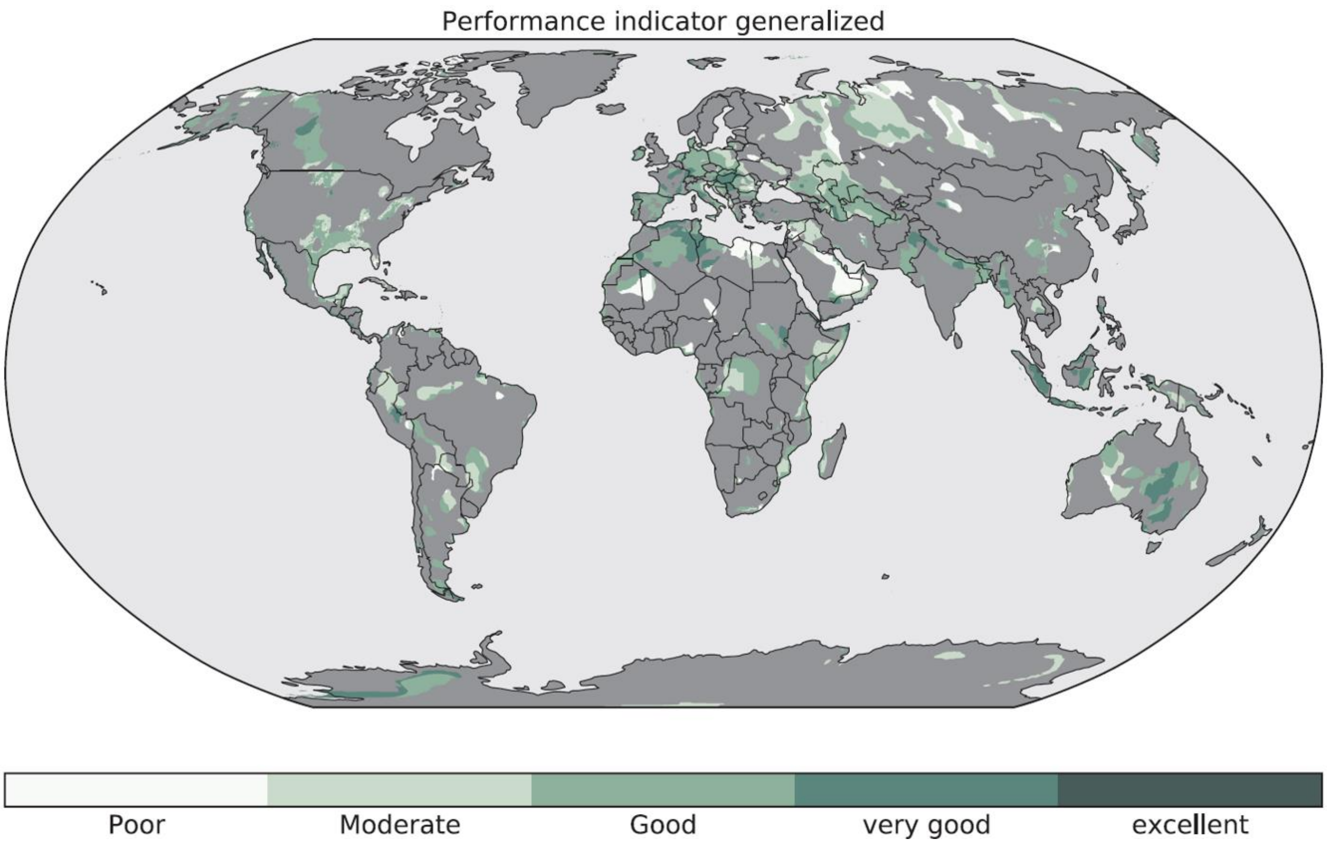

Figure 1.9. Global performance indicator for direct heat applications. This qualitative indicator is shown for regions that have a technical potential and is based on the minimum production depth required for generalized direct heat use (from Limberger et al., 2018).

1.2.3 Heating and cooling from abandoned mines

Although mine sites require significant capital investment to operate, they have always been considered to have little value after closure. There are, however, potentially positive uses for mines that are currently inactive, in particular the production of renewable geothermal energy (Hall et al., 2011; Peralta Ramos et al., 2015; Loredo et al., 2016; Al-Habaibeha et al., 2018). After closure, most mines become flooded by groundwater and runoff. The thermal inertia of this body of water can be exploited through the use of geothermal heat pump systems. This technology can be deployed in any type of geological environment and can result in significant energy savings.

When installing ground-source heat pump systems, the main costs are related to drilling. In the case of an abandoned and flooded mine, this geothermal resource is directly accessible through the existing underground gallery networks or from the open pit. After recovering the heat contained in the water pumped through heat exchangers, this water can be returned to another location in the mine. This type of geothermal system is called "open-loop" because it allows the ground water in the mine to be pumped directly from the ground (**Figure 1.10**).

The energy extracted or transferred with a heat pump from or to the mine water can be used to heat and cool commercial, industrial and institutional buildings located near these mines or energy-intensive businesses such as greenhouse complexes or data centres.

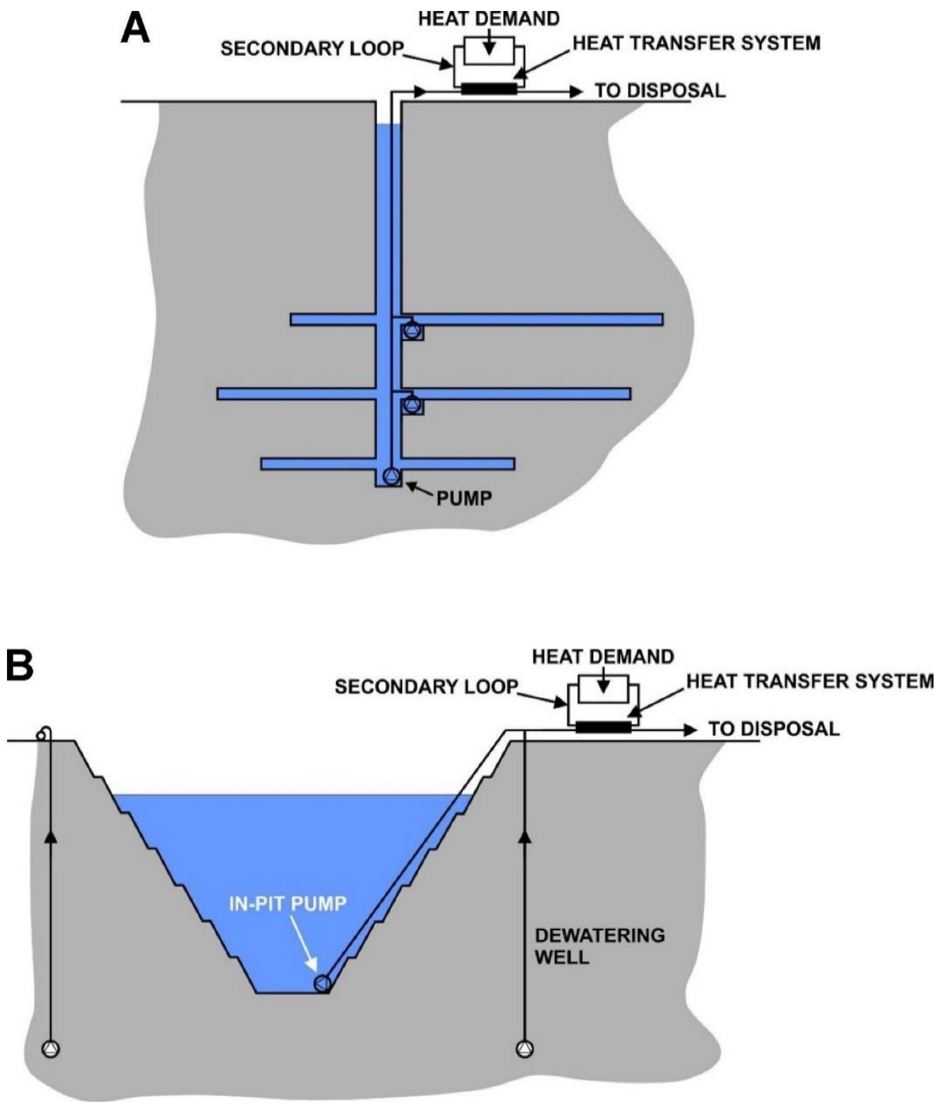

Figure 1.10. Ground-source heat pump systems using water from closed and flooded mines. A) Underground mine; B) Open pit mine (adapted from Preene and Younger, 2014).

1.3 References

Al-Habaibeha, A., Athresha, A.P., Parker, K., 2018. Performance analysis of using mine water from an abandoned coal mine for heating of buildings using an open loop based single shaft GSHP system. Applied Energy 21(1): 393-402. https://doi.org/10.1016/j.apenergy.2017.11.025

Axelsson, G., 2010. Sustainable geothermal utilization - case histories; definitions; research issues and modelling. Geothermics 39(4):283–91. https://doi.org/10.1016/j.geothermics.2010.08.001

Barton, C.A., Zoback, M.D., Burns, K.L., 1988. In-situ stress orientation and magnitude at the Fenton Hill geothermal site, New Mexico, determined from wellbore breakouts. Geophysical Research Letters 15(5):467–70. https://doi.org/10.1029/GL015i005p00467

Breede K, Dzebisashvili K, Liu X, Falcone G., 2013. A systematic review of enhanced (or engineered) geothermal systems: past, present and future. Geothermal Energy 1(4):1–27. https://doi.org/10.1186/2195-9706-1-4

Diaz, A.R., Kaya, E., Zarrouk, S., 2016. Reinjection in geothermal fields – a worldwide review update. Renew Sustain Energy Rev 53:105–62. https://doi.org/10.1016/j.rser.2015.07.151

Dijkshoorn, L, Speer, S., Pechnig, R., 2013. Measurements and design calculations for a deep coaxial borehole heat exchanger in Aachen. Germany. International Journal of Geophysics 2013: 16541. https://doi.org/10.1155/2013/916541

DiPippo, R., 2016. Geothermal Power Plants 4th Edition: Principles, Applications, Case Studies and Environmental Impact. Elsevier Science. 800 p.

Gehringer, M. and Loksha, V., 2012. Geothermal Handbook: Planning and Financing Power Generation. ESMAP Technical Report 002/12. World Bank, Washington, DC, 150 p. http://hdl.handle.net/10986/23712

Hall, A., Scott, J.A., Shang, H., 2011. Geothermal energy recovery from underground mines. Renewable and Sustainable Energy Reviews 15(2): 916-924. https://doi.org/10.1016/j.rser.2010.11.007

Huttrer, G., 2020. Geothermal Power Generation in the World 2015-2020 Update Report. Proceedings World Geothermal Congress 2020 Reykjavik, Iceland, April 26-May 2, 2020, 17 p.

Kaya, E., Zarrouk, S., O'Sullivan, M., 2011. Reinjection in geothermal fields – a review of worldwide experience. Renew Sustain Energy Rev 15(1):47–68. https://doi.org/10.1016/j.rser.2010.07.032

Loredo, C., Roqueñí, N. et Ordóñez, A., 2016. Modelling flow and heat transfer in flooded mines for geothermal energy use: A review. International Journal of Coal Geology 164: 115-122. http://dx.doi.org/10.1016/j.coal.2016.04.013

Lopez S, Hamm V, Brun M Le, Schaper L, Boissier F, Cotiche C, Giuglaris, E., 2010. 40 years of Dogger aquifer management in Île-de-France. Paris Basin, Fr, Geothermics 39(4):339–56. https://doi.org/10.1016/j.geothermics.2010.09.005

Lu S-M., 2017. A global review of enhanced geothermal system (EGS). Renewable and Sustainable Energy Reviews 81(2):2902-2921. https://doi.org/10.1016/j.rser.2017.06.097

Lund J.W. (2015) Geothermal Energy Utilization. In: Meyers R. (eds) Encyclopedia of Sustainability Science and Technology. Springer, New York, NY. https://doi.org/10.1007/978-1-4939-2493-6_231-3

Lund, J.W. and Boyd, T.L., 2016. Direct utilization of geothermal energy 2015 worldwide review. Geothermics 60: 66-93. http://dx.doi.org/10.1016/j.geothermics.2015.11.004

Lund, J.W. and Toth, A.N., 2020. Direct Utilization of Geothermal Energy 2020 Worldwide Review. Proceedings World Geothermal Congress 2020 Reykjavik, Iceland, April 26 – May 2, 2020, 39 p.

Moeck, I.S., 2014. Catalog of geothermal play types based on geologic controls. Renewable and Sustainable Energy Reviews 37: 867-882 https://doi.org/10.1016/j.rser.2014.05.032

Oberderfer, P., 2014. Modeling Geothermal Processes with COMSOL Software. Retrieved from: https://www.comsol.com/blogs/modeling-geothermal-processes-comsol-software/

Olasolo, P., Juárez, M.C., Morales, M.P., D´Amico, S., Liarte, I.A.., 2016. Enhanced geothermal systems (EGS): A review. Renewable and Sustainable Energy Reviews 56:133-144. https://doi.org/10.1016/j.rser.2015.11.031

Parker, R., 1999. The Rosemanowes HDR project 1983-1991. Geothermics 28(4–5):603–15. https://doi.org/10.1016/S0375-6505(99)00031-0

Peralta Ramos, E., Breede, K et Falcone, G., 2015. Geothermal heat recovery from abandoned mines: a systematic review of projects implemented worldwide and a methodology for screening new projects. Environmental Earth Sciences 73(11): 6783–6795. https://doi.org/10.1007/s12665-015-4285-y

Preene, M. et Younger, P.L., 2014. Can you take the heat? – Geothermal energy in mining. Transactions of the Institutions of Mining and Metallurgy, Section A: Mining Technology 123(2): 107-118. https://doi.org/10.1179/1743286314Y.0000000058

Sapinska-Sliwa, A., Rosen, M., Gonet, A., Sliwa, T., 2016. Deep Borehole Heat Exchangers — A Conceptual and Comparative Review. International Journal of Air-Conditioning and Refrigeration 24(1):1630001. https://doi.org/10.1142/S2010132516300019

Tester, J,W, Anderson, B.J., Batchelor, A.S., Blackwell, D.D., DiPippo, R., Drake, E.M., Petty, S., 2006. The future of geothermal energy – impacts of enhanced geothermal systems (EGS) on the United States in the 21st century. Massachusetts Institute of Technology, Cambridge, 384 p.

Valley, B., Evans, K.F., 2010. Stress heterogeneity in the granite of the Soultz EGS reservoir inferred form an analysis of wellbore failure. Proceedings World Geothermal Congress 2010. Bali, Indonesia, 25-29 April 2010.

van der Meer, F., Hecker, C., van Ruitenbeek, F., van der Werff, H., De Wijkerslooth, C., Wechsler, C., 2014. Geologic remote sensing geothermal exploration: a review. International Journal of Applied Earth Observation and Geoinformation 33:255-2569. http://dx.doi.org/10.1016/j.jag.2014.05.007

Wyborn, D., 2010. Update of development of the geothermal field in the granite at Innamincka, South Australia. Proceedings World Geothermal Congress 2010. Bali, Indonesia, 25-29 April 2010.

2. EXAMPLES OF INDUSTRIAL DEVELOPMENTS AROUND THE WORLD

Geothermal energy potential is broadly distributed across Canada (**Figure 2.1**). Nova Scotia is in part covered by sedimentary basins that contain warm fluids in porous rocks and shows a moderate potential for a direct-use of heat. The potential for EGS application in non-sedimentary rocks of the province was considered low, however, recent innovations have raised questions about its potential. Knowledge of the geological framework of Canada can significantly reduce exploration risk by defining regions with the best geological conditions to host a geothermal resource.

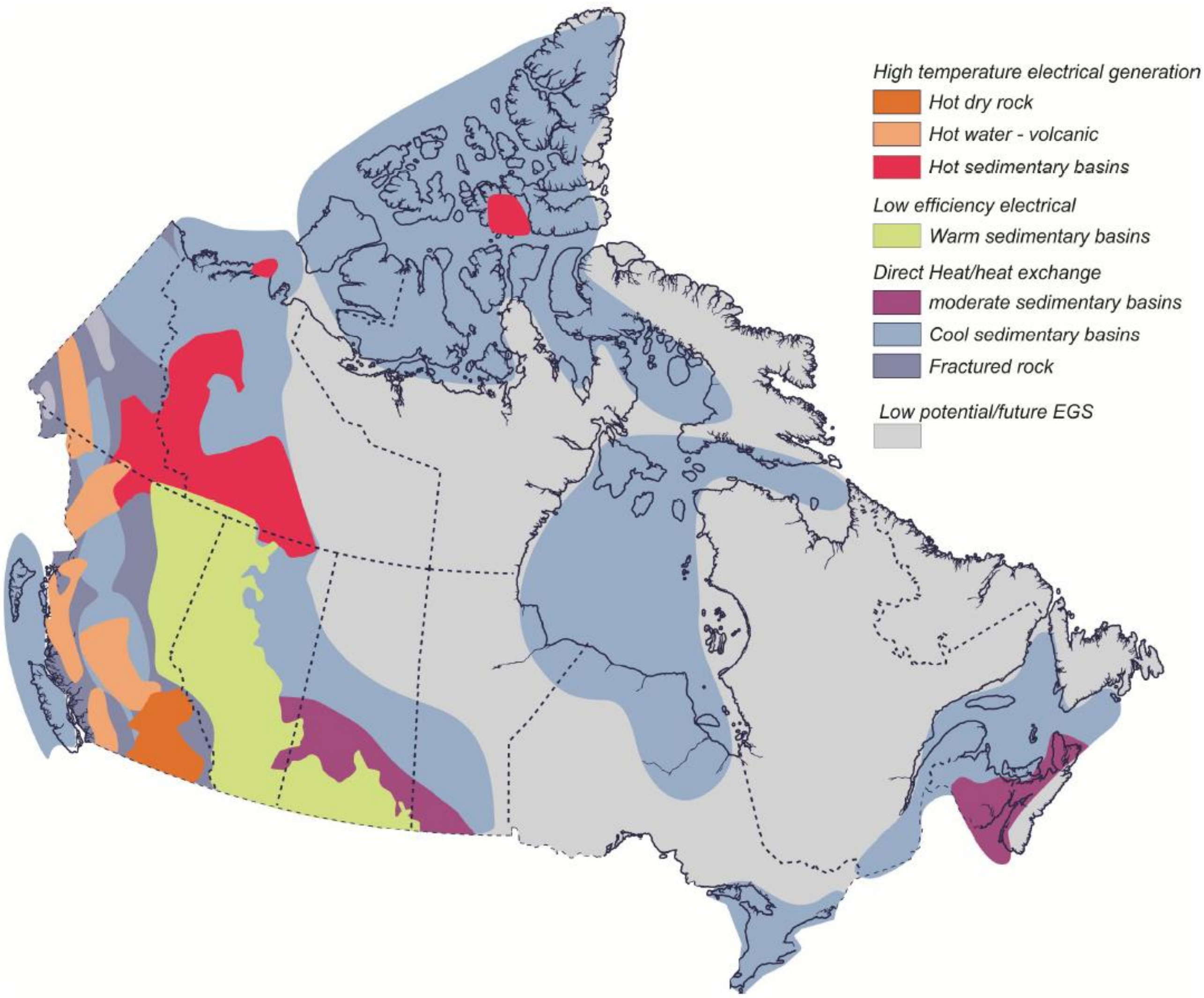

Figure 2.1. Map showing the distribution of the geothermal potential in Canada based on end use (from Grasby et al., 2012).

A total of 179 base metal and 213 coal mines with abandoned and flooded underground excavations have been inventoried in Nova Scotia in 1992 by Arkay (2000). Those abandoned mines contain warm waters that can be used to heat homes, businesses, and institutions through geothermal heat pumps. Water in flooded coal mines has already been used as a heat source in Nova Scotia at the Springhill coal mine (Jessop et al., 1995), the first development of this kind anywhere in the world, which has now evolved into a geothermal industrial park. Water at about 18 ºC is pumped from the mine workings and is used with heat pumps to heat industrial, educational and community-use buildings (presently used by a total of 11 buildings). This low enthalpy energy has a huge potential for both heating and cooling buildings. Thus, this section gives examples of relevant successful development projects from around the world highlighting the types of resource development most likely for Nova Scotia. For this reason, the focus has been set on resources from sedimentary basins (both electricity generation and direct-use of heat) and abandoned mines, with a quick look on both Enhanced geothermal systems (EGS) and deep Borehole heat exchanger (BHE).

As a further reference, it is also advisable to consult the report of the United Nations Framework Classification for Resources (UNFC, 2017), in which a set of 14 case studies on the applications to geothermal energy from Australia, Germany, Hungary, Iceland, Italy, Netherlands, New Zealand, Philippines and Russian Federation. The case studies are presented to illustrate the application of the geothermal energy specifications for the uniform use of UNFC in different contexts. These application examples from different countries provide a range of scenarios in the classification of geothermal resources in a manner consistent with the classification of other energy resources. Thus, it should be noted that of these examples, only those from Germany and the Netherlands can be considered as analogues to Nova Scotia. Indeed, the other examples are related to magmatic systems involving very high levels of heat flux, which is not observed in Eastern Canada.

2.1 Electricity generation from deep sedimentary aquifers

2.1.1 Germany

Neustadt-Glewe, the first German geothermal power plant, began operations in 1995, with an installed power of 0.23 MW, and then transitioned from heating to power generation in 2003 via the exploitation of hot water aquifers. Four years later a 3 MW power plant was installed in Landau. In the following years, additional plants were commissioned proving that power generation from low-enthalpy reservoirs via binary power plant concepts, such as the Organic Rankine Cycle (ORC) or Kalina Cycle, is feasible in Germany. These technologies allow power production even at temperatures as low as 100 °C. Today, ten geothermal plants with an installed capacity of approximately 40 MW are connected to the German grid, seven of which combine heat and electricity (**Table 2.1**).

Although a great theoretical potential for geothermal power generation is attributed to EGS, commercial project development to date focuses on hydrothermal resources in sedimentary systems. The most significant geologic systems hosting proven geothermal reservoirs at depths greater than 1,000 m in Germany are the North German Basin, the South German Molasse Basin and the Upper Rhine Graben.

The North German Basin sediment thickness ranges from 2 to 10 km. Salt tectonic movements are responsible for the intense and complex deformation of the Mesozoic and Cenozoic overburden formations. Affected by these salt tectonics, the geologic successions vary in depth and thickness which lead to strong variations of temperature and energy content of the individual geothermal resources on a regional scale (Weber et al., 2019). The Mesozoic successions of the North German Basin consist of siliciclastic rocks and carbonates with evaporitic layers. Aquifers of high permeability are the main horizons of interest for geothermal use in this region. Porous sedimentary aquifers suitable for geothermal use are defined by a minimum aquifer thickness of 20 m, a porosity > 20%, and a permeability > 250 mD.

Table 2.1. Plant characteristics of geothermal projects with power generation in Germany (from Eyerer et al., 2020). NGB, North German Basin; SGM, South German Molasse Basin; URG, Upper Rhine Graben.

Plant	Region	Initial operation	Electricity (MW)	Heat (MW)	Depth (m)	Temp. (ºC)	Gradient (ºC km^{-1})	Flow (l s^{-1})
Landau	URG	2007	3.0	5	3,300	160	44	70
Bruchsal	URG	2009	0.6	1.2	1,877	124	63	23
Unterhaching	SMB	2009	3.4	38	3,350	122	32	150
Insheim	URG	2012	4.8	–	3,800	165	39	80
Dürrnhaar	SMB	2012	5.5	–	3,926	138	32	130
Kirchstockach	SMB	2013	5.5	–	3,882	135	32	135
Sauerlach	SMB	2013	5.0	4	4,757	140	26	110
Laufzorn	SMB	2014	4.3	40	4,083	128	29	140
Traunreut	SMB	2016	4.1	12	5,067	118	20	165
Taufkirchen	SMB	2017	4.3	40	3,763	136	32	120

The Molasse Basin in southern Germany is a foreland basin that extends over more than 300 km, from Switzerland in the southwest to Austria in the east. The basin fill comprises primarily Tertiary Molasse sediments, Cretaceous, Upper (Malm) to Middle (Dogger) Jurassic and Triassic sediments. The Upper Jurassic Malm Formation is composed of karstic-dolomitic fractured carbonate rocks and is one of the most important hydrothermal energy reservoirs in Central Europe (Weber et al., 2019). The aquifer's geothermal potential and its hydraulic properties have been subject to intense research and development activities since the early 1990s. Due to the southward deepening and wedge-shaped geometry of the basin, reservoir temperatures and depth of the Malm reservoir increase towards the Alps from 40 °C in the north to more than 160 °C in the south of the basin near the Alpine Molasse. Thus, district heating plants can be found in the northern part of the basin while combined heat and power plants are located in the South. Temperatures suitable for power generation are reached south of Munich where several power plants are in operation.

The Upper Rhine Graben belongs to a large European rift system which crosses the northwestern European plate (Villemin et al., 1986). The graben was formed by repeated reactivations of complex fault patterns. Crustal extension 45-60 million years ago formed depocenters along a pre-existing fault associated with up-doming of the crust-mantle boundary and magmatic intrusions at 80-100 km depth (Pribnow and Schellschmidt, 2000). Major exploration targets for geothermal projects in the Upper Rhine Graben are the Upper Muschelkalk and Bunter formations in combination with fault zones (Hurter and Haenel, 2002).

2.1.2 Saskatchewan (Canada)

The Canadian market poses several challenges to geothermal energy development. First, there has been a lack of early-stage supportive policies and funding programs, both provincially and federally. Also, several provincial and territorial jurisdictions have not developed regulatory frameworks for geothermal energy development, with the notable exceptions of Nova Scotia and British Columbia. This creates an uncertain environment for investors and makes it difficult for developers to advance projects beyond the exploration phase (Huttrer, 2020). To address these shortcomings, recent initiatives include:

- maintenance of the Canadian National Geothermal Database;
- provincial and territorial geothermal favorability mapping;
- energy literacy improvement programs;

- various efforts on the part of the Canadian Geothermal Industry Association to build provincial and federal policy support for the geothermal industry.

The federal focus has shifted in recent years towards clean technologies, which led to an increase of funding. Added to the downturn in oil and gas activities, there is now an interest for green energies. Consequently, there are currently 8 geothermal power production projects in various stages of exploration in Canada ranging from permit acquisition, through conduct of surface geoscientific studies and drilling of well(s), to building of demonstration facilities. This work is being undertaken in British Columbia (3), the Northwest Territories (1), the Yukon Territory (1), Alberta (2), and Saskatchewan (1).

The DEEP project proponents in Saskatchewan hope to become the first geothermal electricity production facility in Canada (Deep Earth Energy Production Corp., 2020). Analysis of thousands of public well records revealed the presence of a vast hot sedimentary aquifer in the Williston Basin (**Figure 2.2**). After a $2M Pre-feasibility Study funded in partnership by SaskPower and Natural Resources Canada was completed in 2014, the geothermal developer signed an Electricity Purchasing Agreement with the provincial government in 2018. Finally, the deepest well ever drilled in the province (3,530 metres with a temperature of 120 ºC and a geothermal gradient of 32 ºC km^{-1}) was completed in 2018. In 2019 the federal government announced $25.6M funding through Natural Resources Canada to provide approximately 50% of the total project funding for the first five-megawatt power facility, targeted for construction completion in early 2022. DEEP's long-term goal is to develop 5-20 MW power plants, each of which could power up to 5,000 to 20,000 households.

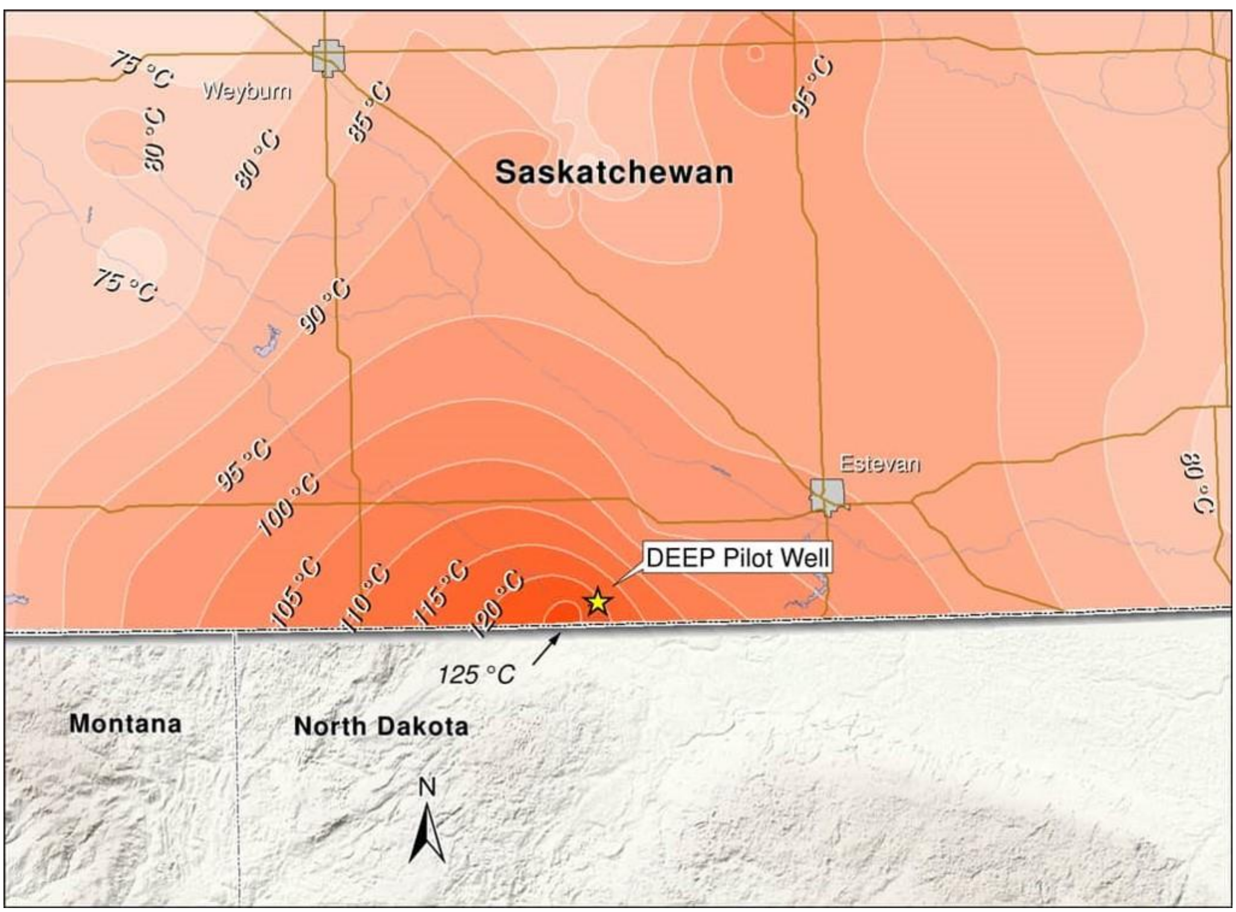

Figure 2.2. Aquifer temperature isocontours of the DEEP geothermal project in Saskatchewan, a few km north of the US border (from Deep Earth Energy Production Corp., 2020).

2.1.3 British Columbia (Canada)

Geoscience BC has previously commissioned two research studies with the purpose of quantifying the potential amount of electrical energy that can be harnessed from the nearby geothermal resources, and the cost of that energy. The first study (Palmer-Wilson et al., 2018) focuses on the techno-economic assessment of the Western Canada Sedimentary Basin (WCSB), while the second (Renaud et al., 2018) is a geological assessment of the Clarke Lake Reservoir, which is in the WCSB and was considered a promising location due to its geological characteristics, the nearby town of Fort Nelson, and existing natural gas development that provides significant geological data.

Palmer-Wilson et al. (2018) used data available on geological criteria and economic criteria relevant to the favourability of geothermal power to produce a geothermal power development favorability map in the Western Canada Sedimentary Basin section located in northeastern British Columbia. According to this algorithm, regions of high favorability show a better opportunity for geothermal power development as compared to regions of low favorability. The criteria (**Table 2.2**) are put together in a weighted summation to produce the favorability score for the locations studied within the Western Canada Sedimentary Basin. The data is geographical in nature, and thus can be evaluated to produce a map. tThe favorability map identified four regions of high favorability, where the Clarke Lake Reservoir area is one of them.

Table 2.2. Geological and economic criteria and their relative weights in the favorability score used by Palmer-Wilson et al. (2018).

Criteria	Weight
Geological Criteria	
Temperature of geothermal resource	25%
Indicated Aquifer *evidence of permeable aquifers*	25%
Economic Criteria	
Gas Activity *potential for natural gas industry as a customer*	13.7%
Electrical Infrastructure *proximity to transmission lines and substations*	13.7%
Proposed Electrical Infrastructure *electrical infrastructure in planning*	13.7%
Towns and Communities *proximity to communities for worker housing and potential for excess heat sales*	13.7%

The Clarke Lake area is situated in the Western Canadian Sedimentary Basin (WCSB), shown in **Figure 1**. The WCSB is a relatively lower temperature region, so it receives less attention with regards to potential geothermal development. Significant oil and gas development in the region, however, has provided a database of wells available from the BC Oil and Gas Commission, which can be used to estimate electrical and heating generation potential. This database was analyzed by Palmer-Wilson et al. (2018).

In 2018, Geoscience BC commissioned Associated Engineering (2019) to conduct a pre-feasibility study to further assess the feasibility of implementing a project from a site servicing perspective, as well as assessing the potential customer base for power and potential heat recovery. A total plant development cost estimate was developed, since the previous studies identified an achievable well production rate in the range of 30 to 100 L/s. This results in two scenarios: one with 47 wells required, and one with 15 wells. Because well drilling is a major cost of a geothermal plant, the results show a cost estimate in the range of $139 million to $285 million ($CAD). Considering only the potential revenue and an estimate for the annual operations and maintenance costs, the payback was estimated to be in the range of 12-24 years for plant construction and commissioning.

2.2 Direct-use of heat from mid-depth sedimentary aquifers

2.2.1 Germany

Due to favorable geological conditions (see **Section 2.1.1**) 19 geothermal plants using direct-use of heat have been constructed in the Molasse Basin in Southern Germany and in the North German Basin (**Table 2.3**). In 2018 the geothermal installed capacity of direct-use of heat applications reached approximately 200 MW. In addition, there are seven other district heating plants (140 MW) that combine heat and electricity (**Table 2.1**). Geothermal well doublets consisting of a production and an injection well are typically used for district heating. Furthermore, there are five deep borehole heat exchangers (Sapinska-Sliwa et al., 2015) operating in Germany in tight rocks: Arnsberg, (2,835 m, heating a spa); Prenzlau (2,786 m, used for district heating); Heubach (773 m, providing heat for industry); Landau (800 m, for space heating) and Marl (700 m, for local heating).

Table 2.3. Plant characteristics of geothermal projects with direct-use of heat in Germany (from Agemar et al., 2014; Büscher, 2014; Weber et al., 2015; Weber et al., 2019). NGB, North German Basin; SGM, South German Molasse Basin.

Plant	Region	Initial operation	Heat (MW)	Depth (m)	Temp. (ºC)	Gradient (ºC km^{-1})	Flow (L s^{-1})
Aschheim	SMB	2009	10.7	2,630	85	29	75
Erding	SMB	1998	7.7	2,359	62	23	48
Freiham	SMB	2016	13	3,132	90	26	90
Garching	SMB	2012	8	2,226	74	29	100
Holzkirchen	SMB	2017	21	5,100	155	29	55
Ismaning	SMB	2013	7.2	1,906	78	36	85
Kirchweidach	SMB	2013	30.6	3,882	139	34	120
München Riem	SMB	2006	13	2,747	95	31	85
Neustadt-Glewe	NGB	1994	4	2,450	97	36	35
Poing	SMB	2012	10	3,049	76	22	100
Prenzlau	NGB	1994	0.2	2,790	108	36	3
Pullach	SMB	2005	15.5	3,505	104	27	79
Simbach-Braunau	SMB	2001	9	2,000	80	36	80
Straubing	SMB	1996	2.1	824	36	34	50
Unterföhring I	SMB	2009	10	1,986	86	39	75
Unterföhring II	SMB	2015	11.3	2,341	93	36	90
Unterschleißheim	SMB	2003	8	2,000	78	35	93
Waldkraiburg	SMB	2012	14	2,720	106	41	65
Waren	NGB	1984	1.3	1,500	63	34	17

The development of direct-use of heat from geothermal energy is still growing rapidly in Germany. The best example is Munich's vision to completely supply the city's district heating network with renewable energies by 2040, where geothermal energy will act as a major contributor to achieving this goal (Weber et al., 2019).

2.2.2 Netherlands

During the last decade, the development of geothermal resources in the Netherlands has accelerated. In 2007, only one geothermal system was present; by 2018 over 20 had been built. Beginning in 2013 Dutch public opinion turned increasingly against natural gas production due to the increase of earthquakes from hydrofracturing. This, combined with the country's national commitment to a 49% reduction of greenhouse gas emissions by 2030, opened new market opportunities for the geothermal sector (Provoost et al., 2019). The geothermal sector in 2018 published the *Master Plan for Geothermal Energy in the Netherlands*, a collaboration of sectoral partners and government on future developments and ambitions for geothermal energy in the Netherlands. The ambition is for geothermal energy to meet 23% of the total energy demand for heat by 2050 with 700 deep geothermal systems (**Figure 2.3**).

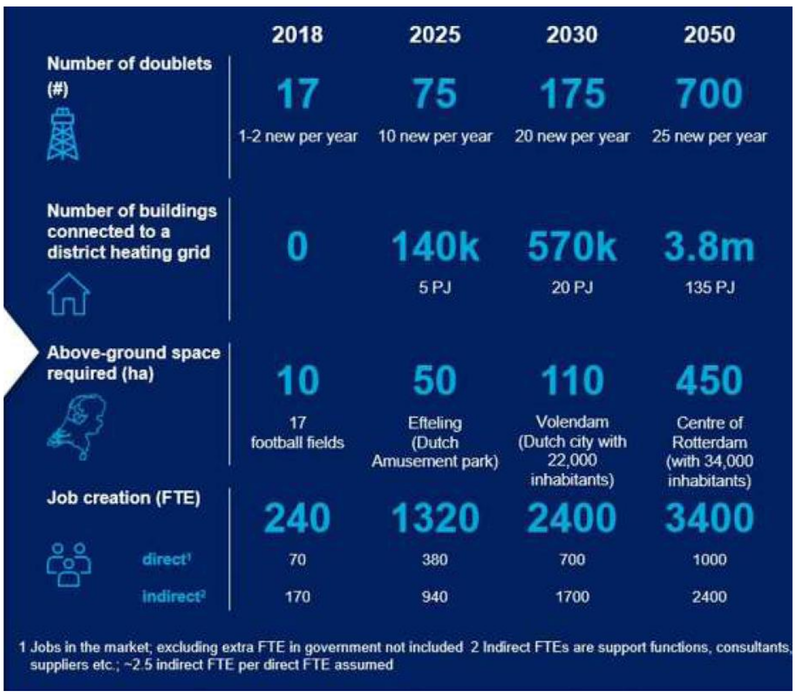

Figure 2.3. Ambitions for geothermal energy as stated in the 'Master Plan geothermal energy in the Netherlands' (from Provoost et al., 2019).

In the Netherlands, the geothermal sources are located in the same reservoirs/aquifers in which the oil and gas accumulations are hosted. These include from youngest to oldest reservoirs in the Cenozoic, Upper Jurassic to Lower Cretaceous, Triassic and late Carboniferous to early Permian (e.g., the Rotliegend Group). The heat is produced from depth intervals between 1,600 and 2,800 metres and from various geological units (**Figure 2.4**), with a total capacity of around 200 MW of sustainable heat (Provoost et al., 2019). For geothermal applications, a permeability of 10 mD is presently thought to be a minimum value for a standard doublet system (Mijnlieff, 2020). Geothermal energy is presently direct-use, mostly for greenhouses and district heating purposes (**Figure 2.4**). Direct use for industrial purposes and possibly conversion to power are expected in future applications. Moreover, some wells coproduced minor quantities of natural gas, which was also used for heating.

In 2019, the *Nederlandse Organisatie voor Toegepast Natuurwetenschappelijk Onderzoek* (TNO or Netherlands Organisation for Applied Scientific Research) an independent research organization that focuses on applied science launched the website www.ThermoGis.nl. This public web-based geographical information system supports companies and the government to develop geothermal energy in the Netherlands. TNO used the abundance of available subsurface data and its broad knowledge of the Dutch subsurface to create ThermoGIS, a tool to evaluate the geothermal plays on a sub-regional scale.

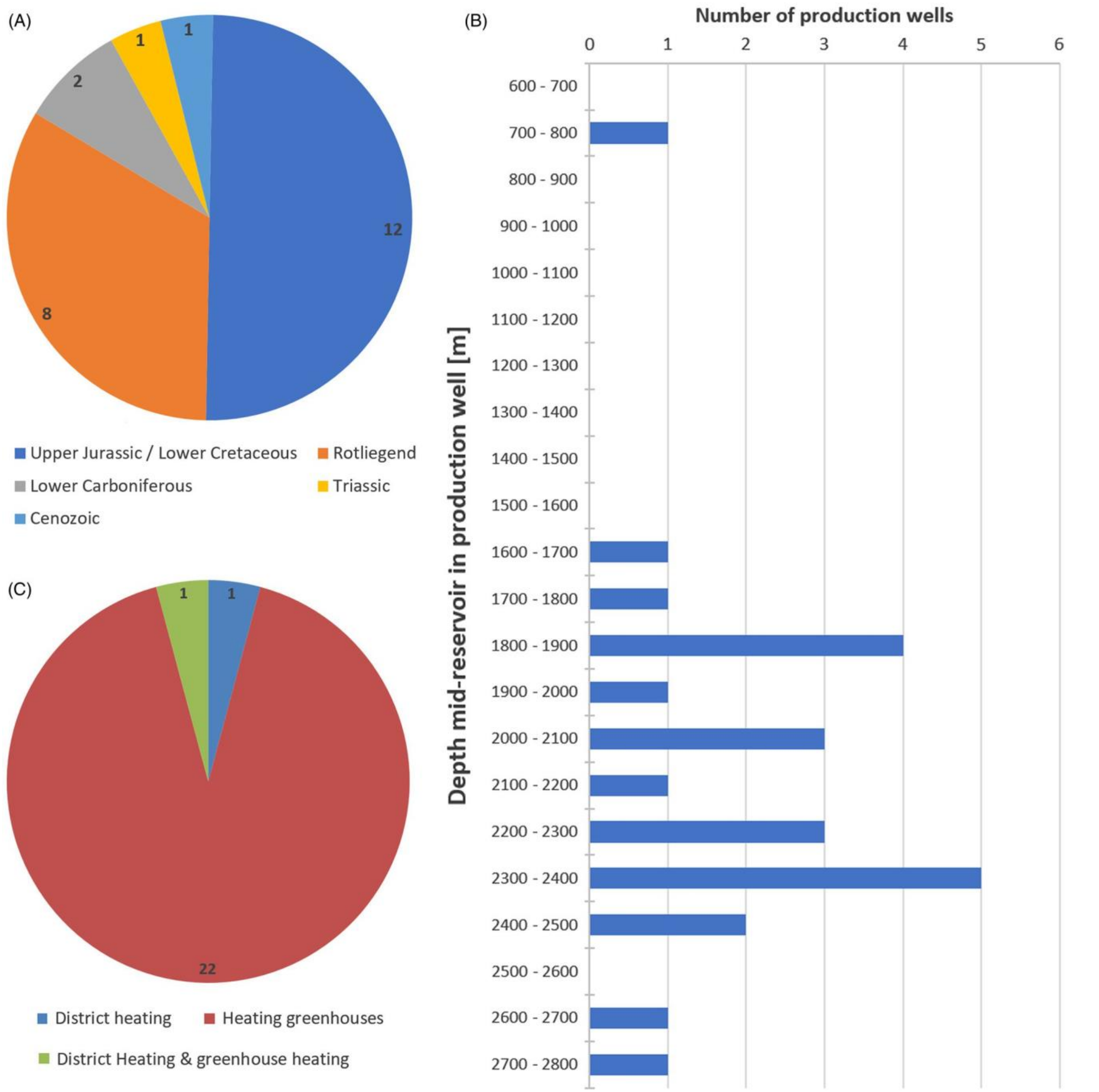

Figure 2.4. Fingerprint of the achieved Dutch geothermal systems: (A) stratigraphy of the productive interval, (B) depth of production wells used for direct-use of heat, (C) uses of the heat produced (MEA, 2018).

2.2.3 Denmark

At present, three geothermal district heating plants are operating in Denmark providing 36 MW of heat, with several more in the planning stage. All the geothermal plants use geothermal heat pumps to optimize heat for district heating. Furthermore, all the geothermal plants use the doublet concept: warm formation water is pumped to the surface from a production well without stimulation of the geothermal reservoir. After heat is extracted and distributed to the district heating system, the cooled water is returned to the reservoir through injection wells (Poulsen et al., 2019).

In Thisted, the production well produces approximately 44 °C warm water from the Gassum Formation at a depth of 1,250 m (geothermal gradient of 30 °C km^{-1}), where the water has a salinity of 15%. The plant produces up to 7 MW of heat from the deep aquifer and transfers 10 MW net of heat to the district heating by heat exchange and through absorption heat pumps driven by biomass boiler. In Sønderborg, the production well produces 48 °C warm water from the Gassum Formation at a depth of 1,200 m (geothermal gradient of 30 °C km^{-1}), where the water has a salinity of 15%. The plant is designed to produce up to 12 MW of heat with the use of geothermal heat pumps driven by biomass. The Margretheholm plant exploits an aquifer in the Lower Triassic Bunter Sandstone Formation at 2,600 m depth, where 19% saline water is produced at approximately 74°C, corresponding to a geothermal gradient of 26 °C km^{-1}. The plant is designed to extract 14 MW of heat and transfer 27 MW of heat to the district heating net by heat exchange and through three absorption heat pumps driven by 14 MW of steam primarily from a wood pellet-based CHP plant (Mathiesen and Røgen, 2020).

2.2.4 France

The direct use of geothermal heat is well developed in France, distributed within the two major sedimentary basins: the Paris Basin (for which Paris is the geographical centre) and the Aquitaine Basin in southwest France. The geothermal resources are found at depths between 600 and 2,000 m. The nature of the existing resources has led France to favour thermal applications of geothermal resources. To this end, 112 deep exploration wells have been drilled or rehabilitated since 1961, 97 of which were brought into operation mainly between 1980 and 1987.

The Paris Basin has five large aquifers, including the most notable Dogger carbonate formation, which has the largest number of low-energy geothermal operations in the world. The Dogger carbonate hosts 40 district geothermal heating plants providing geothermal energy to about 6-7% of the total population of 11 million people (Boissavy et al., 2019). The Dogger covers an area of over 150,000 km^2 with temperatures measured directly below the Paris region varying between 56 °C and 85 °C depending on reservoir depth which ranges from 1,600 and 1,800 m This corresponds to a geothermal gradient between 30 and 40 °C km^{-1}.

2.2.5 United Kingdom

In a worldwide context, the exploitation of geothermal energy in the UK remains small. Only low to moderate temperature fluids have been accessed by drilling in sedimentary basins in the south and northeast of England. Elevated temperature gradients and high heat flows have been measured in and above some granitic intrusions, particularly in southwest England. These granites were previously the site of the *UK Hot Dry Rock Programme* in Cornwall and currently host the *United Downs Deep Geothermal Project* (Curtis et al., 2019).

The city of Southampton remains the only significant user of low enthalpy geothermal energy in the UK (Lund and Toth, 2020). In the 1980s the Department of Energy undertook a research and development program to examine the geothermal potential of UK aquifers. In 1986, an aquifer in the Wessex Basin's Triassic Sandstone containing 76 ºC fluids was drilled to approximately 1,800 m (geothermal gradient of 37 ºC km^{-1}). Construction of a district-heating network began in 1987 in Southampton (100 km southwest of London), and this has since expanded to become a combined heat and power development for 3,000 homes, 10 schools and numerous commercial buildings. At the moment, the total capacity amounts to 2 MW of heat (Curtis et al., 2019). UK geothermal research is largely concentrated on developing the potential of less conventional resources since deep hot sedimentary aquifers are only found in a few regions and often not in regions of high heat demand.

2.3 Enhanced geothermal systems (EGS) and deep Borehole heat exchanger (BHE)

EGS and deep BHE geothermal energy extraction technologies can be used for specific recreational and industrial applications. In many countries, 40 °C geothermal water sources are used to heat recreational pools and residential houses while industrial uses of 40-70 °C water include aquaculture, greenhouse heating, water desalination and district heating (Bai et al., 2010). Although an effective district heating system requires fluid temperatures of a minimum of 40 °C (Lund and Lienau, 1997), lower water temperatures (23 °C) combined with locally installed heat pumps is a viable alternative (Kulcar et al, 2008; Østergaard and Lund, 2011).

The economic viability of EGS and deep BHEs depends on improving and enhancing 'enabling technologies' such as prospecting techniques, drilling technologies and reservoir stimulation technologies as well as energy costs in the region, resource longevity, etc. For example, fracture network stimulation in a sedimentary reservoir requires different procedures compared to a similar stimulation in an igneous reservoir due to differences in fluid migration, pore pressures, and cementation/crystallization (Tester et al., 2006). While the economic viability of EGS remains a research topic, deep BHE designs are based on well-established shallow BHE technologies (Lund and Boyld, 2016). Given its lesser dependence on uncertain fracture networks, the economic viability of deep BHEs depends almost entirely on regional energy prices (Śliwa and Kotyza, 2003). In fact, heat exchanger insulation design/cost may determine deep BHE project feasibility (Śliwa and Kotyza, 2003; Dijkshoorn et al., 2013). **Table 2.4** lists some existing deep BHE projects in Germany (**Section 2.2.1**) and Switzerland. These examples make use of a coaxial tube configuration consisting of two concentric tubes: one carrying fluid down and the other bringing fluid back to surface through the center of the tube. This deep BHE configuration has been proven viable in various locations around Europe (Śliwa et al., 2014).

Table 2.4. Existing deep BHE sites. EWT: Entering water temperature (from Caulk et Tomac, 2017).

Site name	Country	EWT (°C)	Depth (m)	Flow rate (l/s)
Aachen,	Germany	25 - 55	2,500	2.77
Prenzlau	Germany	–	2,786	6
Weissbad	Switzerland	15	1,200	2.9
Weggis	Switzerland	40	2,300	0.8 - 1.75

Closed-loop geothermal systems are gaining attraction as a globally scalable method for producing geothermal energy. Notably, closed-loop systems do not utilize hydraulic fracturing to create subsurface reservoirs and thus avoid many of the regulatory and public relations hurdles that EGS and other geothermal concepts face. Closed-loop systems are also not expected to present the risk of seismicity, a topic that has landed EGS in the news. The concept of closed-loop is broad and encompasses several different methodologies including pipe in pipe GreenLoop configurations pursued by GreenFire Energy (https://www.greenfireenergy.com) and Eavor-Loops drilled by Eavor Technologies (https://eavor.com). No matter the methodology, the broad concepts are the same: 1) the use of oil and gas horizontal drilling technology to design two vertical wells joined by two multilateral legs; 2) the circulation of a fluid through those wells; and 3) the production of electricity or heat with the resulting output.

The Eavor demonstration project is located near Rocky Mountain House (Alberta) and consists of large U- shaped tube wells drilled to depths exceeding 3 kilometres, with several kilometres of multilateral or connecting horizontal wellbores. Two drilling rigs are operated simultaneously from both sites and intersect the multilateral wellbores at depth. (**Figure 2.5**). The rationale for this design, which is not intended to be commercially viable, is to prove and demonstrate the critical elements of Eavor's technologies at the lowest cost possible. This demonstration is designed to achieve the most efficient path to acceptance and commercialization of the technology for project developers and commercial financiers.

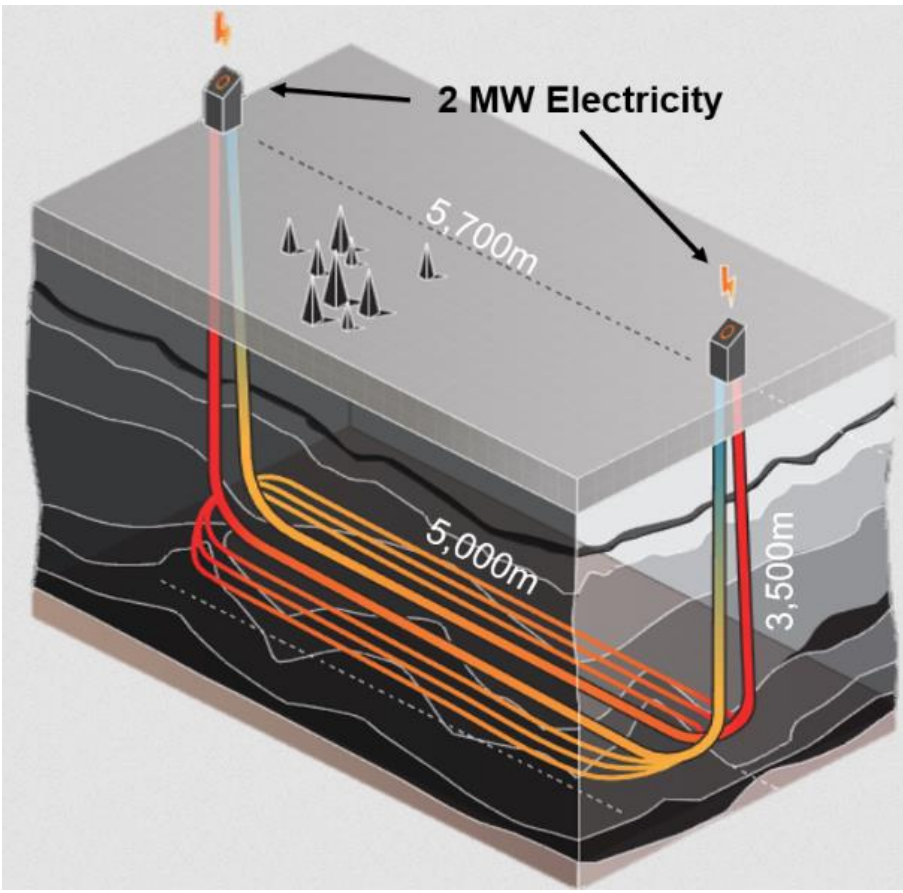

Figure 2.5. Diagram of an Eavor-Loop system (from https://eavor.com). Horizontal multilateral wells are connected at depth creating a network of wells allowing for heat transfer via conduction from the surrounding rock to fluid in the wells. Each surface location is projected to produce 2 MW of electricity or 20 MW thermal energy.

Abandoned oil and gas wells have the potential to contribute to the rising global demand for energy without requiring additional land disturbance that would result from the deep drilling needed for geothermal energy extraction via more traditional methods. Furthermore, Śliwa and Kotyza (2003) concluded that plugging an abandoned oil and gas well may in some cases be more expensive than refurbishing it for thermal extraction. A study performed on the reuse of abandoned oil wells in the Carpathian Mountains (Poland) concluded that the benefits were ubiquitous with the only downside being the challenging optimization of design parameters (Śliwa et al., 2014). Finally, another economic benefit of retrofitting abandoned oil and gas wells is the large number wells available for upscaling BHE extraction capacity to match larger scale EGS operations (Caulk and Tomac, 2017). Although the reuse of abandoned wells removes prospecting and drilling risks, the remaining design and resource assessment factors still require focused research (Caulk and Tomac, 2017). Currently this concept remains at the experimental stage and no operational examples currently exist in the world.

2.3.1 France

In France, and particularly in the Upper Rhine Graben, geothermal development occurred over decades thanks to the expertise developed for EGS, with the European pilot project at Soultz-sous-Forêts. The Soultz geothermal project is a milestone in geothermal development. It is the first time that a deep heat exchanger was created by reactivating pre-existing fractures in a hot granite basement and coupled to a power plant (Koelbel and Genter, 2017).

Starting in 1984, over the next 20 years, the Soultz experimental geothermal site has been explored in detail by a two main phases: 1) a preparatory and compilation phase; 2) drilling, exploration and reservoir development phase. Data on geology, fluid geochemistry, temperature, microseismicity, hydraulics and geomechanics have been collected and interpreted by the various teams from the participating European countries and their international collaborators. Finally, the creation of the deep hot reservoir started in the year 2001. Geology was well known as the region hosts one of the oldest oil fields worldwide. In addition to the existing oil wells, four deep wells were drilled to 4,000 m and 5,000 m (**Figure 2.6**). After successful hydraulic and chemical stimulations from 2001 to 2006, an Organic Rankine Cycle unit was installed, and the power plant commissioned in 2008. The power plant has been operational since 2011, feeding renewable power to the grid. Nevertheless, this is just one milestone enabling further research and demonstration to meet new challenges resulting from operations, e.g., scaling and corrosion, high temperature pump applications, induced micro seismicity monitoring, and to enhance coupled thermal–hydraulic–mechanical–chemical models for better reservoir understanding.

The Soultz site was successfully commissioned in 2016 as an industrial geothermal electricity facility thanks to geothermal fluids at temperatures exceeding 150 °C. Since the geothermal water has a high salinity, the heat is extracted via heat exchangers by a 1.7 MW Organic Rankine Cycle (ORC) unit. The brine is brought at 150°C to the surface and then reinjected into the granite reservoir at 60-70°C through two reinjection wells. The geothermal loop is composed of one production well and two reinjection wells. All three wells are 5 km deep and are cased to roughly 4.5 km in the granitic section. Induced seismicity monitoring of this site is performed on a continuous basis through a network of seismological stations installed on the surface (Maurer et al., 2017). The seismic events induced by reservoir stimulation and system operation are reportedly below the level that can be felt by the local population. For both 2017 and 2018, the geothermal Soultz-sous-Forêts plant operated 90% of the time, with regular weeks of planned maintenance stop.

In 2015, the organization GEODEEP was founded. Its membership includes large companies with expertise in research and development, project development, power plant equipment and operation and maintenance engineering. Its primary objective is mitigation of the risks inherent in geothermal exploration on the French mainland as perceived by investors, developers, and insurers.

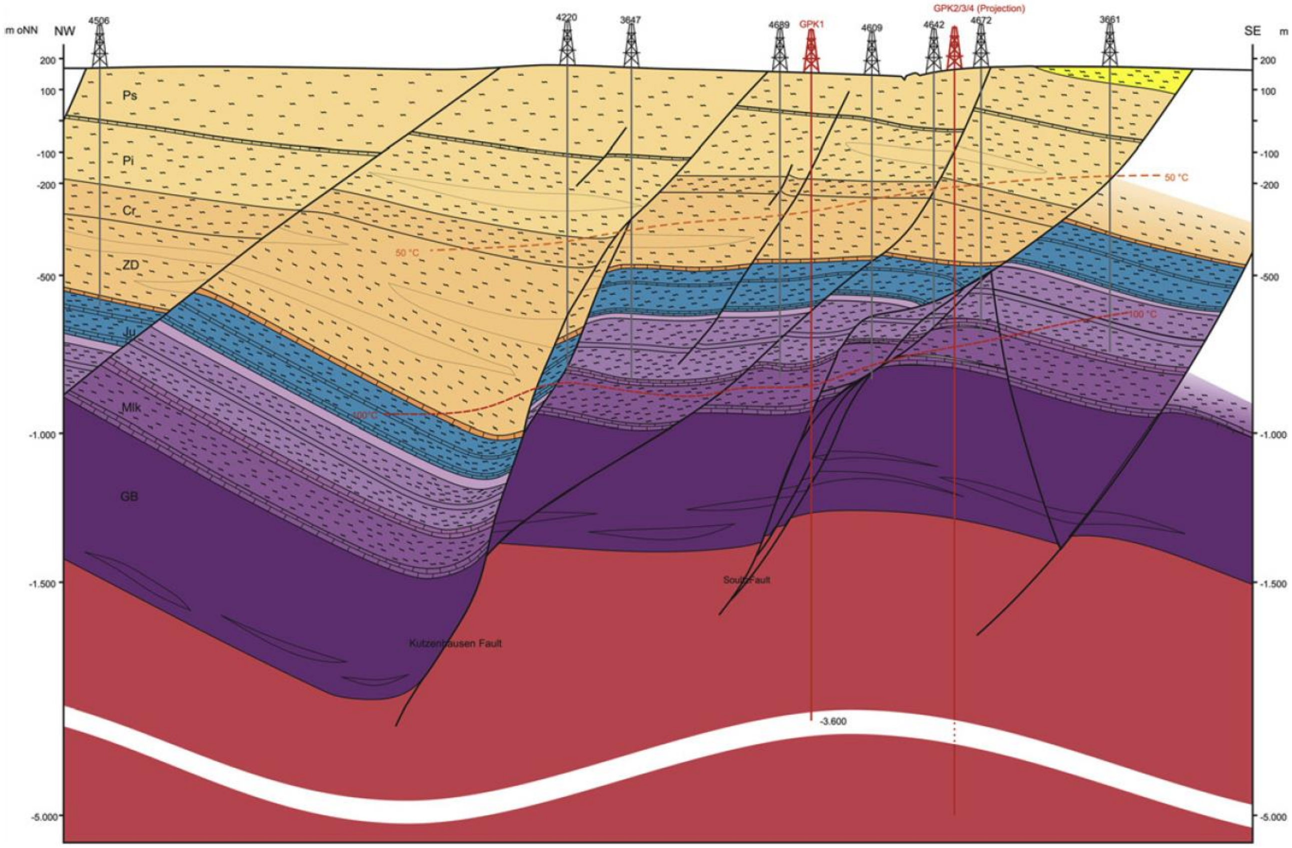

Figure 2.6. Geological cross-section at the Soultz geothermal project (from Vidal et al., 2015). Numerous large-scale crustal faults originate in the basement granite (in red pattern) and cross the overlaying sedimentary cover (in a purple, blue and yellow pattern). Vintage oil wells are shown in black and the geothermal boreholes in red.

2.3.2 Québec (Canada)

The development of deep stimulated geothermal energy (Enhanced Geothermal System, EGS) makes it possible to consider developing geothermal energy in environments that do not naturally have the elements required for conventional hydrothermal geothermal energy such as sufficient heat, fluids and a permeable geological formation. With typical average gradients of less than 30 °C km^{-1}, the development of traditional geothermal resources in north-eastern North America is a challenge.

With this in mind, the Hydro-Québec's research institute (IREQ; Richard, 2006) developed a simulation tool for stimulated deep geothermal systems as part of a 3-year research project on the integration of deep geothermal energy in the Canadian energy portfolio. The simulation tool estimates the potential performance of an EGS system in Québec (without targeting a specific site) to better understand the impact of this technology as it evolves and to identify future research opportunities.

The results of Hydro-Québec’s simulation tool suggest the following:

- The formations considered most likely to serve as geothermal reservoirs for generating electricity in Québec are the deepest geological units of the St. Lawrence Lowlands sedimentary basin and the underlying Precambrian granitic basement (Canadian Shield).
- With a gradient limited to 25 °C km^{-1}, as found in southern Québec, it is possible to generate a power of a few megawatts with attractive potential costs from reservoirs with temperatures of

about 175 °C, which implies depths of 7,000 m or more. Although geothermal drilling has so far been limited to about 5,000 m, wells exceeding 9,000 m are being drilled for hydrocarbon production.

- The temperatures initially targeted in the project, i.e. 85 to 150 °C, do not provide sufficient performance for commercial power generation in the short to medium term. This temperature range corresponds to a depth on the order of 3,500 to 6,000 m, respectively.
- Considering these depths and low permeability geological units, only stimulation techniques and EGS can generate sufficient permeability by a high number of thermally active main fractures, which in turn greatly affects the performance of the system.
- Given the low thermal-to- electrical conversion efficiency intrinsic to the exploitation of a low-temperature resource, the production of heat alone or in combination with electricity is an attractive alternative if there is a nearby market for heat.
- The research concludes that an experimental EGS project in Québec should focus on the demonstration and development of advanced methods for creating artificial geothermal reservoirs in a site that is highly representative of the targeted geological environment in Québec. To be profitable development of the resource must be adapted to the geothermal gradients, the type of fracture network and the surface temperature of Québec.

2.4 Heating and cooling from abandoned mines

2.4.1 Germany

The geothermal system installed at Castle Freudenstein at Freiberg supplies the base requirements of the infrastructure while a conventional system accommodates peak load and air conditioning requirements. The low-enthalpy heat is harnessed from the water flowing in the *Alter Tiefer Fürstenstollen* gallery which is located at a depth of 60 m. Mine water at a constant 10.2 ºC is accumulated in this gallery using a dam (Kranz and Dillenardt, 2010). Two submersible rotary pumps with a combined capacity of 21.6 m^3/h raise the water to a height of 50 m to the shaft head where a heat exchanger is placed, and then the water is returned to the gallery. The heat exchanger captures the heat and transfers it to a secondary loop (ΔT of 5 ºC), which at the same time transfers the heat to a heat pump located 230 m away in a building behind the castle. The heat pump has a maximum heat capacity of 130 kW.

2.4.2 Netherlands

The full-scale Mine Water Project in Heerlen is one of the world's largest district geothermal heating systems sourced by mine water. The project evolved in stages: Mine Water 1.0 running from 2003 to 2008 used a pilot system to determine how the low-enthalpy heat stored in the flooding water of the abandoned Oranje Nassau mine could be harnessed for building heating and air-conditioning (Verhoeven et al., 2014). In 2014, the Mine Water project was upgraded to a smart grid for heating and cooling with a full-scale hybrid sustainable energy structure called Mine Water 2.0. By 2015 a total of 500,000 m^2 of floor space was heated by mine water.

For the assessment of the pilot project, detailed studies (geological, mechanical, hydraulic, thermal and chemical) and pumping tests were carried out. Study and test results along with historical maps were used as inputs to numerical simulations which aided the pilot project design. Based on the chemical analysis of the water titanium was used in the heat exchanger and high-grade polypropylene for the piping system. The pilot project is an open-loop configuration, which extracts the warm mine water at a temperature of 28 ºC through two wells from a depth of about 700 m. In addition, cold water (16 ºC) was supplied from a depth of 250 m using two wells. Each working well has a submersible pump located at a depth of 130 m to avoid thermal losses. Every building has its own energy station consisting of a titanium heat exchanger, heat pumps, and gas-fired high-efficiency boilers. After leaving the energy stations, the mine water is reinjected into the abandoned mine at a depth of 350 m.

2.4.3 Norway

A mine water heat pump system was installed in 1998 at the *Folldal Gamle Gruver* mining museum, located in Folldal. The flooded mine water has a temperature of 6 ºC. The heat of the mine water was harnessed through a closed-loop system to heat the Wormshall chamber, which is 125 m underground. This configuration was selected because the mine water is heavily polluted with sulphides. A mixture of water and anti-freezing agent was circulated in the loop to capture the heat of the mine water and transport it to a water-air heat pump system (Peralta Ramos et al., 2015). The heat pump provided a temperature of 22 ºC and a heat capacity of 18 kW.

2.4.4 Nova Scotia (Canada)

Over 200 years of subsurface coal mining in Nova Scotia has left many square kilometers of abandoned mines, often located directly beneath the towns that grew to support the past mining industry (Zaradic, 2018) This is the case of Springhill, which was the original world leader in the use of groundwater from flooded workings to heat and cool buildings (Jessop et al., 1995). The town is famed for having some of the deepest coal mines in North America, with depths reaching 1,323 m. The first application of mine water geothermal was made in 1989 at Ropak Can-Am Plastics. Two wells were drilled into the mines, one to a depth of 140 metres from which water was extracted at a year-round temperature of 18˚C and a second, shallower well into which water was returned at 13˚C (with heat pumps operating in heating mode) or 23˚C (when operating in cooling mode). Today, there are multiple users (i.e. school and manufacturers) of geothermal energy in Springhill, with many users satisfied with the benefits of their geothermal systems used for both heating and cooling purposes (Grasby et al., 2012). The most detailed estimate of the volume of water in the workings (No. 2 Seam) are about 6 millions m^3 (MacAskill and Power, 2015). There is still significant opportunity for taking further advantage of the geothermal resource. An engineering team found that using the mine water for free cooling process could result in an additional savings of over 1,000 MWh/year (EfficiencyOne, 2017).

2.4.5 Québec (Canada)

In addition to the mine water district heating project in Springhill (Nova Scotia), an open-loop system that utilizes mine water from the Goyer Quarry in Québec has been constructed. The Goyer Quarry has a total flooded volume of 8,064,000 m^3 and is used to supply heating and cooling to 6 apartment buildings (36 units each) using geothermal heat pumps. The project is designed as a decentralized system, with heat pumps located at each customer site. The installed heat pumps have capacities in the range of 3.6-5.3 kW (Raymond et al., 2008).

2.4.6 Spain

In the city of Asturias, a geothermal system was successfully implemented for two buildings (a research centre and a residence) on the campus of the University of Oviedo and for the new *Álvarez Buylla* hospital. The heat source, which is a nearby abandoned coal mine is estimated to contain about 5.8 million m^3 of water. Water temperature ranges from 17 to 23 ºC and is used for both heating and cooling (Jardón et al., 2013). The shaft which is used to extract the mine water is close to the university buildings, some 250 m away. The mine water is used to warm clean water circulating in a closed-loop. Afterwards, the clean water enters the heat pumps at 14 ºC, where it is cooled to 7 ºC as the heat is extracted. Total annual energy savings are estimated at 73% (1,112,050 kWh/year) with a 39% annual reduction of CO_2 emissions and monetary savings of 15% for the student residence and up to 20% for the research facility.

For the system at the hospital, an open-loop configuration was installed to capture the temperature of the mine water. The fluid is pumped to the surface at a rate of 400 m^3/h. In heating mode, the mine water temperature decreases from 23 ºC to 13.9 ºC during its passage through the heat exchanger before it is discharged to waste. Using the heat exchanger, clean water which is transported to the end-user about 2 km away is warmed from 12 ºC to 19 ºC.

2.4.7 United Kingdom

The Shettleston Colliery (Glasgow, Scotland) produced coal from 1872 until its abandonment in 1923. Since 1999 a geothermal space heating project has operated using mine water from the abandoned coal mines. The mine water with a temperature of 12 ºC is extracted at a depth of 100 m using a well specifically drilled for this purpose. Heat pumps use the mine water to increase the temperature of water that is collected in tanks to store the heat. Meanwhile, the mine water temperature is reduced to 3 ºC and returned to the abandoned mine via a re-injection well. A total of 16 houses are supplied with heat from this system. Annual savings of 80% on heating costs have been estimated (Watzlaf and Ackman, 2006).

2.4.8 USA

Mine water has been used for heating and air-conditioning the municipal building in Park Hills, Missouri since 1995. The source is the flood water from abandoned mines located 10 to 133 m underneath the town, which have approximately 265 million m^3 of water at a constant temperature of 13.9 ºC (Peralta Ramos et al., 2015). An open-loop configuration was installed to extract mine water from a 122 m deep well by means of a 17 m^3/h submersible pump. At the surface, a plate and frame heat exchanger transfers heat from the mine water to clean water, which circulates in a closed-loop. The mine water is then returned via a second 122 m deep well. The closed-loop transports the heat to nine water-to-air heat pumps which are located directly in the rooms. The heat pump system generates a combined capacity of 112.5 kW.

2.4.9 Summary

The important reservoir parameters (temperature and volume) for the different geothermal systems using abandoned mines described above is summarized on **Table 2.5**. The variation of these parameters highlights that the implementation of a system is generally possible irrespective of reservoir size. For instance, the water temperature in the reservoir shows that different systems can be designed to exploit a wide range of the mine water temperatures, ranging from as low as 6 ºC in the case of Folldal (Norway) to a maximum of 32 ºC in Heerlen (Netherlands). The reservoir capacity is based on temperature and volume which in turn defines the heating requirements the reservoir can fulfil.

Table 2.5. Reservoir properties and end-users of the selected operational geothermal systems installed in abandoned mines. [a] Information available only for the plastic transformation factory; [b] Corresponding to the estimated potential and not the energy extracted by users, due to a lack of operational data.

Country	Projects location	End-user	Volume (million m^3)	Temp, (°C)	Heating area (m^2)	Heating capacity (kW)
Canada	Nova Scotia (Springhill)	Plastic transformation factory School and manufacturers	6	18	16,700[a]	8,000[b]
	Québec	Apartment buildings	8	8	6,039	3.6 – 5.3
Germany	Freiberg	Castle and mineralogical museum	495	10.2		130
Netherlands	Heerlen	Offices buildings and university	10 – 11	27 - 32	500,000	
Norway	Folldal	Wormshall (Cavern)		6	1,599	18
Spain	Asturias	Research centre and student residence	6	17 - 23	57,393	1,000
		Hospital				3,600
UK	Shettleston	Building (16 houses)		12	28,000	
USA	Park Hills	Municipal building	265	13,9	753	113

The size and type of the end users also differ (**Table 2.5**). The extent of the heated area also varies considerably across the projects, from single buildings to urban areas of over 125,000 m^2. Moreover, as the end users are also located in different physical environments and so have different heating and cooling requirements, so the system needs to be designed specifically for each location. In all the cases, the source and end user are closely linked together; a heat pump system needs to be designed such that it can supply the end user requirements while maintaining a sustainable geothermal system over the long term. Most of the systems presented here use floor heating for heat distribution, which is the most effective way of distributing heat, especially for low enthalpy sources. In some cases, water-to-air heat pumps are used to provide the required air conditioning.

2.5 References

Agemar, T., Weber, J., Schulz, R., 2014. Deep Geothermal Energy Production in Germany. Energies 7(7):4397-4416. https://doi.org/10.3390/en7074397

Arkay, K., 2000. Geothermal energy from abandoned mines: A methodology for an inventory, and inventory data for abandoned mines in Québec and Nova Scotia. Geological Survey of Canada, Open file report 3825, 45 pp. https://doi.org/10.4095/211648

Bai, F., Akbarzadeh, A., Singh, R., 2010. Combined freshwater production and power generation from geothermal reservoirs. Proceedings World Geothermal Congress, Bali, Indonesia, 25-29 April 2010, 6 p.

Boissavy, C., Henry, L., Genter, A., Pomart, A., Rocher, P., Schmidlé-Bloch, V., 2019. Geothermal Energy Use, Country Update for France. European Geothermal Congress 2019. Den Haag, The Netherlands, 11-14 June 2019, 18 p.

Büscher, E., 2014. Development of Geothermal District Heating in Germany. Geothernal Research Council Transactions 38, 4 p.

Caulk, R. and Tomac, I., 2017. Reuse of abandoned oil and gas wells for geothermal energy production. Renewable Energy 112:388-397. https://doi.org/10.1016/j.renene.2017.05.042

Curtis, R., Busby, J., Law, R., Adams, C., 2019. Geothermal Energy Use, Country Update for United Kingdom. European Geothermal Congress 2019 Den Haag, The Netherlands, 11-14 June 2019, 7 p.

Deep Earth Energy Production Corp., 2020. https://deepcorp.ca

Dijkshoorn, L, Speer, S., Pechnig, R., 2013. Measurements and design calculations for a deep coaxial borehole heat exchanger in Aachen. Germany. International Journal of Geophysics 2013: 16541. https://doi.org/10.1155/2013/916541

EfficiencyOne, 2017. Springhill Geothermal Energy Use Study. Prepared for Cumberland Energy Authority. 61 p.

Eyerer, S., Schifflechnera, C., Hofbauer, S.,Bauer, W., Wielanda, c.,Spliethoff, H., 2020. Combined heat and power from hydrothermal geothermal resources in Germany: An assessment of the potential. Renewable and Sustainable Energy Reviews 120:109661. https://doi.org/10.1016/j.rser.2019.109661

Goldbrunner, J., Goetzl, G., 2019. Geothermal Energy Use, Country Update for Austria. European Geothermal Congress 2019 Den Haag, The Netherlands, 11-14 June 2019, 10 p.

Grasby, S.E., Allen, D.M., Bell, S., Chen, Z., Ferguson, G., Jessop, A., Kelman, M., Ko, M., Majorowicz, J., Moore, M., Raymond, J., and Therrien, R., 2012. Geothermal Energy Resource Potential of Canada. Geological Survey of Canada, Open File 6914, 322 p. https://doi.org/10.4095/291488

Hurter, S. and Haenel, R. 2002. Atlas of Geothermal Resources in Europe. Office for Official Publications of the European Communities, Luxemburg.

Huttrer, G., 2020. Geothermal Power Generation in the World 2015-2020 Update Report. Proceedings World Geothermal Congress 2020 Reykjavik, Iceland, April 26-May 2, 2020, 17 p.

Jardón, S., Ordóñez, A., Álvarez, R., Cienfuegos, P., Loredo, J., 2013. Mine water for energy and water supply in the Central Basin of Asturias (Spain). Mine Water and the Environment volume 32:139–151. https://doi.org/10.1007/s10230-013-0224-x

Jessop, A.M., MacDonald, J.K. and Spence, H., 1995, Clean energy from abandoned mines at Springhill, Nova Scotia: Energy Sources 17:93-106. https://doi.org/10.1080/00908319508946072

Koelbel, T., Genter, A., 2017. Enhanced Geothermal Systems: The Soultz-sous-Forêts Project. In: Uyar T. (eds) Towards 100% Renewable Energy. Springer Proceedings in Energy. Springer, Cham: 243-248. https://doi.org/10.1007/978-3-319-45659-1_25

Kranz, K. and Dillenardt, J., 2010. Mine water utilization for geothermal purpose in Freiberg, Germany: determination of hydrological and thermophysical rock parameters. Mine Water and the Environment 29(1):68–76. https://doi.org/10.1007/s10230-009-0094-4

Kulcar, B., Goricanec, D., Krope, J. 2008. Economy of exploiting heat from low temperature geothermal sources using a heat pump. Energy and Buildings 40(3):323-329. https://doi.org/10.1016/j.enbuild.2007.02.033

Lund, J.W. and Lienau, P.J., 1997. Geothermal district heating. Proceedings of International Course on Geothermal District Heating Schemes, Çeşme, Izmir, Turkey, 19-25 October, 1-27.

Lund, J.W. and Boyd, T.L., 2016. Direct utilization of geothermal energy 2015 worldwide review. Geothermics 60: 66-93. http://dx.doi.org/10.1016/j.geothermics.2015.11.004

Lund, J.W. and Toth, A.N., 2020. Direct Utilization of Geothermal Energy 2020 Worldwide Review. Proceedings World Geothermal Congress 2020 Reykjavik, Iceland, April 26 – May 2, 2020, 39 p.

MacAskill, D. and Power, C., 2015. Researching the Geothermal Potential of the Former Springhill Mine. Report to Cumberland energy Authority. Verschuren Centre for Sustainability in Energy and the Environment, Cape Breton University, 24 p.

Mathiesen, A., Nielsen, L. H., Vosgerau, H., Poulsen, S. E., Bjørn, H., Røgen, B., Ditlefsen, C., Vangkilde-Pedersen, T.: Geothermal Energy Use, Country Update Report for Denmark. Proceedings, World Geothermal Congress 2020, Reykjavik, Iceland, (2020), 14 p.

Mijnlieff, HF., 2020. Introduction to the geothermal play and reservoir geology of the Netherlands. Netherlands Journal of Geosciences 99(e). https://doi.org/10.1017/njg.2020.2
Ministry of Economic Affairs and Climate Policy (MEA). Directorate-General Energy, Telecommunications and Competition, 2018. Natural resources and geothermal energy in the Netherlands, 2017. Annual review. An overview of exploration, production and underground storage. MEA (The Hague), 139 p.
Moeck, I.S., 2014. Catalog of geothermal play types based on geologic controls. Renewable and Sustainable Energy Reviews 37:867-882 https://doi.org/10.1016/j.rser.2014.05.032
United Nations Framework Classification for Resources (UNFC), 2017. Application of UNFC to Geothermal Energy Resources - Selected Case Studies. ECE Energy Series 51, 96 p. https://shorturl.at/dlHR2
Østergaard, P.A. and Lund, H., 2011. A renewable energy system in Frederikshavn using low-temperature geothermal energy for district heating, Applied Energy 88(2):479-487. https://doi.org/10.1016/j.apenergy.2010.03.018
Palmer-Wilson, K., Banks, J., Walsh, W., Robertson, B., 2018. Sedimentary basin geothermal favorability mapping and power generation assessments. Renewable Energy 127:1087-1000. https://doi.org/10.1016/j.renene.2018.04.078
Peralta Ramos, E., Breede, K and Falcone, G., 2015. Geothermal heat recovery from abandoned mines: a systematic review of projects implemented worldwide and a methodology for screening new projects. Environmental Earth Sciences 73(11):6783–6795. https://doi.org/10.1007/s12665-015-4285-y
Poulsen, S.E., Bjørn, H., Mathiesen, A., Nielsen, L.H., Vosgerau, H., Vangkilde-Pedersen, T., Ditlefsen, C., Røgen, B., 2019. Geothermal Energy Use, Country Update for Denmark. European Geothermal Congress 2019Den Haag, The Netherlands, 11-14 June 2019, 9 p.
Pribnow, D. and Schellschmidt, R, 2000. Thermal tracking of upper crustal fluid flow in the Rhine graben. Geophysical Research Letters 27(13):1957-1960. https://doi.org/10.1029/2000GL008494
Provoost, M., Albeda, L., Godschalk, B., van der Werff, B., Schoof, F., 2019. Geothermal Energy Use, Country Update for The Netherlands. European Geothermal Congress 2019 Den Haag, The Netherlands, 11-14 June 2019, 8 p.
Raymond, J., Therrien, R., Hassani, F., 2008. Overview of Geothermal Energy Resources in Québec (Canada) Mining Environments. International Mine Water Association. 12 p.
Richard, M.A., 2016. Production d'électricité avec des systèmes géothermiques stimulés au Québec : analyse des résultats d'un outil de simulation. IREQ-2016-0001, 164 p.
Śliwa, T. and Kotyza J., 2003. Application of existing wells as ground heat source for heat pumps in Poland. Appl. Energy 74(1-2):3-8. https://doi.org/10.1016/S0306-2619(02)00125-3
Śliwa, T., Rosen, M.A., Jezuit, Z., 2014. Use of oil boreholes in the carpathians in geoenergetic systems: historical and conceptual review. Research Journal of Environmental Sciences 8(5):231-242. https://doi.org/10.3923/rjes.2014.231.242
Verhoeven, R., Willems, E., Harcouët-Menou, V., De Boever, E., Hiddes, L., Op't Veld, P., Demaollin, E., 2014. Minewater 2.0 Project in Heerlen the Netherlands: Transformation of a Geothermal Mine Water Pilot Project into a Full Scale Hybrid Sustainable Energy Infrastructure for Heating and Cooling. Energy Procedia 46:58-67. https://doi.org/10.1016/j.egypro.2014.01.158
Vidal, J., Genter, A., Schmittbuhl, J., 2015. How do permeable fractures in the Triassic sediments of Northern Alsace characterize the top of hydrothermal convective cells? Evidence from Soultz geothermal boreholes (France). Geothermal Energy 3:8. https://doi.org/10.1186/s40517-015-0026-4

Villemin, T., Alvarez, F., Angelier, J., 1986. The Rhinegraben: Extension, subsidence and shoulder uplift. Tectonophysics 128(1-2):47-59. https://doi.org/10.1016/0040-1951(86)90307-0

Watzlaf, G., Ackman, T., 2006. Underground mine water for heating and cooling using geothermal heat pump systems. Mine Water and the Environment 25:1-14. https://doi.org/10.1007/s10230-006-0103-9

Weber, J., Ganz, B., Schellschmidt, R., Sanner, B., Schulz, R., 2015. Geothermal Energy Use in Germany. Proceedings World Geothermal Congress 2015 Melbourne, Australia, 19-25 April 2015, 15 p.

Weber, J., Born, H., Moeck, I., 2019. Geothermal Energy Use, Country Update for Germany 2016 – 2018. European Geothermal Congress 2019, Den Haag, The Netherlands, 11-14 June 2019, 16 p.Zaradic, A., 2018. Direct Use Geothermal Projects State of the Nation in Canada 2018. GRC Transactions, Vol. 42, 15 p.

3. GEOLOGY OVERVIEW OF NOVA SCOTIA

This section summarizes the main geological features of onshore Nova Scotia to contextualize the geothermal evaluation. Additional geological information on the topics presented here can be found in the Decade of North American Geology (Barr et al., 1995; Erdmer and Williams, 1995; Gibling, 1995; Keppie et al., 1995; Schenk, 1995; Williams, 1995).

3.1 General setting

Two contrasted zones are recognized onshore Nova Scotia across the Cobequid-Chedabucto Fault (**Figure 3.1**). This ca 300 km-long strike-slip fault system separates the Cambro-Ordovician Meguma terrane to the south (then part of Gondwana) from the Pre-Cambrian to Early Carboniferous Avalon Zone to the north (then part of Laurasia). Deformation along this fault zone stopped some 40 My ago and lasted more than 400 My. Devonian magmatic intrusives are essentially present within the Meguma terrane but are also locally recognized in the Avalon zone. A sedimentary cover, Carboniferous to Triassic in age, overlies both zones.

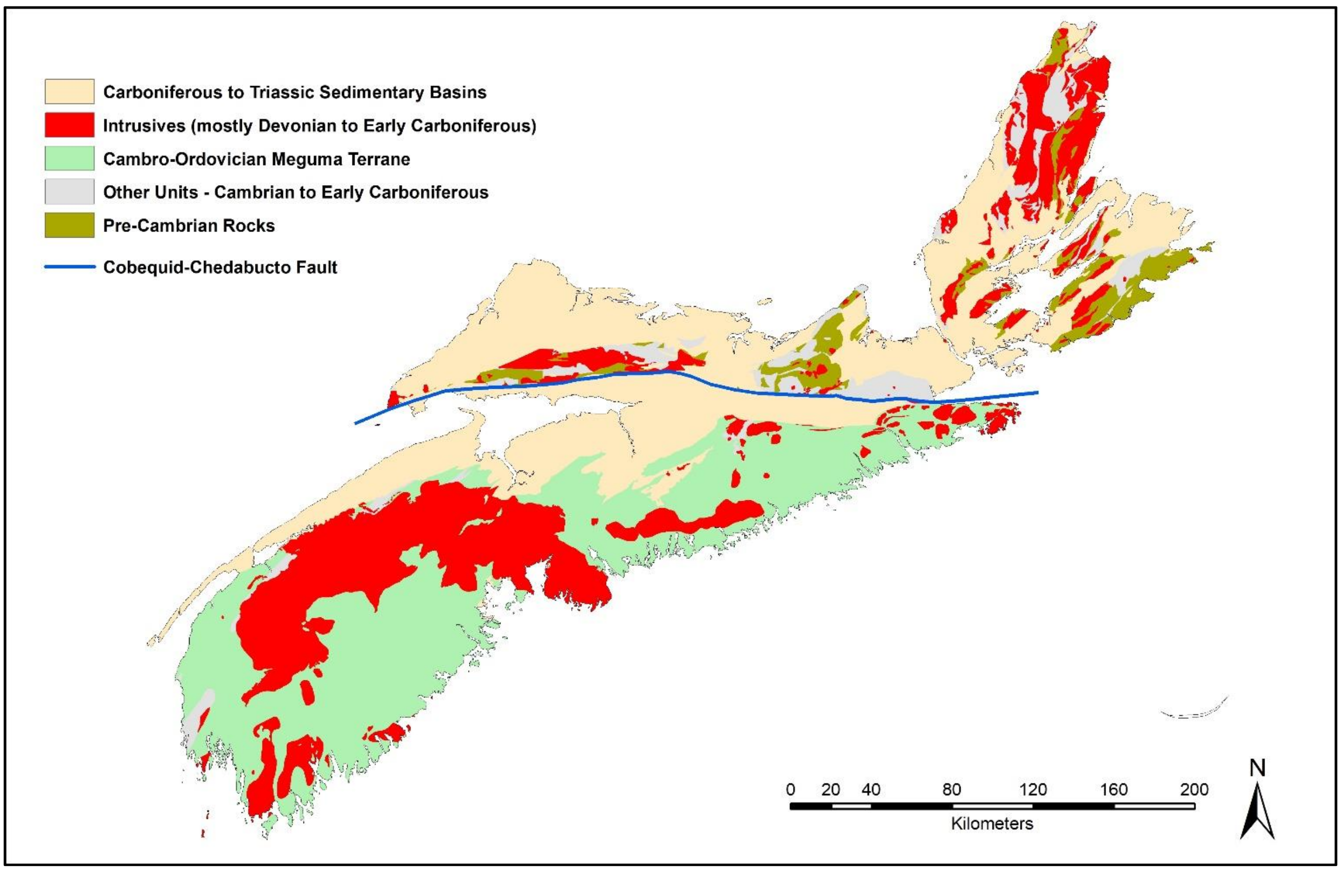

Figure 3.1. Main geological assemblages of onshore Nova Scotia. Cartographic background: NSDNR (2006).

3.2 Avalon Zone

The Avalon Zone outcrops north of the Cobequid-Chedabucto Fault in the Cobequid Highlands, the Pictou-Antigonish Highlands and in Cape Breton, where it is the most exposed. It is comprised of four assemblages of distinct affinities and characteristics. From north to south:

- The Blair River Complex is made of quartzo-feldspathic and amphibolitic gneisses with ancillary amounts of calcareous rocks, intruded by magmatic rocks. This one billion-year-old rock have an affinity with the Canadian Shield and the complex is correlated with the Humber Zone in Newfoundland.
- The Aspy terrane (metamorphosed volcanic and sedimentary rocks of Ordovician to Silurian age) and the Bras d'Or terrane (sedimentary and volcanic rocks with a low metamorphic grade, intruded by Early Cambrian magmatic rocks) are regionally correlated with the Gander and Exploits zones in Newfoundland.
- Finally, the Mira terrane in southern Cape Breton Island is dominated by Late Precambrian volcanics and magmatic intrusions, overlain by sandstones and conglomerates and followed by Cambrian shales and siltstones. The sedimentary record extends until the Devonian and is interspersed with Late Ordovician to Silurian volcanics. This terrane is correlated with the Avalon Zone (or the Avalon terrane) in Newfoundland.

3.3 Meguma terrane

The Meguma terrane has been thrust over a southern extension of the Avalon Zone and is located south of the Cobequid-Chedabucto Fault, but extends offshore underneath the Grand Banks of Newfoundland. The terrane is essentially comprised of metamorphosed, fine-grained sandstones and shales (slates). Ancillary volcaniclastics, conglomerates and carbonates are also locally abundant. The sandstones of the basal Meguma Supergoup have a higher mudstone content than in the overlying Annapolis Supergroup. The age of the base of the Meguma Supergoup is obscured by granitic intrusions but the earliest fossils recorded are Middle Cambrian in age. The top of the Annapolis Supergroup corresponds to the Acadian unconformity (Early Devonian).

3.4 Devonian intrusives

Late Devonian to Early Carboniferous granitoids intruded extensive parts of the Meguma rocks, along with smaller areas north of the Cobequid-Chedabucto Fault. The South Mountain Batholith alone occupies about one half of the southern part of the province. Dominant lithologies include granodiorites, monzogranites and granites. Lesser amounts of pre-Devonian magmatic rocks are documented north of the Cobequid-Chedabucto Fault, in the Avalon Zone.

3.5 Maritimes Basin

After the end of the Acadian Orogeny (Late Devonian), sediments accumulated in depressions and fault-bounded compartments individualizing sub-basins throughout the Carboniferous. These sub-basins are part of a larger, composite basin, the Maritimes Basin, which extends over parts of Nova Scotia, New Brunswick and Newfoundland, covers the entire Prince Edward Island and stretches up the offshore Labrador and the Grand Banks. A tectonostratigraphic synthesis of this basin is illustrated on **Figure 3.2**.

The earliest phase of the formation of the Maritimes Basin took place at the end of the Acadian Orogeny and is characterised by volcanic rocks. Rocks of the Early Carboniferous in Nova Scotia can be divided into three groups (**Figure 3.3**). The basal Horton Group is made of clastic rocks (conglomerates, sandstones and shales). It corresponds to flood-plain, river and lacustrine depositional environments. The overlying Windsor Group is dominated by salt deposits (although absent in the Stellarton Basin), limestones and mudstones, resulting from a regional-scale marine invasion in a restricted, evaporitic environment. Finally, the Mabou Group is essentially made of mudstones, sandstones and incipient amounts of limestones, with some evaporites at the base. It corresponds to a river and lacustrine depositional environment. Two main groups characterize the Late Carboniferous assemblages (**Figure 3.3**), namely the Cumberland Group (formerly referred to as the Morien Group in the Sydney Basin) and the overlying Pictou Group. Both are dominated by sandstones and thick coal seams. In spite of a relatively consistent stratigraphic framework for the Maritimes Basin across onshore Nova Scotia, local lithostratigraphic and biostratigraphic differences exist due to the development of partially connected depocenters and unconformities or disconformities. This led to the recognition of several basins or sub-basins (**Figure 3.4**). For practical purposes, they are all referred to as "basins" in the present document. Detailed stratigraphy of each basin or sub-basin can be found in Waldron et al. (2017).

3.6 Fundy Basin

The Permian period marks a phase of uplifting and erosion, followed by a period of extension and the formation of half-grabens during the Middle Triassic. These depressions were then filled by sediments until the Middle Jurassic. The architecture of the Fundy Basin is thus made of three half-grabens filled with up to 12,000 m of sediments. The Fundy Group comprises volcanics, sandstones, mudstones and shales and is part of the Newark Supergroup that extents to the Gulf of Mexico. Depositional environments correspond to lacustrine, playas, braided plains and alluvial fans.

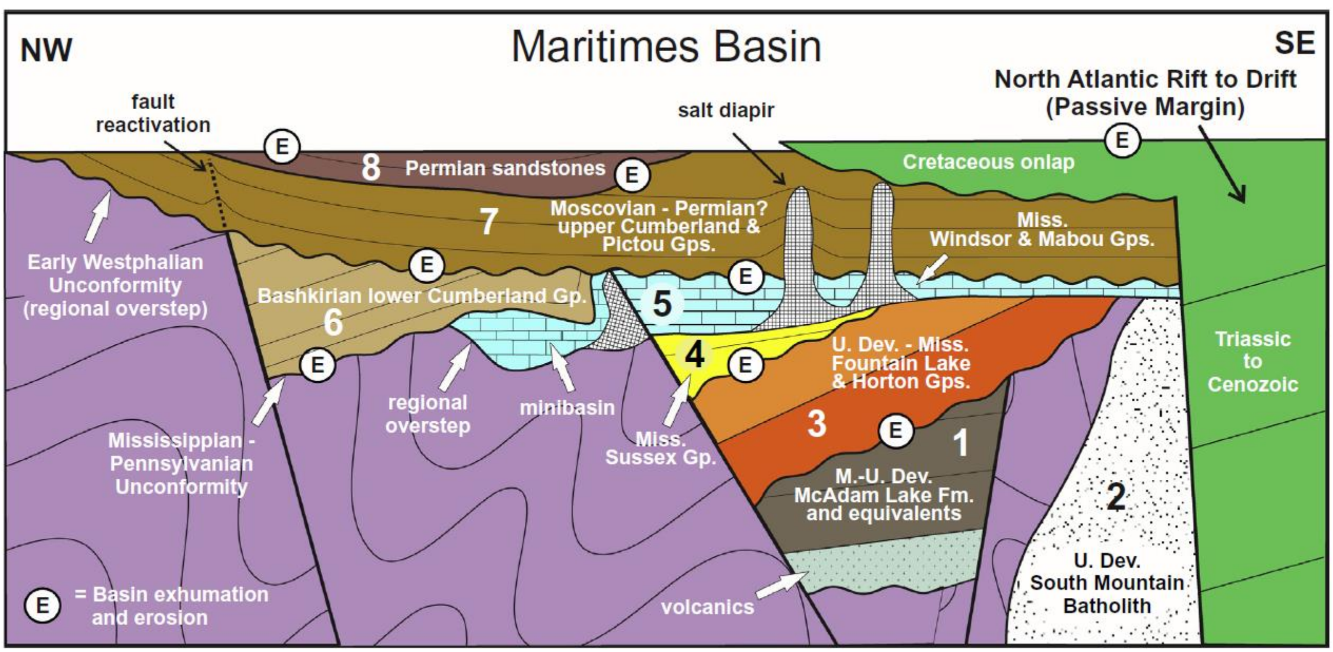

Figure 3.2. General tectonostratigraphic overview of the Maritimes Basin. Figure taken from Gibling et al. (2019).

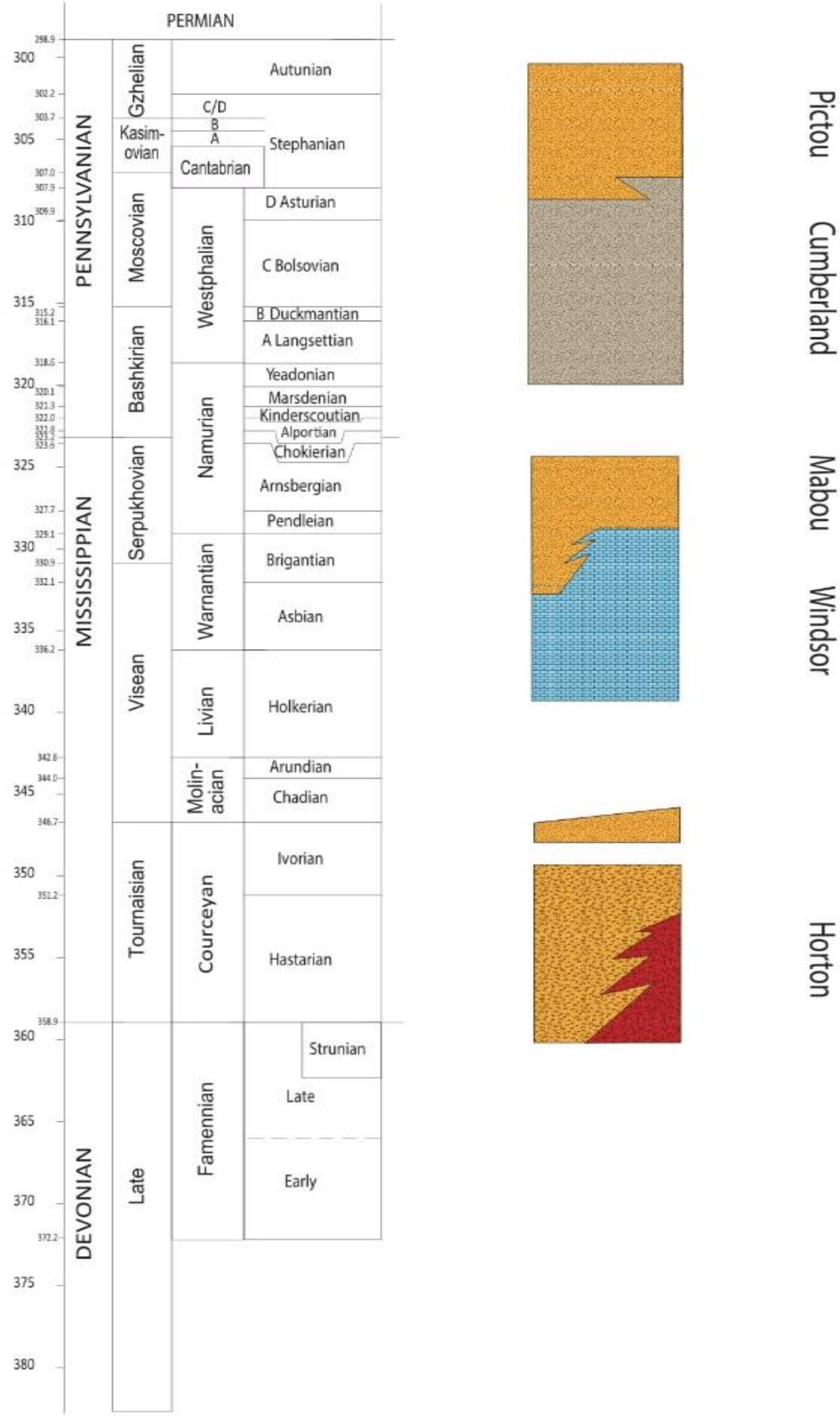

Figure 3.3. General stratigraphy of the Maritimes Basin in Nova Scotia (courtesy of Xiochun Cen, NSDEM, 2020).

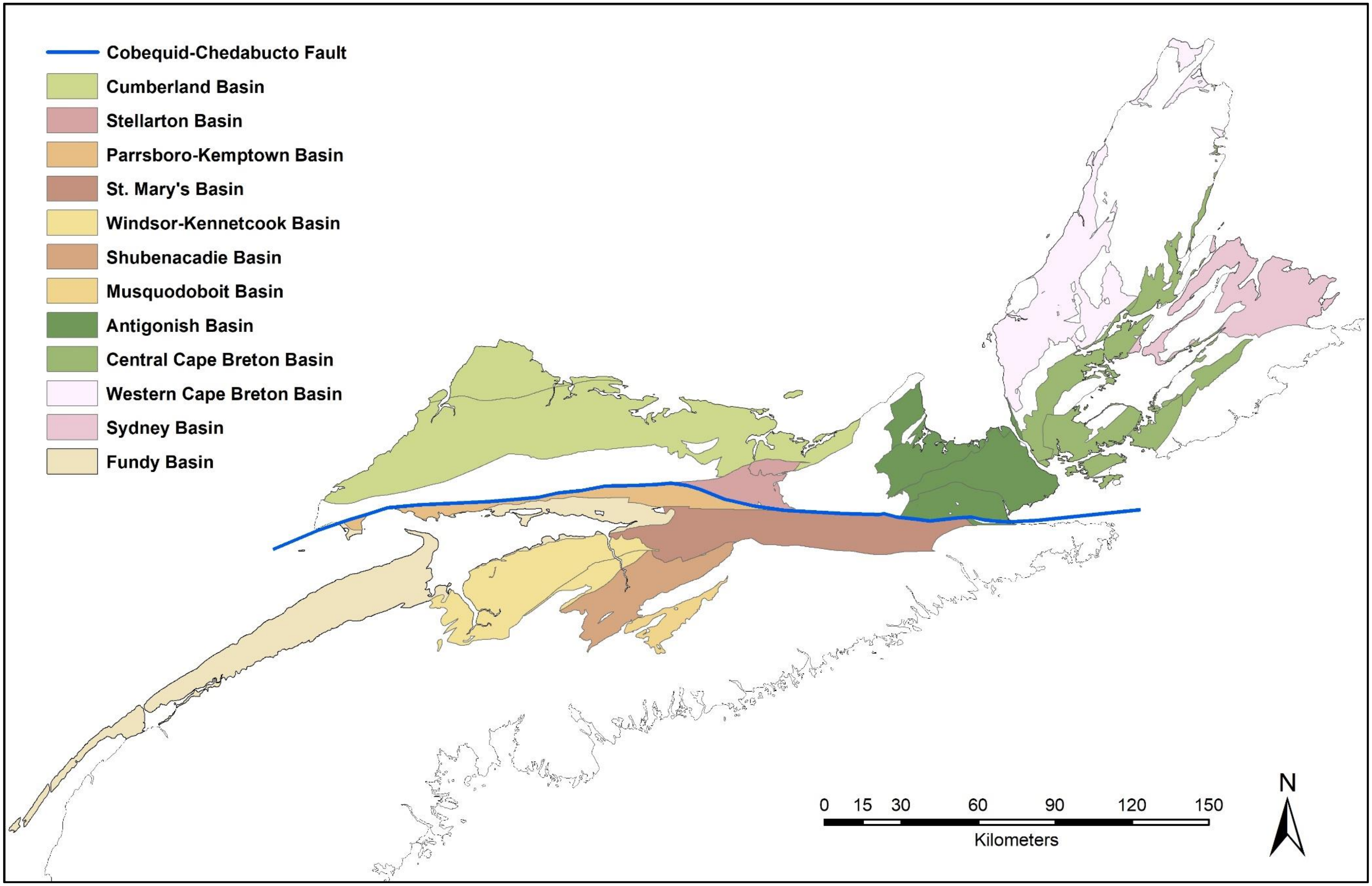

Figure 3.4. Extent of sedimentary basins onshore Nova Scotia. Cartographic background: NSDNR (2006) and NSDEM (2020).

3.7 References

Barr, S.M., Raeside, R.P., Jamieson, R.A., 1995. Gander Zone-Cape Breton Island, Nova Scotia. In: Chapter 3 of Geology of the Appalachian-Caledonian Orogen in Canada and Greenland, Ed.: Williams, H. Geological Survey of Canada, Geology of Canada, No 6, p. 212-216.

Erdmer, P., Williams, H., 1995. Grenville basement rocks (Humber Zone). In: Chapter 3 of Geology of the Appalachian-Caledonian Orogen in Canada and Greenland, Ed.: Williams, H. Geological Survey of Canada, Geology of Canada, No 6, p. 50-61.

Gibling, M.R., 1995. Upper Paleozoic rocks, Nova Scotia. In: Chapter 5 of Geology of the Appalachian-Caledonian Orogen in Canada and Greenland, Ed.: Williams, H. Geological Survey of Canada, Geology of Canada, No 6, p. 493-523.

Gibling, M.R., Culshaw, N., Pascucci, V., Waldron, J.W.F., Rygel, M.C., 2019. The Maritimes Basin of Atlantic Canada: Basin Creation and Destruction During the Paleozoic Assembly of Pangea. In: The Sedimentary Basins of the United States and Canada (Second Edition), p. 267-314. https://doi.org/10.1016/B978-0-444-63895-3.00006-1

Keppie, J.D., Murphy, J.B., Nance, R.D., Dostal, J., 1995. Avalon Zone-Nova Scotia. In: Chapter 3 of Geology of the Appalachian-Caledonian Orogen in Canada and Greenland, Ed.: Williams, H. Geological Survey of Canada, Geology of Canada, No 6, p. 238-249.

NSDNR, 2006. Geological map of the province of Nova Scotia, Scale 1:500 000, Compiled by J. D. Keppie, 2000. Digital Version of Nova Scotia Department of Natural Resources Map ME 2000-1. DP ME 43, Version 2.

NSDEM, 2020. Digital contours of sedimentary basins. Nova Scotia Department of Energy and Mines, unpublished data.

Schenk, P.E., 1995. Meguma Zone. In: Chapter 3 of Geology of the Appalachian-Caledonian Orogen in Canada and Greenland, Ed.: Williams, H. Geological Survey of Canada, Geology of Canada, No 6, p. 261-277.

Waldron, J. W. F., Giles, P.S., and Thomas, A.K., 2017, Correlation chart for Late Devonian to Permian stratified rocks of the Maritimes Basin, Atlantic Canada. Nova Scotia Department of Energy Open File Report 2017-02

Williams, H., 1995. Temporal and spatial divisions. In: Chapter 2 of Geology of the Appalachian-Caledonian Orogen in Canada and Greenland, Ed.: Williams, H. Geological Survey of Canada, Geology of Canada, No 6, p. 21-44.

4. COMPILATION OF GEOTHERMAL DATA IN NOVA SCOTIA

4.1 Previous studies

4.1.1 Geothermal data

In the years 1981-1985, the Geothermal Service of Canada mandated J. A. Leslie and Associates Ltd. to gather available data relevant to the evaluation of the geothermal energy resources. The scope of this project, initially focussed on Nova Scotia and Prince Edward Island, was later expanded to all Atlantic Provinces. Results were published in a series of Open Files (Leslie, 1981, 1982, 1983, 1984, 1985). The aim of the program was to compile existing data: no evaluation of the geothermal potential of Nova Scotia was made during the course of this study.

4.1.2 Abandoned mines

In 1991, the Earth Physics Branch of the Federal Department of Energy, Mines and Resources (the future Geological Survey of Canada) mandated K. Arkay to develop a "methodology for an inventory of abandoned mines, with the objective of identifying sites of potential interest as sources of geothermal energy" (Arkay, 2000). The report, completed in 1992 and published in 2000, also presents an inventory of abandoned underground mines in Nova Scotia for metals, industrial minerals and coal.

In the methodology, Arkay (2000) acknowledges that some of the smallest abandoned underground mines might not have been included in the compilation, especially for the oldest mines. In some cases, clusters of small mines have also been aggregated into "districts".

4.1.3 Abandoned coal mines applications

The town of Springhill, Nova Scotia (Municipality of Cumberland) hosts some of the deepest coal mines of North America. These were in operation between 1849 and 1958 and are now flooded. The world's first successful exploitation of the groundwater from flooded coal mines for heating and cooling buildings took place in Springhill in 1989, after a feasibility study initiated by the Earth Physics Branch of the Federal Department of Energy, Mines and Resources in 1985 (Jessop et al., 1995). The geothermal energy of these coal mines is still in use today and its technical and economic parameters continue to be actively studied (MacAskill, 2015; EOS, 2017; CBCL, 2017).

Encouraged by the successful example of Springhill, other studies have since focussed on the geothermal potential of flooded coal mines in other localities in Nova Scotia, such as the Cochrane Mine in the River Hebert and Joggins area (Whitford, 1993), the Stellarton coal field (Michel, 2007) and the Sydney coal field (MacSween et al., 2013).

4.1.4 OERA's assessment program

In March 2020, the Offshore Energy Research Association (OERA) initiated an assessment of geothermal resources in onshore Nova Scotia. The present study corresponds to the initial stage of this program ("Part 1: Setting the stage, demonstrating value, and identifying next steps").

4.2 Surface temperatures

Although not directly related to the geothermal potential of an area, surface temperatures are used in the calculation of the geothermal gradients.

Annual mean surface temperatures were gathered from Environment Canada (2020) for 42 weather stations located across the province. The range of the data span over 30 years, from 1981 to 2010. The data from each weather station have been used to build a 2D map of the annual mean surface temperatures over the entire province (**Figure 4.1**).

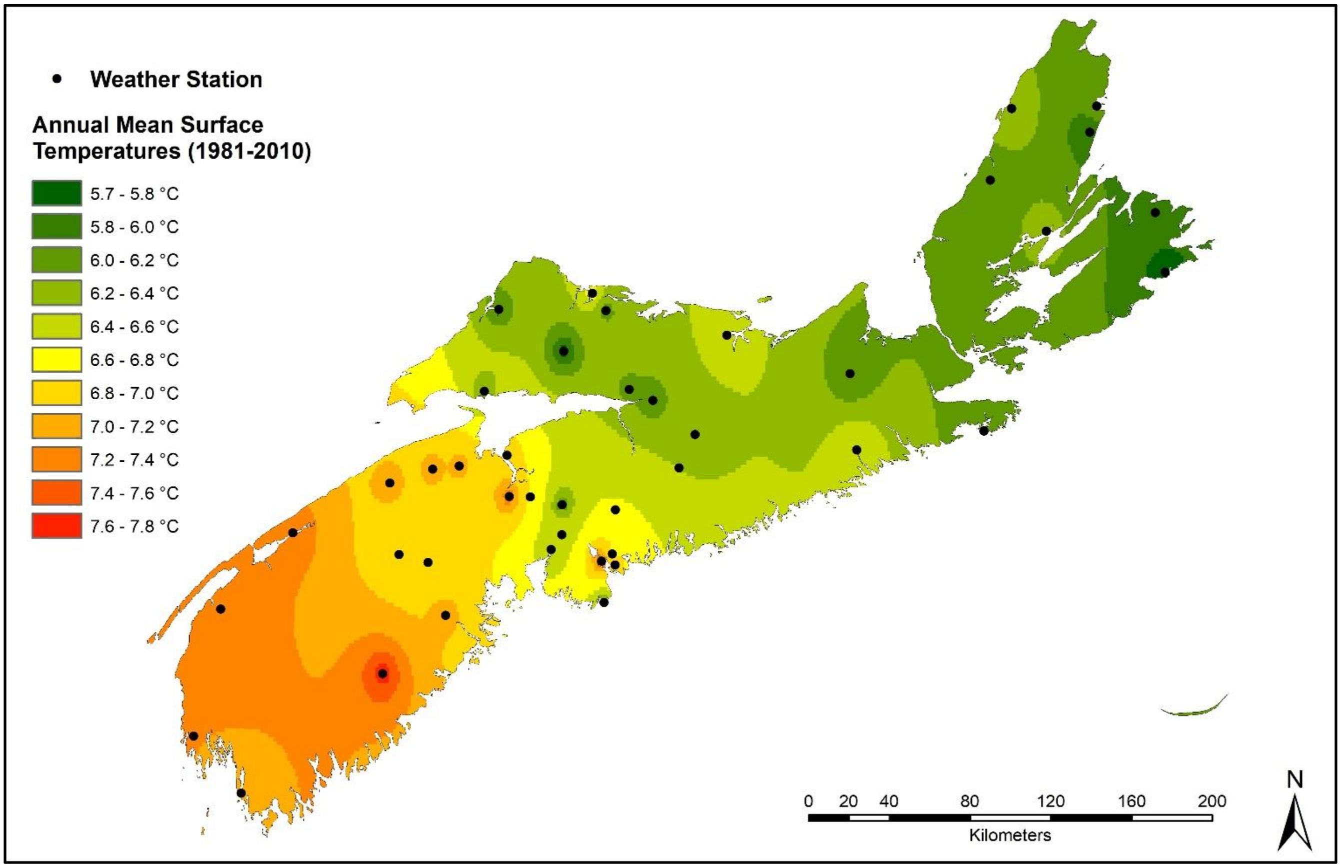

Figure 4.1. Annual mean surface temperatures (1981-2010) for Nova Scotia.

4.3 Underground temperatures

Underground temperature data were obtained from published reports and papers and from petroleum well petrophysical logs. **Figure 4.2** shows the spatial distribution of these datasets.

4.3.1 From published sources

As indicated in **Section 4.1**, many underground temperature data can be found in Leslie (1981; 1982; 1983; 1984; 1985). These data and more recent ones are also compiled in Jessop et al. (2005). The original sources referenced in these compilations have been consulted to confirm the accuracy of the data reported (Jessop, 1968; Jessop and Judge, 1971; Drury et al., 1987; Chatterjee and Dostal, 2002). The most important contribution of these compilations are temperature profiles. They correspond to temperature measurements made in wells several months or years after circulation of drilling mud had stopped, at a moment when the temperature of the mud is considered to have had enough time to equilibrate with the temperature of the surrounding rock.

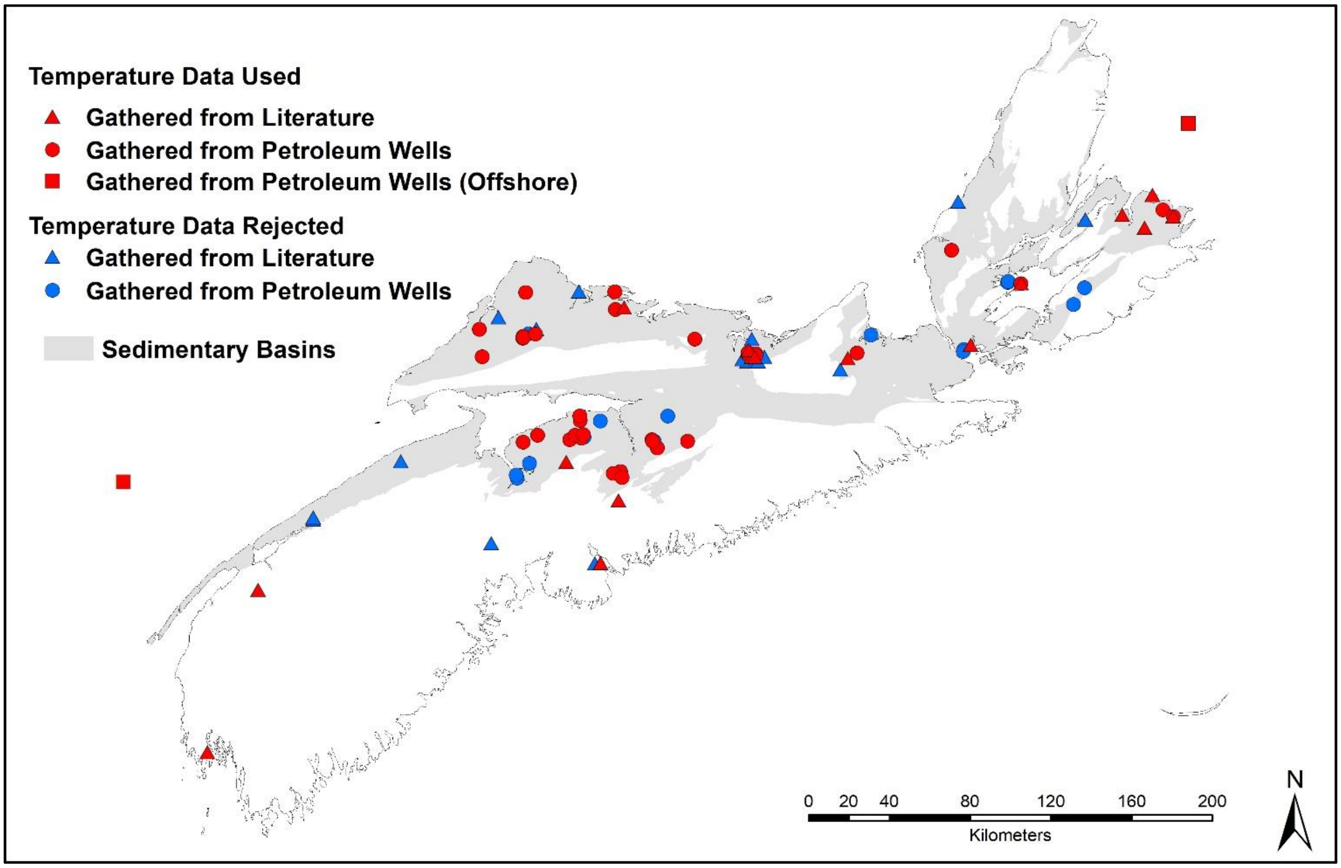

Figure 4.2. Spatial distribution of the underground data that have been used or rejected in the course of the present study. Refer to text for details.

Complementary data have been gathered from various literature sources, including a geothermal gradient calculated from temperatures measured at equilibrium in a coal mine (Young, 1997) and a geothermal gradient estimated from the thermal maturity of the coal (Hacquebard and Donaldson, 1970). For a few localities, heat flux and thermal conductivity data are also reported in the published compilations, associated with the original temperature data at equilibrium (Misener, 1955; Lachenbruch, 1957; Paterson and Law, 1966; Rankin and Hyndman, 1971; Rankin, 1974; Hyndman et al., 1979; Drury et al., 1987).

Table 4.1 illustrates the content of data collected from the literature review while the entire dataset is presented in **Appendix I**. Twenty-seven out of the 31 data points correspond to wells for which a temperature profile is available. In these cases, the deepest temperature measurement has been selected along with the corresponding depth. In two other cases, the depth and temperature reported in the database correspond to the only information mentioned in the original references, with no temperature profile available. In the two remaining cases, the original references did not indicate any temperature measurement but provided an estimation of the geothermal gradient, which is reported in the Comment section of **Appendix I**. Whenever possible, geographic coordinates more accurate than those indicated in the original sources were provided by the Nova Scotia Department of Energy, and have been preferred over the original coordinates.

Table 4.1. Example datasheet for the temperature data gathered from the literature for the well NSDME P-54. Refer to **Appendix I** for the entire dataset.

AMST: Annual Mean Surface Temperature
TEMP.: Temperature, as indicated in the original reference

<table>
<tr><td rowspan="5">NSDME P-54</td><td>BASIN:</td><td colspan="2">Stellarton (Cumberland)</td><td>SITE:</td><td colspan="2">New Glasgow</td></tr>
<tr><td>AMST (°C)</td><td>EASTING</td><td>NORTHING</td><td>DEPTH (m)</td><td>TEMP. (°C)</td><td>EQUILIBRIUM</td></tr>
<tr><td>6.5</td><td>526 521</td><td>5 048 552</td><td>950.0</td><td>28.1</td><td>Yes</td></tr>
<tr><td>SOURCE(S):</td><td colspan="3">Jessop et al. (2005); Drury et al. (1987); Leslie (1984)</td><td>CONFIDENCE:</td><td>VERY GOOD</td></tr>
<tr><td>COMMENT:</td><td colspan="5">Jessop et al. (2005) refer to Drury et al. (1987) but the latter do not mention this well. Leslie (1984) provides the temperature profile.</td></tr>
</table>

4.3.2 From petroleum well data

Most petrophysical logs recorded in oil and natural gas wells contain temperature data. These data correspond to the temperature of the drilling mud some time (typically a few hours) after the circulation of the mud has stopped, but not long enough to have reached an equilibrium with the surrounding rock. These temperatures represent nonetheless a very valuable source of information on the underground thermal regimes at mid-depths.

The petrophysical logs available from onshore Nova Scotia petroleum wells were systematically reviewed to gather temperature data. The logs were provided by the Nova Scotia Department of Energy and Mines (NSDEM) in their original format (LAS, TIFF, PDF or DLIS). Some are accessible in Bianco (2017), the others come from the archives of the NSDEM. End of drilling reports were also consulted whenever necessary.

Table 4.2 illustrates the content of data collected while the entire dataset is presented in **Appendix II**. For each well, all temperatures, measured depths and times since the mud circulation ceased have been extracted. Whenever a deviation survey was available, a true vertical depth was gathered or calculated using the minimum curvature method. The temperatures of the mud, the mud filtrate and the mud cake were also compiled in an effort to better assess the accuracy of the temperatures reported in the logs. These mud temperature values are not reported in the database because they were not used in estimating the temperature gradients.

The compilation of all temperature data from all logs for a given well allowed for the cross-verification of the data and the filtering of erroneous, suspect or inconsistent data. For each well, only one was ultimately selected for the compiled temperatures, depths and times since the mud circulation ceased. These selected values serve as input to estimate the temperature gradients in the vicinity of each well. When multiple choices were possible the rationale for the selection is explained in the Comment section (**Table 4.2**), accompanied with an appreciation of their level of confidence (see **Section 4.3.3**).

A total of 98 individual logs were reviewed, corresponding to 42 wells. The well CCSNS#1 (3 logs), drilled for carbon capture and storage in 2014, has been added to this list because of the quality of the data available. Two offshore wells have also been added, to further document the underground temperatures in poorly documented areas: Well F-24 in the Sydney Basin (10 logs) and well N-37 (5 logs) in the Fundy Basin (location on **Figure 4.2**).

Table 4.2. Example datasheet for the temperature data gathered for the petroleum well P-120. Refer to **Appendix II** for the entire dataset.

AMST: Annual Mean Surface Temperature
KBG: Elevation of the Kelly bushing or rotary table and the ground level
MD: Total Measured Depth of the well or of a log
TVD: True Vertical Depth of the well or of a log. When empty: no deviation survey available
Max T: Maximum Temperature, as reported in the log considered
BHT: Bottom Hole Temperature, as reported in the log considered
TSC: Time Since the mud Circulation has stopped, before the logging tool reaches the bottom
SOURCES: 1: Open File 2017-09 (Bianco, 2017); 2: Nova Scotia Department of Energy and Mines, archived data

P-120	**SPUD:**	2005	**NAME:**	Hardwoodlands #1		
	SOURCE(S):	1	**BASIN:**	Shubenacadie		
	AMST (°C)	**EASTING**	**NORTHING**	**KBG (m)**	**MD (m)**	**TVD (m)**
	6.5	459 530	4 987 591	4.06	835.0	833.7
	LOG #	**MD (m)**	**TVD (m)**	**Max T (°C)**	**BHT (°C)**	**TSC (hrs)**
	1	745.6	744.6	27.0	27.0	4.9
	2	832.5	831.2	24.0	23.0	9.0
	3	832.5	831.2	24.0	24.0	9.0
	4	298.0	298.0		25.0	
	SELECTION:	23 °C at 831.2 m after 9 hrs			**CONFIDENCE:**	**GOOD**
	COMMENT:	BHT in LOG # 2 is confirmed by a temperature log.				

4.3.3 Level of confidence

A level of confidence has been attributed to each of the temperature data gathered from literature and petroleum wells: NONE, POOR, GOOD and VERY GOOD.

For the temperatures obtained from the literature (31 wells), the level of confidence is considered very good whenever a temperature profile at equilibrium was available at a depth greater than 300 m (11 wells). For wells with a temperature profile at the equilibrium that do not exceed 300 m (15 wells), the level of confidence is considered to be none. Five data points have a poor level of confidence, three of them because a single temperature was provided and the original data were not available for review, one because a geothermal gradient was provided from temperatures at equilibrium, but not the original data, and one corresponding to a geothermal gradient inferred from the level of thermal maturity of coal.

For the temperatures filtered from petroleum wells, the level of confidence is good overall, but not very good because the temperatures were not measured at equilibrium. Three wells have a poor level of confidence because some residual ambiguities could not be resolved. Three other wells have been rejected (level of confidence: none) because of their shallow depths.

The threshold of 300 m used to dismiss some temperature data due to surface and shallow subsurface effects that can impact underground temperatures. Temperatures measured at equilibrium at shallow depths may not be suitable to extrapolate the temperature at greater depths. Most authors agree that temperatures measured between 200 and 400 m below ground level should not be used for such purposes (Beck, 1979; Jessop, 1990; Rolandone et al., 2002; Jaupart and Mareschal, 2011).

4.4 Volumes of abandoned mines

As indicated in **Section 4.1**, Arkay (2000) provides a comprehensive compilation of the abandoned underground mines until 1992. The data relevant to the present study include:

- For coal: the name of the mine, some location information (closest community, township and map sheet) and the volume of ore removed.
- For metals and industrial minerals: the name of the mine, its latitude and longitude, the volume of ore removed and the maximum depth of the mine.

This dataset is complemented by a compilation of coordinates prepared by the Nova Scotia Department of Natural Resources in 2014 for the National Orphaned/Abandoned Mines Initiative (NOAMI), which includes:

- The extracted volume for open-pit mines, along with the type of commodity.
- The extracted volume for five additional underground coal mines closed after 1992.

These two datasets have been combined to create a new database that includes at a minimum the name of the mine, its location and the volume of ore extracted and, whenever possible, the maximum depth of the mine for underground metals and industrial mineral mines. Mines with an extracted volume of less than 1 metric tonne were discarded. **Figure 4.3** illustrates the location of the abandoned mines included in the database. The entire dataset is presented in **Appendix III**.

Salt mines have not been included in this compilation due to a lack of specific data, although abandoned mines exploited by solution mining may be considered in the future. Abandoned salt mines have an overall better potential for compressed air energy storage than for geothermal energy.

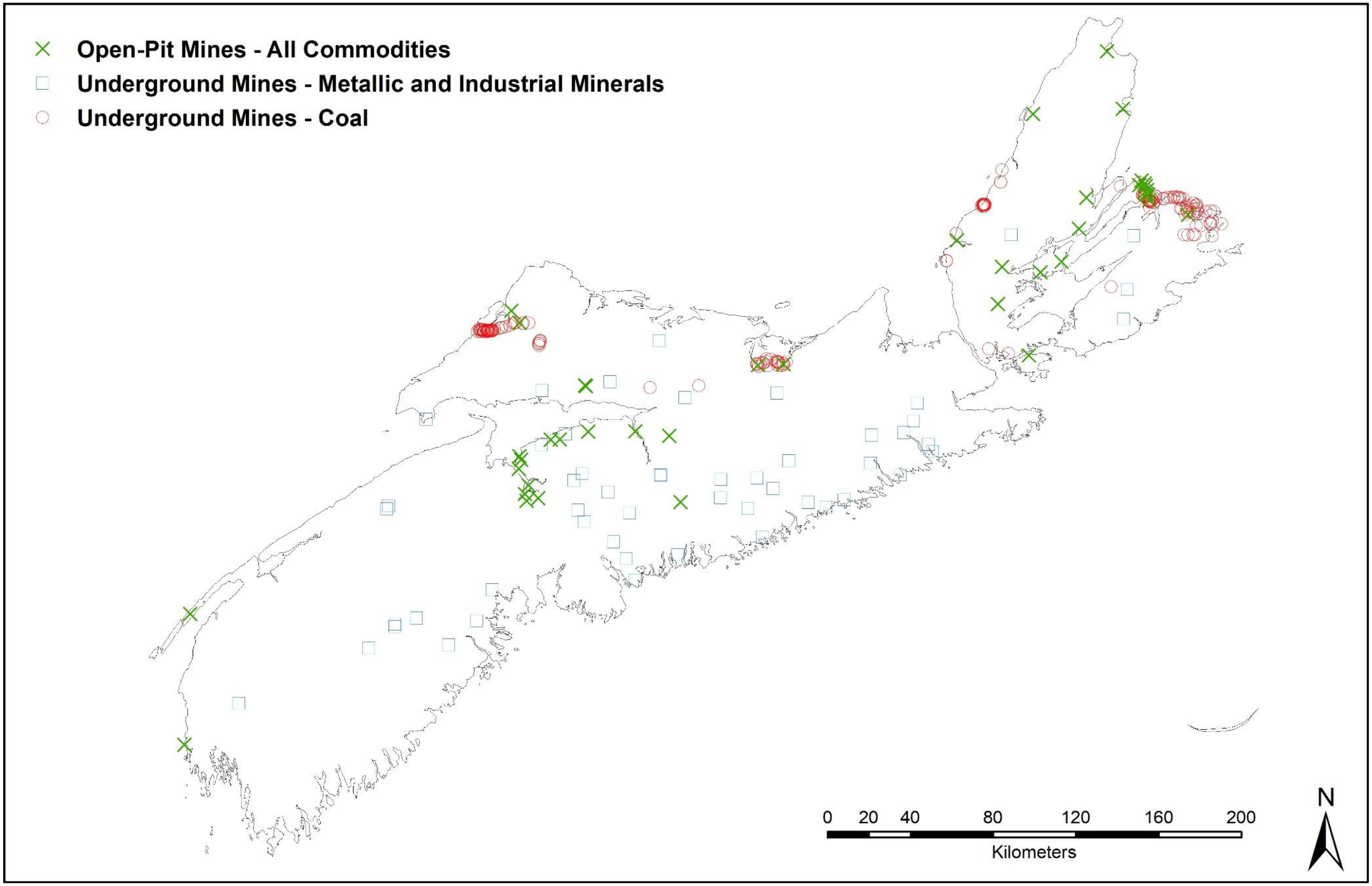

Figure 4.3. Location of the abandoned mines included in the database.

4.5 References

Arkay, K., 2000. Geothermal energy from abandoned mines: A methodology for an inventory, and inventory data for abandoned mines in Quebec and Nova Scotia. Geological Survey Open File 3825, 388 p. https://doi.org/10.4095/211648

Beck, A.E., 1977. Climatically perturbed temperature gradients and their effect on regional and continental heat-flow means. Tectonophysics 41(1–3):17-39. https://doi.org/10.1016/0040-1951(77)90178-0

Bianco, E., 2017. Preliminary petroleum well log database, onshore Nova Scotia. Nova Scotia Department of Energy Open File Report 2017-09.

CBCL, 2017. Mine workings spatial analysis review and deep well test boreholes, Springhill, Nova Scotia. CBCL Limited, Report prepared for the Municipality of Cumberland, 12 p.

Chatterjee, A.K., Dostal, J., 2002. Deep drill hole in the Devonian South Mountain batholith, Nova Scotia: a potential for hidden mineral deposits within the batholith. Atlantic Geology 38(1):1-10. https://doi.org/10.4138/1251

Drury, M.J., Jessop, A.M., Lewis, T.J., 1987. Thermal nature of the Canadian Appalachian crust. Tectonophysics 133 (1–2):1-14. https://doi.org/10.1016/0040-1951(87)90276-9

Environment Canada (2020). Station Results - 1981-2010 Climate Normals and Averages. Government of Canada. https://shorturl.at/hqEGT. Consulted online 2020-05-26.

EOS, 2017. Springhill geothermal energy use study. Efficiency One Services, Report prepared for Cumberland Energy Authority, 61 p.

Hacquebard, P.A., Donaldson, J.R., 1970. Coal metamorphism and hydrocarbon potential in the Upper Paleozoic of the Atlantic Provinces, Canada. Canadian Journal of Earth Sciences 7 (4):1139-1163. https://doi.org/10.1139/e70-108

Hyndman, R.D., Jessop, A.M., Judge, A.S., 1979. Heat flow in the Maritime Provinces of Canada. Canadian Journal of Earth Sciences 16 (6):1154–1165. https://doi.org/10.1139/e79-102

Jaupart, C., Mareschal, J.-C., 2011. Heat generation and transport in the Earth. Cambridge University Press. Cambridge; New York, 464 p.

Jessop, A.M., 1968. Three measurements of heat flow in eastern Canada. Canadian Journal of Earth Sciences 5 (1):61–68. https://doi.org/10.1139/e68-006

Jessop, A.M., Judge, A.S., 1971. Five measurements of heat flow in southern Canada. Canadian Journal of Earth Sciences 8(6):711-716. https://doi.org/10.1139/e71-069

Jessop, A.M., MacDonald, J.K. Spence, H. 1995. Clean energy from abandoned mines at Springhill, Nova Scotia. Energy Sources 17(1):93-106. https://doi.org/10.1080/00908319508946072

Jessop, A.M., Allen, V.S., Bentkowski, W., Burgess, M., Drury, M., Judge, A.S., Lewis, T., Majorowicz, J., Mareschal, J.-C., Taylor, A.E., 2005. The Canadian geothermal data compilation. Geological Survey of Canada, Open File 4887, 12 p. https://doi.org/10.4095/220364

Leslie, J.A., 1981. Investigation of geothermal energy resources - Nova Scotia and Prince Edward Island. Energy, Mines and Resources Canada, Earth Physics Branch Open File 81-9, 120 p.

Leslie, J.A., 1982. Investigation of geothermal energy resources - Atlantic Provinces. Energy, Mines and Resources Canada, Earth Physics Branch Open File 82-8, 119 p.

Leslie, J.A., 1983. Investigation of geothermal energy resources - Atlantic Provinces. Energy, Mines and Resources Canada, Earth Physics Branch Open File 83-20, 37 p.

Leslie, J.A., 1984. Investigation of geothermal energy resources - Atlantic Provinces. Energy, Mines and Resources Canada, Earth Physics Branch Open File 84-5, 41 p.

Leslie, J.A., 1985. Investigation of geothermal energy resources - Atlantic Provinces. Energy, Mines and Resources Canada, Earth Physics Branch Open File 85-8, 64 p.

MacAskill, D., Power, C. 2015. Researching the geothermal potential of the former Springhill Mine. Verschuren Centre for Sustainability in Energy and the Environment, Report to Cumberland Energy Authority, 24 p.
MacSween, J., Raman, C., Kaliaperumal, R., Oakes, K., Mkandawire, M., 2013. Modeling potential impact of geothermal energy extraction from the 1B Hydraulic System of the Sydney Coalfield, Nova Scotia, Canada. In: Reliable Mine Water Technology, Eds: Wolkersdorfer, Brown and Figueroa, p. 1035-1040.
Michel, F.A., 2007. Evaluation of the geothermal energy potential in Stellarton, Nova Scotia, final report. Prepared for: Nova Scotia Department of Energy, Nova Scotia Department of Natural Resources, and the Town of Stellarton, 29 p.
Rankin, D.S., 1974. Heat flow production studies in Nova Scotia. Ph.D. thesis, Dalhousie University, 188 p.
Rankin, D.S., Hyndman, R.D., 1971. Shallow water heat flow measurements in Bras d'Or Lake, Nova Scotia. Canadian Journal of Earth Sciences 8(1):96–101. https://doi.org/10.1139/e71-006
Rolandone, F., Jaupart, C., Mareschal, J.-C., Gariepy, C.,Bienfait, G., Carbonne, C., Lapointe, R., 2002. Surface heat flow, crustal temperatures and mantle heat flow in the Proterozoic Trans-Hudson Orogen, Canadian Shield. Journal of Geophysical Research 107(B12):ETG 7-1-ETG 7-19. https://doi.org/10.1029/2001JB000698
Whitford, J., 1993. Earth Energy Assessment of Cochrane Mine, River Hebert, Nova Scotia. Jacques Whitford Environment Limited, Report submitted to River Hebert and Joggins Area Development Association, 38 p.
Young, D.A., 1997. Methane and ventilation studies in coal mining in the Sydney Coalfield, Nova Scotia. M.Sc. thesis, McGill University, 173 p.

5. METHODOLOGY OF THE GEOTHERMAL POTENTIAL EVALUATION

5.1 Sedimentary basins

5.1.1. Underground temperatures

5.1.1.1 Drilling disturbance

The drilling operations disturb the temperature of the underground environment through friction and heat exchange with the drilling mud, resulting in a temporary cooling of the rock (Jessop, 1990). This cooling effect vanishes within a few days to several months after mud circulation stops, while the temperature data obtained from wireline logging are generally measured only a few hours after the drilling operations cease, before equilibrium can be reached (Kehle et al., 1970; Harrison et al., 1983; Jessop, 1990; Beardsmore and Cull, 2001; Kutasov and Eppelbaum, 2010).

Several methods are available to reduce the uncertainties associated with estimates of temperature data at equilibrium from petroleum wells. The most direct and reliable method is to use formation temperature data obtained from drill stem tests to calibrate the wireline logging temperatures. In the present case, however, very few drill stem tests (DST) results were available and they had no or unreliable temperature information. An alternative method consists in using a Horner plot (Horner, 1951) to compare three temperature measurements taken in the same well at the same depth at three different times after mud circulation has stopped (Timko and Fertl, 1972; Beardsmore and Cull, 2001). None of the wells reviewed in the course of the present study had enough information to use this method. Other, empirical methods have been published to correct the wireline logging temperatures, three of which were applied to the Nova Scotia data and are discussed below.

Correction for the depth only

The temperature correction proposed by Harrison et al. (1983) is based on a direct relationship between temperature and the depth of the measurement (**eq. 5.1**). It is expressed in Celsius and was originally calibrated for the depth interval 914 to 3,048 m (3,000 to 10,000 ft):

$$\Delta T = -16.51 + (1.827 \times 10^{-2} \times Z) - (2.345 \times 10^{-6} \times Z^2) \qquad \textbf{(eq. 5.1)}$$

With: ΔT: Temperature correction to add to the measured temperature (°C)
Z: Depth (m)

Recent studies suggest this correction can be used for a depth interval of 600 to 3,932 m (Blackwell and Richards, 2004; Blackwell et al., 2010; Frone and Blackwell, 2010). For depths greater than 3,932 m, Blackwell et al. (2010) suggest a correction expressed in Fahrenheit that is later converted into Celsius (**eq. 5.2**):

$$\Delta T = 34.3\ \text{°F} + 0.05\ \text{°F (at every 500 feet)} \qquad \textbf{(eq. 5.2)}$$

The correction of Blackwell et al. (2010) was applied only to well P-85 because all other wells had temperature measurements shallower than 3,932 m. For practical purposes, the temperatures measured at depths shallower than 1,045 m were not corrected using **eq. 5.1** because the correction was negative (i.e., corrected temperatures were cooler than those measured).

Correction for the depth and for the time since the circulation of the mud has stopped

Other authors have proposed temperature corrections that are based on a relationship between temperature, measurement depth and the time since mud circulation stopped. The rationale behind these corrections is that the longer the delay between the end of mud circulation and the moment at which the temperature is recorded, the more time the system has had to approach a state of thermal equilibrium. Three corrections of this type were tried and compared in **Figure 5.1**. the equations below describe the correction proposed by Wapples and Ramly (2001) for the depth interval 1,000 to 3,500 m (**eq. 5.3**), its extension for depths beyond 3,500 m (**eq. 5.4**, Wapples et al., 2004) and the correction proposed by Zare-Reisabadi et al. (2015) for the depth interval 1,550 to 4,719 m (**eq. 5.5**).

$$T_C = T_S + [(-0.1462 \times \ln(TSC) + 1.699) / (0.572 \times Z^{0.075})] \times (T_M - T_S) \quad \textbf{(eq. 5.3)}$$

$$T_C = T_S + 1.32866^{(-0.005289 \times TSC)} \times (T_M - T_S) - 0.001391 \times (Z - 4{,}498) \quad \textbf{(eq. 5.4)}$$

$$T_C = T_S + [(1.012 - 0.0057 \times \ln(TSC) + (375.42 / Z)] \times (T_M - T_S) \quad \textbf{(eq. 5.5)}$$

With: T_C: Corrected temperature (°C)
T_S: Surface temperature (°C)
TSC: Time since the circulation of the mud has stopped (hours)
Z: Depth (m)
T_M: Measured temperature (°C)

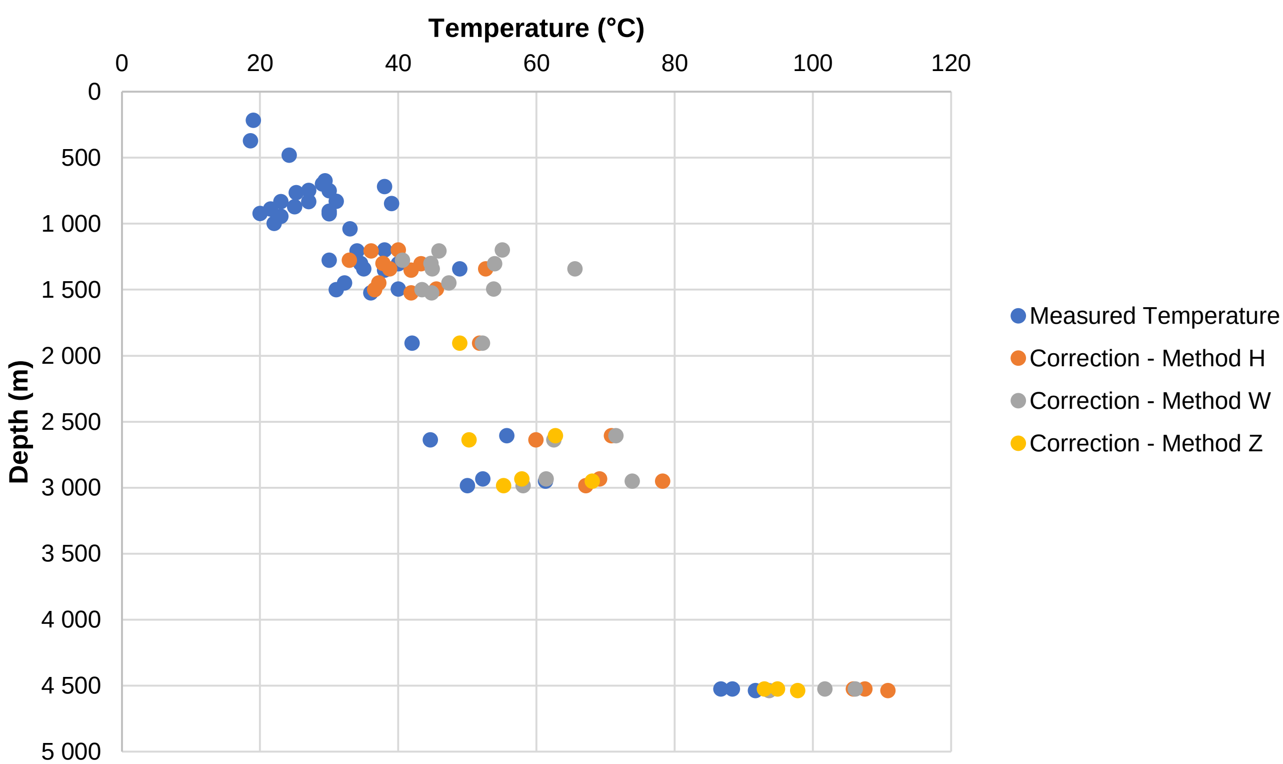

Figure 5.1. Comparison of the temperatures corrected by the different methods. Method H: Harrison et al. (1983) or Blackwell et al. (2010); Method W: Wapples and Ramly (2001) or Wapples et al. (2004); Method Z: Zare-Reisabadi et al. (2015).

Selection of the correction method

Discrepancies were noticed when comparing the temperatures corrected by using only the direct relationship between the measured temperature and the depth (**eqs. 5.1** and **5.2**) with the temperatures corrected by also using the time since mud circulation stopped (**eqs. 5.3** to **5.5**). For depths greater than 2,636 m, the correction proposed by Wapples and Ramly (2001) and Wapples et al. (2004) resulted in corrected temperatures lower than those corrected by the method of Harrison et al. (1983) or Blackwell et al. (2010). Similarly, for depths greater than 1,905 m, the correction proposed by Zare-Reisababi et al. (2015) resulted in corrected temperatures lower than those corrected by the method of Harrison et al. (1983) or Blackwell et al. (2010). Two main reasons can explain these discrepancies: 1) the time since mud circulation stopped may not have always been reported in a consistent manner in the original wireline logs data and 2) the correction methods have been validated in other basins which may not be suitable for Nova Scotia.

The correction methods proposed by Harrison et al. (1983) or Blackwell et al. (2010) have been selected for the present study for practical reasons:

- In the absence of formation temperatures obtained from drill stem tests for the studied wells, it is not possible to confirm which correction method is the most appropriate.
- The record of the time since mud circulation stopped is uncertain and its use may introduce further uncertainties to the correction of the measured temperatures with the methods proposed by Wapples and Ramly (2001), Wapples et al. (2004) and Zare-Reisababi et al. (2015).
- The correction proposed by Zare-Reisababi et al. (2015) is applicable here to less than 50% of the wells for which a correction can be attempted.

Based on the methods considered here, and on the results obtained, the consequence of correcting the measured temperatures without taking into account the time since the circulation of the mud stopped is that the corrected temperatures may be slightly underestimated below 2,000 m and slightly overestimated beyond this depth (**Figure 5.1**). The impact of this analytical bias is mitigated by the fact that the calculated geothermal gradient for a given sedimentary basin takes into account all of the corrected temperatures available at various depths (see **Section 5.1.2**).

5.1.1.2 Paleoclimatic effect

The thick ice sheets that have cyclically covered the Canada over the past 300,000 years have induced variations in the surface temperatures that have propagated at depth by thermal diffusion (Guillou-Frottier, 2006; Jaupart and Mareschal, 2011). Because the thermal diffusivity of the rocks is in the order of 0.8 to 2.5 $mm^2 sec^{-1}$, it is possible to observe the thermal signature induced by the long glacial periods of the Quaternary at several hundreds of meters (Beck, 1977; Jessop, 1990; Jaupart and Mareschal, 2011). The resulting cooling effect continues to propagate at depth today and most of the underground temperatures collected at depths are impacted by the thermal signature of the past glacial periods. These temperatures, although corrected to equilibrium with the host rock (see **Section 5.1.1.1**), are not at equilibrium with respect to the paleoclimate changes. Therefore, temperatures extrapolated beyond the deepest temperature measurement will be underestimated if the corresponding geothermal gradients are not corrected to account for the paleoclimatic effect (Birch, 1948; Beck, 1977; Chouinard and Mareschal, 2009). **Figure 5.2** illustrates the impact of the corrections on the measured temperatures. The correction of the geothermal gradient for the paleoclimatic effect allows adjustment of the instantaneous gradient at all points of a temperature profile at depth so as to obtain the gradient at equilibrium.

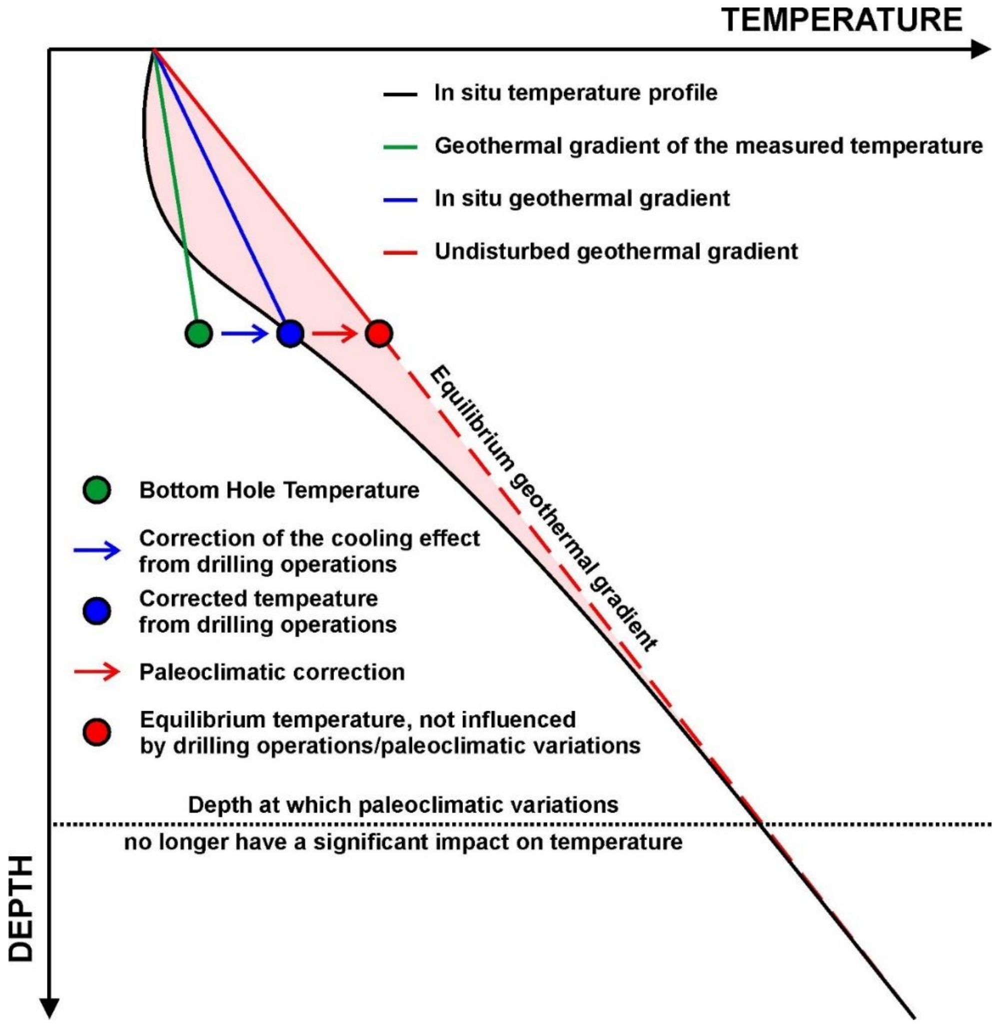

Figure 5.2. Impacts of the corrections applied to the temperatures measured in the petroleum wells (modified from Bédard et al., 2016).

To correct the temperatures for the paleoclimatic effect, it is necessary to consider each variation of the historical temperature so as to obtain the global cumulative effect of the correction (**eq. 5.6**) because the impacts of each ice age are additive (Jessop, 1971; Beck, 1977; Westaway et Younger, 2013). The correction depends on the temperature at the base of the ice sheet and on the start and end dates of the glacial period (**Figure 5.3**). It is maximum at 1,554 m (2.442 °C) and tends toward 0 °C beyond 7,000 m (**Figure 5.4**).

$$\Delta T = \sum_i (Ti) \times \left(erf\left(\frac{z}{\sqrt{4st_{i1}}}\right) - erf\left(\frac{z}{\sqrt{4st_{i2}}}\right)\right) \qquad \textbf{(eq. 5.6)}$$

With: ΔT: Temperature correction to add to the measured temperature (°C)
Ti: Mean temperature variation between the glacial period and today (-5 °C)
erf: Error function
s: Thermal diffusivity (1.2×10^{-6} m^2/sec)
$ti1$: End of the glacial period (sec, 31,557,600 sec/year)
$ti2$: Start of the glacial period (sec, 31,557,600 sec/year)
z: Depth (m)

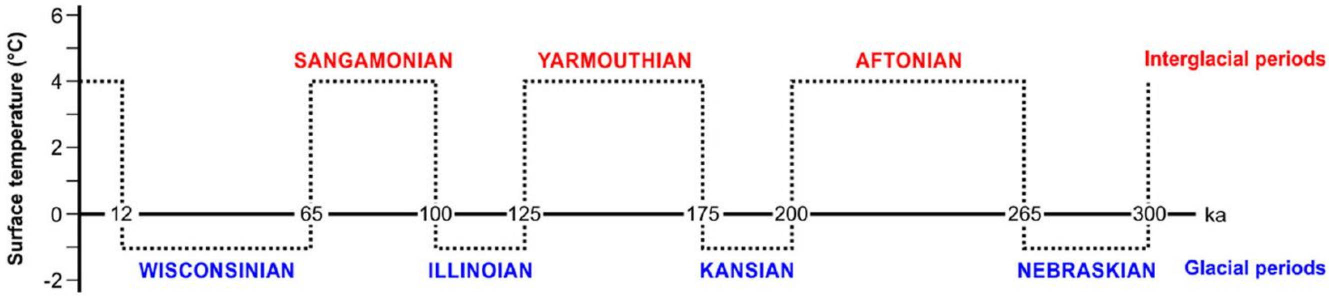

Figure 5.3. Chronology of the glacial periods considered in the present study (modified from Bédard et al., 2016).

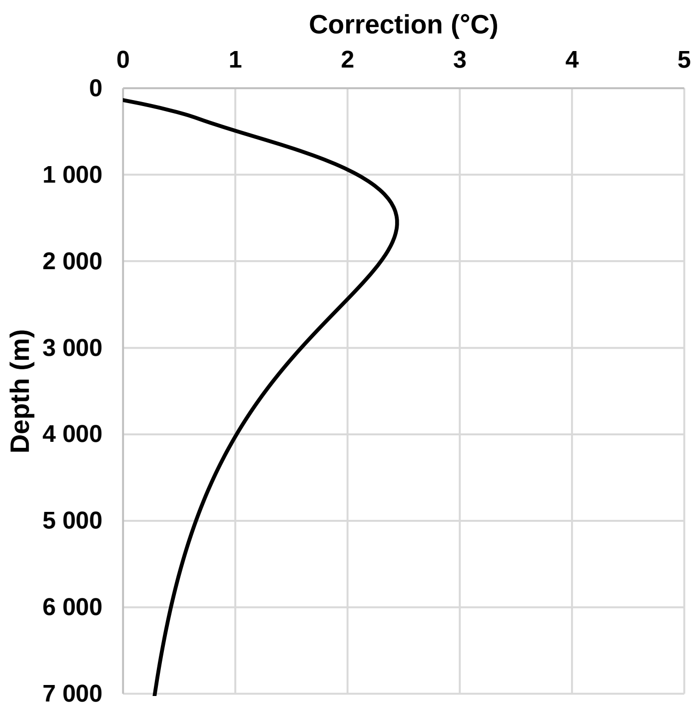

Figure 5.4. Evolution of the paleoclimatic correction with depth.

5.1.2 Geothermal gradients

Average geothermal gradients have been calculated for each sedimentary basin by integrating the geothermal gradients derived from the temperatures measured in wells for which a good or a very good level of confidence has been established and from the annual mean surface temperature corresponding to the location of these wells. The median values have been calculated for basins that have five wells or more, the average values have been used in the other cases. The standard deviation (or half the difference between the maximum and minimum value) reflect the margin of error on the calculated gradients.

For depths deeper than 1,045 m, the temperatures have been corrected by the methods of Harrison et al. (1983) or Blackwell et al. (2010). For depths shallower than 1,045 m, the temperatures measured at equilibrium have been preferred. Two geothermal gradients have been calculated for each basin, one representative of the temperatures at depths shallower than 1,000 m and one representative of greater depths.

Because the temperatures were measured at moderate depths (shallower than 3,000 m except for the well P-85 at about 4,500 m), extrapolated temperatures at greater depths were calculated taking into consideration the paleoclimatic effect. Expected temperatures and depths at representative intervals were then calculated as a guide considering that the correction for the paleoclimatic effect that is not linear.

The Fundy Basin is a notable exception to this otherwise consistent methodology. Because of the lack of deep underground temperature data, the geothermal gradient of this basin has been theorised using low- and high-end values of 20 and 30 °C km^{-1}. Temperatures measured at equilibrium in 4 wells at very shallow depths (55 to 153 m-deep) support this range of temperatures (16.2 to 27.5 °C km^{-1}, uncorrected), but do not give any level of confidence in the actual geothermal gradient.

The level of confidence in the geothermal gradients obtained for all basins are ranked GOOD on account for the GOOD or VERY GOOD level of confidence in the input data. The only exceptions are the Central Cape Breton Basin (POOR) due to the overall poor level of confidence in the input data and the Fundy Basin (NONE) due to the lack of reliable data. The results for each basin are synthesized in **Appendix IV**.

5.1.3 Sedimentary aquifers

The most difficult parameter to evaluate in Nova Scotia's onshore sedimentary basins is the quality of the lithological characteristics, that is, the combined porosity and permeability characteristics that permit an aquifer to freely produce heated water. In the absence of producing conventional reservoirs, the quality of potential aquifers can be incompletely inferred from porosity and permeability measurements undertaken on key lithologies, either from outcrop rock samples or from cores. In this respect, most of the relevant data has already been compiled in Cen (2017) and Bibby and Shimeld (2000), completed by recent work from Cameron (2018). Available data are summarized in **Figure 5.5**. However, the analyses of rock samples from outcrops tend to overestimate the actual porosity and permeability of equivalent rocks at depth and the results of core analyses from isolated, non-producing wells may not reflect the properties of a given aquifer across the basin.

In an effort to evaluate and rank the lithological characteristics with a reasonable level of confidence and uniformity across a given basin, the most prospective petroleum reservoirs are used as a general guideline. Hayes et al. (2017) provided such guidelines for the Cumberland and Windsor-Kennetcook basins, estimating undiscovered volumes of hydrocarbons in place for selected formations. Key seismic horizons were used as proxies for some of these prospective petroleum reservoirs (**Figures 5.6** and **5.7** for the Cumberland and Windsor-Kennetcook basins, respectively). For the other basins the information regarding the quality, if not the confirmed occurrence, of potential aquifers is limited. As an alternative, it was assumed that these basins contain prospective petroleum reservoirs laterally equivalent to those considered in the Cumberland and Windsor-Kennetcook basins.

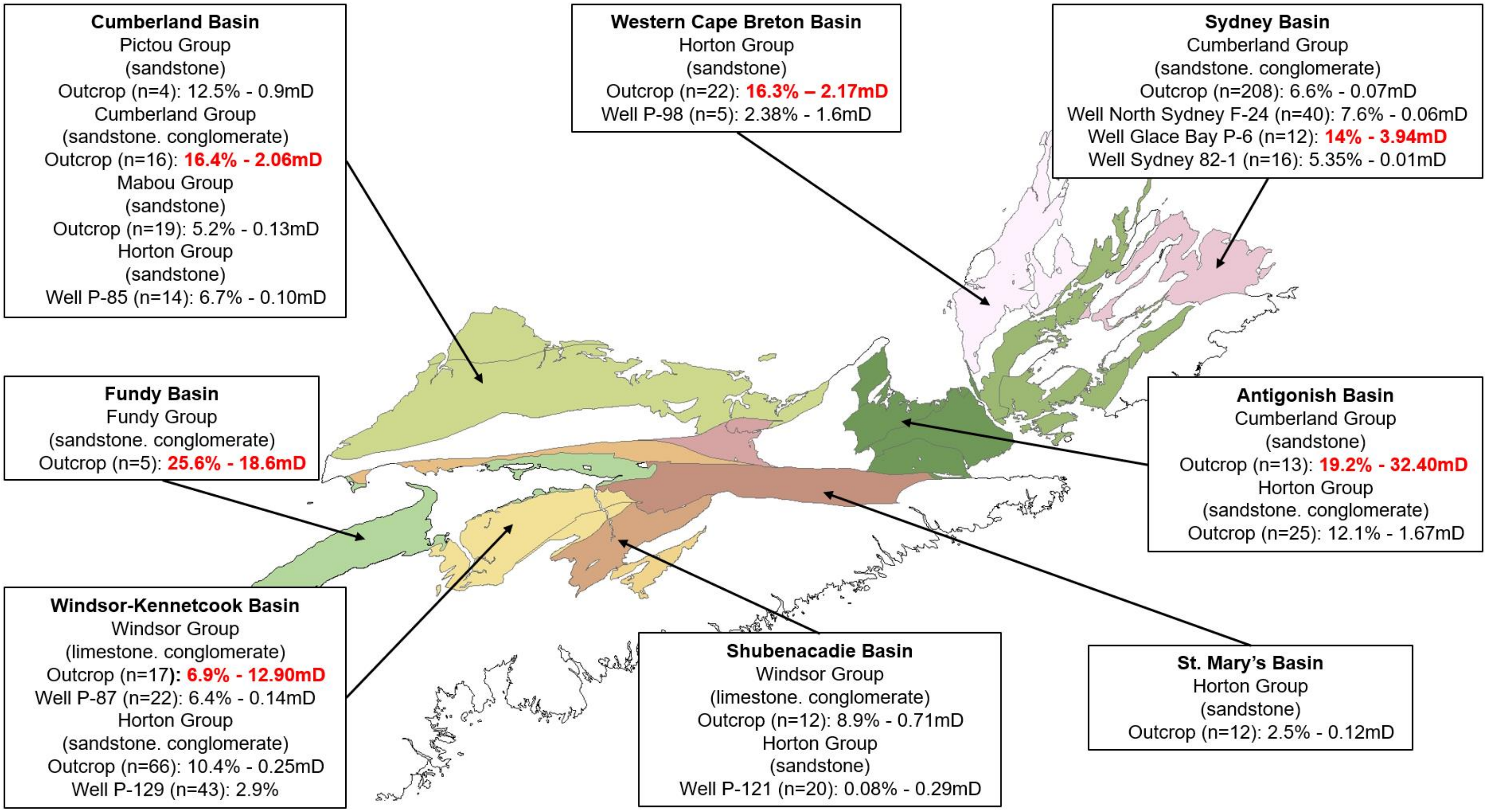

Figure 5.5. Summary of the porosity and permeability measurements for key lithologies onshore Nova Scotia. Cartographic background: NSDEM (2020).

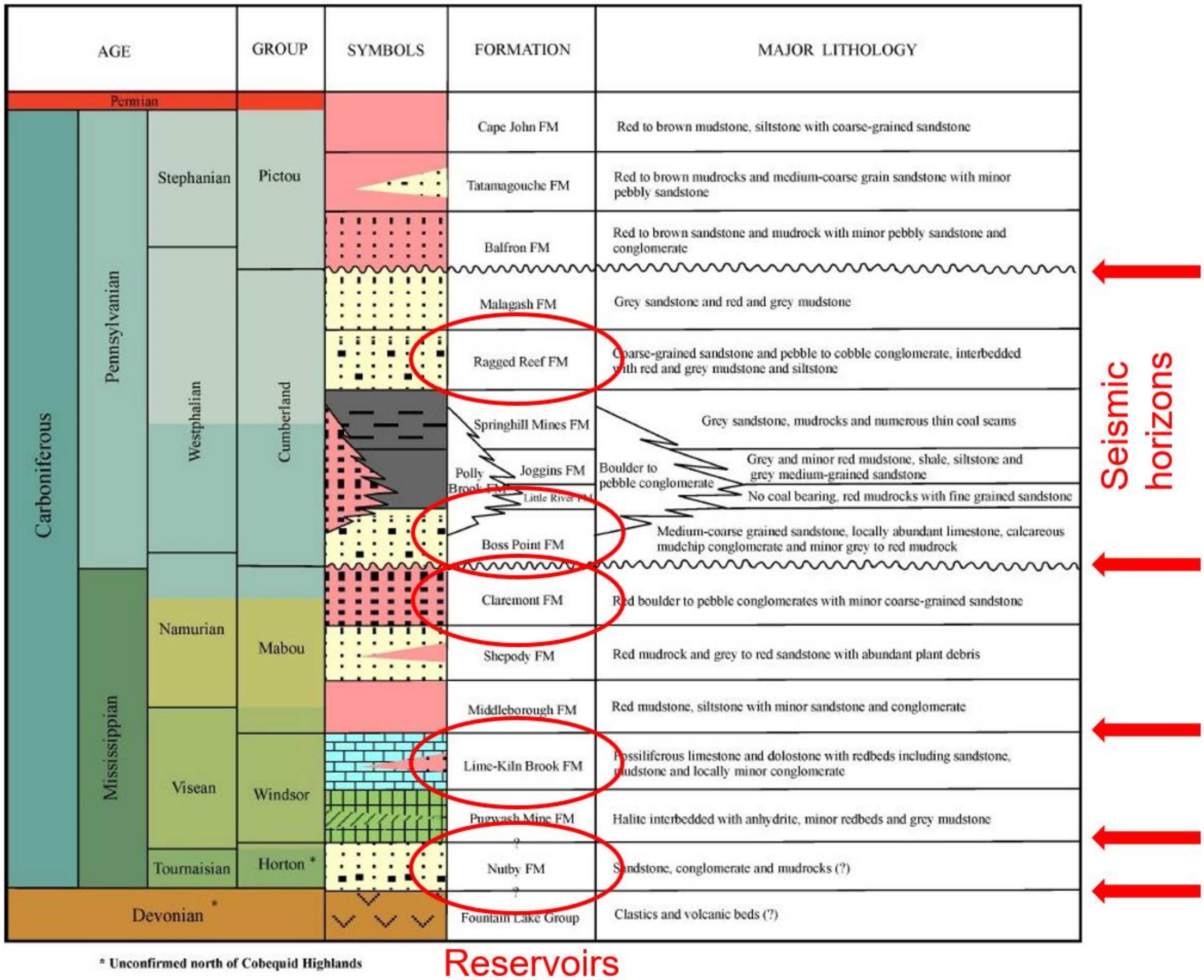

Figure 5.6. Stratigraphy of the Cumberland Basin with the most prospective petroleum reservoirs (potential aquifers) and the key seismic horizons used as proxies for these reservoirs. Adapted from Hayes et al. (2017) and NSDOE.

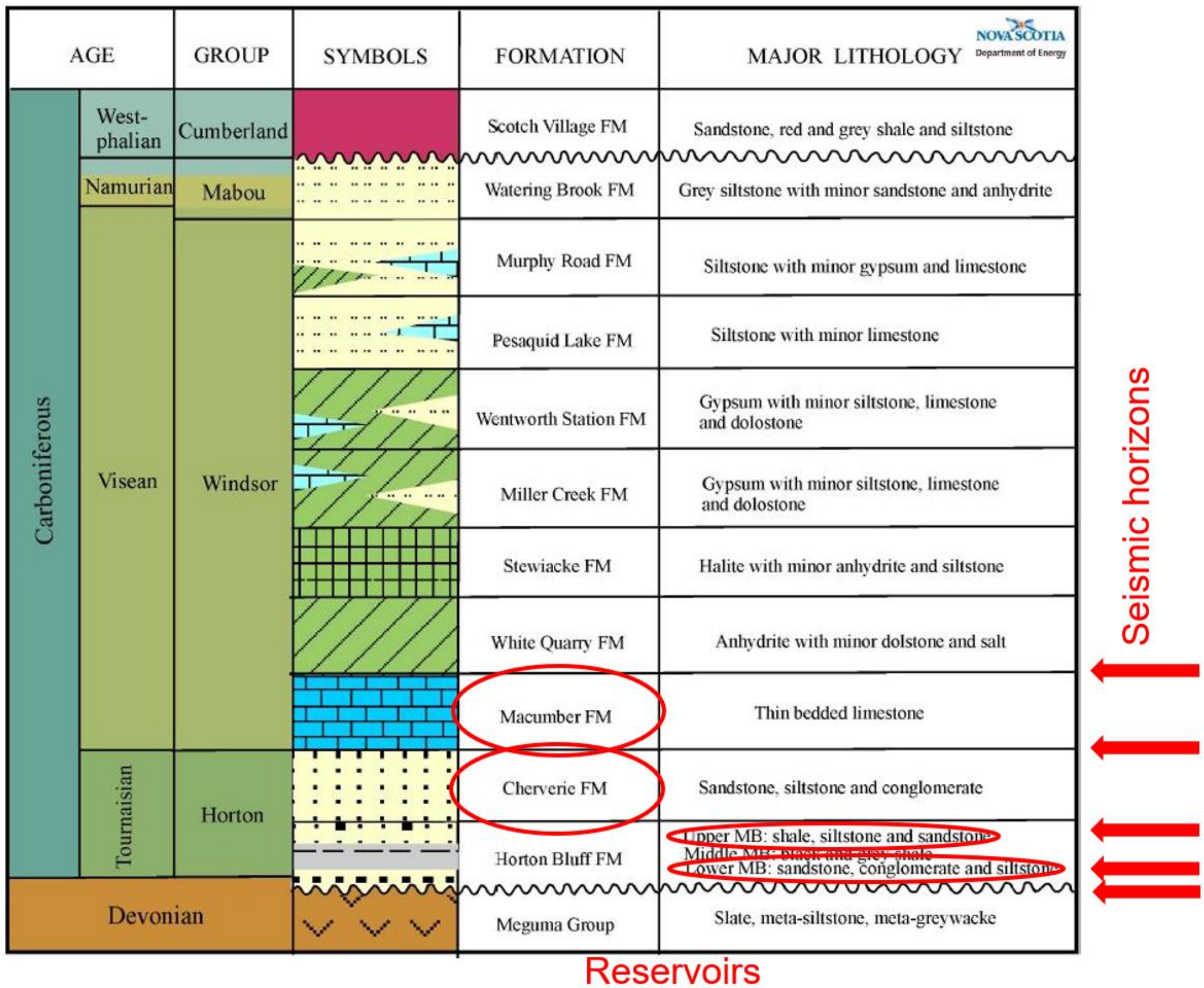

Figure 5.7. Stratigraphy of the Windsor-Kennetcook Basin with the most prospective petroleum reservoirs (potential aquifers) and the key seismic horizons used as proxies for these reservoirs. Adapted from Hayes et al. (2017) and NSDOE.

5.1.4 Ranking of the geothermal potential

The methodology used to identify and rank the geothermal potential for electricity generation and for direct-use of heat is adapted from Richard et al. (2016). It is based on five criteria, to which different weight factors are attributed in consideration of their relative importance:

- Temperature of the reservoir (× 3)
- Depth of the reservoir (× 3)
- Lithology of the reservoir (× 2)
- Temperature uncertainty at the scale of the basin (× 1)
- Geological uncertainty at the scale of the basin (× 1)

Each criterion is evaluated with a system of marks as follows:

Mark	Value	Description
+ or ++	+ 1 or + 2	**Positive or Very positive:** Promising potential, no negative impact expected
O	0	**Neutral:** Some technical limitations expected that can be resolved or mitigated
– or – –	- 1 or - 2	**Negative or Very negative:** Significant technical limitations, difficult to resolve or mitigate
⬢	Rejected	**Major hurdle:** Drawback that cannot be resolved or mitigated

5.1.4.1 Temperature of the reservoir

Reservoir temperature is the most critical parameter in determining geothermal potential. Although it is ultimately the temperature of the fluid produced at surface that dictates the performance of the system, the initial temperature of the reservoir at depth is the most practical characteristic that can be analysed. Reservoir temperature is estimated from the corrected temperatures presented in **Section 5.1.1**. Because of its importance, a weight factor of 3 is attributed to this parameter. Two different sets of intervals are defined for direct-use of heat and electricity generation. In the first case the minimum threshold to exploit the heat is 20 °C. For electricity generation this threshold is 80 °C.

Direct-use of heat	
++	≥ 80 °C
+	≥ 60 °C to < 80 °C
O	≥ 40 °C to < 60 °C
–	≥ 20 °C to < 40 °C
⬢	< 20 °C

Electricity generation	
++	≥ 160 °C
+	≥ 140 °C to < 160 °C
O	≥ 120 °C to < 140 °C
–	≥ 100 °C to < 120 °C
– –	≥ 80 °C to < 100 °C
⬢	< 80 °C

5.1.4.2 Depth of the reservoir

The drilling cost of a deep well increases exponentially with depth and can represent more than 60% of the total capital cost of a geothermal project (Tester et al., 2006). Although modern technology allows greater depths to be reached, the geothermal wells drilled to date have been limited to about 5 000 m (**Section 2**; Lukawski et al., 2014). The reservoir depth is inferred from the seismic horizons available for the Cumberland and Windsor-Kennetcook basins (Hayes et al., 2017) and from the formation tops for petroleum wells for the other basins. Because of its importance, a weight factor of 3 is attributed to this parameter. Two different sets of intervals are defined for direct-use of heat and for electricity generation. In the first case the maximum threshold to exploit the heat is set at 4 km. For electricity generation this threshold is set at 7 km. Depth ranges between 3-4 and 5.5-7 km, respectively for direct-use of heat and for electricity generation, can be considered but would have a detrimental impact on the economics of a project.

Direct-use of heat	
++	≤ 1 km
+	> 1 km to ≤ 2 km
O	> 2 km to ≤ 3 km
–	> 3 km to ≤ 4 km
⬣	> 4 km

Electricity generation	
++	≤ 3 km
+	> 3 km to ≤ 4 km
O	> 4 km to ≤ 5.5 km
–	> 5.5 km to ≤ 7 km
⬣	> 7 km

5.1.4.3 Lithological characteristics

A hydrothermal geothermal system must contain a hot fluid in a porous and permeable host rock. Some sedimentary rocks have sufficient porosity and permeability to provide the necessary water flow. They are referred to as potential reservoirs, in the petroleum sense. In other cases, the flow capability of the rock must be stimulated to attain an acceptable flux: the hydrothermal geothermal system is then referred to as an EGS (see **Section 1.1.3**). The more the host rock is stimulated, the more heat content becomes accessible. Sandstones that have a good permeability are considered the best aquifers. Carbonates (limestones and dolostones) tend to have a lower permeability, and fine-grained siliciclastics (mudstones, shales, siltstones) are assumed too tight to be considered without an EGS. The basement that underlies the sedimentary basins, made of magmatic or metamorphic rocks, must also be stimulated (EGS). Further discussion on the criteria used to identify the potential aquifers in sedimentary basins of Nova Scotia is presented in **Section 5.1.3**. No threshold is defined for the lithological characteristics of an aquifer, but a negative mark indicates that the rock must be stimulated in order to be considered as an aquifer. Because of its importance, a weight factor of 2 is attributed to this parameter.

Direct-use of heat and Electricity generation	
++	Sandstones / conglomerates or limestones with good porosity and permeability documented
+	Sandstones / conglomerates
O	Limestones
–	Mudstones / shales / siltstones / metamorphic and igneous rocks

5.1.4.4 Temperature uncertainty

The level of uncertainty regarding reservoir temperature is quite variable depending on the quality and the amount of data available. This parameter impacts the level of risk associated with site selection. The level of uncertainty is a subjective parameter used for comparing different locations, and a common value is attributed to all potential aquifers within a given basin. The number of temperature data used as input and their depths impact the level of uncertainty regarding reservoir temperature. Only the input temperature data measured at more than 1,000 m and for which a good level of confidence has been estimated are used here to evaluate this parameter. No evaluation can be done if the temperature data are of poor quality or absent.

Direct-use of heat and Electricity generation	
++	4 or more
+	3
O	2
–	1
⬣	Poor or no data

5.1.4.5 *Subsurface geological uncertainty*

The level of uncertainty regarding reservoir geology (its geometry, structure, lithology, etc.) is variable depending on the quality and the amount of data available. Similar to temperature uncertainty, this parameter impacts the level of risk associated with site selection. The level of uncertainty is a subjective parameter used for comparing different locations and a common value is attributed to all potential aquifers within a given basin. To evaluate this parameter, the number of wells and the amount of seismic coverage available at least in some representative areas of a given basin are considered. No evaluation can be done in the absence of well control.

Direct-use of heat and Electricity generation	
++	Good well control and extensive seismic interpretation available
+	Fair well control and fair seismic coverage
O	Poor well control and poor seismic coverage
–	Poor well control and no seismic coverage
⬣	No well control

5.2 Meguma terrane and the Devonian intrusives

The geothermal gradients for the Meguma terrane and for the Devonian intrusives have been calculated from temperature data by applying the correction for the paleoclimatic effect (**Section 5.1.1.2**).

In the case of the Meguma terrane, only two temperature data points are available, both measured at equilibrium at depths shallower than 1,000 m (333 and 607 m). Individual geothermal gradients have been calculated for each case, then averaged to obtain a final geothermal gradient calculated at 12.63 °C km^{-1} ± 0.04 at 470.5 m (n=2). The level of confidence is considered VERY GOOD.

Only two temperature data are available in the case of the Devonian intrusives as well, but only one of them is measured at equilibrium (at 480 m) while the second, measured at 1,450 m, has been attributed a poor level of confidence because the temperature reported in the original reference could not be verified. These results have not been averaged to obtain a single geothermal gradient for all Devonian intrusives because 1) the resulting calculated geothermal gradients are very different, 2) the level of confidence is different in both cases and 3) the differences can reflect different contents in radioactive minerals. Instead, the two separate geothermal gradients are used as low- and high-end scenarios, respectively calculated at 17.92 °C km^{-1} at 480 m and 41.86 °C km^{-1} at 1,450 m. The level of confidence is POOR in both cases.

It must be emphasized that the geothermal gradients calculated for both the Meguma terrane and the Devonian intrusives are based on only two temperature measurements in each case, which, on account of the spatial extent of the area considered, might not be sufficient to establish geothermal gradients representative over the whole area.

5.3 Abandoned mines

Because of the inconsistent nature of the data available for the abandoned mines (see **Section 4.4**), a methodology different than the one used for the sedimentary basins has been developed to evaluate the geothermal energy available from these mines. In the absence of depth data for coal mines, it was not possible to apply the geothermal gradients calculated for the corresponding sedimentary basins. In the absence of geothermal gradients for the metallic and industrial mineral mines located outside of a sedimentary basin, it was not possible to estimate a temperature despite the available depth data. The open-pit mines lacked both depth and temperature data. The common parameter to these various sub-datasets is the volume of ore extracted. Leveraging on this common ground, the geothermal energy potential has been evaluated based on a temperature differential, i.e., the difference between the surface temperature and the temperature of the water in the flooded underground mines or open-pits (**Figure 5.8**).

5.3.1 Assumptions

Several assumptions were necessary in order to overcome the lack of data in some cases and their wide diversity in other cases. For practical purposes, and to ensure that each mine can be compared to the others, the following parameters have been applied to all mines by default:

All mines
- System is operated over 25 years
- Groundwater recharge to the system is negligible
- Density of the ore: 2,700 kg/m^3
- Potential for heating: above 2 °C
- Potential for cooling: below 20 °C

Open-pit mines
- Maximum depth: 100 m
- Heat balance corrected with bedrock: 1.25 × water
- ΔT for heating: 5 °C
- ΔT for cooling: 13 °C

Underground mines
- Geothermal gradient: 20 °C km^{-1}
- Backfill: 75%
- Heat balance corrected with bedrock: 25 water

Coal mines
- Maximum depth: 500 m
- ΔT for heating: 10 °C
- ΔT for cooling: 8 °C

Metallic and industrial mineral mines
- Maximum depth: 250 m
- ΔT for heating: 7.5 °C
- ΔT for cooling: 10 °C

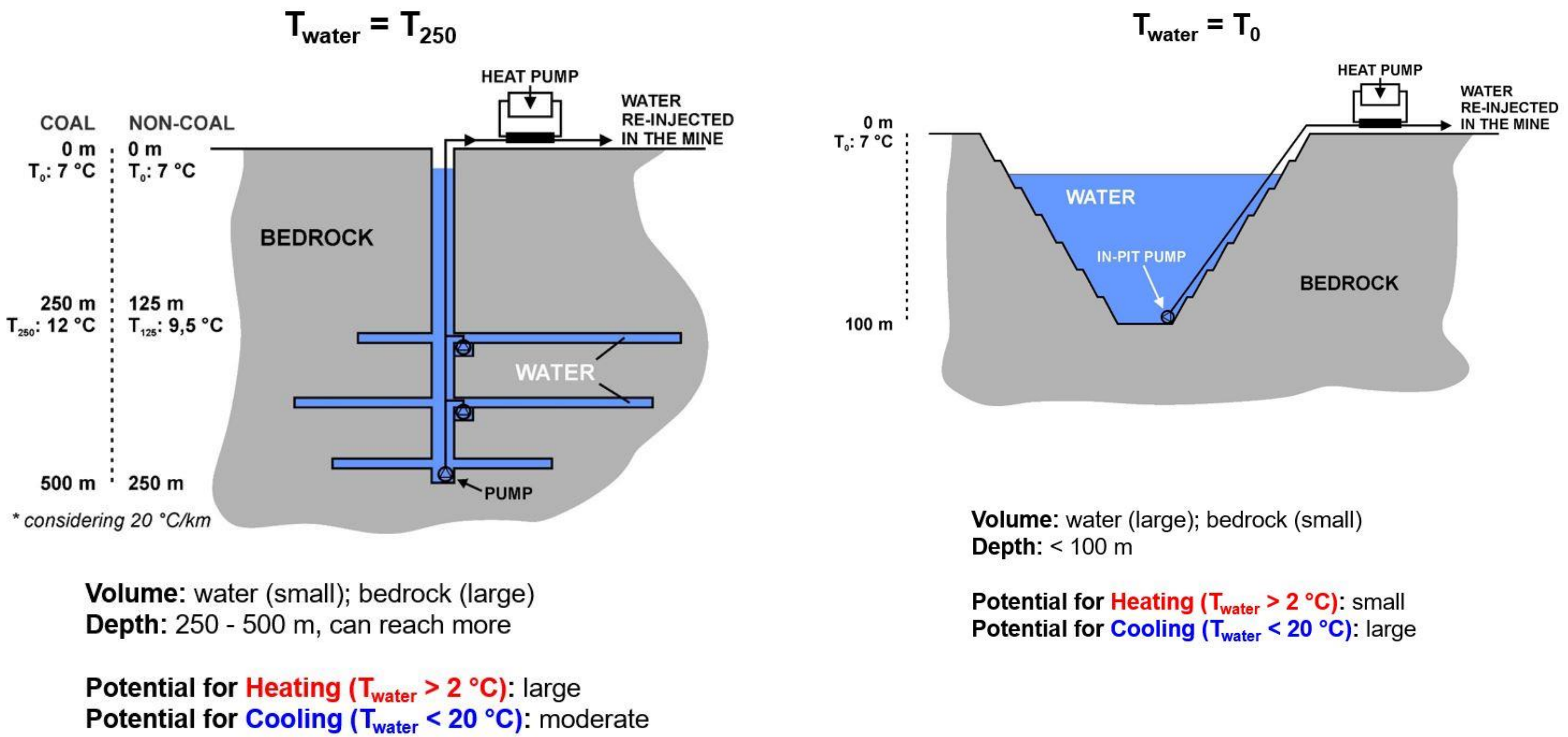

Figure 5.8. Schematic vertical profile of an open-pit mine with some of the assumptions considered.

5.3.2 Criteria

5.3.2.1 Objective criteria

The geothermal heating or cooling capacity of an abandoned underground or open-pit mine is directly related to its volume. Therefore, the calculated heating or cooling capacity expressed in Megawatts per hour (MWh) can be used as a direct indicator of the geothermal potential of a mine. In practice, the end-user facilities should not be located further than 2 km from the source. Mines that are consequently within a radius distance of 2 km from each other have been aggregated and their individual heating or cooling capacity have been summed.

As a point of reference, the heating of one hectare of greenhouses requires 7,000 MWh per year (2,832.8 MWh acre^{-1}) in southern Québec (Pelletier and Godbout, 2017). The engineering firm SNC Lavalin also estimated that a 0.1-hectare data centre (2.471 acres) has a cooling energy needs in southern Québec equivalent to 8,000 MWh per year (Comeau et al., 2019). For practical purpose, mines or aggregated mines with heating or cooling capacity of less than 10 MWh have been excluded from the evaluation.

Several assumptions have been applied to the calculation of mine geothermal heating or cooling capacity (see **Section 5.3.1**). The consequence is that the results are generalized and do not reflect the actual geothermal potential of a given mine but allow for quick appraisal of the overall potential from one area or mine to another. One of these assumptions is the geothermal gradient, which was set at 20 °C km^{-1} across the entire province. The actual geothermal gradients calculated for the different sedimentary basins are often higher than this value (see **Section 6**), which results in an increased geothermal heating capacity for the mines located in these basins. On the other hand, the geothermal gradient calculated for the Meguma terrane in the southern part of the province is lower than 20 °C km^{-1}so that the actual geothermal heating capacity for the mines in this area must be reduced accordingly. The opposite relationship has to be considered for the cooling capacity.

5.3.2.2 Subjective criteria

Aside from the objective criteria of the heating or cooling capacity of a mine expressed in MWh, its location relative to potential end-users can impact its value. This is a major difference from the potential for direct-use of heat at mid-depth or for electricity generation at greater depths, which typically extend across large areas. For this reason, the results are overlaid on the population distribution. The population map was prepared based the civic addresses and the community boundaries files available from the Government of Nova Scotia (2020). Each civic address has been assigned a population density of 2.1 inhabitants based on the most recent census (2016) from Statistics Canada. The total population of the province has been stable since the previous census of 2011 so that little changes are expected for the next census, scheduled in 2021. For reference purposes, the locations of existing greenhouses are also shown, based on the data available from the Government of Nova Scotia (2020). Other potential end-users can be added as needed.

These subjective criteria are useful to quickly identify the areas with promising heating or cooling geothermal potential that coincide with populated areas or with the presence of large greenhouse infrastructures, but they should not hinder the future potential of a less developed area where a high geothermal potential exists.

5.3.3 Energy balance

The overall energy available from mine water actually comes from the sum of the heat balance of the volume of water and the surrounding rock influenced by changes in water temperature. The extraction or injection of heat from mine water depends on the temperature of the water and rock, as well as their volume. The results of the heat balance calculation were based on a 25-year life cycle.

The consequence of applying the common assumptions of **Section 5.3.1** is that the results are generalized and do not reflect the actual geothermal potential of a given mine. For instance, some of the coal mines can be significantly deeper than the generic depth of 500 m (1,323 m in the case of Springhill). Conversely, it allows a quick appraisal of the overall potential from one area or mine to another. The actual parameters of a specific area or a specific mine can then be used to fine tune the initial results, using the following equations to estimate the energy balance calculation (**eqs. 5.7** and **5.8**):

$$P_n = (v \times \Delta T \times c) / t_n \times R \qquad \textbf{(eq. 5.7)}$$

With: P_n: Thermal power from the mine (MW)
v: Water volume (m^3)
ΔT: Temperature difference at which water can be heated/cooled (°C)
C: Volumetric heat capacity of water (4.184 MJ m^{-3} K^{-1})
t_n: Period of time during which energy is extracted (sec: 25 × 365 × 24 × 3,600)
R: Correction coefficient for the bedrock (underground: 25; open-pit: 1.25)

$$v = (O / \rho) \times (100 - B) /100 \qquad \textbf{(eq. 5.8)}$$

With: v: Water volume (m^3)
O: Total production of ore mined (1 tonne = 1,000 kg) (kg)
ρ: Rock density (2.70 kg m^{-3})
B: Backfilling of underground mine workings (75%)

5.3.4 Geothermal energy generation capacity

With a geothermal heat pump system, both heat and cold can be produced efficiently depending on the temperature of the water at the heat pump's inlet, according to a system-specific coefficient of performance (COP). An energy source, usually electricity, is required to operate the compressor of the ground-source heat pump system. This results in energy savings in both heating and cooling modes. However, the amount of energy required to operate the system's compressor is a function of the COP. The COP is calculated differently depending on a heating or cooling application. The geothermal energy generation capacity for heating and cooling is calculated using **Equations 5.9** to **5.13**. Individual results for each mine are detailed in **Appendix III**.

For heating:

$$P_{hp} = P_n / (COP - 1) \qquad \textbf{(eq. 5.9)}$$

$$P_{tot} = P_n + P_{hp} \qquad \textbf{(eq. 5.10)}$$

For cooling:

$$P_{hp} = P_n / (COP + 1) \qquad \textbf{(eq. 5.11)}$$

$$P_{tot} = P_n - P_{hp} \qquad \textbf{(eq. 5.12)}$$

$E_{tot} = P_{tot} \times 24 \times 365$ **(eq. 5.13)**

With: P_n: Thermal power from the mine (MW)
P_{hp}: Electrical power consumed by the heat pump (MW)
COP: Coefficient of performance of the heat pump (heating: 3.5; cooling: 4.5)
P_{tot}: Total power available (MW)
E_{tot}: Total geothermal energy available per year (MWh)

5.4 References

Beck, A.E., 1977. Climatically perturbed temperature gradients and their effect on regional and continental heat-flow means. Tectonophysics 41(1–3):17-39. https://doi.org/10.1016/0040-1951(77)90178-0

Bédard, K., Comeau, F.-A., Millet, E., Raymond, J., Malo, M., Gloaguen, E., 2016. Évaluation des ressources géothermiques du bassin des Basses-Terres du Saint-Laurent. INRS, Centre Eau Terre Environnement, Québec, Rapport de recherche R1659, 100 p. http://espace.inrs.ca/4845

Birch, A.F., 1948. The effects of Pleistocene climatic variations upon geothermal gradients. American Journal of Science 246(12):729-760. https://doi.org/10.2475/ajs.246.12.729

Blackwell, D.D., Richards, M., 2004. The 2004 geothermal map of North America. Explanation of resources and applications. GRC Transactions 28:317-320.

Blackwell, D., Richards, M., Stepp, P., 2010. Texas Geothermal Assessment for the I35 Corridor East - Final report. SMU Geothermal Laboratory, Southern Methodist University, 78 p.

Beardsmore, G.R., Cull, J.P., 2001. Crustal Heat Flow - A guide to measurement and modeling. Cambridge University Press, 324 p.

Chouinard, C., Mareschal, J.C., 2009. Ground surface temperature history in southern Canada: Temperatures at the base of the Laurentide ice sheet and during the Holocene. Earth and Planetary Science Letters 277(1–2)280-289. https://doi.org/10.1016/j.epsl.2008.10.026

Comeau, F.-A., Raymond, J. et Ngoyo Mandemvo, D.D., 2019. Évaluation du potentiel géothermique des mines désaffectées de Société Asbestos limitée à Thetford Mines. INRS, Centre Eau Terre Environnement, Québec, Rapport de recherche R1856, 63 p.

Frone, Z., Blackwell, D.D., 2010. Geothermal Map of the Northeastern United States and the West Virginia Thermal Anomaly. GRC Transactions 34:339-343.

Government of Nova Scotia, 2020. Nova Scotia Civic Address File; Nova Scotia Topographic Database. Geographic Data Directory files. https://nsgi.novascotia.ca/gdd/

Guillou-Frottier, L., 2006. Les empreintes paléothermiques du sous-sol. Geosciences 3:12-17.

Harrison, W.E., Luza, K.V., Prater, M.L., Reddr, R.J., 1983. Geothermal resource assessment in Oklahoma. Oklahoma Geological Survey, Special Paper 83-1, 42 p.

Horner, D.R., 1951, Pressure build-up in wells: Third World Petroleum Congress Proceedings, section II, WPC-4135:503-521.

Jaupart, C., Mareschal, J.-C., 2011. Heat generation and transport in the Earth. Cambridge University Press. Cambridge; New York, 464 p.

Jessop, A.M., 1971. The Distribution of Glacial Perturbation of Heat Flow in Canada. Canadian Journal of Earth Sciences 8(1):162-166, https://doi.org/10.1139/e71-012

Jessop, A.M., 1990. Thermal geophysics. Elsevier Publishing Co., 305 p.

Kehle, R.O., Schoeppel, R.J., Deford, R.K., 1970. The AAPG geothermal survey of North America. Geothermics 2(1):358-367. https://doi.org/10.1016/0375-6505(70)90034-9

Kutasov, I.M., Eppelbaum, L.V., 2010. A new method for determining the formation temperature from bottom-hole temperature logs. Journal of Petroleum and Gas Engineering 1(1):1-8.
NSDEM, 2020. Digital contours of sedimentary basins. Nova Scotia Department of Energy and Mines, unpublished data.
Pelletier, F. and Godbout, S., 2017. Consommation d'énergie et de gaz à effet serre en production serricole au Québec. Institut de recherche et de développement en agroenvironnement. Projet IRDA 400023, 36 p.
Timko, D.J., Fertl, W.H., 1972. How downhole temperatures, pressures affect drilling. World Oil 175:73-78.
Waples, D.W., Ramly, M., 2001. A statistical method for correcting log-derived temperatures. Petroleum Geoscience 7:231-240. https://doi.org/10.1144/petgeo.7.3.231
Waples, D.W., Pacheco, J., Vera, A., 2004. A method for correcting log-derived temperatures in deep wells, calibrated in the Gulf of Mexico. Petroleum Geoscience 10:239-245. https://doi.org/10.1144/1354-079302-542
Westaway, R., Younger, P.L., 2013. Accounting for palaeoclimate and topography: A rigorous approach to correction of the British geothermal dataset. Geothermics 48:31-51. https://doi.org/10.1016/j.geothermics.2013.03.009
Zare-Reisabadi, M., Kamali, M.R., Mohammadnia, M., Shabani, F., 2015. Estimation of true formation temperature from well logs for basin modeling in Persian Gulf. Journal of Petroleum Science and Engineering 125:13-22. https://doi.org/10.1016/j.petrol.2014.11.009

6. EVALUATION OF THE GEOTHERMAL POTENTIAL IN NOVA SCOTIA

Evaluation of the geothermal potential for electricity generation and direct-use of heat is primarily focused on the sedimentary basins because of the possible presence of deep aquifers. **Sections 5.1** and **5.2** describe the methodology used to calculate the geothermal gradients. Direct-use of heat and electricity generation are also theoretically possible in other geological environments when considering deep BHE or EGS (see **Section 1.1.3**). The criteria considered to evaluate the geothermal potential and the results of this evaluation are presented in **Section 5.1.4** for electricity generation and direct-use of heat together.

The geothermal potential of abandoned mines, as established following the methodology presented in **Section 5.3**, is directly related to the volume of ore extracted and is essentially independent from the geological environment of a given mine. Therefore, the evaluation of the geothermal potential of abandoned mines is not restricted to the sedimentary basins. The criteria considered to evaluate this potential are presented in **Section 5.3.2**.

6.1 Sedimentary basins

The spatial distribution and magnitude of the geothermal gradients calculated for individual wells is shown on **Figure 6.1**. The gradients for each sedimentary basin are summarised on **Figure 6.2**. Refer to **Appendix IV** for details.

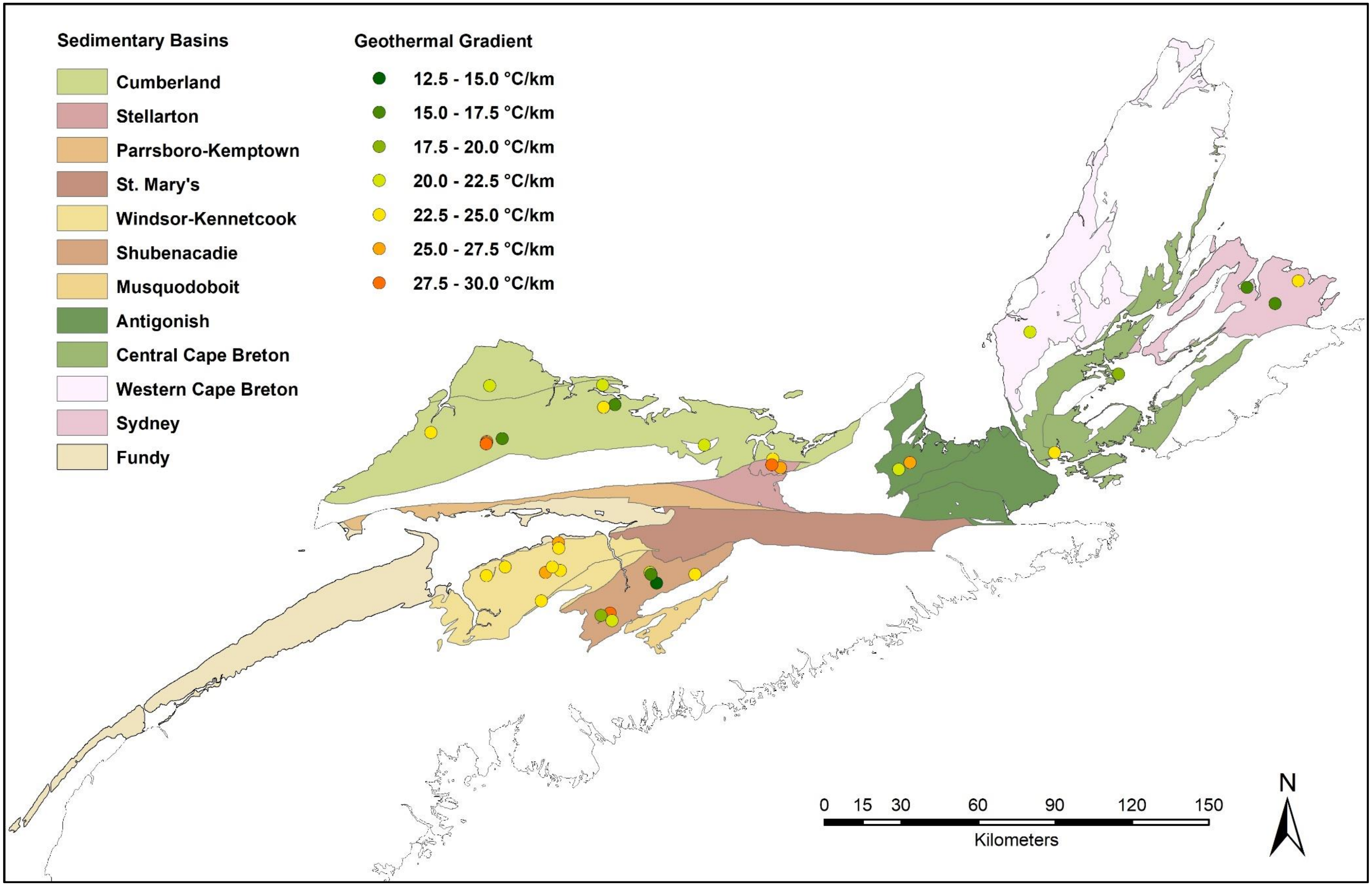

Figure 6.1. Geothermal gradients calculated for each well in the sedimentary basins. Refer to **Appendix IV** for details. Cartographic background: NSDEM (2020).

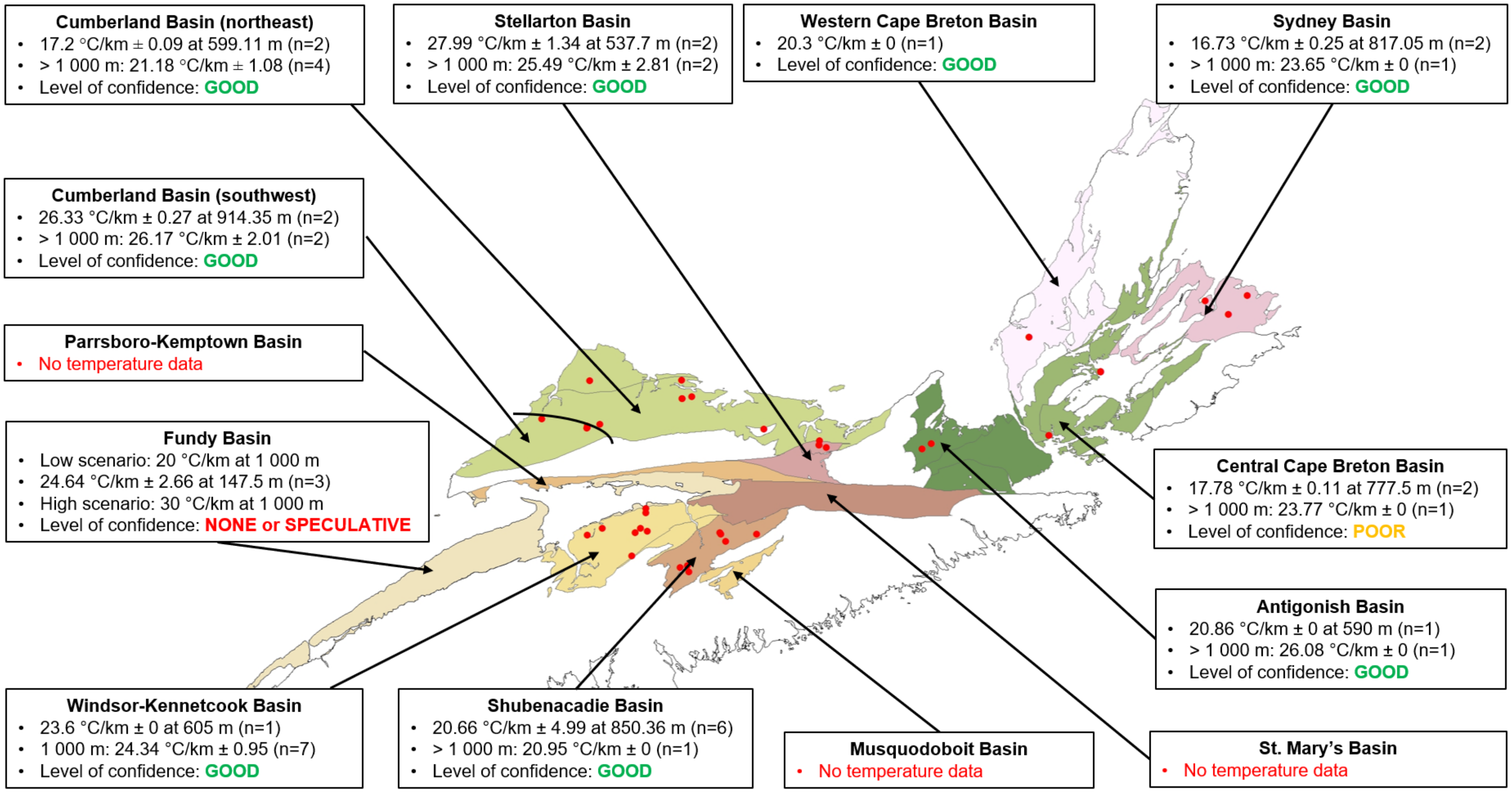

Figure 6.2. Geothermal gradients calculated for the different sedimentary basins. Red dots: wells with temperature data used to calculate the geothermal gradients. Refer to **Appendix IV** for details. Cartographic background: NSDEM (2020).

6.1.1 Cumberland Basin

The Cumberland Basin benefits from a good well control and an extensive seismic coverage, so that a basin-wide evaluation of the geothermal potential is possible in this basin (**Figure 6.3**). Seismic horizons provided by the NSDEM (see Hayes et al., 2017) were used as proxies for potential aquifers (**Figure 5.6**). The altitude in the basin varies from 0 to 237 m above sea level, with a median of 52 m. Consequently, a bulk shift of + 50 m was applied to the seismic horizons, which were provided in metres below mean sea level. Two representative geothermal gradients of the Cumberland Basin at depths greater than 1,000 m were calculated. The distinction was made to account for the greater thickness of the sedimentary strata to the southwest, which resulted in a higher geothermal gradient for this area compared to the northwest. The geothermal gradient is calculated at 21.18 °C km^{-1} ± 1.08 in the northwest, and at 26.17 °C km^{-1} ± 2.01 in the southwest. Detailed results for each gradient are presented in **Appendix IV**. Each potential aquifer is evaluated and ranked for direct-use of heat and electricity generation. The potential aquifers considered include, from top to base:

- The Boss Point and Claremont formations, represented by the seismic horizon of the base of the Cumberland Group
- The carbonates of the Windsor Group, represented by the seismic horizon of the base of the Mabou Group
- The upper part of the Horton Group, represented by the seismic horizon of the base of the Windsor Group
- The top of the underlying basement (as an indication of the conditions at the base of the basin)

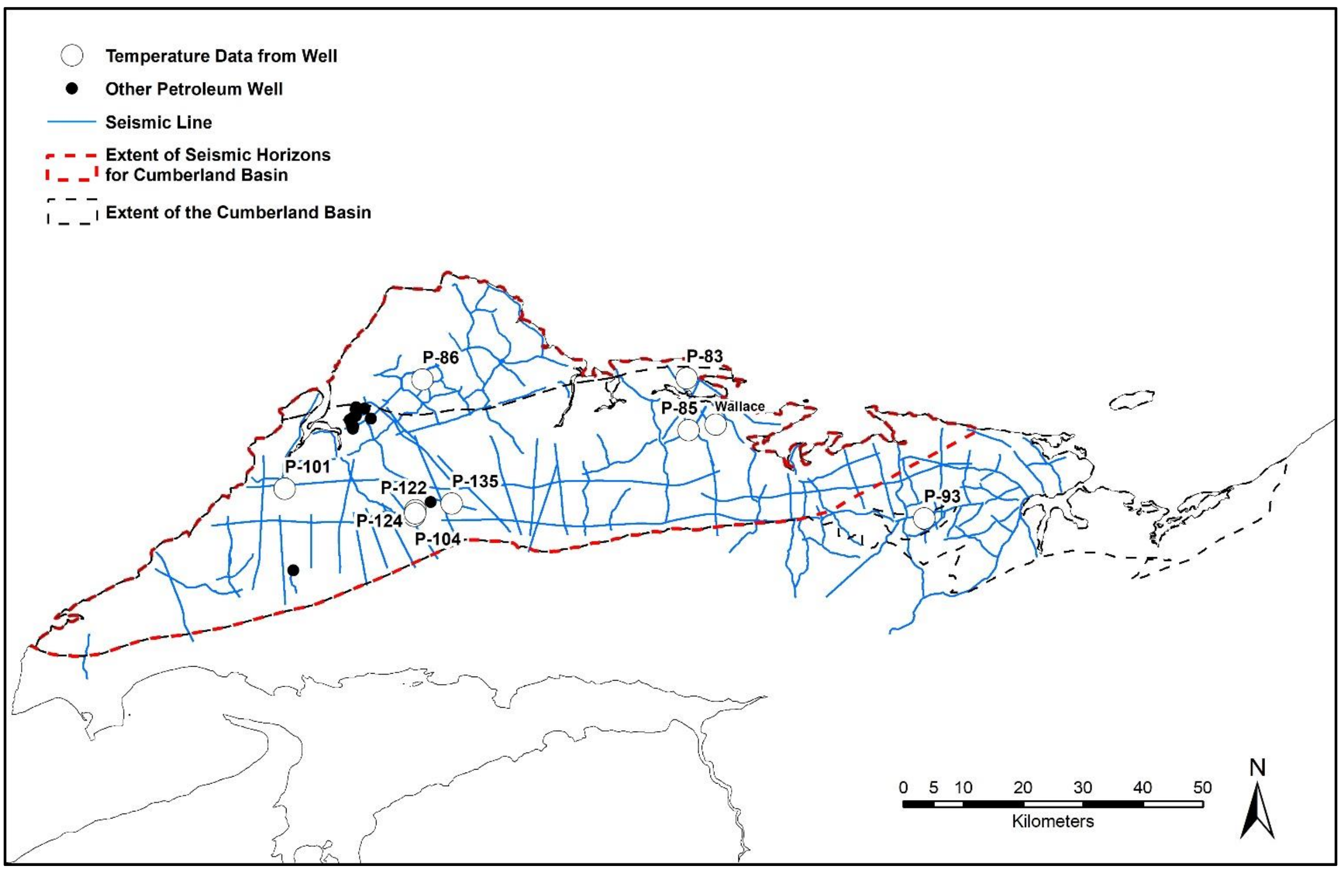

Figure 6.3. Available underground temperatures and subsurface data for the Cumberland Basin. Seismic horizons created from 2D seismic lines span across most of the basin. The evaluation of the geothermal potential is limited to the extent of the seismic horizons.

6.1.1.1 Electricity generation

The individual scores obtained by each potential aquifer for electricity generation vary from – 4 to + 11 points across the basin (**Figure 6.4**). The highest score is assigned to the base of the Cumberland Group (+ 8 to + 11 points), followed by the base of the Mabou Group (+ 7 points). Most of the electricity generation potential of both of these geological groups is in the deepest part of the basin (southwest), but smaller areas of lower potential are also present to the east, with scores in the range of + 1 to + 5 points. The base of the anhydrite of the Windsor Group and the top of the basement are associated with lower scores, with a maximum of + 5 points to the southwest and – 4 or less to the east. These units are too shallow in the northern part of the basin and too deep in the southwestern part of the basin to have any potential for electricity generation.

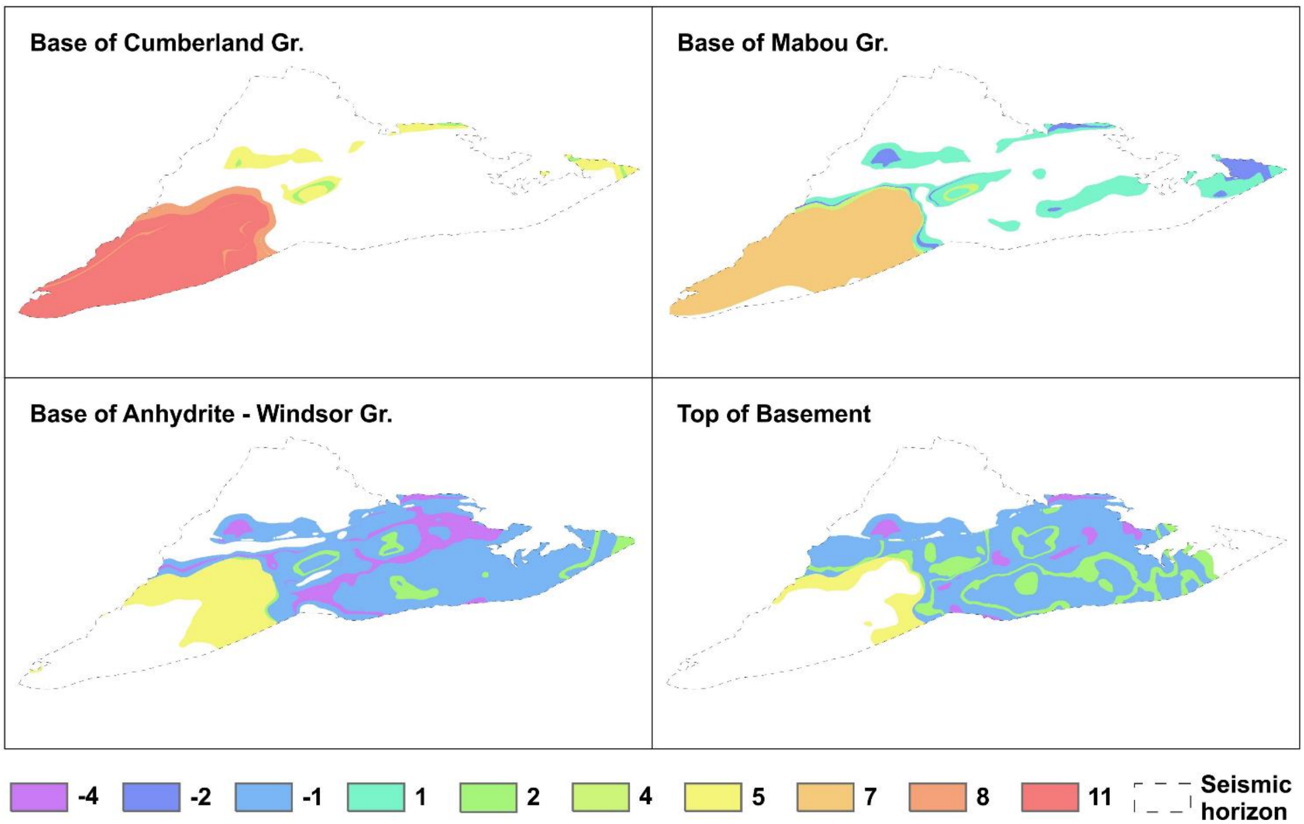

Figure 6.4. Scores obtained for electricity generation for each potential aquifer and for the top of the basement of the Cumberland Basin.

The global score obtained by summing up the individual scores (excluding the top of the basement) varies from – 6 to + 23 across the basin (**Figure 6.5**). This display emphasizes the importance of the southwestern part of the basin for electricity generation, while the northern and eastern parts have only a marginal to non-existent potential. The sharp contact between the southwestern and northeastern zones correspond to a decrease in the depth of strata to the southwest.

Detailed results for the evaluation of Area EG-C (located on **Figure 6.5**) are further presented below. This area is selected for its representativeness of the higher-end scores obtained for electricity generation.

Area EG-C obtains a global score of + 23 points (**Table 6.1**), with the most promising potential represented by the aquifer corresponding to the base of the Cumberland Group (+ 11 points) due to its more favourable lithology. All potential aquifers in this area are encountered at depths between 5.5 and 7 km, and the expected temperature is always above 160 °C except for some parts of the base of the Cumberland Group, where it could be in the range of 140 to 160 °C. The area immediately to the west of Area EG-C shares overall similar characteristics, but it obtains a comparatively lower global score because the base of the anhydrite of the Windsor Group becomes deeper than 7 km and ceases to be considered for electricity generation. Area EG-C covers some 293 km^2 (about 19 x 15 km).

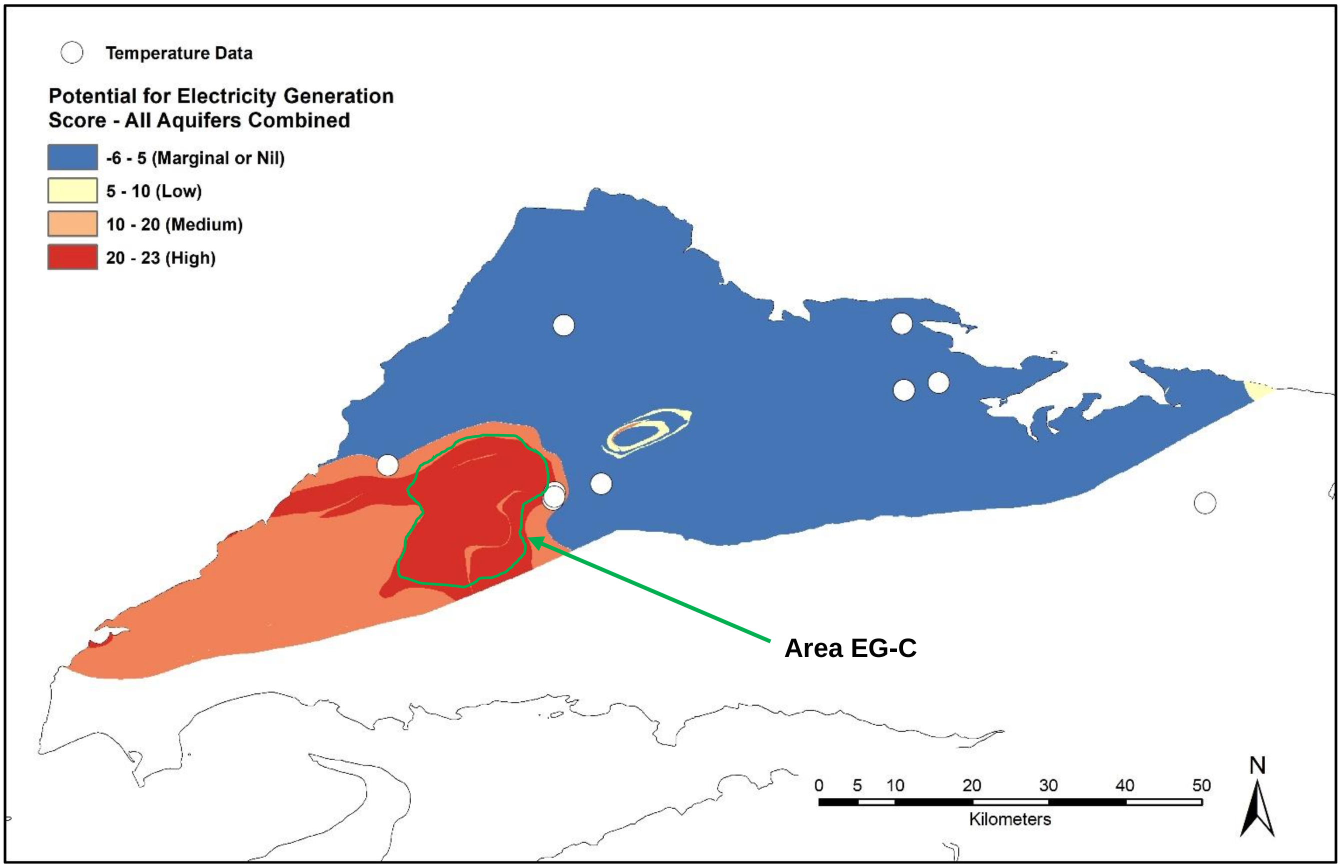

Figure 6.5. Global score obtained for electricity generation by combining all superposed potential aquifers for the Cumberland Basin. Refer to text for details on Area EG-C.

Table 6.1. Ranking of the potential aquifers for electricity generation in Area EG-C.

Potential Aquifer	Temperature of the Reservoir	Depth of the Reservoir	Lithology	Temperature Uncertainty	Subsurface Geological Uncertainty	Score (Aquifer)	Score (Global)
Base Cumberland	++	–	++	++	++	11	23
Base Mabou	++	–	O			7	
Base Anhydrite	++	–	–			5	
Top Basement	++	⬣	–			⬣	

6.1.1.2 Direct-use of heat

The individual scores obtained by each potential aquifer for direct-use of heat vary from + 2 to + 14 across the basin **(Figure 6.6**). The highest score is obtained for the base of the Cumberland Group (+ 11 to + 14), followed by the base of the Mabou Group (+ 6 to + 7). Both potential aquifers have the same spatial extent. The base of the anhydrite of the Windsor Group obtains lower scores (+ 2 to + 5) and its potential is geographically limited to the northern (shallower) part of the basin. The southwestern part of the basin, along with scattered areas to the east, have no potential for direct-use of heat due to their comparatively greater depth. The zoning observed in the score maps is due to the interplay between the marks obtained for different depth and temperature ranges.

The global score obtained by summing up the individual scores (excluding the top of the basement) varies from 0 to +26 across the basin (**Figure 6.7**). In this display, areas corresponding to high scores are more extensively developed to the north, consistent with the absence of potential for the anhydrite at the base of the Windsor Group in the southeast. The southwestern part of the basin has no potential for direct-use of heat.

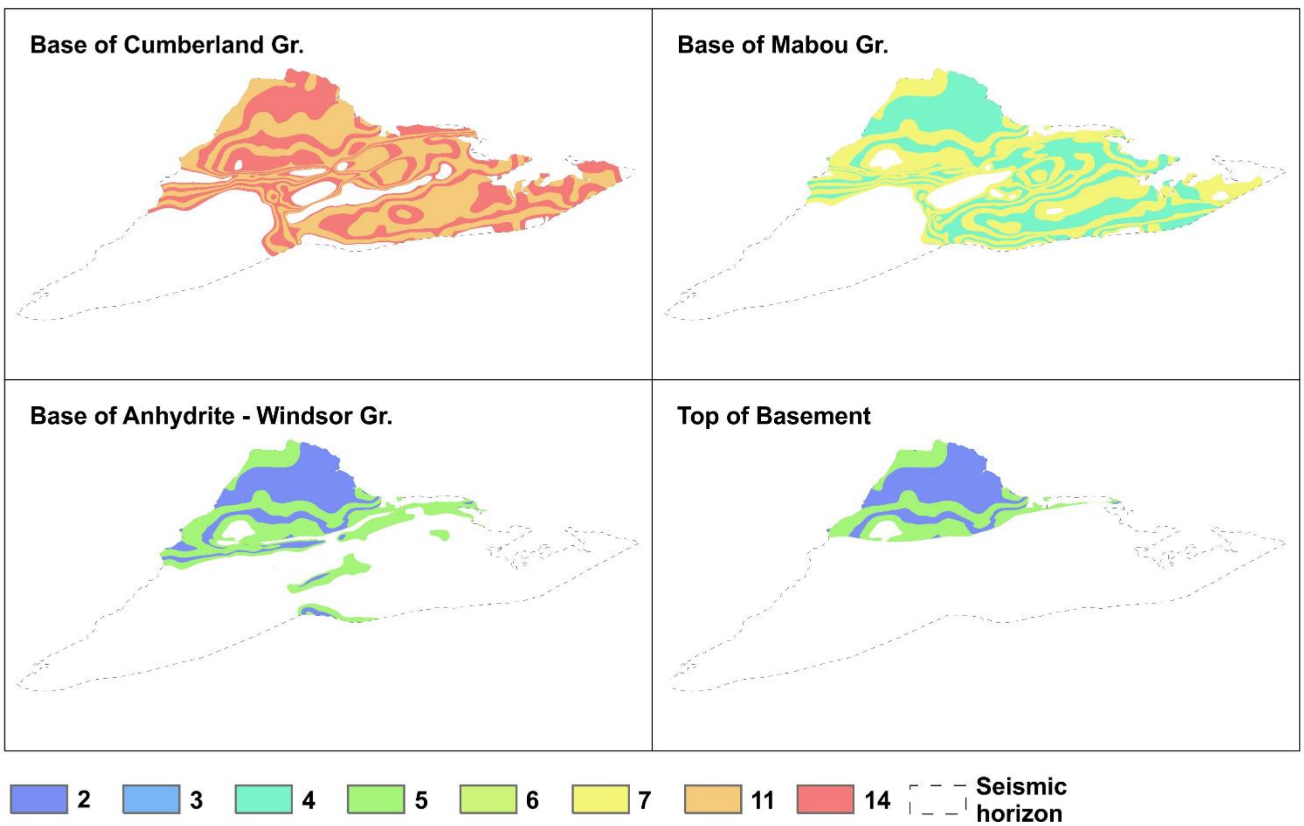

Figure 6.6. Scores obtained for direct-use of heat for each potential aquifer and for the top of the basement of the Cumberland Basin.

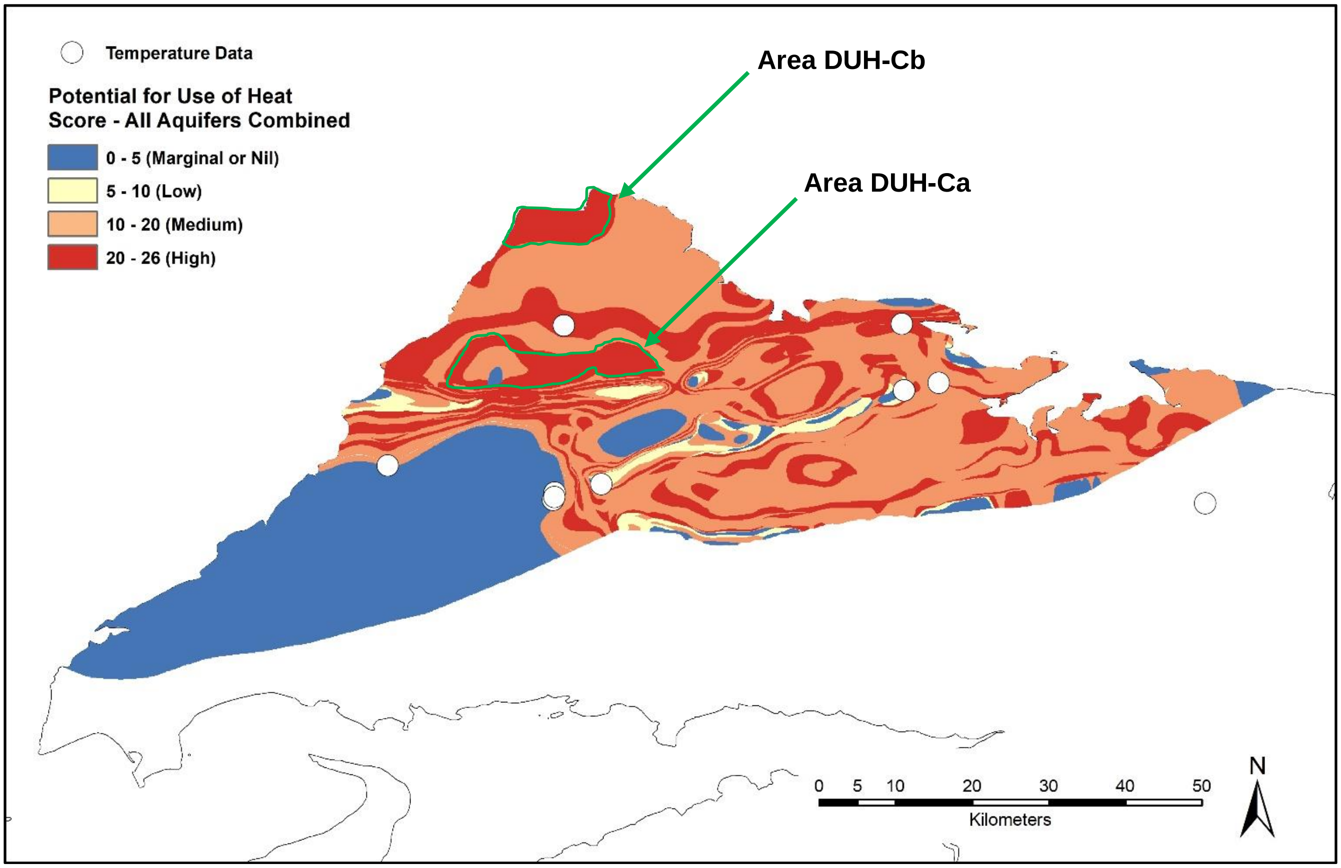

Figure 6.7. Global score obtained for direct-use of heat by combining all superposed potential aquifers for the Cumberland Basin. Refer to text for details on areas DUH-Ca and DUH-Cb.

Detailed results for the evaluation of areas DUH-Ca and DUH-Cb (located on **Figure 6.7**) are further presented below. These areas are selected because they are representative of the higher-end scores obtained for direct-use of heat. However, the identical scores obtained for both areas express significantly different characteristics.

In the case of Area DUH-Ca (**Table 6.2**), the depth of all potential aquifers is between 1 and 2 km and the expected range of temperatures varies between 40 and 60 °C. Although some internal variation (in both temperature and depth) occurs within the aquifer represented by the base of the Cumberland Group, the differences in the individual scores obtained by each potential aquifer are essentially related to their respective lithologies. This area covers some 63 km^2 (about 4 × 15 km).

By contrast, the geothermal potential of Area DUH-Cb (**Table 6.3**) for direct-use of heat is reached at greater depths, between 3 and 4 km, but the expected temperatures exceed 80 °C and a geothermal potential for electricity generation is also present in this area (temperature range of 80 to 100 °C). However, the potential of this area is not uniform, with less potential to the west and a global score up to + 26 to the east. Area DUH-Cb covers some 92 km^2 (about 4 × 23 km).

Table 6.2. Ranking of the potential aquifers for direct-use of heat in Area DUH-Ca.

Potential Aquifer	Temperature of the Reservoir	Depth of the Reservoir	Lithology	Temperature Uncertainty	Subsurface Geological Uncertainty	Score (Aquifer)	Score (Global)
Base Cumberland	O	+	++	++	++	11	23
Base Mabou	O	+	O			7	
Base Anhydrite	O	+	–			5	
Top Basement	O	+	–			5	5

Table 6.3. Ranking of the potential aquifers for direct-use of heat in Area DUH-Cb.

Potential Aquifer	Temperature of the Reservoir	Depth of the Reservoir	Lithology	Temperature Uncertainty	Subsurface Geological Uncertainty	Score (Aquifer)	Score (Global)
Base Cumberland	++	–	++	++	++	11	23
Base Mabou	++	–	O			7	
Base Anhydrite	++	–	–			5	
Top Basement	++	–	–			5	5

6.1.2 Windsor-Kennetcook Basin

Like the Cumberland Basin, the Windsor-Kennetcook Basin benefits from a good well control and an extensive seismic coverage, so that a basin-wide evaluation of the geothermal potential is possible in this basin (**Figure 6.8**). The Rawdon Block outlined on **Figure 6.8**, although part of the Windsor-Kennetcook Basin, was not evaluated. It consists in a horst structure with an overall lower geothermal potential than the rest of the basin.

Seismic horizons provided by the NSDEM (see Hayes et al., 2017) are used as proxies for potential aquifers (**Figure 5.7**). The altitude of the basin varies from 0 to 226 m above sea level, with a median of 49 m. A bulk shift of + 50 m was therefore applied to the seismic horizons, which were provided in metres below mean sea level.

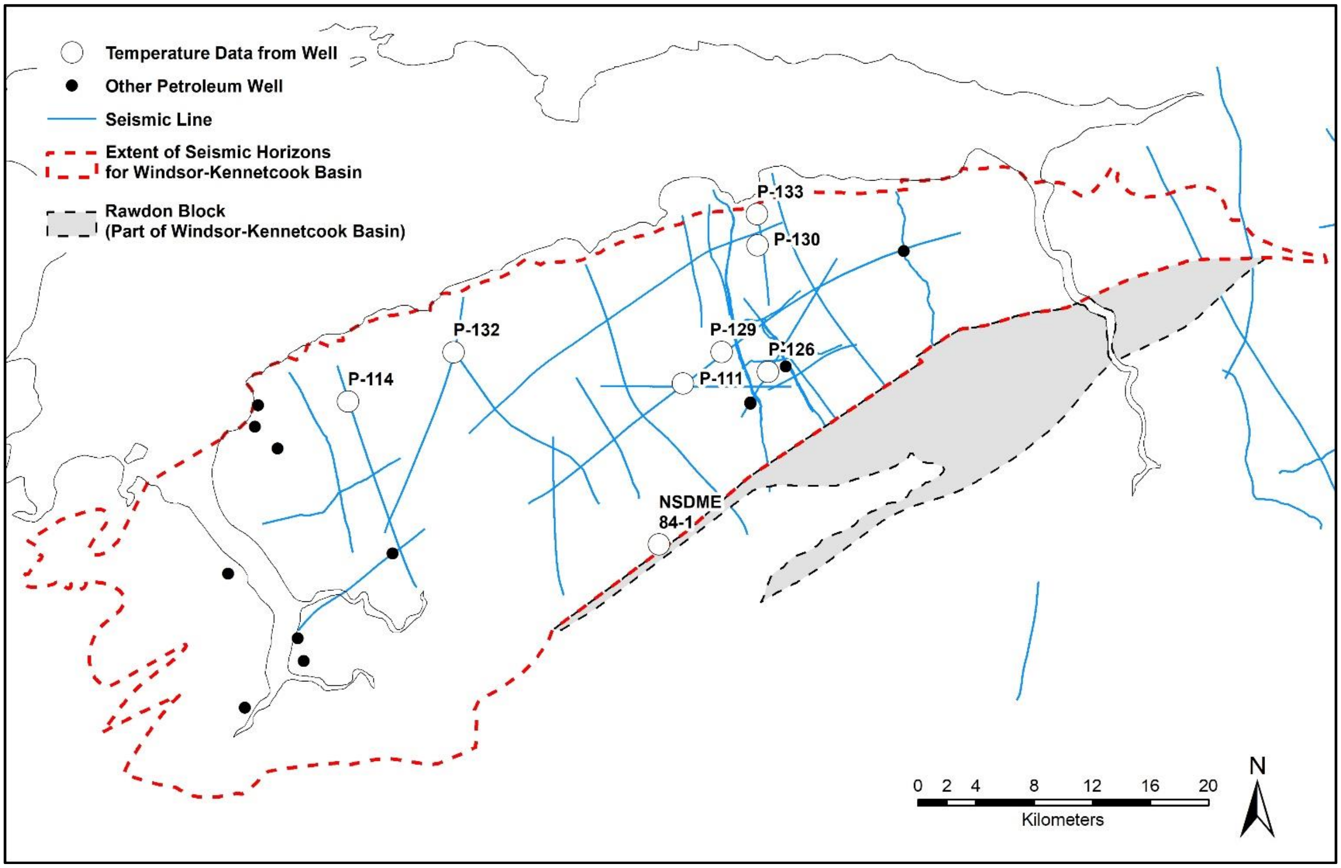

Figure 6.8. Available underground temperature and subsurface data for the Windsor-Kennetcook Basin. The evaluation of the geothermal potential covers the extent of the seismic horizons, excluding the Rawdon Block.

The geothermal gradient representative of the Windsor-Kennetcook Basin at depths greater than 1,000 m is calculated at 24.34 °C km^{-1} ± 0.95. Detailed results are presented in **Appendix IV**.

Each potential aquifer is evaluated and ranked for direct-use of heat and electricity generation. Because a seismic horizon is available to define the top each of these stratigraphic units, the following potential aquifers are considered, from top to base:

- The Macumber Formation
- The Cheverie Formation
- The upper member of the Horton Bluff Formation
- The lower member of the Horton Bluff Formation
- The top of the underlying basement (as an indication of the conditions at the base of the basin)

6.1.2.1 Electricity generation

A geothermal potential for electricity generation exists only along a narrow zone of the lower member of the Horton Bluff Formation and of the underlying basement in the north-centre part of the basin, with individual scores varying from – 1 to + 2 (**Figure 6.9**). The apparent higher score obtained locally for the top of the basement (+ 2) must be considered cautiously because of the deficient seismic control in this specific area (**Figure 6.9**): 1) the quality of a seismic line tends to degrade at its terminations and 2) artifacts can develop at the edges of the interpolated seismic horizons.

The global score obtained by summing up the individual scores of these two units varies from – 2 to + 4 (**Figure 6.10**). The summation of negative individual scores (– 1) results in increasingly negative global scores (– 2), translating the overall negative characteristics of each potential aquifer over a given area.

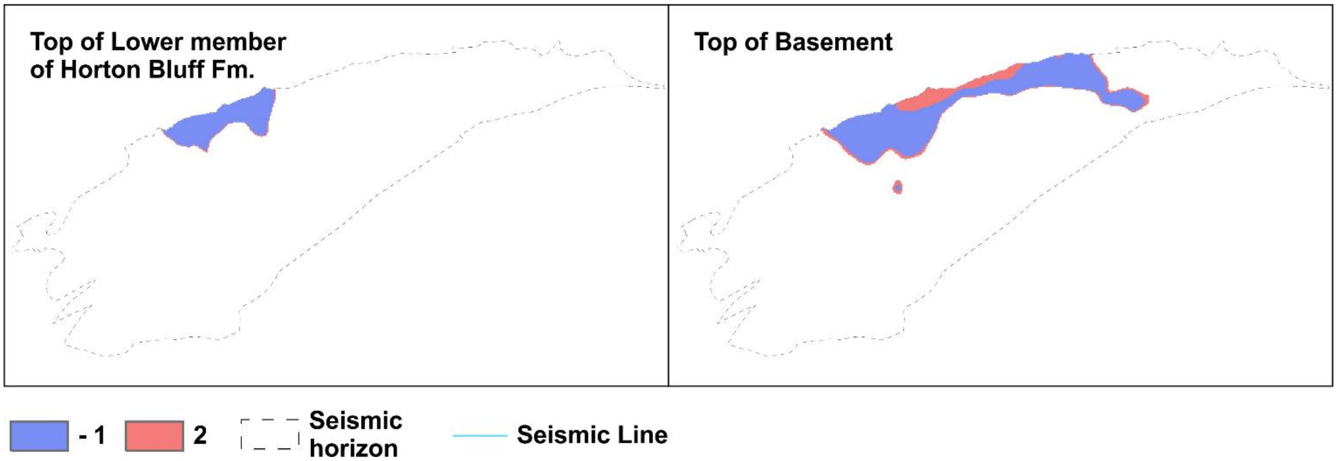

Figure 6.9. Scores obtained for electricity generation for the top of the Lower member of the Horton Bluff Formation and the top of the basement of the Windsor-Kennetcook Basin.

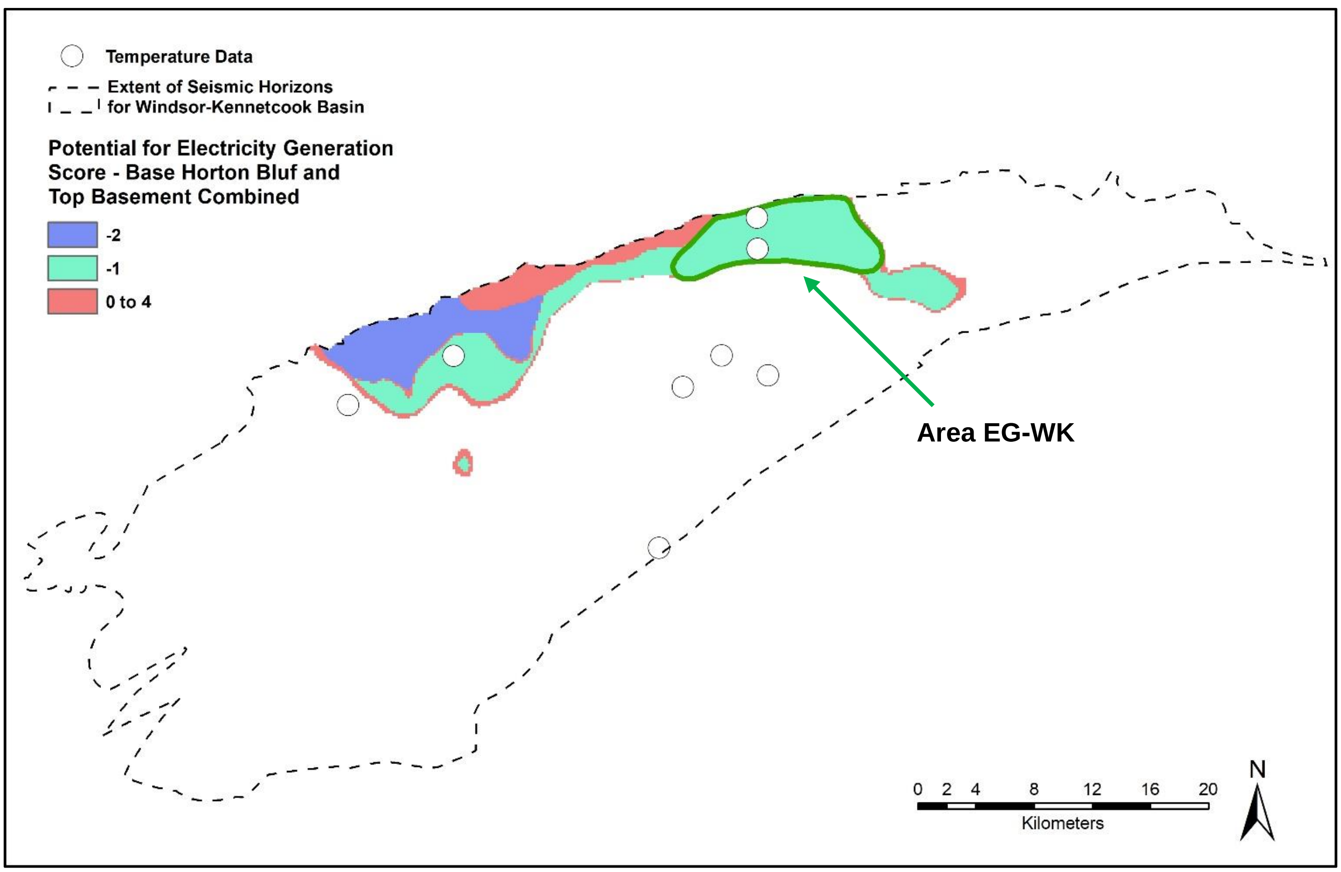

Figure 6.10. Global score obtained for electricity generation by combining the top of the Lower member of the Horton Bluff Formation and the top of the basement for the Windsor-Kennetcook Basin. Refer to text for details on Area EG-WK.

Detailed results for the evaluation of Area EG-WK (located on **Figure 6.10**) are further presented below. This area is selected because it is representative of the potential of the top of the basement for electricity generation. The subsurface control over this area is also better than for the adjacent area with a higher score (see discussion above). Area EG-WK is also comparable to the westernmost part of the area prospective for electricity generation. To the west, the Lower member of the Horton Bluff Formation provides an additional potential aquifer, but it needs to be stimulated (as does the basement), so that the considerations relevant to Area EG-WK also apply to the west. This area covers some 50 km^2 (about 13 × 4 km).

Area EG-K has a global score of – 1 point which corresponds to the individual score of the sole potential aquifer considered here, namely the top of the basement (**Table 6.4**). In this specific case, the score obtained by the basement has to be included in the global score. In this area, the potential for electricity generation is limited to the lowest temperature interval (80 to 100 °C) at the depth of the top of the basement (3 to 4 km). This potential can obviously increase with increasing depth to the basement. This potential aquifer would require stimulation to develop its geothermal potential.

Table 6.4. Ranking of the top of the basement for electricity generation in Area EG-WK.

Potential Aquifer	Temperature of the Reservoir	Depth of the Reservoir	Lithology	Temperature Uncertainty	Subsurface Geological Uncertainty	Score (Aquifer)	Score (Global)
Top Horton Bluff (Lower member)	⬣	+	–	++	++	⬣	-1
Basement	– –	+	–			-1	

6.1.2.2 Direct-use of heat

The individual scores obtained for each potential aquifer vary from + 2 to + 9 across the basin (**Figure 6.11**). The highest score is assigned to the Cheverie and Glass Sand formations, followed by the overlying Macumber Formation. The upper and lower members of the Horton Bluff Formation and the top of the basement obtain the lowest scores. The geothermal potential of the high-score potential aquifers is restricted to the south-centre of the basin, while the spatial extents of the lower member of the Horton Bluff Formation and of the basement span across the whole basin.

The global score obtained by summing up the individual scores (excluding the top of the basement) varies from + 20 to + 40 across the basin (**Figure 6.12**). In this display, the south-centre part of the basin stands out, in agreement with the evaluation of the individual potential aquifers. This global score is representative of the combined geothermal potential of the superposed potential aquifers. It is useful as a tool to quickly appraise the variation of the geothermal potential across the basin, but it can be misleading and must be used with caution in so far as, over a given area, one or more potential aquifers having very low scores can mask the outstanding geothermal potential of another potential aquifer.

Detailed results for the evaluation of Area DUH-WK (located on **Figure 6.12**) are further presented below. This area is selected because it stands out as being representative of the most promising potential for direct-use of heat in the Windsor-Kennetcook Basin, and it has been preferred over other areas in the basin with a comparable score because its extent minimizes the risk of possible unintended mapping effects due to subsurface geological uncertainties. This area covers some 12 km^2 (about 2 × 6 km).

Area DUH-WK has a global score of + 35 points (interval + 30 to + 35 on **Figure 6.12**). The ranking of each potential aquifer is shown in **Table 6.5**. The Cheverie and Glass Sand formations stand out with the highest score (+ 9 points). A temperature of 40 to 60°C is expected between 1 and 2 km depth for these potential aquifers. The Macumber Formation and the Upper member of the Horton Bluff Formation offer similar characteristics in terms of temperature and depth but their lithologies are less favourable in terms of permeability and the second, if targeted, must be stimulated. The underlying Lower member of the Horton Bluff Formation offers higher temperatures (60 to 80°C), but at greater depths (2 to 3 km) and would require stimulation to develop its geothermal potential.

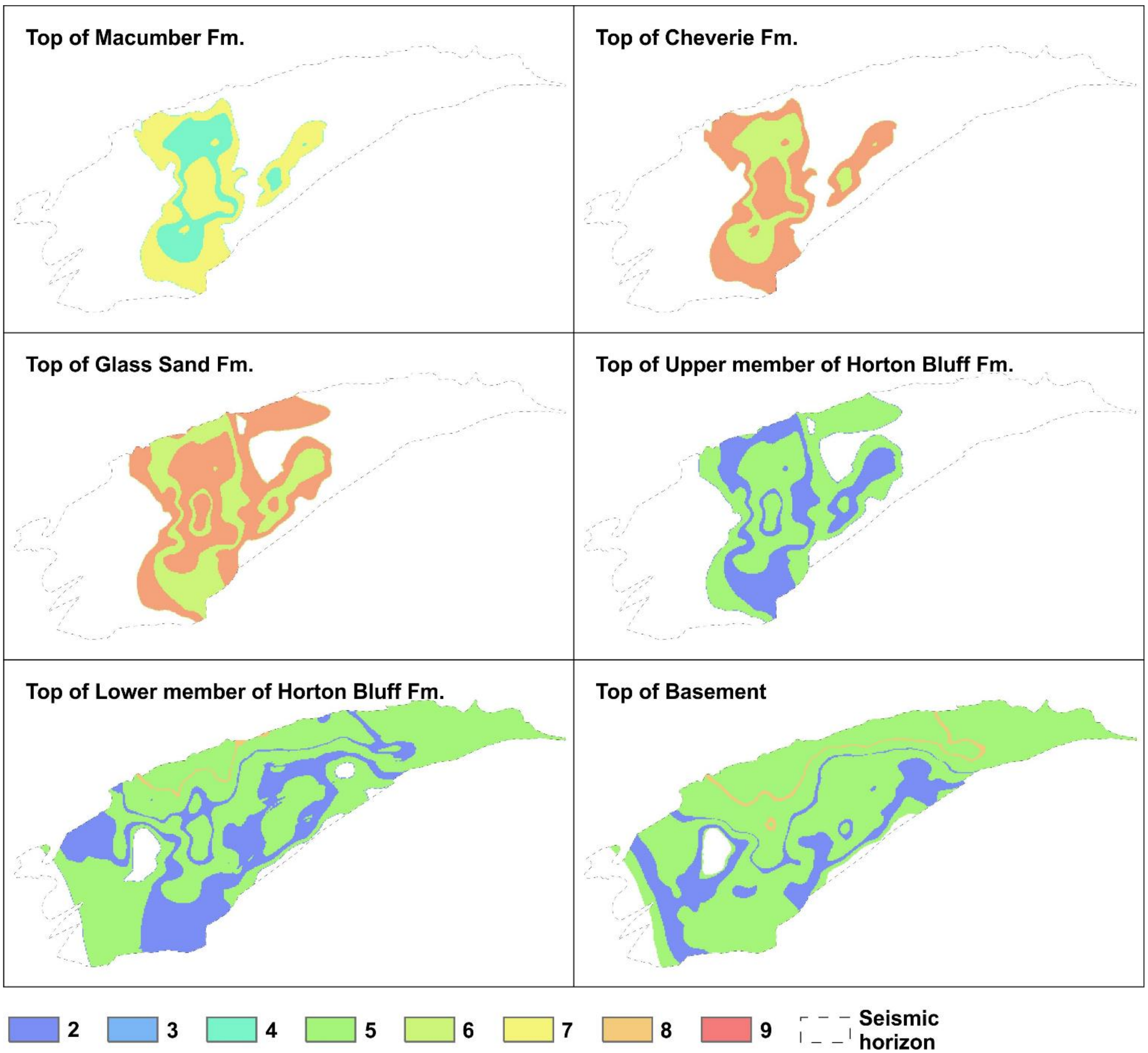

Figure 6.11. Scores obtained for direct-use of heat for each potential aquifer and for the top of the basement of the Windsor-Kennetcook Basin.

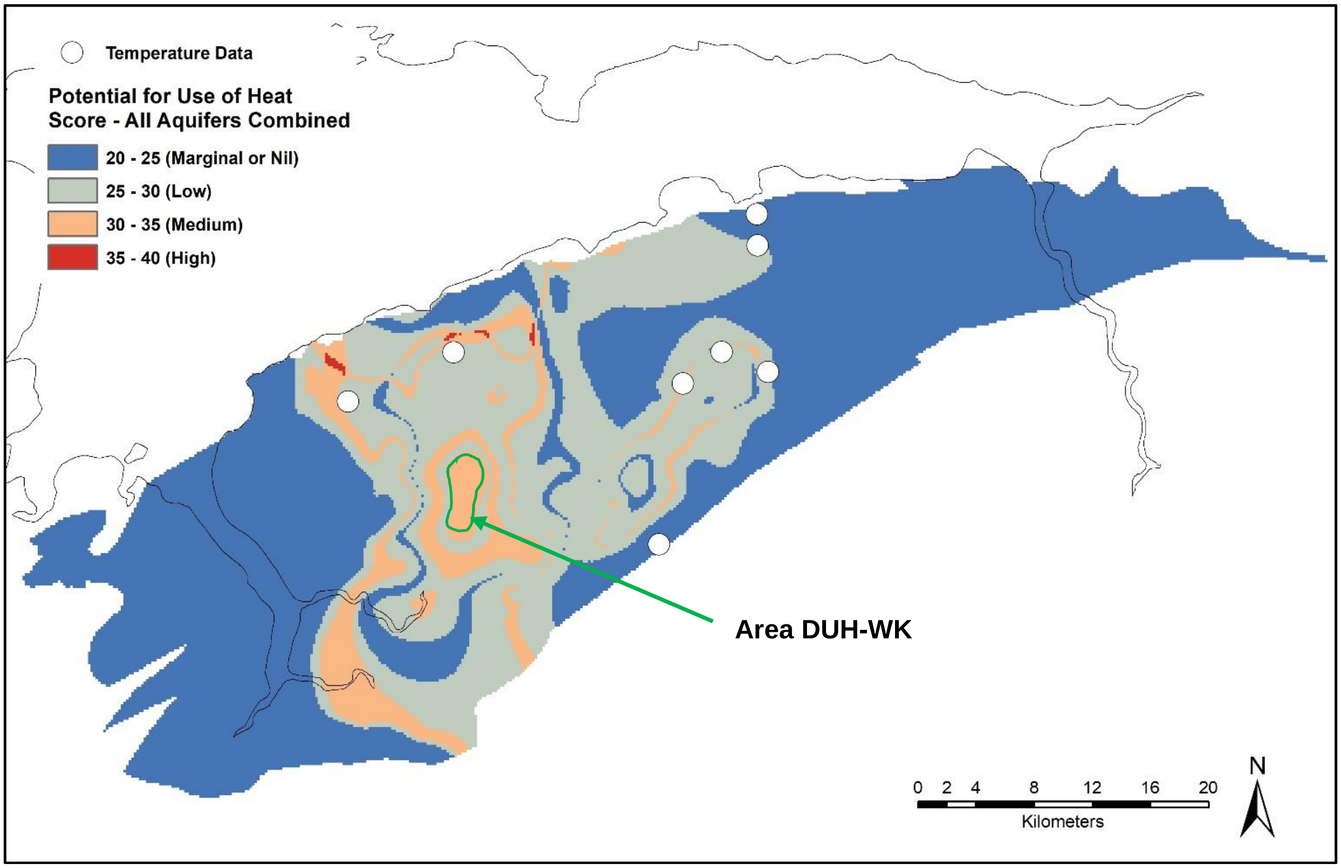

Figure 6.12. Global score obtained for direct-use of heat by combining all superposed potential aquifers for the Windsor-Kennetcook Basin. Refer to text for details on Area DUH-WK.

Table 6.5. Ranking of the potential aquifers for direct-use of heat in Area DUH-WK.

Potential Aquifer	Temperature of the Reservoir	Depth of the Reservoir	Lithology	Temperature Uncertainty	Subsurface Geological Uncertainty	Score (Aquifer)	Score (Global)
Top Macumber (or Top Gays River)	O	+	O	+ +	+ +	7	35
Top Cheverie	O	+	+			9	
Top Glass Sand	O	+	+			9	
Top Horton Bluff (Upper member)	O	+	–			5	
Top Horton Bluff (Lower member)	+	O	–			5	
Top Basement	+	O	–			5	5

6.1.3 Stellarton Basin

The geothermal gradient calculated for the Stellarton Basin is one of the highest obtained for the province. Unfortunately, a comprehensive evaluation of the geothermal potential of this basin is not currently possible due to the current lack of subsurface data. The formation tops available from the wells drilled in the basin cannot be used to identify potential aquifers because the Stellarton Basin has been explored mostly for its coal and oil shale potential. Only one seismic line has been shot across the basin (**Figure 6.13**). The thickness of the basin is also subject to debate, as Jiang et al. (2016) estimate that the top of the basement is shallower than 2,000 m while Smith et al. (1999) place it at a depth greater than 2,500 m.

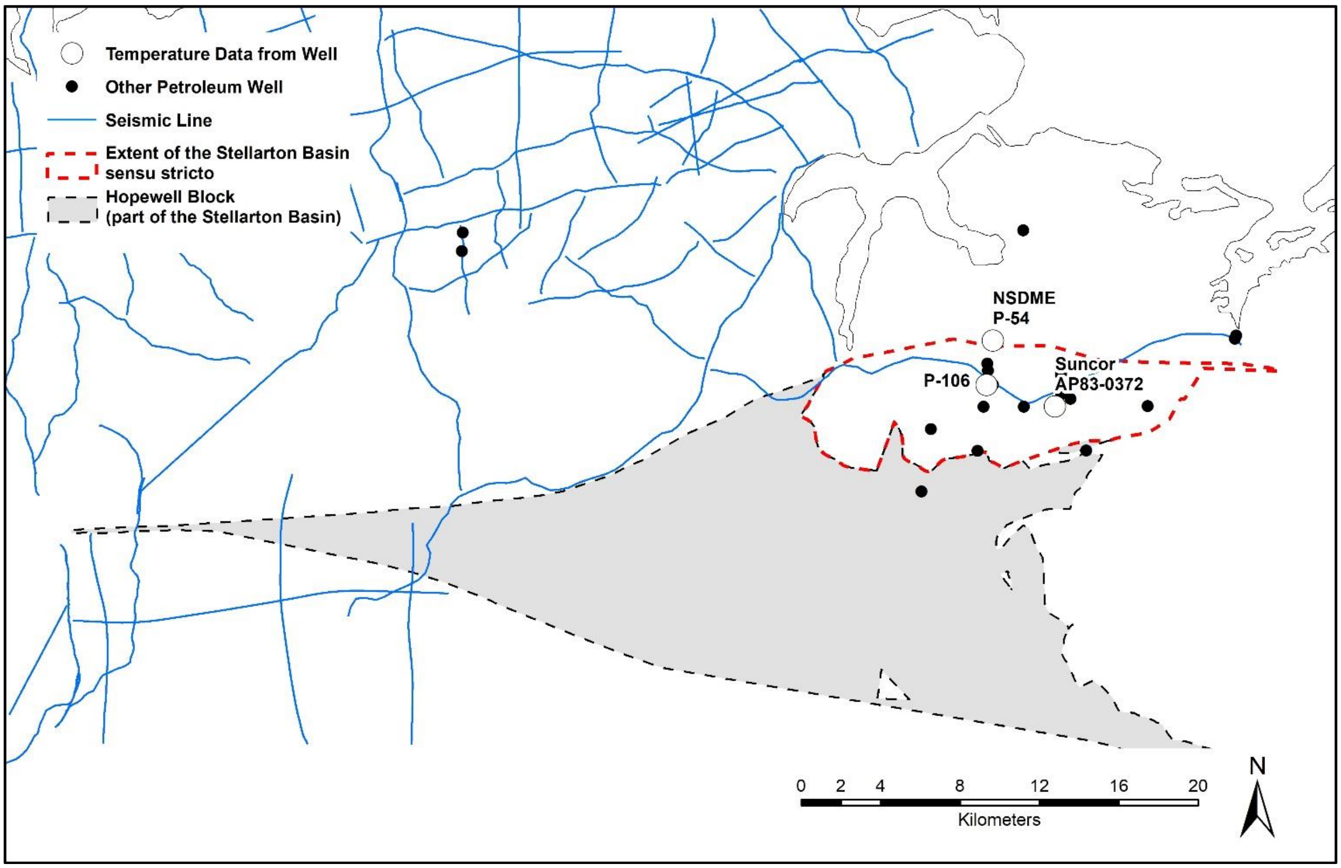

Figure 6.13. Available underground temperature and subsurface data for the Stellarton Basin. The Hopewell Block is included in the Stellarton Basin but has no associated temperature data.

6.1.3.1 Direct-use of heat and electricity generation

Using the geothermal gradient of 25.49 °C km^{-1} ± 2.81 calculated for depths greater than 1,000 m (see detailed results in **Appendix IV**), a hypothetical aquifer at 2,500 m would have an estimated temperature of 70.96 °C ± 7.02. A temperature of 80 °C, beyond which electricity generation can be considered, would be reached at a depth of 2,786 m ± 285.

These values are considered conservative. Currently, the geothermal gradient calculated for the basin is constrained by only two data points. The geothermal gradient representative for depths shallower than 1,000 m is calculated at 27.99 °C ± 1.34 (see **Appendix IV** and Michel, 2007). Drury et al. (1987) discuss the existence of deep-seated hydrothermal fluids migrating through fault conduits to explain the unexpectedly high geothermal gradients observed locally at shallow depths in the basin.

The thickness of the basin is subject to uncertainty (see above). For the sake of the evaluation, hypothetical sandstone aquifers are considered at fixed depths, down to 2,500 m. These hypothetical aquifers are evaluated and ranked for the entire area covered by the Stellarton Basin *sensu stricto* (**Table 6.6**). It is important to note that the existence and the characteristics of these hypothetical aquifers must be confirmed before any further evaluation of the geothermal potential can be undertaken.

It must be additionally noted that the input underground temperature data available for the Stellarton Basin are contrasted and that those retained for the present evaluation are considered conservative. Local geothermal gradients obtained for some individual wells are in the range of 30 to 40 °C km^{-1} at depths below 1,000 m (**Appendix IV**). These unusually high values for the province could correspond to locations where deep-seated hydrothermal fluids are migrating upward along fault zones, as suggested in Drury et al. (1987).

Table 6.6. Ranking of hypothetical aquifers in the Stellarton Basin.

Potential Aquifer	Temperature of the Reservoir	Depth of the Reservoir	Lithology	Temperature Uncertainty	Subsurface Geological Uncertainty	Score (Aquifer)
Hypothetical - 1 000 m	–	+	+	–	O	**1**
Hypothetical - 1 500 m	O	+	+			**7**
Hypothetical - 2 000 m	O	O	+			**1**
Hypothetical - 2 500 m	+	O	+			**7**
Basement	+	O	–			**3**

6.1.4 Shubenacadie Basin

The subsurface of the Shubenacadie Basin is documented by a few seismic lines and a few petroleum wells, from which only one has reached a depth greater than 1,000 m (**Figure 6.14**). The thickness of the basin varies between 830 and 1,055 m based on the well penetrations, but can increase slightly to the northwest. The geothermal gradient representative of the Shubenacadie Basin is in the range of 20 to 21 °C km^{-1} (detailed results are presented in **Appendix IV**).

6.1.4.1 Direct-use of heat and electricity generation

The geothermal potential has been evaluated in the vicinity of well P-108 (**Figure 6.14**), the deepest well drilled in the basin. This well intersects two potential aquifers, the Macumber and Cheverie formations, at 996 m and 1,008 m respectively. The basement is reached at 1,055 m, a depth that corresponds to an expected temperature of about 28 °C. Therefore, only the potential for direct-use of heat is evaluated.

As expected, the results of the evaluation (**Table 6.7**) indicate that, for the area around well P-108, the Macumber and Cheverie formations have a low potential for direct-use of heat, limited to the lowest temperature range (20 to 40 °C). The score of the Macumber Formation carbonates is slightly higher than for the Cheverie Formation sandstones because of the relative depth of each unit, but the difference is minimal. As discussed earlier, it is possible that this potential increases slightly to the northwest of the well P-108 but the absence of subsurface data makes it difficult to confirm this hypothesis.

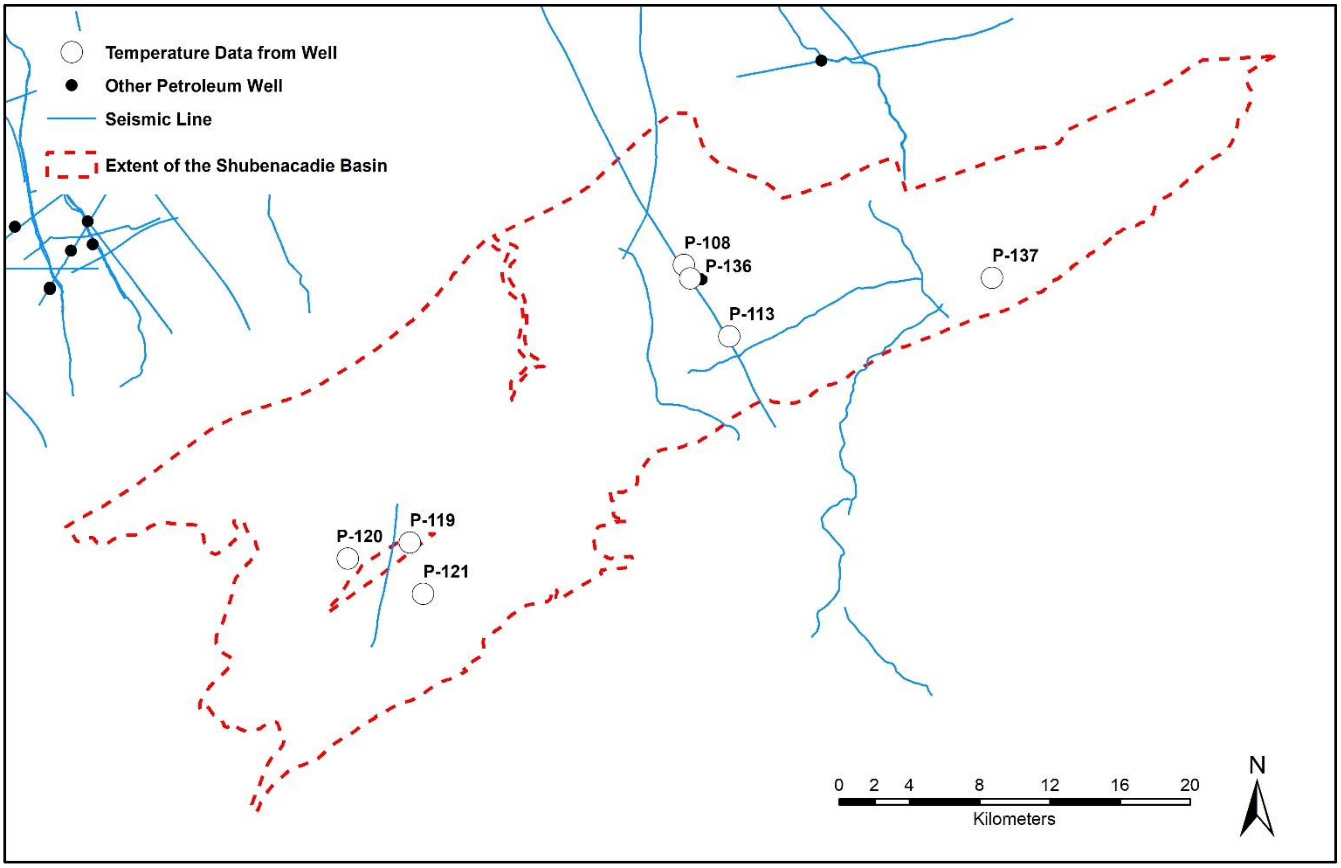

Figure 6.14. Available underground temperature and subsurface data for the Shubenacadie Basin.

Table 6.7. Ranking of the potential aquifers for direct-use of heat in the vicinity of well P-108.

Potential Aquifer	Temperature of the Reservoir	Depth of the Reservoir	Lithology	Temperature Uncertainty	Subsurface Geological Uncertainty	Score (Aquifer)	Score (Global)
Top Macumber	–	++	O	–	O	2	1.5
Top Cheverie	–	+	+			1	
Top Basement	–	+	–			-3	

6.1.5 Antigonish Basin

The subsurface of the Antigonish Basin is documented by a few seismic lines and a few petroleum wells, mostly located in the central part of the basin (**Figure 6.15**). The thickness of the basin in the central part is estimated to be about 1,025 m based on two well penetrations. The geothermal gradient representative of the Central Antigonish Basin for depths greater than 1,000 m is calculated to be 26.08 °C km^{-1} (see detailed results in **Appendix IV**).

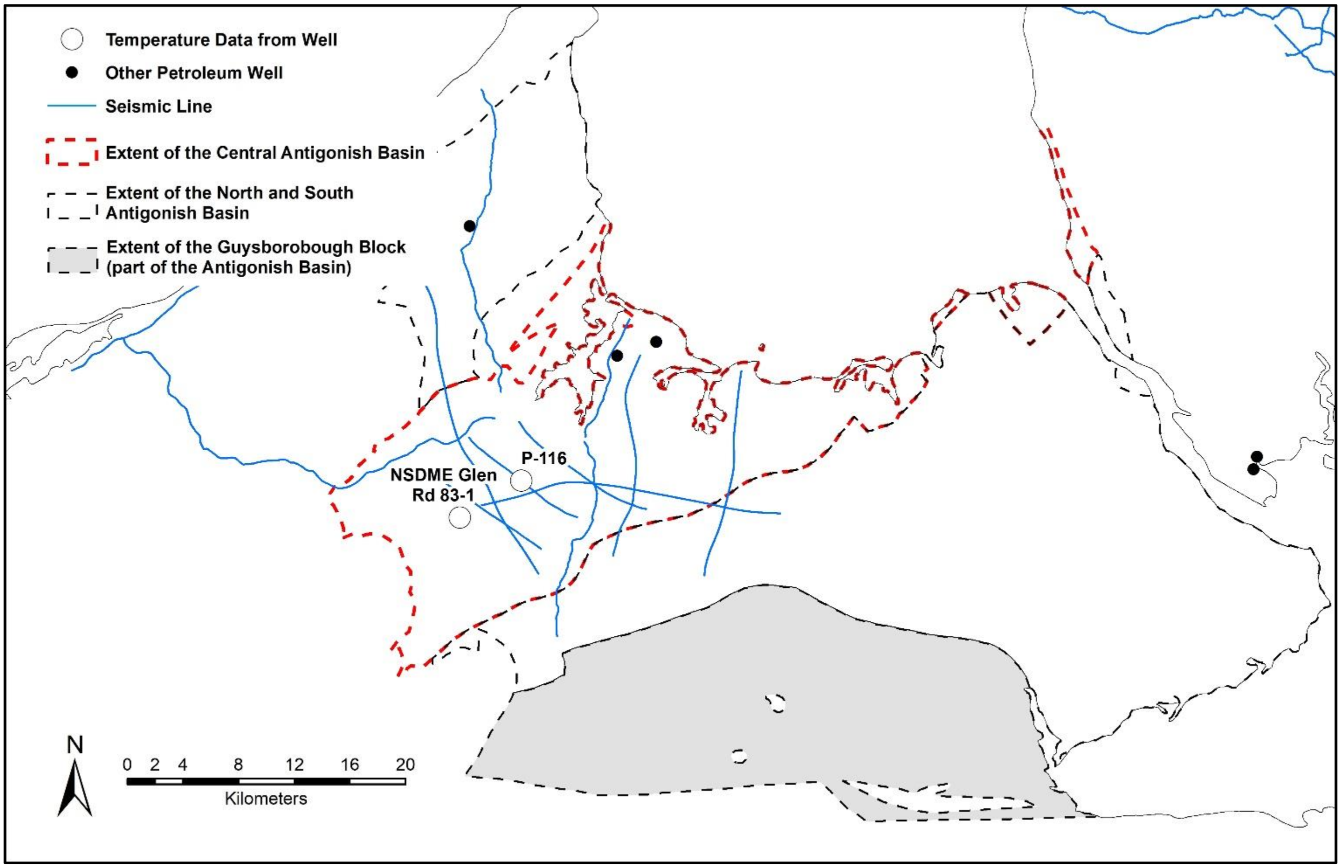

Figure 6.15. Available underground temperature and subsurface data for the Antigonish Basin.

6.1.5.1 Direct-use of heat and electricity generation

The geothermal potential is evaluated for the Central Antigonish Basin (**Figure 6.15**), where data on temperature and formation tops were available. The only potential aquifer documented by the well data is the Macumber Formation in well P-116. The depth expected to reach a minimum temperature of 80 °C is estimated to about 2,750 m. Therefore, only the potential for direct-use of heat is evaluated.

As expected, the results of the evaluation (**Table 6.8**) indicate that, for the Central Antigonish Basin, the Macumber Formation has a low potential for direct-use of heat, limited to the lowest temperature range (20 to 40 °C). Other potential aquifers may be present at greater depths, but the data available are insufficient to characterise then.

Table 6.8. Ranking of a potential aquifer for direct-use of heat in the Central Antigonish Basin.

Potential Aquifer	Temperature of the Reservoir	Depth of the Reservoir	Lithology	Temperature Uncertainty	Subsurface Geological Uncertainty	Score (Aquifer)	Score (Global)
Top Macumber	–	+	O	–	O	-1	-1
Top Basement	–	+	–			-3	

6.1.6 Western Cape Breton Basin

The subsurface of the Western Cape Breton Basin is documented by a few seismic lines and close to 50 petroleum wells (**Figure 6.16**). However, 75% of these wells do not exceed 500 m and formation tops are available for only 15% of the wells. The thickness of the basin cannot be estimated based on the well penetration data.

The geothermal gradient representative of the Western Cape Breton Basin for depths greater than 1,000 m is calculated to be 20.30 °C km^{-1} (see detailed results in **Appendix IV**).

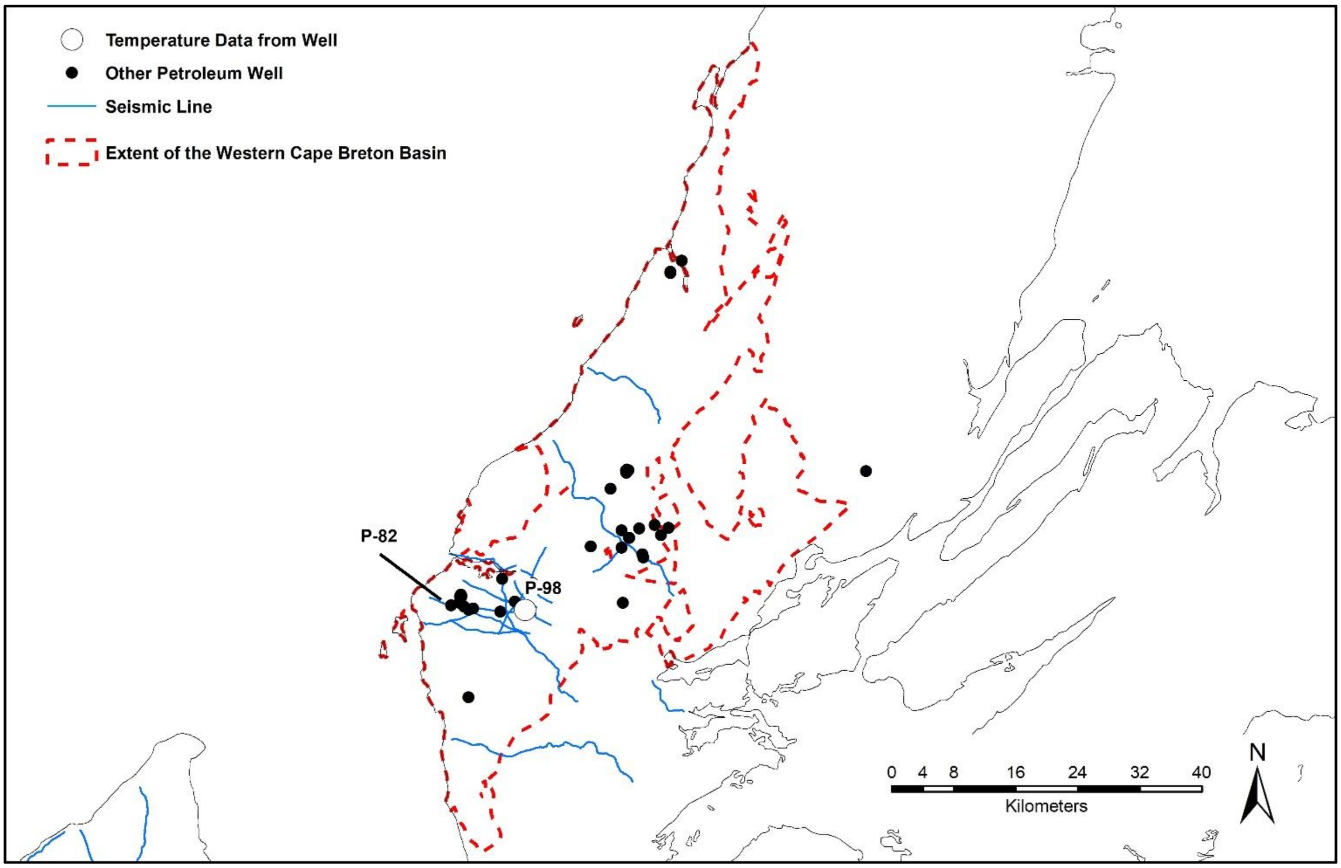

Figure 6.16. Available underground temperature and subsurface data for the Western Cape Breton Basin. The northern part of the basin, at the northern-most tip of Cape Breton Island, is devoid from any subsurface data and is not represented here.

6.1.6.1 Direct-use of heat and electricity generation

Only the area in the vicinity of well P-82 (**Figure 6.16**) has sufficient data to evaluate its geothermal potential. This well, drilled to a total depth of about 3,000 m, did not reach the basement but penetrated the top of the Hood Island Formation limestones (Windsor Group) at 1,628 m and the top of the Macumber Formation limestones at 2,956 m. The seismic line PW09-AINS-08 (NSDOE, 2017) shows that the basin deepens to the northwest of the well, suggesting that the geothermal gradient derived from a thinner area of the basin (well P-98, **Figure 6.16**) can be underestimated in the area of interest.

Using the current calculated geothermal gradient, the depth needed to reach a minimum temperature of 80 °C in the area of interest is estimated be to about 3,500 m. A geothermal potential for electricity generation can be considered in this area if aquifers are present underneath the Macumber Formation (e.g., Wilkie Brook, Ainslie or Creignish formations). Until the presence of such aquifers is confirmed, the evaluation of the geothermal potential can only focus on direct-use of heat.

The results of the evaluation (**Table 6.9**) indicate that a geothermal potential exists for direct-use of heat in the vicinity of well P-82. Assuming that both potential aquifers share a similar lithology, the difference between the scores obtained by the Hood Island and the Macumber formations are only due to the respective depths of these two units. In the vicinity of well P-82, the temperature expected for the Macumber Formation is in the range of 60 to 80 °C. As indicated earlier this potential could be higher northwest of this well.

Table 6.9. Ranking of the potential aquifers for direct-use of heat in the vicinity of the well P-82.

Potential Aquifer	Temperature of the Reservoir	Depth of the Reservoir	Lithology	Temperature Uncertainty	Subsurface Geological Uncertainty	Score (Aquifer)
Top Hood Island	–	+	O	–	–	**-2**
Top Macumber	+	O	O			**4**
Top Horton	?	?	–			**?**
Base Horton	?	?	–			**?**
Top Basement	?	?	–			**?**

6.1.7 Central Cape Breton Basin

The subsurface of the Central Cape Breton Basin is documented by few seismic lines onshore and few wells (**Figure 6.17**). Formation tops are available for only two wells (P-90 and P-91), which indicate that the top of the basement is no deeper than 355 m in the central part of the basin. Two other wells, for which no formation tops are available, have been drilled to total depths of 1,091 and 1,255 metres, suggesting that the thickness of the sediments varies significantly across the basin.

6.1.7.1 Direct-use of heat and electricity generation

Neither the thickness of the basin nor the depth of potential aquifers can be estimated based on the well penetration data available, so an evaluation of the geothermal potential of the basin is not possible. Nonetheless, a geothermal gradient representative of the Central Cape Breton Basin for depths greater than 1,000 m has been calculated to be 23.77 °C km^{-1} (see detailed results in **Appendix IV**).

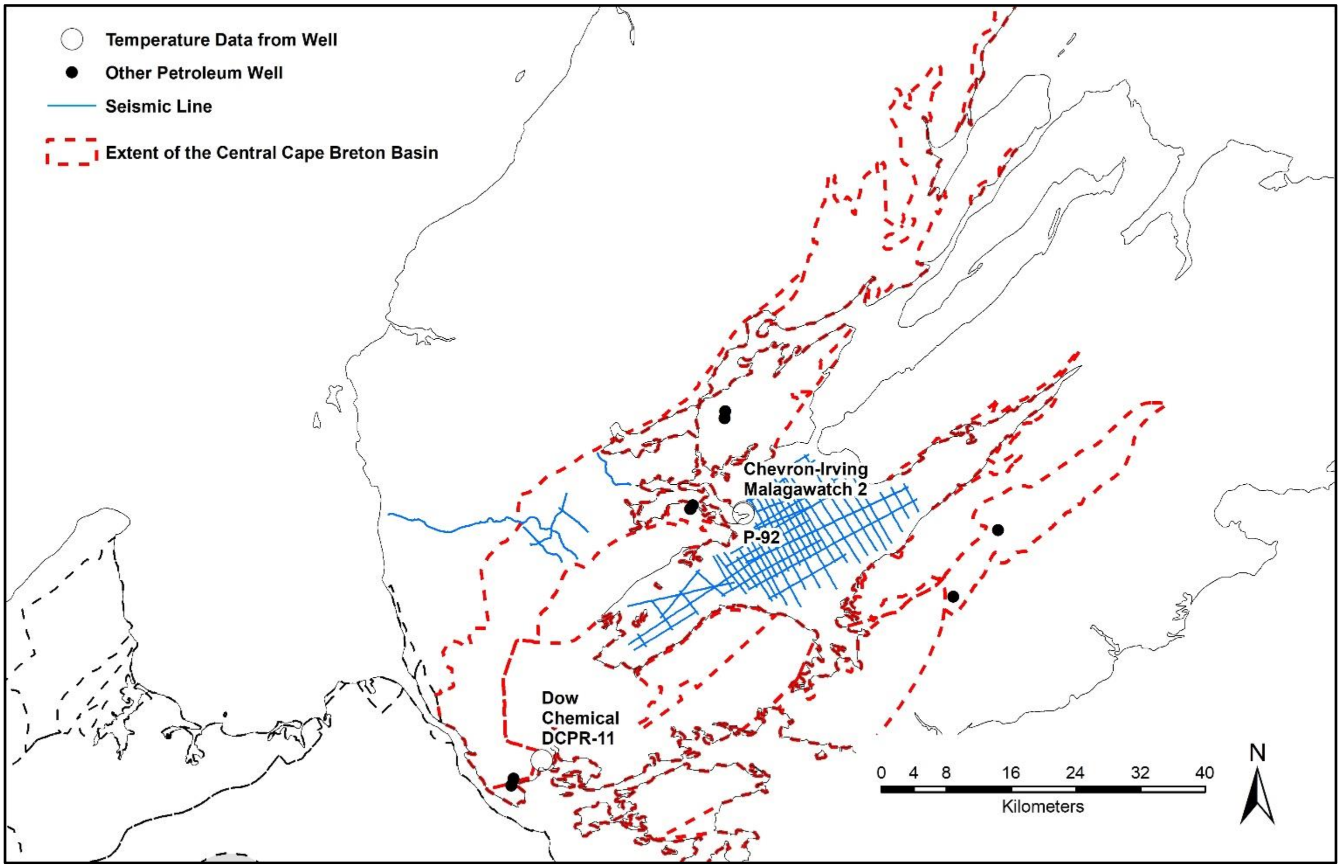

Figure 6.17. Available underground temperature and subsurface data for the Central Cape Breton Basin. The northern tip of the basin has no underground data and is not represented here.

6.1.8 Sydney Basin

The subsurface of the onshore part of the Sydney Basin is documented by little seismic data and few wells (**Figure 6.18**). A recent well drilled for carbon capture and storage encountered the top of the basement at 1,373 m. Elsewhere in the basin, the thickness of the sediments is expected to be lower than 2,000 m (Jiang et al., 2000), except along the shore near the town of North Sydney where the depth of the basement increases to about 2,500 m (NSDOE, 2017).

An evaluation of the geothermal potential of the basin is not possible at the present time, as for the Central Cape Breton Basin (see **Section 6.1.7.1**). The area along the shore near the town of North Sydney is a notable exception, where a series of seismic horizons have been interpreted in the offshore part of the basin (NSDOE, 2017). This underground dataset stops are the shore and its extrapolation onshore is debatable. For this reason, an evaluation of the geothermal potential of the Sydney Basin is proposed for this area only and should not be extrapolated to the rest of the onshore Sydney Basin.

The geothermal gradient representative of the Sydney Basin for depths greater than 1,000 m is calculated at 23.65 °C km^{-1} (see detailed results in **Appendix IV**). It is based on one temperature datapoint measured in a part of the basin where the top of the basement is thinner than in the area of interest, so that the temperatures estimated from this gradient in the North Sydney area might be underestimated. For comparison purposes, underground temperature data from logs have been reviewed for offshore well F-24 located some 40 km northeast of the coast (**Figure 4.2**, **Appendix II**), where the thickness of the basin is about 5.5 km (NSDOE, 2017). A geothermal gradient was calculated at 32.03 °C km^{-1} for this well, significantly higher than for the thinner, onshore part of the basin.

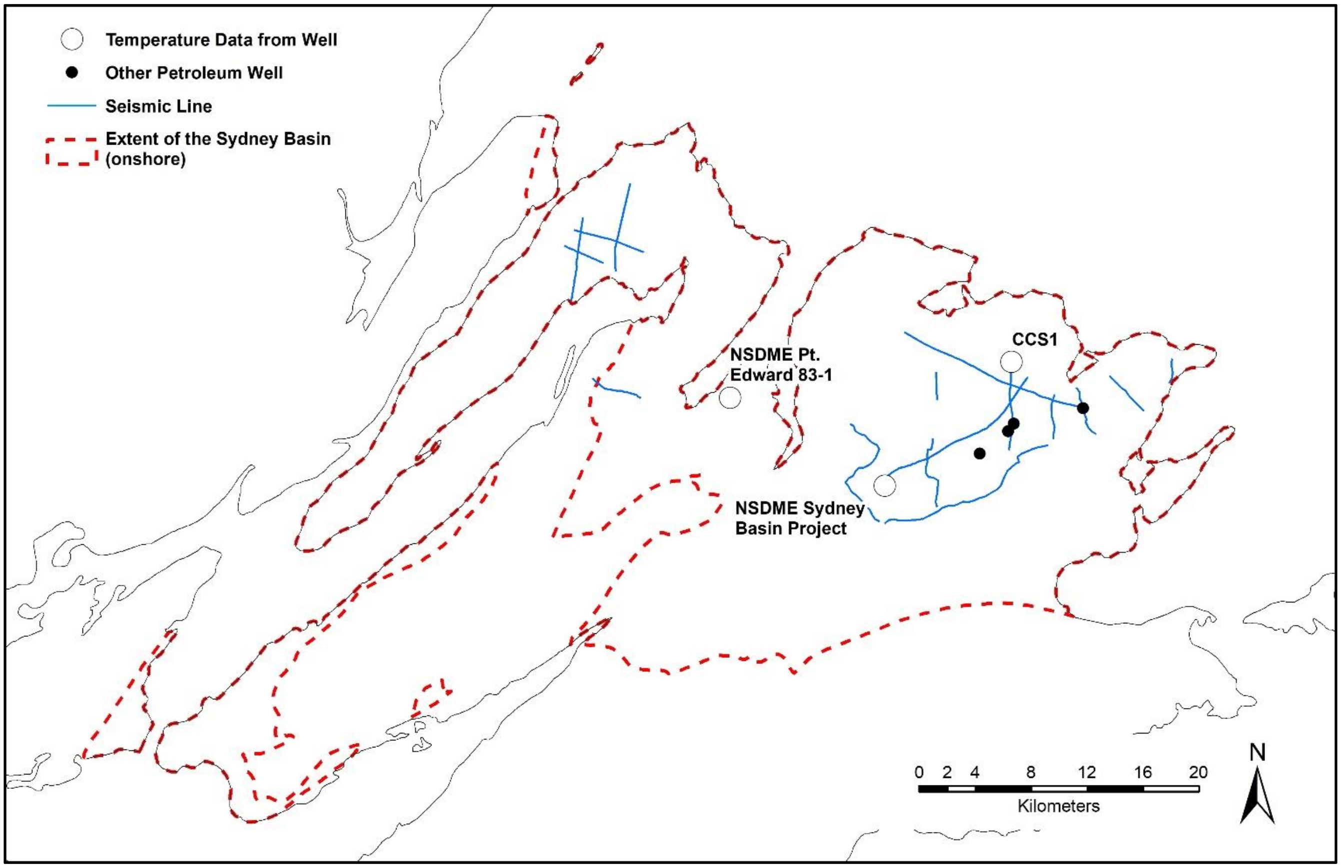

Figure 6.18. Available underground temperature and subsurface data for the onshore part of the Sydney Basin.

6.1.8.1 Direct-use of heat and electricity generation

In the vicinity of the town of North Sydney the basement does not exceed 2,500 m while the minimum temperature of 80 °C, beyond which electricity generation can be considered, is expected to be reached at a depth of about 3,065 m. Only the potential for direct-use of heat has, therefore, been evaluated. The potential aquifers considered include, from top to base (depths indicated are below sea level):

- The South Bar Formation (700 m)
- The Point Edward Formation (800 m)
- The Woodbine Formation (1,000 m)
- The top of the Horton Group (1,750 m)

A seismic horizon is available to define the top each of these stratigraphic units. For indicative purposes, a score has also been calculated for the top of the underlying basement and is presented as well.

The results of the evaluation (**Table 6.10**) indicate a low geothermal potential for direct-use of heat for the shallow sandstones of the South Bar and Point Edward formations and for the underlying limestones of the Woodbine Formation, limited to the lowest temperature range (20 to 40 °C). The comparatively lower score obtained for the Woodbine Formation is due to its carbonate lithology. The expected temperature range increases for the top of the underlying Horton Group (40 to 60 °C) but its greater depth and its lithology impair the score of this latter unit. As indicated earlier, these results are most likely underestimated for the area of interest. They must also be considered with great care in so far as they do not reflect the potential of the rest of the onshore Sydney Basin. Unless new data become available to point to other areas of the onshore basin that share similar or greater thickness, the geothermal potential of the rest of the onshore Sydney Basin is likely lower than the results presented in **Table 6.10**.

Table 6.10. Ranking of the potential aquifers for direct-use of heat along the shore of the Sydney Basin, near the town of North Sydney.

Potential Aquifer	Temperature of the Reservoir	Depth of the Reservoir	Lithology	Temperature Uncertainty	Subsurface Geological Uncertainty	Score (Aquifer)	Score (Global)
Top South bar	–	++	+	–	–	3	4
Top Point Edward	–	++	+			3	
Top Woodbine	–	+	O			-2	
Top Horton	O	+	–			0	
Top Basement	+	O	–			0	

6.1.9 Fundy Basin

The subsurface of the offshore part of the Fundy Basin is documented by extensive seismic surveys and two wells drilled close to New Brunswick. Based on these data, it is estimated that the onshore part of the basin is about 1,000 m-thick at the latitude of Digby Neck (Wade et al., 1996), with the basalts of the North Mountain Formation cropping out in this area. No well penetration deeper than 150 m (**Appendix I**) or seismic data are available to document otherwise the subsurface of the onshore part of the Fundy Basin, so that estimates of the subsurface depths remain uncertain (**Figure 6.19**).

A reliable geothermal gradient representative of the Fundy Basin cannot be calculated either, as the only available temperature data have been measured at very shallow depths (four data points, between 55 and 153 m).

By all practical means, the evaluation of the geothermal potential of the basin cannot be completed with the data available. For indicative purposes only, a tentative evaluation has been made using two hypothetical geothermal gradients of 20 and 30 °C km^{-1} (see detailed results in **Appendix IV**). This range of geothermal gradients is qualitatively supported, but not confirmed, by the geothermal gradients calculated from the above-mentioned shallow temperature measurements (between 16.2 and 27.5 °C km^{-1}, uncorrected). For comparison purposes, underground temperature data from logs have been reviewed for offshore well N-37 located some 60 km northwest of the coast, close to New Brunswick (**Figure 4.2**, **Appendix II**), where the thickness of the basin ranges between 2 and 4 km (Wade et al., 1996). A geothermal gradient was calculated at 26.29 °C km^{-1} for this well, within the range considered for the onshore part of the basin.

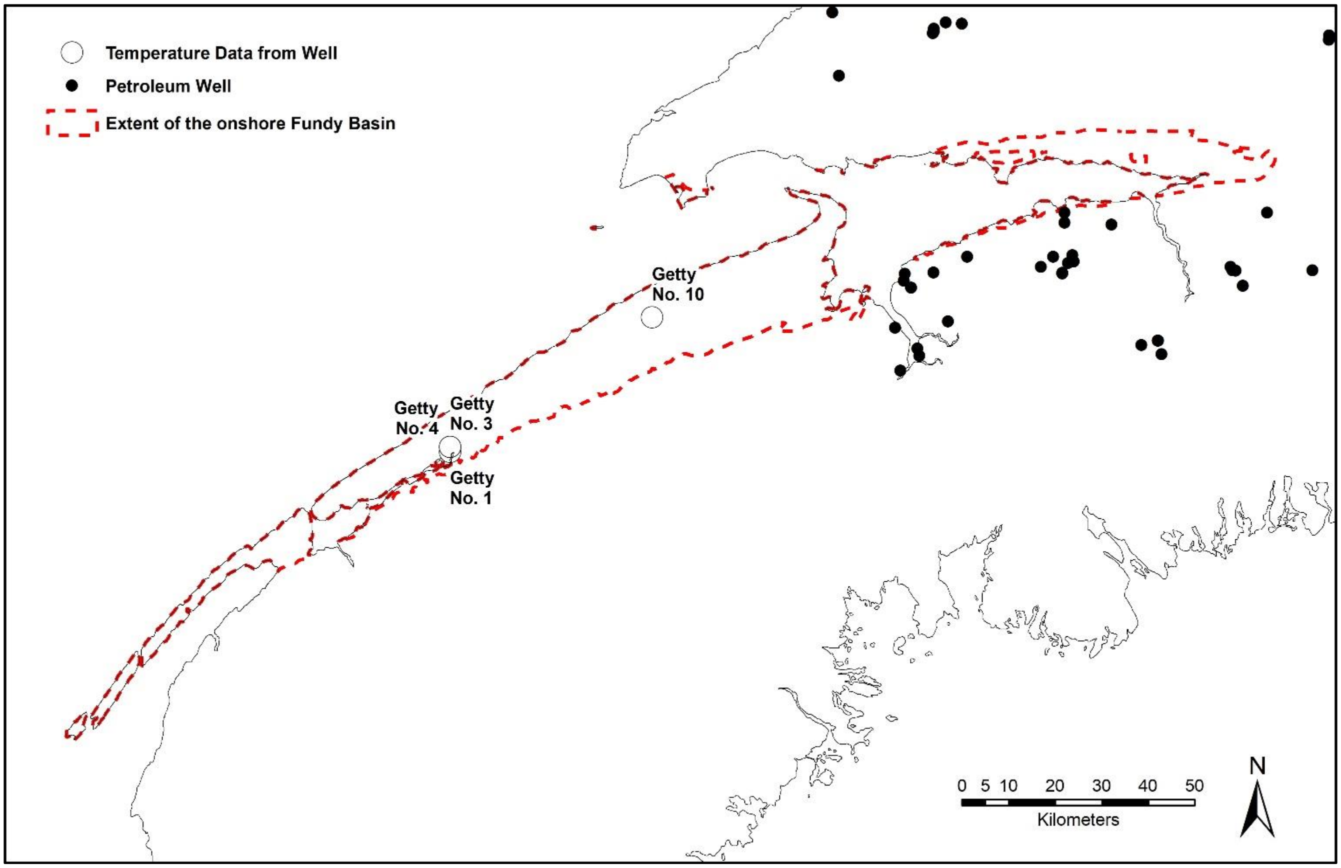

Figure 6.19. Available underground temperature and subsurface data for the onshore part of the Fundy Basin.

6.1.9.1 Direct-use of heat and electricity generation

The geothermal potential of the onshore part of the Fundy Basin is evaluated assuming a sediment thickness of about 1,000 m. The temperature expected at this depth does not exceed about 35 °C when considering the high-end scenario of 30 °C km^{-1}. Therefore, only the potential for direct-use of heat is evaluated. The basal Wolfville Formation is the only potential aquifer that can be considered in the area. Its lithology is dominated by clean sands that may have a very good aquifer potential.

The results of the evaluation are presented in **Table 6.11**. The scores assigned to the Wolfville Formation at various depths are similar regardless of the scenario considered for the temperature of the reservoir and fall within the low temperature range (20 to 40 °C). The underlying basement has a comparatively much lower score, essentially due to the increased depth and basement lithology which would require stimulation. Of course, higher temperatures can be reached at greater depths below the top of the basement.

For the sake of the evaluation, the criteria related to the uncertainty about the reservoir temperature and the subsurface control have not been considered.

Table 6.11. Ranking of the potential of the Wolfville Formation for direct-use of heat with two different geothermal gradients in the Fundy Basin. For the sake of the evaluation, the uncertainty criteria have not been considered.

Potential Aquifer	Temperature of the Reservoir	Depth of the Reservoir	Lithology	Temperature Uncertainty	Subsurface Geological Uncertainty	Score (Aquifer)	Score (Global)
Wolfville at 500 m	⬣	++	++			⬣	7
Base Wolfville at 1 000 m	–	++	++			7	
Top Basement	–	+	–			-2	

6.2 Meguma terrane and Devonian intrusives

Although the Cambro-Ordovician Meguma terrane and the Devonian intrusives make up most of the southern part of the province, few temperature data are available to constrain their geothermal potential (**Figure 6.20**).

In the case of the Meguma terrane, a low geothermal gradient is calculated at 12.63 °C km^{-1} from two temperature datapoints measured at the equilibrium at shallow depths (333 m for the Dalhousie well and 607 m for the NSDM Oldham well, **Figure 6.20**). Detailed results are reported in **Appendix IV**.

In the case of the Devonian intrusives, a low geothermal gradient of 17.92 °C km^{-1} is calculated based on one temperature datapoint measured at equilibrium at shallow depth (480 m, well EPB No. 18, **Figure 6.20**). This gradient is higher but consistent with the results obtained for the Meguma terrane, but it contrasts with a second gradient calculated at 41.86 °C km^{-1} based on a poorly constrained temperature data point from the well MRRD-01 (**Figure 6.20)**. Refer to **Section 5.2** for the methodology and to **Appendix IV** for detailed results). If this second value can be trusted, the difference could be related to the relative concentrations in radioactive elements that are responsible for radiogenic heat generation or the thermal conductivity of the igneous rock that can be insulating when containing a high concentration of feldspar.

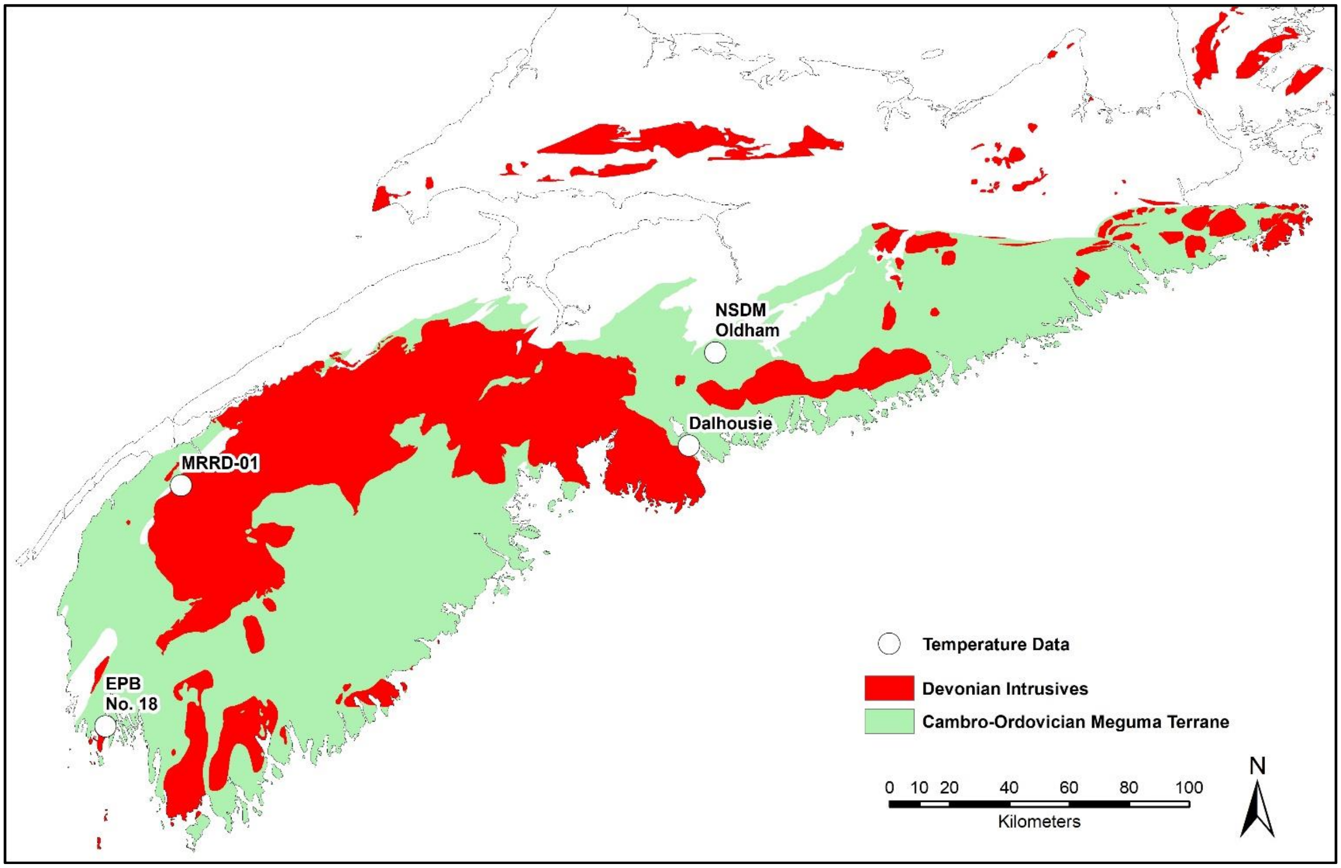

Figure 6.20. Surface map of the Meguma terrane and the Devonian intrusives in the southern part of the province, with location of the underground temperature data available. Cartographic background: NSDNR (2006).

6.2.1 Direct-use of heat and electricity generation

The geothermal potential of the Meguma terrane and the Devonian intrusives can hardly be evaluated based on the few shallow and scattered temperature data available. Although these results are somewhat consistent and point to a low geothermal gradient in the order of 12 to 18 °C km^{-1}, the occurrence of an outlier at about 42 °C km^{-1} casts strong doubts on the homogeneity of the geothermal properties of this area. Until further data can be gathered, two scenarios can be inferred from the available data. In a pessimistic scenario (geothermal gradient of 12.63 °C km^{-1} for the Meguma terrane), the minimal temperature required for direct-use of heat is reached at about 1,080 m and the minimal temperature required for electricity generation is reached at about 5,100 m. In an optimistic scenario (geothermal gradient of 41.86 °C km^{-1} for the Devonian intrusives), these depths are about 350 m and 1,740 m, respectively. The wide gap between these two end-members highlights the necessity to gather additional data in order to ascertain the geothermal potential of this large area. This is particularly important for populated areas of the province that are close to the contact between the intrusives and the rocks of the Meguma terrane, such as the City of Halifax.

Regardless of the thermal properties of the area, the rocks that make up the Meguma terrane and the Devonian intrusives would require some sort of stimulation in order to be considered as aquifers (EGS or BHE, see **Section 1.1.3**).

6.3 Abandoned mines

6.3.1 Heating capacity

The calculated geothermal heating capacity of the abandoned mines is presented in **Figure 6.21**, along with the nature of the mine (open-pit versus underground) and the commodity that was exploited (coal versus metallic and industrial mineral). Details for each mine are compiled in **Appendix III**.

Overall, the total heating capacity is dominated by the underground coal mines, which make up 97.9% of the total heating capacity calculated for the whole dataset. This is due to the comparatively larger volumes of ore extracted for the coal mines. Consequently, this geothermal potential is essentially concentrated in localized areas of Cumberland, Pictou and Cape Breton counties, with ancillary locations in the Colchester and Inverness counties.

The underground metallic and industrial mineral mines account for 1.9% of the total heating capacity of the province. Although they have a smaller contribution to the overall potential for the province, these mines cover a larger area and dominate in the non-coal basins, especially in Hants, Halifax and Guysborough counties.

The geothermal potential is only marginal in the southwest of the province, and so is the geothermal potential of open-pit mines (0.2%).

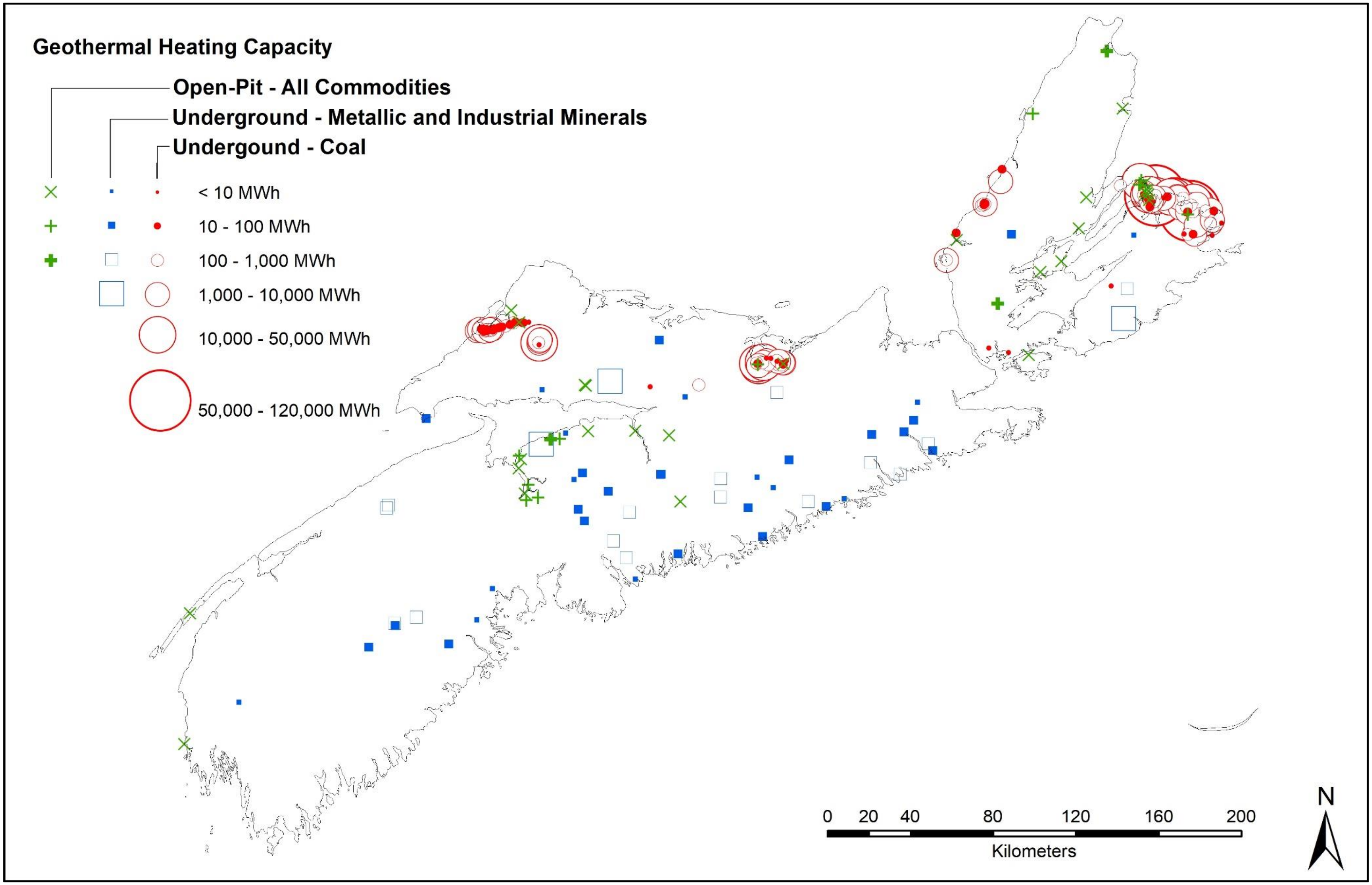

Figure 6.21. Heating capacity calculated for the abandoned mines. Refer to **Appendix III** for the details of each mine.

6.3.2 Cooling capacity

The geothermal cooling capacity of the abandoned mines is presented in **Figure 6.22**, along with the nature of the mine (open-pit versus underground) and the commodity that was exploited (coal versus metallic and industrial minerals). Details for each mine are compiled in **Appendix III**.
As was determined for the heating capacity, the total cooling capacity is dominated by the underground coal mines, which make up 97.1% of the total cooling capacity calculated for the whole dataset. This geothermal potential is essentially concentrated in localized areas of Cumberland, Pictou and Cape Breton counties, with ancillary locations in Colchester and Inverness counties.

The underground metallic and industrial mineral mines account for 1.9% of the total heating capacity of the province. Although they have a much smaller contribution to the overall potential for the province, these mines cover a larger area and dominate in the non-coal basins, especially in Hants, Halifax and Guysborough counties. Open-pit mines account for only 1.0% of the total capacity. Large open-pit mines with significant cooling capacity are limited to coal and gypsum.

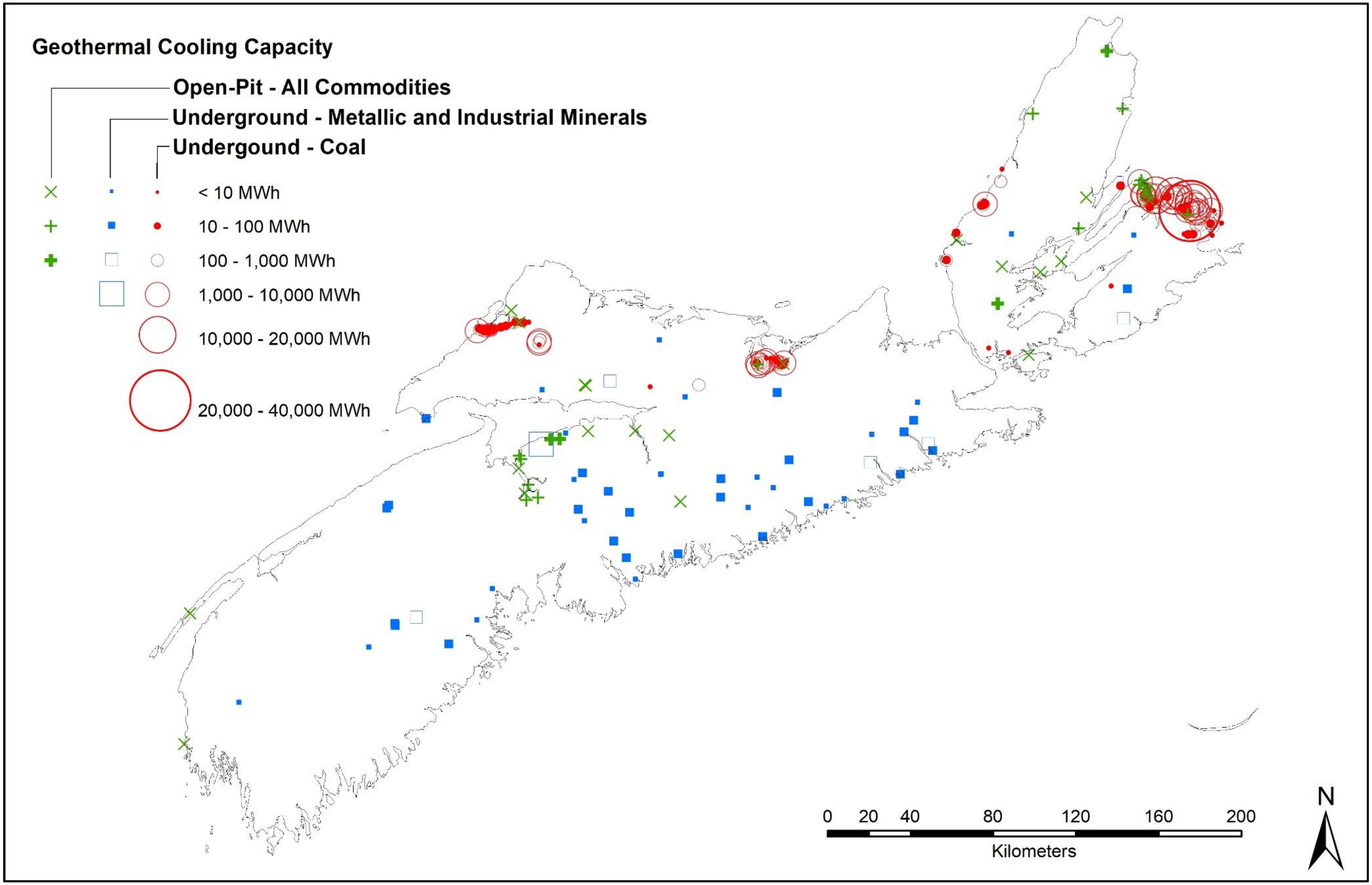

Figure 6.22. Cooling capacity calculated for the abandoned mines. Refer to **Appendix III** for the details of each mine.

6.4 References

Bibby, C., Shimeld, J.W., 2000. Compilation of reservoir data for sandstones of the Devonian-Permian Maritimes Basin, Eastern Canada. Geological Survey of Canada, Open File Report 3895, 102 p. https://doi.org/10.4095/211514

Cameron, R., 2018. A geophysical, petrological and reservoir potential study of the Glass Sand marker unit and associated sandstones in the Upper Horton Bluff Formation, Horton Group, Windsor Basin, Nova Scotia. B.Sc. thesis, Acadia University, 80 p.

Cen, X., 2017, Preliminary petrophysics database, onshore Nova Scotia. Nova Scotia Department of Energy Open File Report 2017-10.

Drury, M.J., Jessop, A.M., Lewis, T.J., 1987. Thermal nature of the Canadian Appalachian crust. Tectonophysics 133(1-2):1-14. https://doi.org/10.1016/0040-1951(87)90276-9

Government of Nova Scotia, 2020. Geographic data directory. https://nsgi.novascotia.ca/gdd/ Accessed online 2020-05-15.

Hayes, B.J.R., Dorey, K., Longson, C.K., 2017. Assessment of Oil and Gas Potential, Windsor and Cumberland Basins, Onshore Nova Scotia. For Nova Scotia Department of Energy by Petrel Robertson Consulting Limited, Open File Report 2017-03.

Jiang, C., Lavoie, D., Rivard, C., 2016. An Organic Geochemical Investigation of the Carboniferous Mabou Group Intersected by Groundwater Wells in McCully Gas Field, Southern New Brunswick. Its Hydrocarbon Source Potential and Character. Geological Survey of Canada, Open File 8071, 34 p. https://doi.org/10.4095/298803

Lukawski, M.Z., Anderson, B.J., Augustine, C., Capunao, L.E. Jr., Beckeres, K.F., Livesay, B., Tester, J.W., 2014. Cost analysis of oil, gas, and geothermal well drilling. Journal of Petroleum Science and Engineering 118:1-14. https://doi.org/10.1016/j.petrol.2014.03.012

Michel, F.A., 2007. Evaluation of the geothermal energy potential in Stellarton, Nova Scotia, final report. Prepared for: Nova Scotia Department of Energy, Nova Scotia Department of Natural Resources, and the Town of Stellarton, 29 p.

NSDNR, 2006. Geological map of the province of Nova Scotia, Scale 1:500 000, Compiled by J. D. Keppie, 2000. Digital Version of Nova Scotia Department of Natural Resources Map ME 2000-1. DP ME 43, Version 2.

NSDOE, 2011, Play fairway analysis offshore Nova Scotia, Sydney Basin offshore, Chapter 3 Stratigraphy. Nova Scotia Department of Energy

NSDOE, 2017. Schedule of 2D Seismic Data, onshore Nova Scotia. Nova Scotia Department of Energy Open File Report 2017-07.

NSDEM, 2020. Digital contours of sedimentary basins. Nova Scotia Department of Energy and Mines, unpublished data.

Richard, M.-A., Comeau, F.-A., Bédard, K., Malo, M., 2016. Géothermie profonde : grille de sélection de sites géothermiques. Institut de recherche d'Hydro-Québec, Rapport IREQ-2016-0023, 78 p. http://espace.inrs.ca/7688

Smith, W.D., Naylor, R.D., Kalkreuth, W.D., 1989. Oil shales of the Stellarton basin, Nova Scotia, Canada: Stratigraphy, depositional environment, composition and potential uses. Atlantic Geology 25:20-38.

Tester, J.W., Anderson, B.J., Batchelor, A.S., Blackwell, D.D., DiPippo, R., Drake, E.M., Garnish, J., Livesay, B.J., Moore, M.C., Nichols, K., Petty, S., Taksoz, M.N., Veatch, R.W.J., 2006. The future of geothermal energy. Impact of enhanced geothermal systems (EGS) on the United States in the 21st century. Massachusetts Institute of Technology, Idaho National Laboratory. INL/EXT-06-11746. 372 pages.

Wade, J.A., Brown, D.E., Traverse, A., Fensome, R.A., 1996. The Triassic-Jurassic Fundy Basin, eastern Canada: regional setting, stratigraphy and hydrocarbon potential. Atlantic Geology 32(3):189-231. https://doi.org/10.4138/2088

7. ECONOMIC OPPORTUNITIES FOR NOVA SCOTIA

Section 6 of the present report demonstrates the potential for shallow to deep geothermal resource development in Nova Scotia: heating and cooling from abandoned mines, direct-use of heat at mid-depths and electricity generation at greater depths can all be legitimately considered.

Review and analysis of the available data (**Sections 4** and **5**) however, show that this potential is not equally distributed across the province. In addition, our understanding of the geothermal potential varies from one area to another depending on the nature, quality and quantity of subsurface data available.

The current level of knowledge on the geothermal potential for Nova Scotia is illustrated in **Figure 7.1**. The divisions are based on the primary geological features of the province (**Section 3**). Some areas have not been evaluated due to the absence of underground temperature data.

For each area considered, the spatial extent of the potential for electricity generation and direct-use of heat in aquifers is shown on **Figure 7.2**. The geothermal potential for electricity generation with Enhanced Geothermal Systems (EGS) at a depth of 7 km and for direct-use of heat with deep Borehole Heat Exchanger (BHE) at a depth of 4 km are shown respectively on **Figures 7.3 and 7.4**. Finally, the geothermal potential for heating and cooling from abandoned mines are shown respectively on **Figures 7.5** and **7.6**. These characteristics are summarized in **Table 7.1**.

The depths of 7 km for EGS and 4 km for deep BHE represent the maximum theoretical limits for the use of these technologies to extract geothermal energy. In contrast, of the constructed EGS and deep BHE pilot projects (**Section 2.3**), depths are typically approximately 5.5 and 3 km respectively. These EGS and BHE pilot projects, however, have not yet reached a commercial stage. Further development of these technologies may provide access to deeper resources in the future.

Economic opportunities that benefit from geothermal resources can be considered, wherever a suitable resource is present, but their development will ultimately be constrained by the pace at which the missing subsurface data can be gathered and by the presence of end users (current or future). **Figure 7.7** illustrates the present-day spatial distribution of some of the potential end users, showing populated areas, greenhouses, fish hatcheries and electric transmission lines.

The remainder of this section highlights the primary economic opportunities that can be considered for each area based on the current understanding of the geothermal potential.

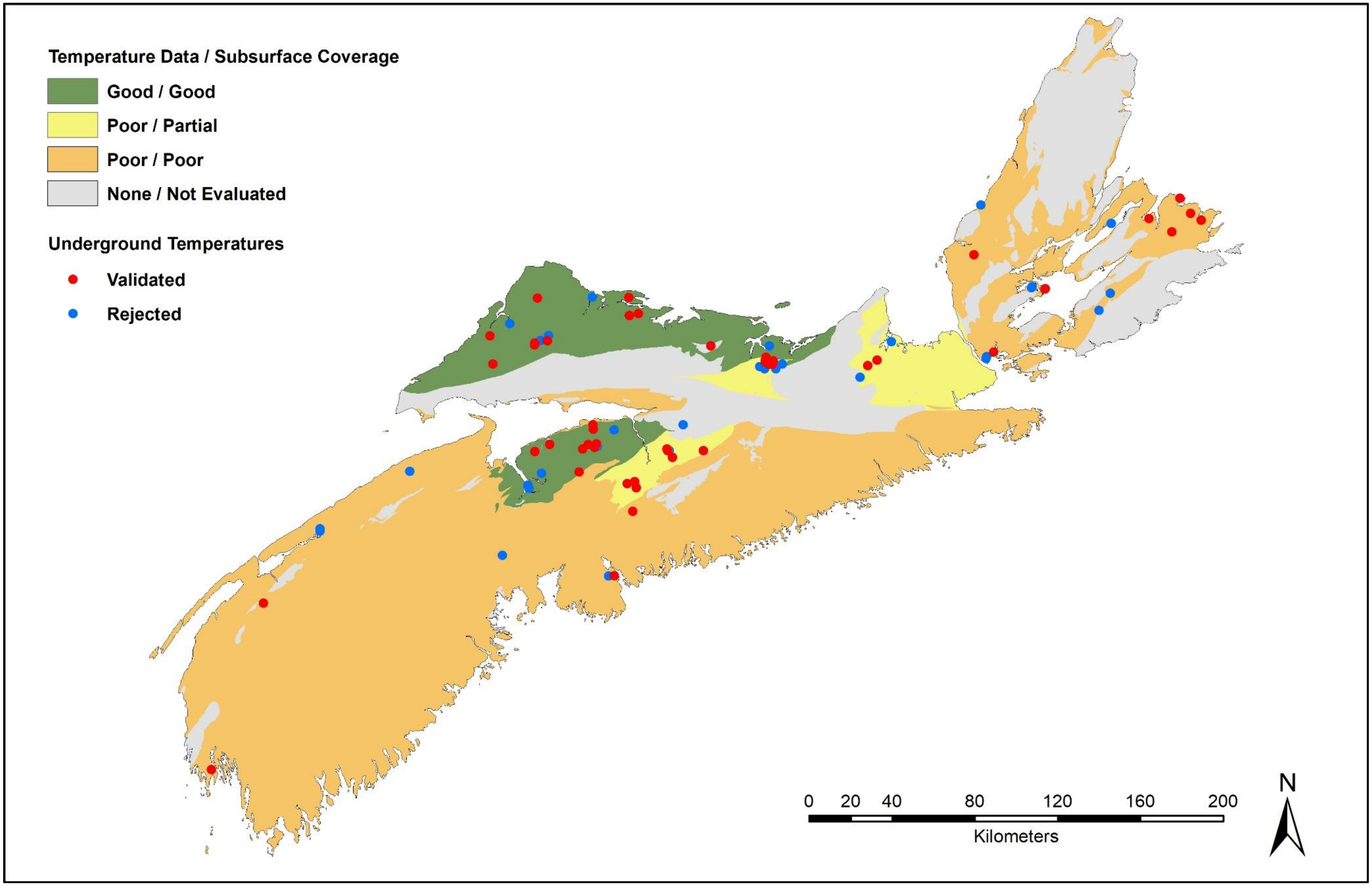

Figure 7.1. Current understanding of the geothermal potential of Nova Scotia. Cartographic background: NSDNR (2006) and NSDEM (2020).

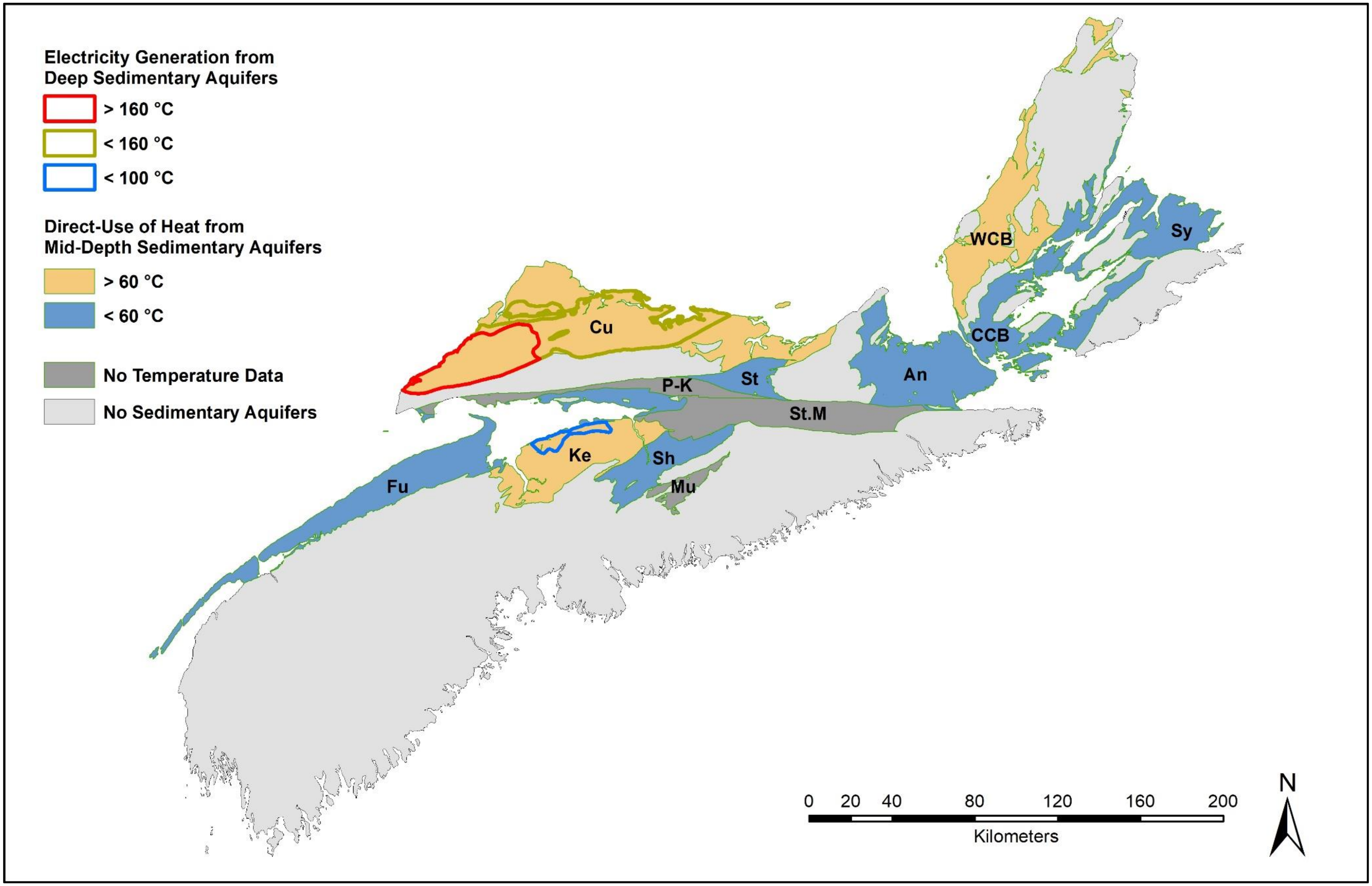

Figure 7.2. Spatial extent of the potential for electricity generation and direct-use of heat from aquifers. Areas with no aquifer correspond to magmatic or metamorphic rocks. Sedimentary basins: An: Antigonish; CCB: Central Cape Breton; Cu: Cumberland; Fu: Fundy; Ke: Windsor-Kennetcook; Mu: Musquodoboit; P-K: Parrsboro-Kemptown; Sh: Shubenacadie; St: Stellarton; St.M: St. Mary's; Sy: Sydney; WCB: Western Cape Breton. Cartographic background: NSDNR (2006) and NSDEM (2020).

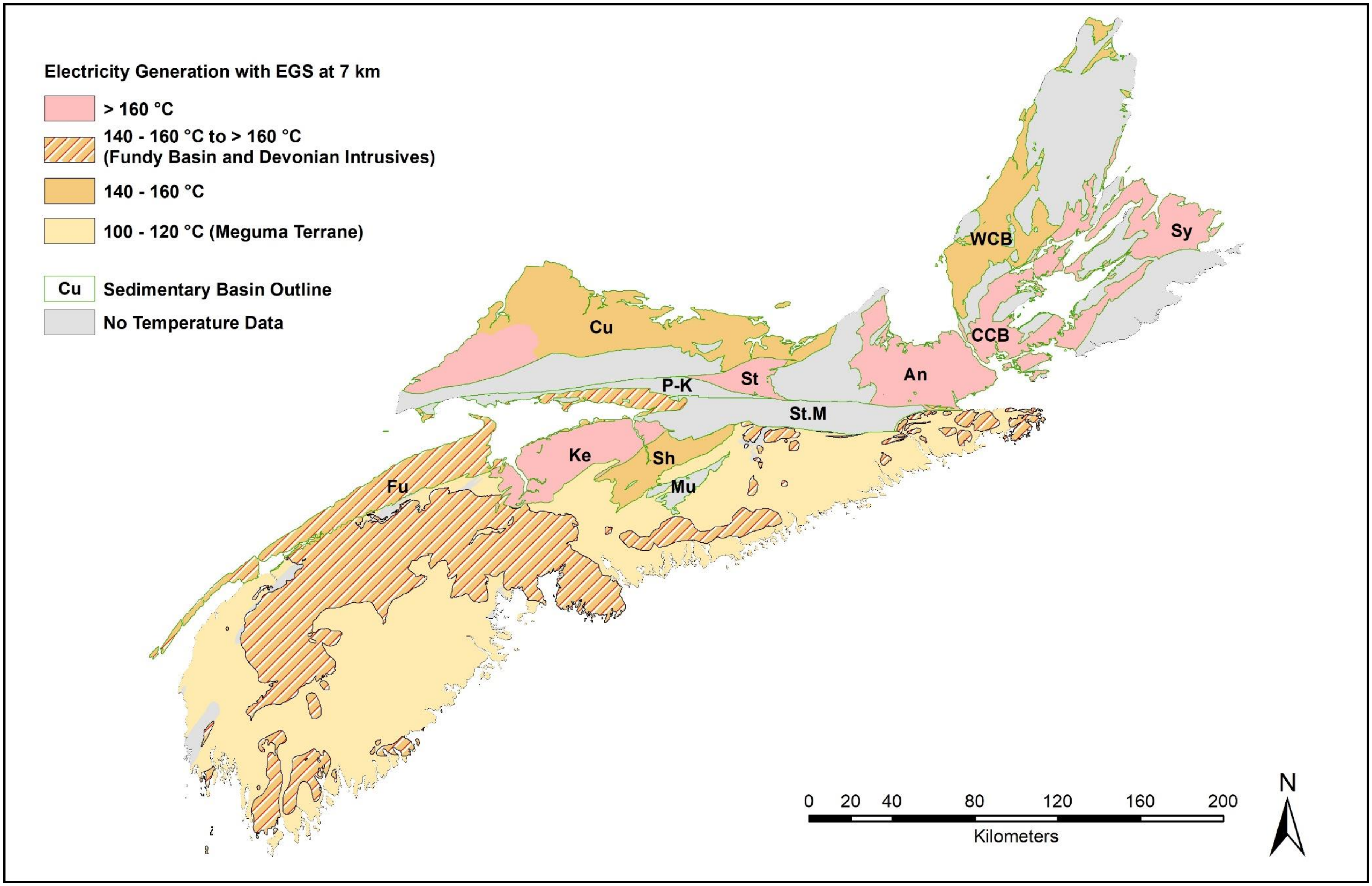

Figure 7.3. Spatial extent of the potential for electricity generation with Enhanced Geothermal Systems (EGS) at a depth of 7 km. Two temperatures ranges are presented for the Fundy Basin and the Devonian intrusives to account for the level of uncertainty in the input underground temperature data. Sedimentary basins: An: Antigonish; CCB: Central Cape Breton; Cu: Cumberland; Fu: Fundy; Ke: Windsor-Kennetcook; Mu: Musquodoboit; P-K: Parrsboro-Kemptown; Sh: Shubenacadie; St: Stellarton; St.M: St. Mary's; Sy: Sydney; WCB: Western Cape Breton. Cartographic background: NSDNR (2006) and NSDEM (2020).

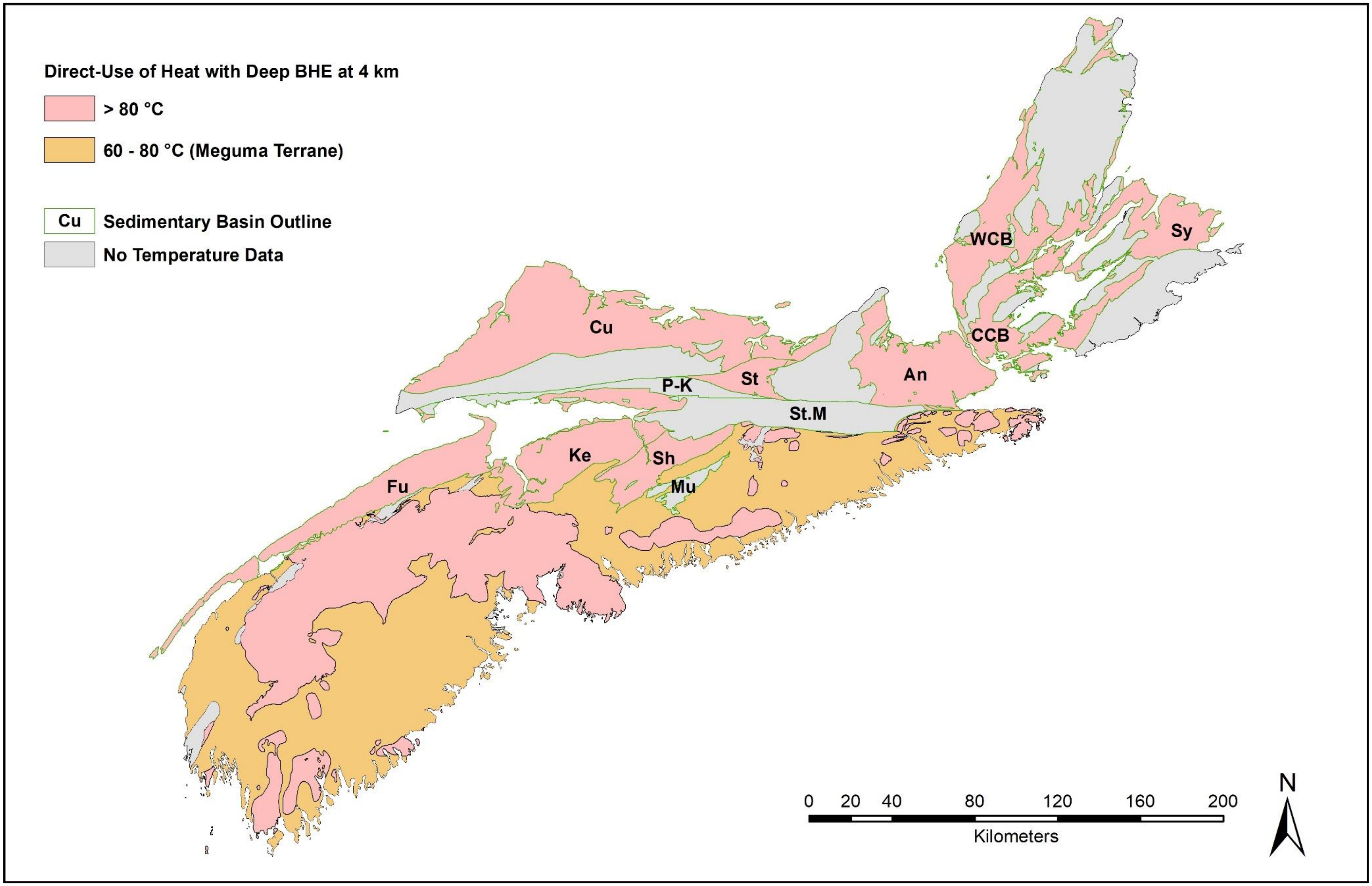

Figure 7.4. Spatial extent of the potential for direct-use of heat with deep Borehole Heat Exchangers (BHE) at a depth of 4 km. Sedimentary basins: An: Antigonish; CCB: Central Cape Breton; Cu: Cumberland; Fu: Fundy; Ke: Windsor-Kennetcook; Mu: Musquodoboit; P-K: Parrsboro-Kemptown; Sh: Shubenacadie; St: Stellarton; St.M: St. Mary's; Sy: Sydney; WCB: Western Cape Breton. Cartographic background: NSDNR (2006) and NSDEM (2020).

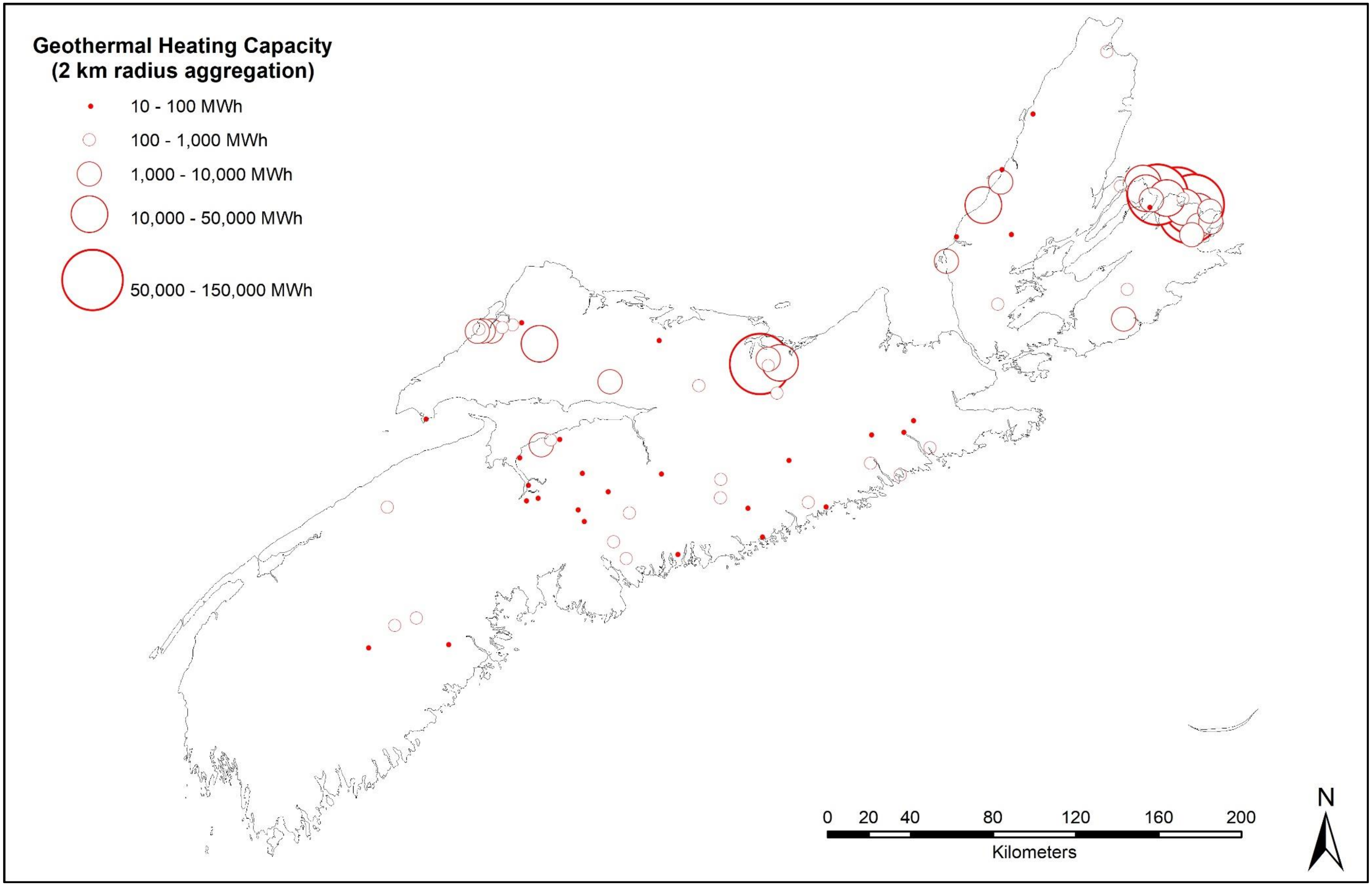

Figure 7.5. Potential for geothermal heating from abandoned mines. Mines within a radius of 2 km from each other have been aggregated for clarity purposes.

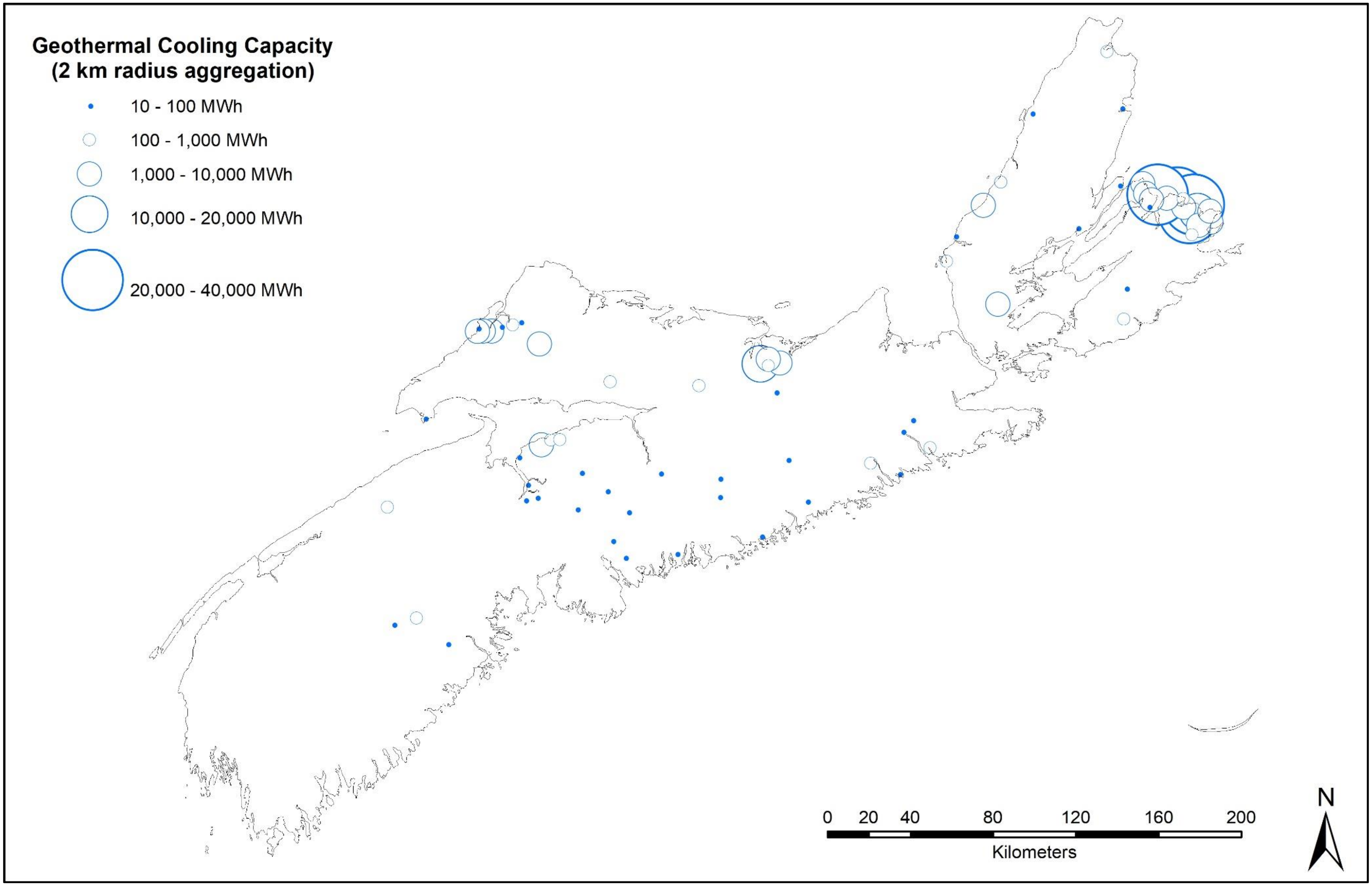

Figure 7.6. Potential for geothermal cooling from abandoned mines. Mines within a radius of 2 km from each other have been aggregated for clarity purposes.

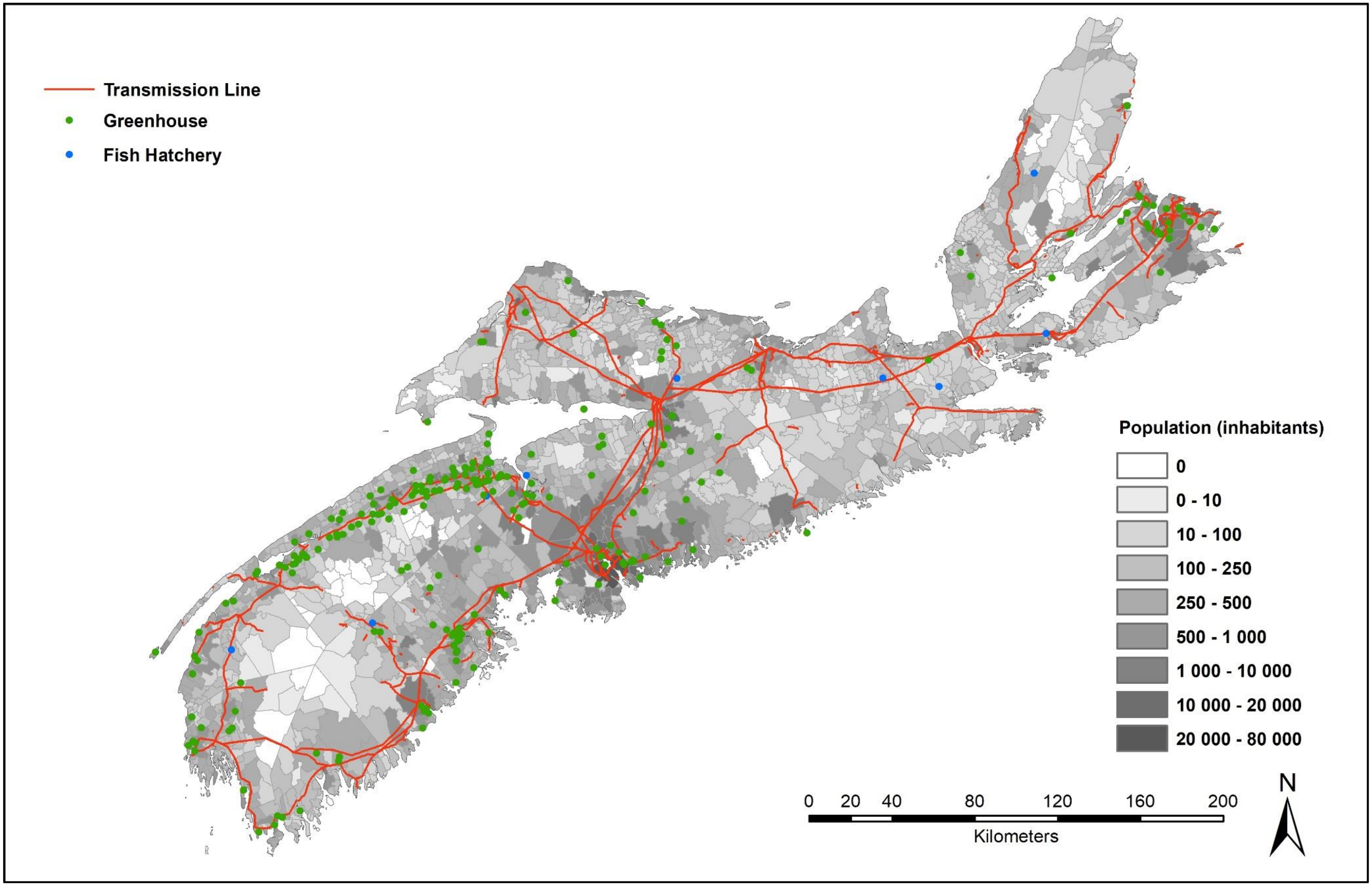

Figure 7.7. Spatial distribution of some potential end users: population, green houses, fish hatcheries, electric transmission lines. Cartographic background: Government of Nova Scotia (2020).

Table 7.1. Main characteristics of the areas considered in the evaluation of the geothermal potential of Nova Scotia. (1): Values for northeastern and southwestern parts of the basin, respectively. (2): Hypothetical values. (3): From two different intrusives. N.A.: Not applicable.

			Sedimentary Reservoirs		EGS and Deep BHE		Abandoned Mines		
			Expected Temperature (°C, Deepest Aquifer)		Expected Temperature (°C)			Total Capacity (MWh)	
Area	**Level of Understanding (Temperature / Subsurface)**	**Geothermal Gradient (°C km^{-1})**	**Electricity Generation (< 7 km)**	**Direct-Use of Heat (< 4 km)**	**EGS (at 7 km)**	**Deep BHE (at 4 km)**	**Nb**	**Heating**	**Cooling**
Cumberland	Good / Extensive	21.18 / 26.17 (1)	> 160	100-120	140-160 / > 160	80-100 / 100-120	57	48,479	14,944
Windsor-Kennetcook	Good / Extensive	24.34	80-100	60-80	> 160	100-120	13	6,183	2,164
Stellarton	Poor / Partial	25.49	N.A.	40-60	> 160	100-120	30	86,473	25,789
Shubenacadie	Poor / Partial	20.95	N.A.	20-40	> 160	80-100	3	40	13
Antigonish	Poor / Partial	26.08	N.A.	20-40	> 160	100-120	1	6	2
Western Cape Breton	Poor / Poor	20.3	Theoretical	60-80	140-160	80-100	22	15,737	5,390
Central Cape Breton	Poor / Poor	23.77	N.A.	20-40	> 160	100-120	9	777	1,123
Sydney	Poor / Poor	23.65	N.A.	40-60	> 160	100-120	95	636,894	187,616
Fundy	Poor / Poor	20.00 / 30.00 (2)	N.A.	20-40	140-160 / > 160	80-100 / 120-140	2	86	25
Musquodoboit	None / Not Evaluated	N.A.	N.A.	N.A.	N.A.	N.A.	1	< 1	< 1
St. Mary's	None / Not Evaluated	N.A.	N.A.	N.A.	N.A.	N.A.	1	3	1
Parrsboro-Kemptown	None / Not Evaluated	N.A.	N.A.	N.A.	N.A.	N.A.	3	499	174
Devonian intrusives	Poor / Poor	17.92 / 41.86 (3)	N.A.	N.A.	140-160 / > 160	80-100 / > 160	0	0	0
Meguma terrane	Poor / Poor	12.63	N.A.	N.A.	100-120	60-80	35	4,378	1,281
Other	None / Not Evaluated	N.A.	N.A.	N.A.	N.A.	N.A.	13	4,998	1,465

7.1 Relevance of geothermal resources in Nova Scotia's energy portfolio

Nova Scotia generated 9.6 terawatt hours (TW.h) of electricity in 2018, whose primary source is coal, accounting for more than 60%, but also from oil, natural gas, hydro, wind, and biomass (**Figure 7.8**). As energy requirements turned out to be higher, the province needed to import approximately 0.6 TW.h of electricity from New Brunswick in 2018 to meet the shortfall. It is noteworthy that the share from renewable sources has grown from 16% in 2005 to 24% in 2018 (Canada Energy Regulator, 2019). Nevertheless, the largest greenhouse gas emitting sectors in Nova Scotia are electricity generation with 42% of emissions, followed by transportation at 31%, and buildings (residential and commercial) with 14% (**Figure 7.8**).

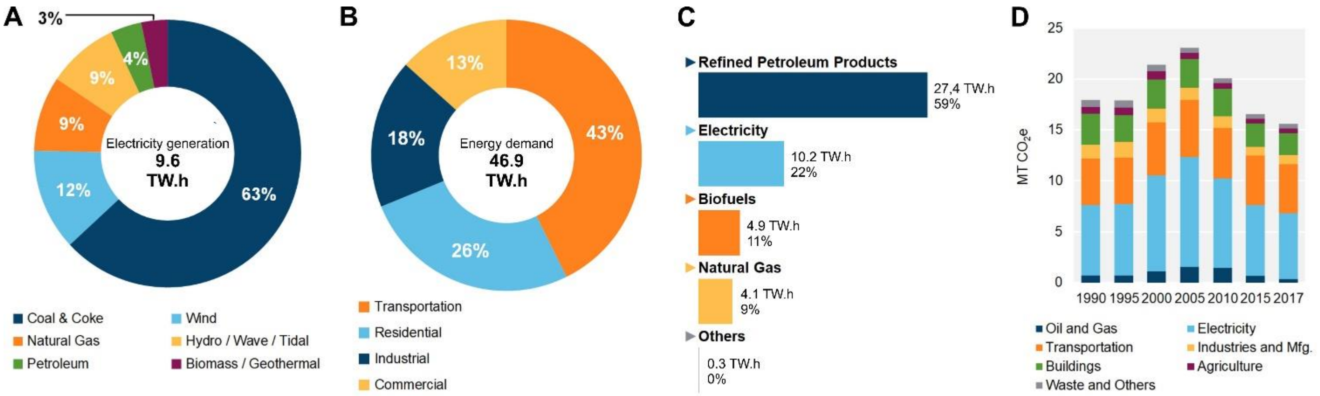

Figure 7.8. A) Electricity generation by source, B) end-use energy demand by sector, and C) end-use demand by fuel type in Nova Scotia in 2018 (adapted from Canada Energy Regulator, 2019).

Nova Scotia Power, a subsidiary of Emera, generates the majority of electricity of the province and is responsible for power transmission and distribution. The cost of electricity in 2020 ranges from 10.52 to 17.03 ¢/kW.h for industrial customers in manufacturing, depending on peaks and daily energy demands, while an average residential price was estimated at 15 ¢/kW.h over the year (Nova Scotia Power, 2020).

According to the IRENA (2017), the standard cost of producing geothermal electricity from conventional hydrothermal systems varies between 38 and 62 €/MWh (5.9 and 9.6 ¢/kW.h in Canadian dollar). However, the cost of producing geothermal electricity from EGS systems is currently difficult to evaluate given the still very limited number of installations in service. It can be estimated at around 160 €/MWh (25 ¢/kW.h in Canadian dollar) for a 3 MW installation with two deep drillings representing a total investment cost of around 30 M€ (45 M CAN$). These figures are similar to those of Hydro-Québec (2017), which estimates capital costs for an EGS, including the power plant, drilling and hydraulic stimulation, amount to at least $10,000/kW, with an electricity cost between 22 and 32 ¢/kWh. Compared to conventional hydrothermal systems in volcanic environments, the drillings are deeper and the temperature reached is lower, such that the cost of the electric MWh will in any case remain higher. A decrease in the cost can be envisaged when it will be possible to reduce the cost of deep drilling and to systematically combine the production of electricity with the production of heat. From now on, industry professionals are committed to a logic of cost reduction to reach a target of 100 €/MWh (15 ¢/kW.h in Canadian dollar) of electricity in 2028, which is consistent with international literature data (Joint Research Centre, 2018).

France has 71 deep geothermal installations using resources up to about 2,000 m. In 2018, the heat production of this sector reached 1.78 TW.h (ADEME, 2020), which represents about 15% of the energy demand for the entire residential sector in Nova Scotia (**Figure 7.8**). The levelized cost of energy for the production of heat by the deep geothermal field in France is estimated between 15 and 55 €/MWh (2.3 and 8.5 ¢/kW.h in Canadian dollar). However, this estimate does not include the cost of heat distribution.

7.2 Cumberland Basin

The Cumberland Basin benefits from good temperature and subsurface coverage. A significant geothermal potential for electricity generation, direct-use of heat from aquifers and from abandoned mines has been identified, sometimes present over the same area. Results from the evaluation are summarized in **Table 7.1** and illustrated on **Figure 7.9**.

7.2.1 Electricity generation

The Cumberland Basin has by far the most promising area for electricity generation from deep aquifers in the province. In the southwestern part of the basin, the combination of potential aquifers at great depths (ranging from 5.5 to 7 km) and a high geothermal gradient calculated at 26.17 °C km^{-1} (the highest for the province) results in temperatures exceeding 160 °C throughout this area. Three superimposed potential aquifers can be considered in this area, the base of the Cumberland Group had the highest score on account of its comparatively shallower depth and better aquifer properties. Examples of operational electricity generation facilities worldwide do not exceed a depth of 5.5 km (**Section 2.1**). Because the potential identified in the Cumberland Basin is present at depths greater than 5.5 km, its development will be challenged by technological or economical constraints which may be overcome in the future.

A geothermal potential for electricity generation also exists for aquifers in the northeastern part of the basin, although shallower depths and a lower geothermal gradient result in expected temperatures below 160 °C. In this area, the potential aquifer that has the largest spatial extent is at the base of the Windsor Group anhydrite, which requires stimulation to be considered for electricity generation. The expected temperature range is 80 to 100 °C between 4 and 5.5 km depth. The two other potential aquifers, which do not require stimulation, have smaller spatial extents and an expected temperature range of 80 to 140 °C between 3 and 5.5 km. Electricity generation with EGS can also be theoretically considered throughout the basin, with expected temperatures at 7 km depth exceeding 160 °C in the south-west and in the range of 140 to 160 °C in the north-east.

7.2.2 Direct-use of heat

The potential for direct-use of heat is limited to the northeastern part of the basin because the potential aquifers are too deep in the southwest. The geothermal gradient is calculated at 21.18 °C km^{-1} for the northeastern area, where temperatures in the range of 40 °C to > 80 °C are expected at depths between 1 and 4 km. Results from the evaluation show the potential is not distributed homogeneously throughout the area, due to variations in the depth of the three potential aquifers considered. To the south, the lowermost potential aquifer (below the base of the Windsor Group anhydrite) also becomes too deep to be considered for direct-use of heat. Direct-use of heat with deep BHE can also be considered throughout the basin with expected temperatures at 4 km depth exceeding 80 °C.

7.2.3 Heating and cooling capacity from abandoned mines

The total heating and cooling capacities from abandoned mines in the basin amount to 48,479 and 14,944 MWh, respectively. About 98% of this potential corresponds to the Springhill coal mine (61%) and to a cluster of smaller coal mines in the area of Joggins and River Hebert (37%).

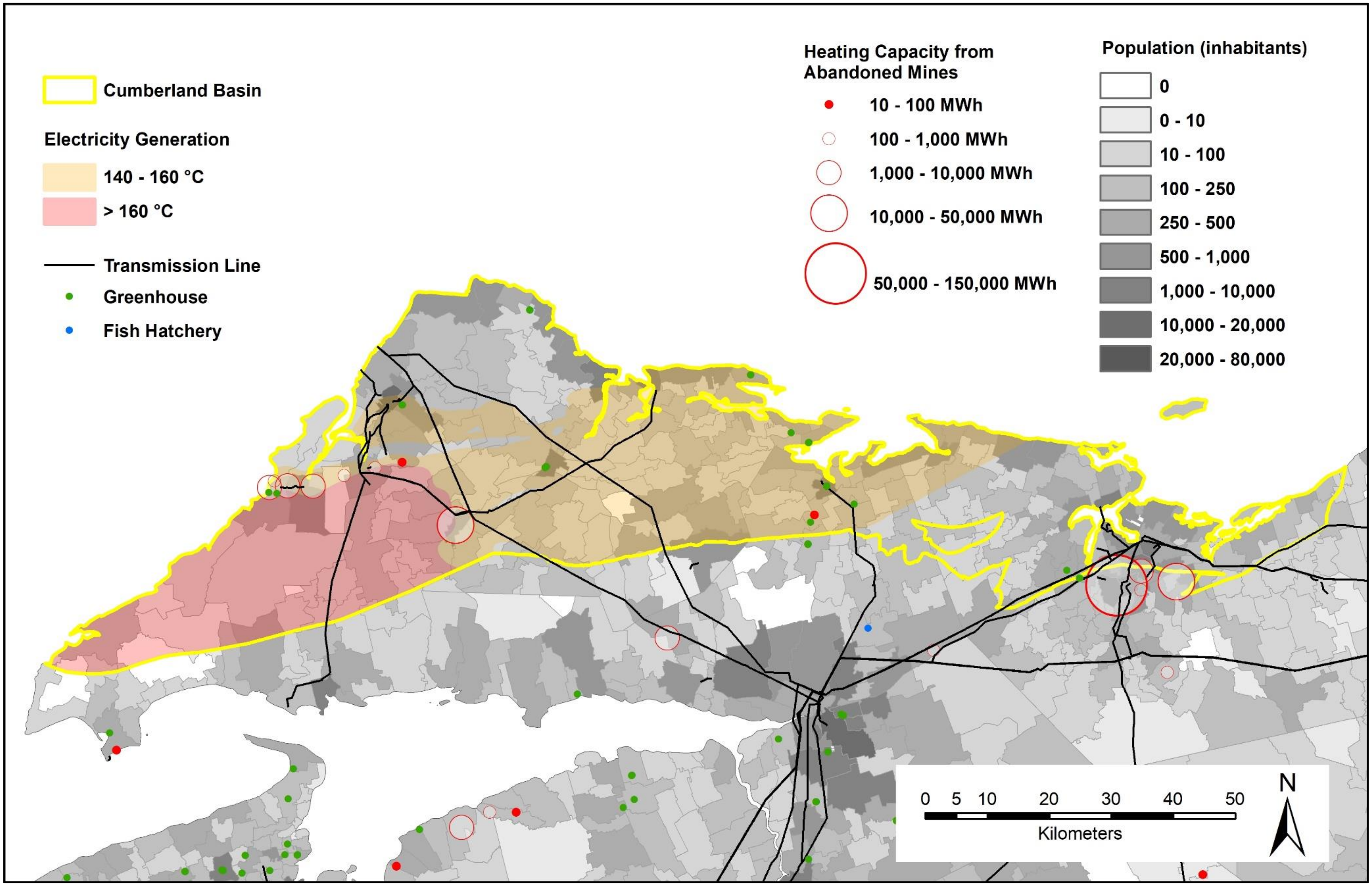

Figure 7.9. Outline of the potential for electricity generation and heating capacity from abandoned mines for the Cumberland Basin. Cartographic background: NSDEM (2020) and Government of Nova Scotia (2020).

7.3 Windsor-Kennetcook

The Windsor-Kennetcook Basin benefits from good temperature and subsurface coverage, and a moderate geothermal potential for electricity generation and direct-use of heat from aquifers and from abandoned mines has been identified. Results from the evaluation are summarized in **Table 7.1** and illustrated on **Figure 7.10**.

7.3.1 Electricity generation

The Windsor-Kennetcook area is the second in rank for electricity generation from deep aquifers in the province. However, its characteristics are much less favourable than for the Cumberland Basin and the potential is restricted to a narrow area along the shore, where temperatures are expected in the range of 80 to 100 °C at depths between 3 and 4 km. Aside from the underlying basement, the only potential aquifer suitable for electricity generation there corresponds to the lower member of the Horton Bluff Formation, which requires stimulation. Electricity generation with EGS can also be considered throughout the basin with expected temperatures at 7 km depth exceeding 160 °C.

7.3.2 Direct-use of heat

The potential for direct-use of heat from aquifers is essentially concentrated in the west-central part of the basin, where up to five potential aquifers are superimposed. The potential aquifers with the highest-ranking scores correspond to the top of the Cheverie Formation and the top of the Glass Sand Formation. The geothermal gradient calculated for the basin is 24.34 °C km^{-1} and temperatures in the range of 40 to 80 °C are expected in this area, at depths between 1 and 3 km. Direct-use of heat with deep BHE can also be considered throughout the basin, with expected temperatures at 4 km depth exceeding 80 °C.

7.3.3 Heating and cooling capacity from abandoned mines

The total heating and cooling capacities from abandoned mines in the basin amount to 6,183 and 2,164 MWh, respectively. 95% of this potential is concentrated in an underground lead mine the area of Pembroke, although isolated open-pits can also be considered in other parts of the basin.

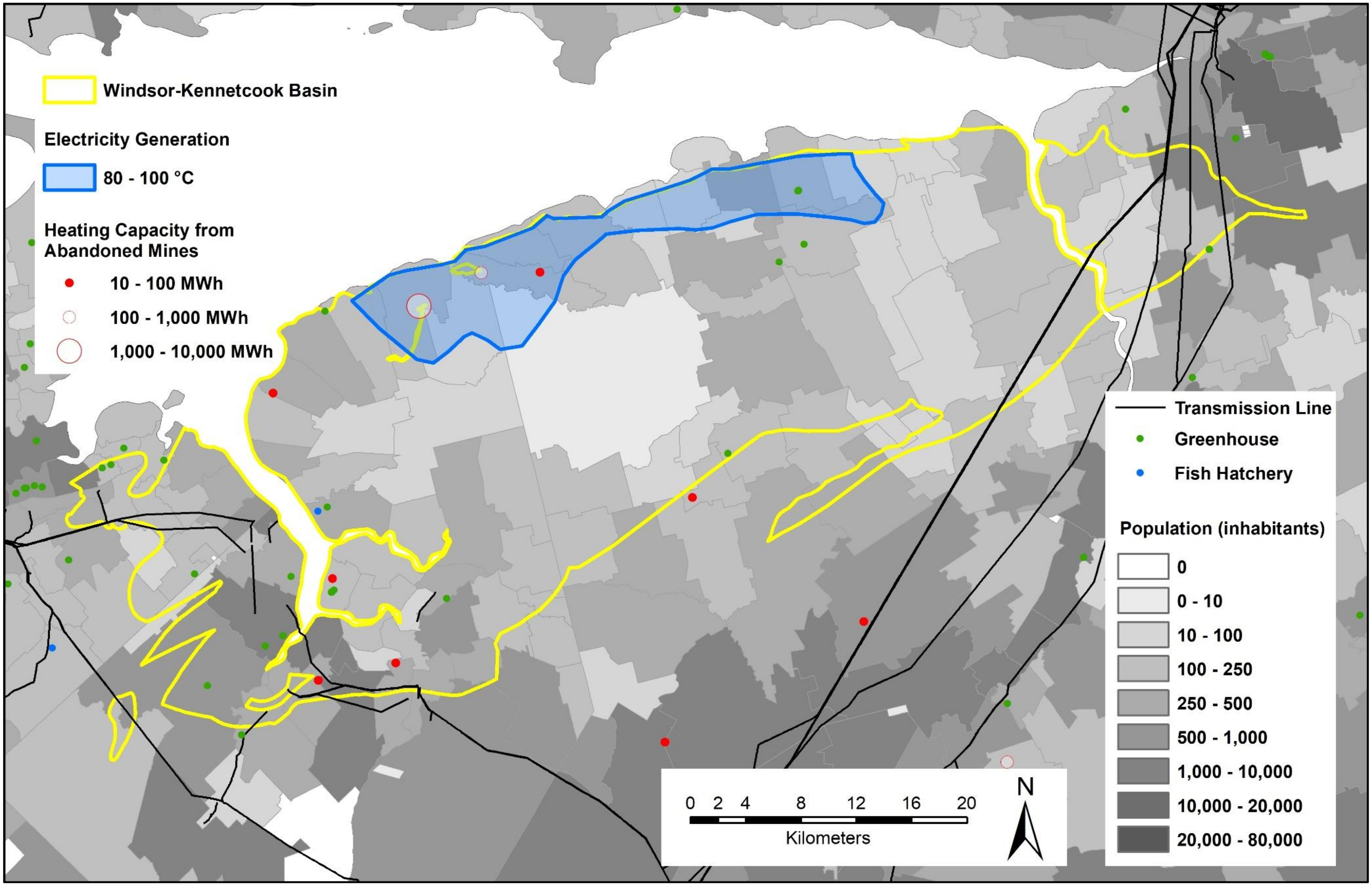

Figure 7.10. Outline of the potential for electricity generation and heating capacity from abandoned mines for the Windsor-Kennetcook Basin. Cartographic background: NSDEM (2020) and Government of Nova Scotia (2020).

7.4 Stellarton Basin

Underground temperatures in the Stellarton Basin are poorly understood, and only partial subsurface coverage is available. The available data are sufficient, however, to confirm a geothermal potential for direct-use of heat and for geothermal energy from abandoned mines. The potential for electricity generation can only be considered with EGS. Results from the evaluation are summarized in **Table 7.1** and illustrated on **Figure 7.11**.

7.4.1 Electricity generation

The basin is not deep enough to host potential aquifers at depths suitable for electricity generation, which can only be achieved in this area with EGS in the underlying basement rocks. Expected temperatures at 7 km depth exceed 160 °C.

7.4.2 Direct-use of heat

The geothermal gradient calculated for the basin (25.49 °C km^{-1}) is one of the highest interpreted for the province, which makes this area one of the most promising for direct-use of heat. However, the existence, depth and characteristics of potential aquifers within the basin cannot be confirmed with the data currently available. Expected temperatures for hypothetical aquifers present in the basin range between 40 and 80 °C, at depths between 1 and 3 km. These temperatures are considered conservative and representative of the whole area, although higher geothermal gradients in the range of 30 to 40 °C km^{-1} are locally observed at depths shallower than 1 km. Direct-use of heat with deep BHE can also be theoretically considered throughout the basin with expected temperatures at 4 km depth exceeding 80 °C.

7.4.3 Heating and cooling capacity from abandoned mines

The geothermal potential from abandoned mines for this basin ranks second after the Sydney Basin, with total heating and cooling capacities in the amount of 86,473 and 25,789 MWh, respectively. This corresponds to about 10% of the total geothermal heating and cooling capacities calculated for the province. The potential is essentially concentrated between the towns of Westville, Stellarton and New Glasgow and the largest mine (Intercolonial/Drummond Mines, close to Westville) has heating and cooling capacities of about 21,000 and 6,100 MWh, respectively.

As for all other areas, a geothermal gradient of 20 °C km^{-1} was considered to calculate the heating capacity of the basin. However, it is worth noticing that significantly higher geothermal gradients are locally documented in the Stellarton Basin, in the range of 30 to 40 °C km^{-1} (**Appendix IV**).

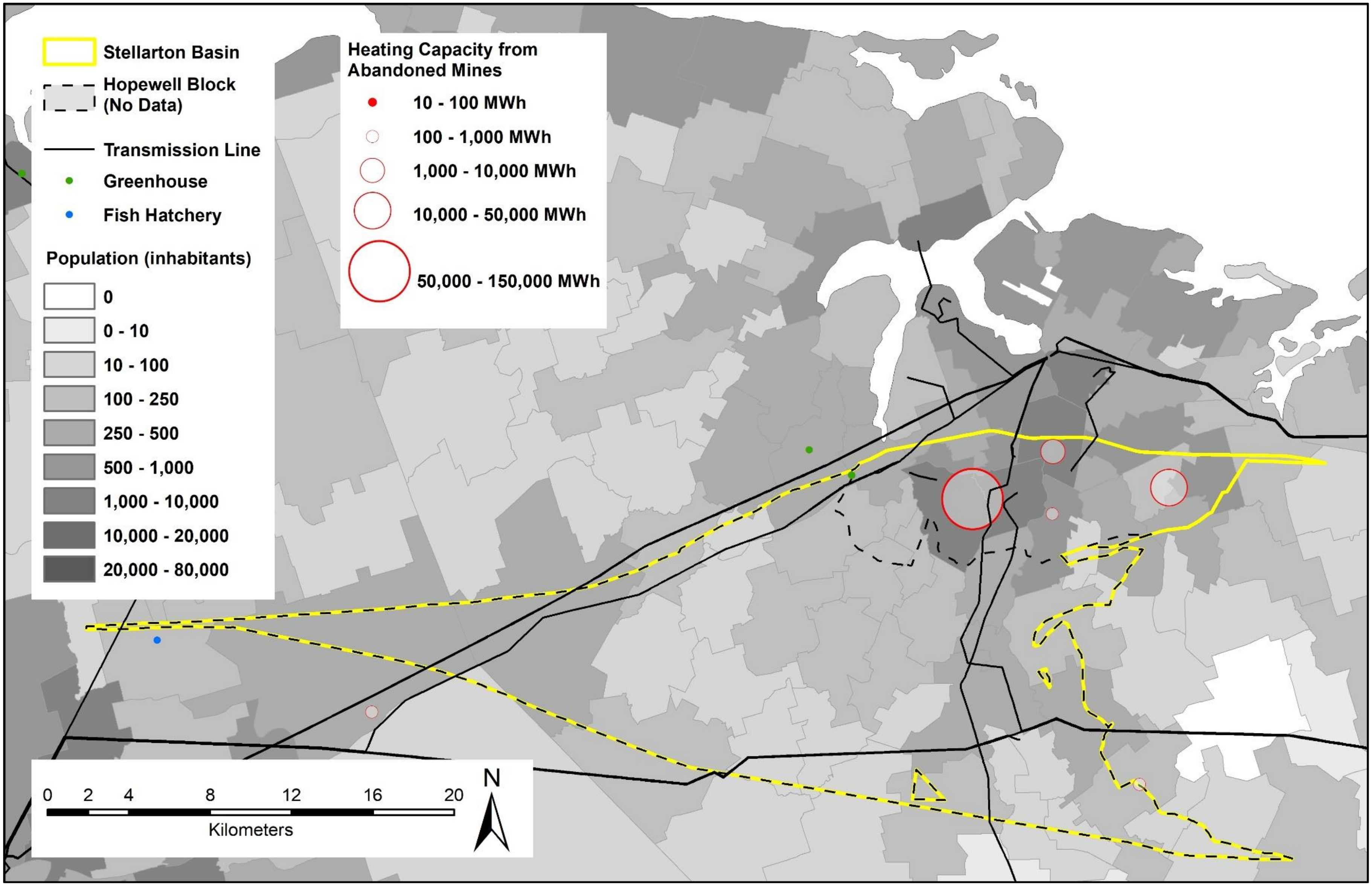

Figure 7.11. Outline of the potential for heating capacity from abandoned mines for the Stellarton Basin. Cartographic background: NSDEM (2020) and Government of Nova Scotia (2020).

7.5 Shubenacadie Basin

Underground temperatures in the Shubenacadie Basin are poorly understood and only partial subsurface coverage is available. The available data are sufficient, however, to confirm a geothermal potential for direct-use of heat from mid-depth aquifers. The geothermal potential from abandoned mines is negligible, and electricity generation can be considered only with EGS. Results from the evaluation are summarized in **Table 7.1** and illustrated on **Figure 7.12**.

7.5.1 Electricity generation

The basin is not deep enough to host potential aquifers at depths suitable for electricity generation, which can only be achieved in this area with EGS in the underlying basement rocks. Expected temperatures at 7 km depth are in the range of 140-160 °C.

7.5.2 Direct-use of heat

The low geothermal gradient calculated for the basin (20.95 °C km^{-1}) combined with the thinness of the sedimentary basin (about 1 km maximum) limits the geothermal potential for direct-use of heat from mid-depth aquifers to temperatures ranging from 20 to 40 °C. The Macumber and Cheverie formations are the two potential aquifers that can be considered in this area. Direct-use of heat with deep BHE can also be considered throughout the basin with expected temperatures at 4 km depth exceeding 80 °C.

7.5.3 Heating and cooling capacity from abandoned mines

Two underground gold mines are present at the south-center margin of the basin, with total heating and cooling capacities in the amount of 39 and 11.5 MWh, respectively. A gypsum open-pit mine in the north makes up the balance of the geothermal potential for this basin.

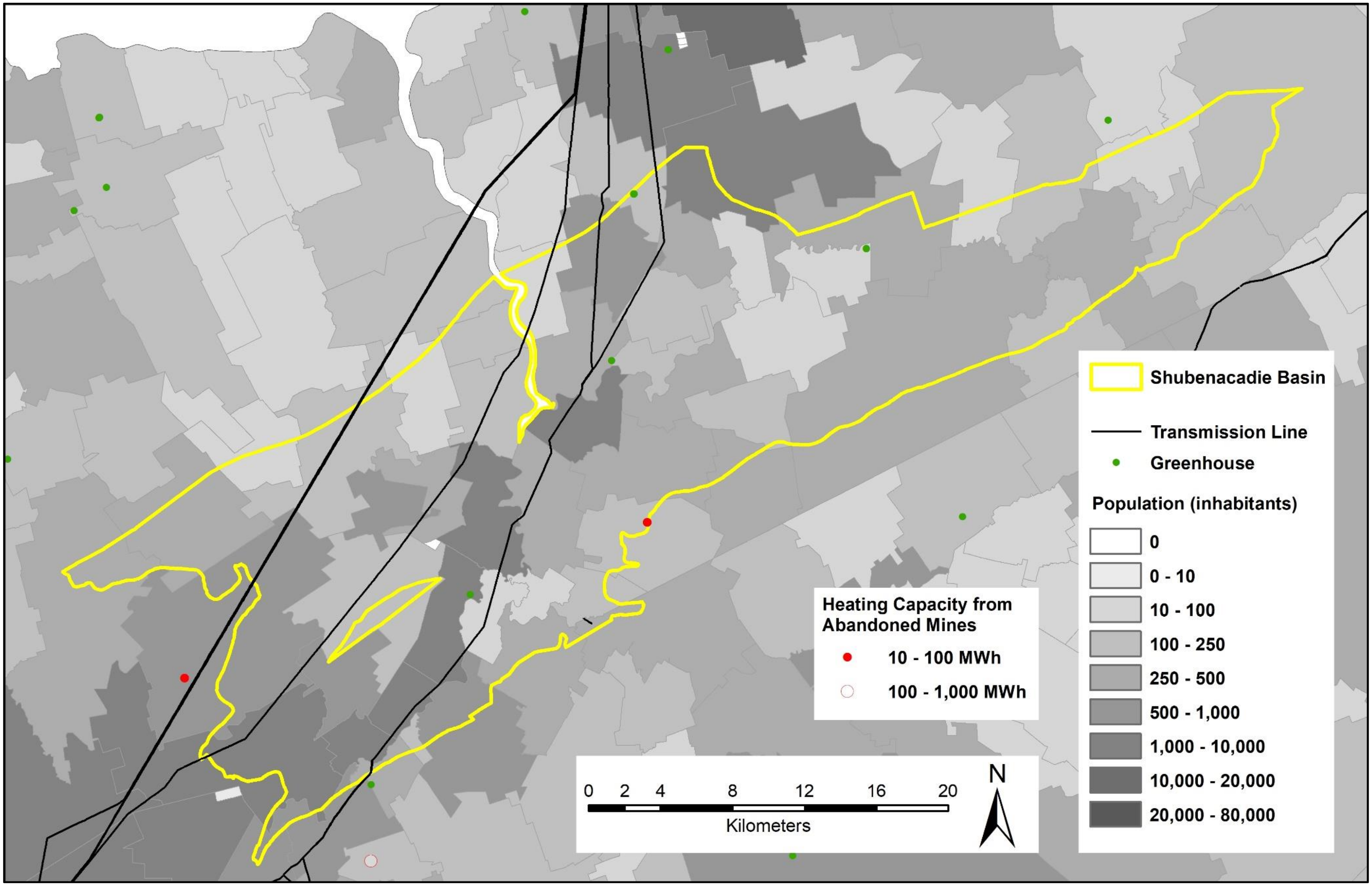

Figure 7.12. Outline of the potential for heating capacity from abandoned mines for the Shubenacadie Basin. Cartographic background: NSDEM (2020) and Government of Nova Scotia (2020).

7.6 Antigonish Basin

Underground temperatures in the Antigonish Basin are poorly understood, and only partial subsurface coverage is available. The available data are sufficient, however, to confirm a geothermal potential for direct-use of heat from mid-depth aquifers. The potential for geothermal energy from abandoned mines is negligible, and electricity generation can be considered only with EGS. Results from the evaluation are summarized in **Table 7.1** and illustrated on **Figure 7.13**.

7.6.1 Electricity generation

The basin is not deep enough to host potential aquifers at depths suitable for electricity generation, which can only be achieved in this area with EGS in the underlying basement rocks. Expected temperatures at 7 km depth exceed 160 °C.

7.6.2 Direct-use of heat

The geothermal gradient representative of the Central Antigonish Basin for depths greater than 1 km is calculated at 26.08 °C km^{-1} based on one data point. The only potential aquifer indicated by the available data is the Macumber Formation, although deeper potential aquifers may be present. Despite the comparatively high geothermal gradient calculated for the area, the potential for direct-use of heat from mid-depth aquifers is limited to the 20 to 40 °C temperature range at 1 to 2 km depth until new subsurface data become available. Direct-use of heat with deep BHE can also be considered throughout the basin with expected temperatures at 4 km depth exceeding 80 °C.

7.6.3 Heating and cooling capacity from abandoned mines

The geothermal potential from abandoned mines in the basin is limited to a single iron mine closed in 1901. Its heating and cooling capacities are at 6 and 2 MWh, respectively.

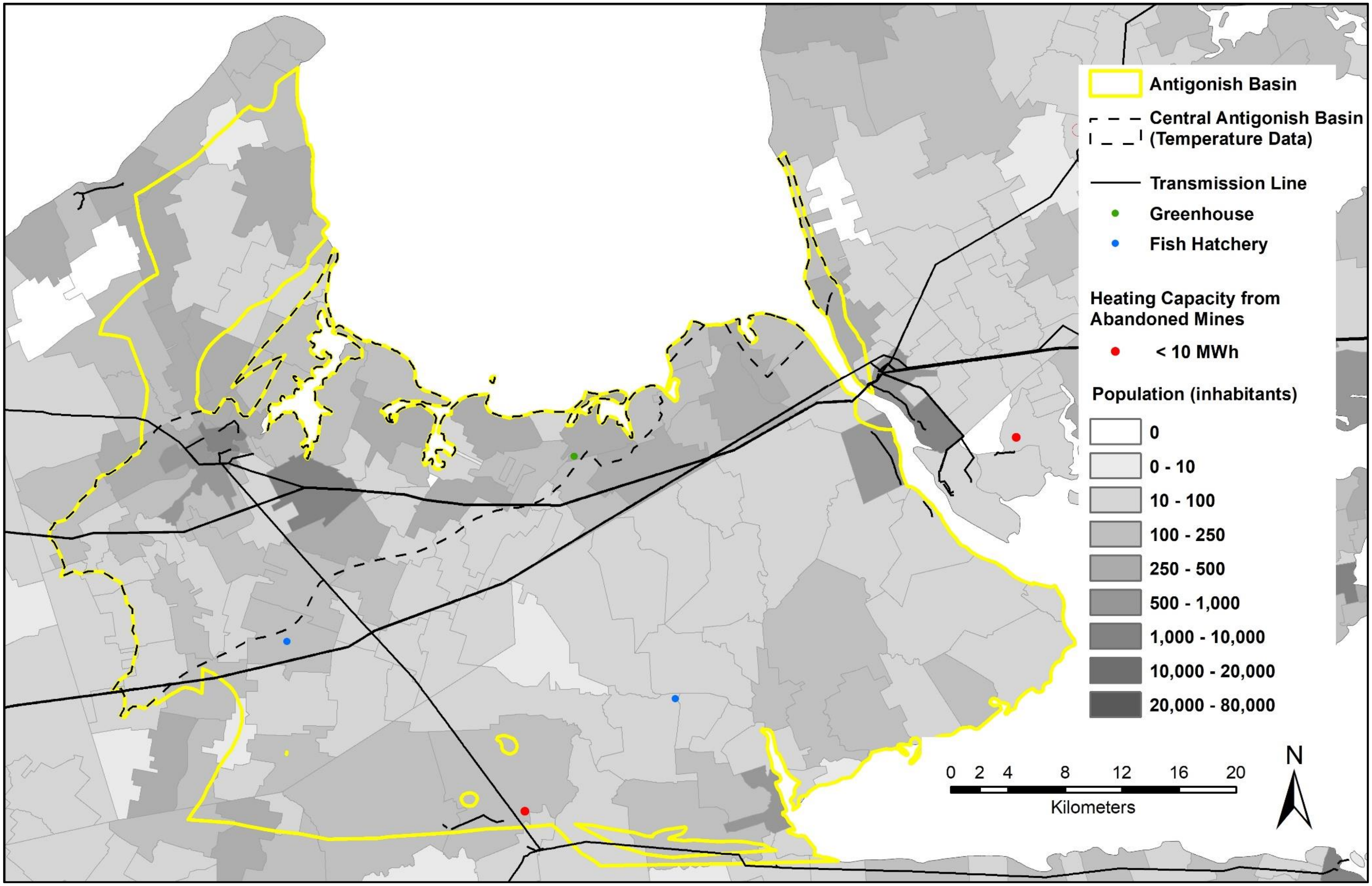

Figure 7.13. Outline of the potential for heating capacity from abandoned mines for the Antigonish Basin. Underground temperature data are available only for the Central Antigonish Basin (black dashes). Cartographic background: NSDEM (2020) and Government of Nova Scotia (2020).

7.7 Western Cape Breton Basin

Underground temperatures and the subsurface geometry of the Western Cape Breton Basin are poorly understood. However, the available data are sufficient to confirm a potential for geothermal energy from abandoned mines. The potential for direct-use of heat from mid-depth aquifers is indicated in a specific area which also has potential for electricity generation from deep aquifers. Results from the evaluation are summarized in **Table 7.1** and illustrated on **Figure 7.14**.

7.7.1 Electricity generation

The vast majority of the basin is either too shallow or lacks sufficient data to support a geothermal potential for electricity generation from deep aquifers. The only exception is the area of Port Hood and Mabou, where a theoretical potential can be considered if aquifers are present underneath the Macumber Formation. Although the geothermal gradient calculated for the basin is relatively low (20.30 °C km^{-1}), it may be slightly higher in this specific area. Electricity generation is also possible with EGS throughout the basin. Expected temperatures at 7 km depth are in the range of 140-160 °C.

7.7.2 Direct-use of heat

Due to the limitations indicated in the previous section, the potential for direct-use of heat from mid-depth aquifers can be evaluated only in the area of Port Hood and Mabou, where temperatures greater than 60 °C can be expected at depths between 3 and 4 km. The Macumber Formation is the only potential aquifer identified in the area based on available data. Direct-use of heat with deep BHE can also be theoretically considered throughout the basin with expected temperatures at 4 km depth exceeding 80 °C.

7.7.3 Heating and cooling capacity from abandoned mines

The total heating and cooling capacities from abandoned mines in the basin amount to 15,737 and 5,390 MWh, respectively. It is essentially concentrated in the coal mines of Inverness, Port Hood and Inverness (96%) and the largest mine is Inverness No.1 and 4 with heating and cooling capacities of about 9,500 and 2,700 MWh, respectively.

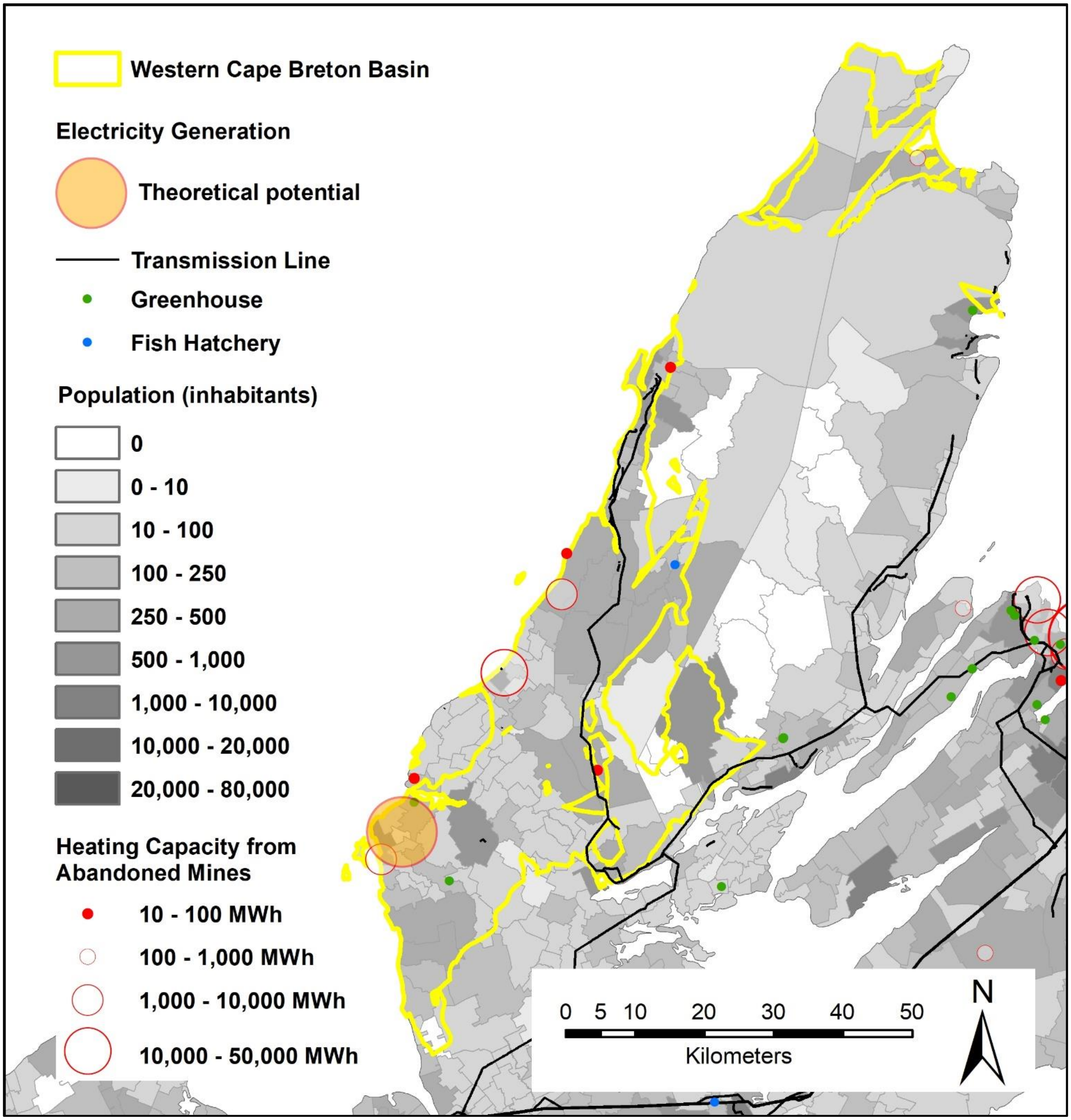

Figure 7.14. Outline of the potential for electricity generation and heating capacity from abandoned mines for the Western Cape Breton Basin. Cartographic background: NSDEM (2020) and Government of Nova Scotia (2020).

7.8 Central Cape Breton Basin

Underground temperatures and the subsurface geometry of the Central Cape Breton Basin are poorly understood. The available data are sufficient, however, to confirm a geothermal potential for direct-use of heat from mid-depth aquifers and a marginal potential for geothermal energy from abandoned mines. Electricity generation can only be considered with EGS. Results from the evaluation are summarized in **Table 7.1** and illustrated on **Figure 7.15**.

7.8.1 Electricity generation

The basin is not deep enough to host potential aquifers at depths suitable for electricity generation, which can only be achieved in this area with EGS in the underlying basement rocks. Expected temperatures at 7 km depth exceed 160 °C.

7.8.2 Direct-use of heat

The few subsurface data available indicate that the thickness of the sedimentary basin varies from less than 300 m to more than 1 km. A geothermal potential for direct-use of heat from mid-depth aquifers can be considered in the latter case based on a calculated geothermal gradient of 23.77 °C km^{-1} with expected temperatures in the range of 30 °C at a depth of 1 km. Direct-use of heat with deep BHE can also be considered throughout the basin, with expected temperatures at 4 km depth exceeding 80 °C.

7.8.3 Heating and cooling capacity from abandoned mines

The total heating and cooling capacities from abandoned mines in the basin amount to 777 and 1,123 MWh, respectively. This corresponds to geographically scattered open-pit mines.

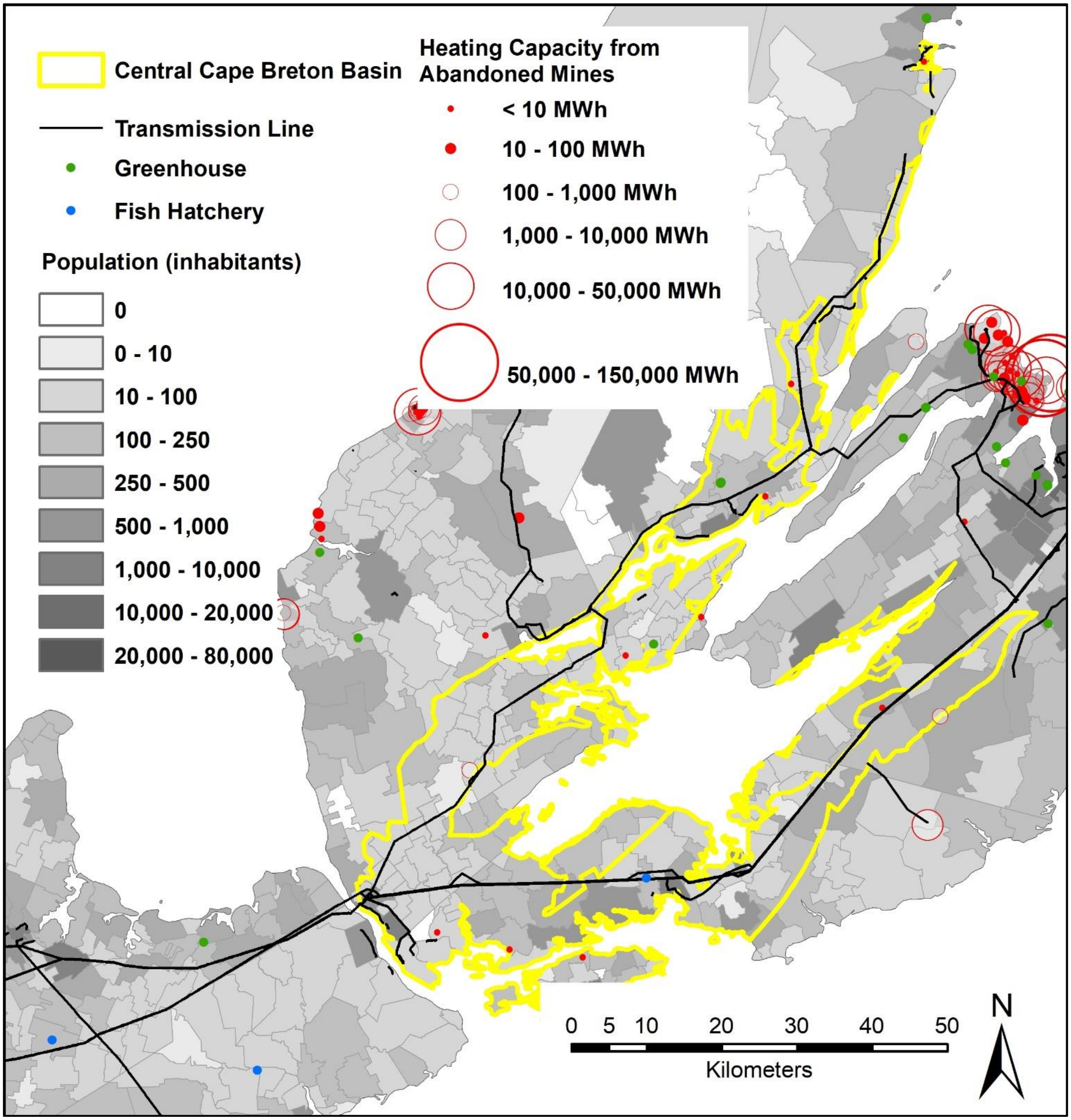

Figure 7.15. Outline of the potential for heating capacity from abandoned mines for the Central Cape Breton Basin. Cartographic background: NSDEM (2020) and Government of Nova Scotia (2020).

7.9 Sydney Basin

Underground temperatures and the subsurface geometry of the Central Cape Breton Basin are poorly understood. However, the available data confirm that this region has the highest geothermal potential for heating and cooling from abandoned mines in Nova Scotia. A geothermal potential for direct-use of heat from mid-depth aquifers is also present over the same area. Electricity generation can only be considered with EGS. Results from the evaluation are summarized in **Table 7.1** and illustrated on **Figure 7.16**.

7.9.1 Electricity generation

The basin is not deep enough to host potential aquifers at depths suitable for electricity generation, which can only be achieved in this area with EGS in the underlying basement rocks. Expected temperatures at 7 km depth exceed 160 °C.

7.9.2 Direct-use of heat

The potential for direct-use of heat from mid-depth aquifers can be evaluated only in the northern part of the basin due to insufficient data to the south. Four specific aquifers are identified in this area and the local geothermal gradient can be slightly higher than the one calculated for the whole basin at 23.65 °C km^{-1}. The expected temperature ranges from 20 to 40 °C at depths lower than 1 km and up to 40 to 60 °C at depths between 1 and 2 km. Although the geothermal potential for direct-use of heat from mid-depth aquifers cannot be evaluated in the southern part of the basin, it is presumed to be lower than in the north based on the few subsurface data available. Direct-use of heat with deep BHE can also be theoretically considered throughout the basin, with expected temperatures at 4 km depth exceeding 80 °C.

7.9.3 Heating and cooling capacity from abandoned mines

The northern part of the Sydney Basin is by far the most promising area for geothermal heating and cooling from abandoned mines, representing about 80% of the total capacity of the province. The total heating and cooling capacities amount to 636,894 and 187,616 MWh, respectively, 98% of which is concentrated in the coal mines offshore of Sydney Mines, New Waterford and Glace Bay. The largest mine (Dominion Colliery, close to Glace Bay) has heating and cooling capacities of about 117,900 and 34,400 MWh, respectively.

As discussed in **Section 5.3** and for comparative purposes, the heating of one hectare of greenhouses requires 7,000 MWh per year (2,832.8 MWh $acre^{-1}$) and a 0.1 hectare data centre (2.471 acres) has a cooling energy needs equivalent to 8,000 MWh per year in southern Québec. This would mean that the abandoned mines in the Sydney area would have the potential to supply the heating needs of nearly 100 hectares of greenhouses as well as the cooling needs of about 25 data centres.

Given that almost all of this potential is contained in the offshore environment, it is very likely that the entire volume of water actually consists of seawater. Thus, this potential would be reduced by 8%, proportional to the difference in the volumetric heat capacity of seawater compared to fresh water. Also, it will be necessary to use suitable equipment to avoid corrosion due to the salinity of sea water.

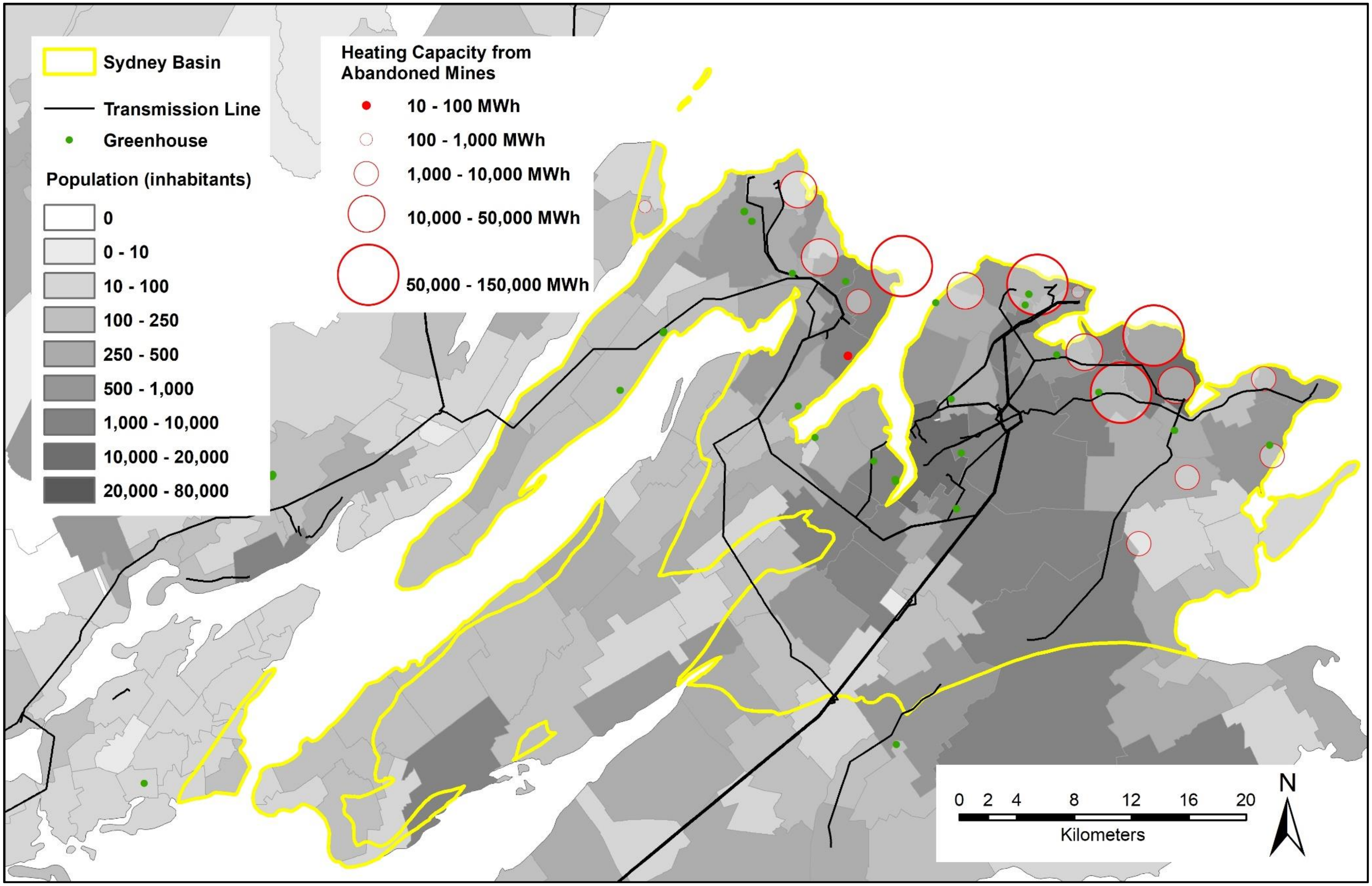

Figure 7.16. Outline of the potential for heating capacity from abandoned mines for the Sydney Basin. Cartographic background: NSDEM (2020) and Government of Nova Scotia (2020).

7.10 Fundy Basin

Underground temperatures and the subsurface geometry of the Fundy Basin are poorly understood and the geothermal potential of the area cannot be evaluated based on the available data. Using realistic ranges of values, a geothermal potential for direct-use of heat from mid-depth aquifers can be considered while electricity generation can only be theoretically considered with EGS. The basin also has a marginal potential for geothermal energy from abandoned mines. Results from the evaluation are summarized in **Table 7.1** and illustrated on **Figure 7.17**.

7.10.1 Electricity generation

The basin is not deep enough to host potential aquifers at depths suitable for electricity generation, which can only be theoretically achieved in this area with EGS in the underlying basement rocks. Expected temperatures at 7 km depth are in the range of 140-160 °C or exceed 160 °C, respectively for the low-end and high-end geothermal gradients considered.

7.10.2 Direct-use of heat

A geothermal potential for direct-use of heat from mid-depth aquifers is expected when considering a realistic range of geothermal gradients (20 to 30 °C km^{-1}) and an approximate thickness of 1 km for the onshore part of the basin. The only potential aquifer is the Wolfville Formation, located at the base of the sedimentary sequence. Temperatures in the range of 20 to 40 °C are expected at a depth of about 1 km for both the high- and low-end scenarios. Direct-use of heat with deep BHE can also be considered throughout the basin, with expected temperatures at 4 km depth exceeding 80 °C for both the low-end and high-end geothermal gradients considered.

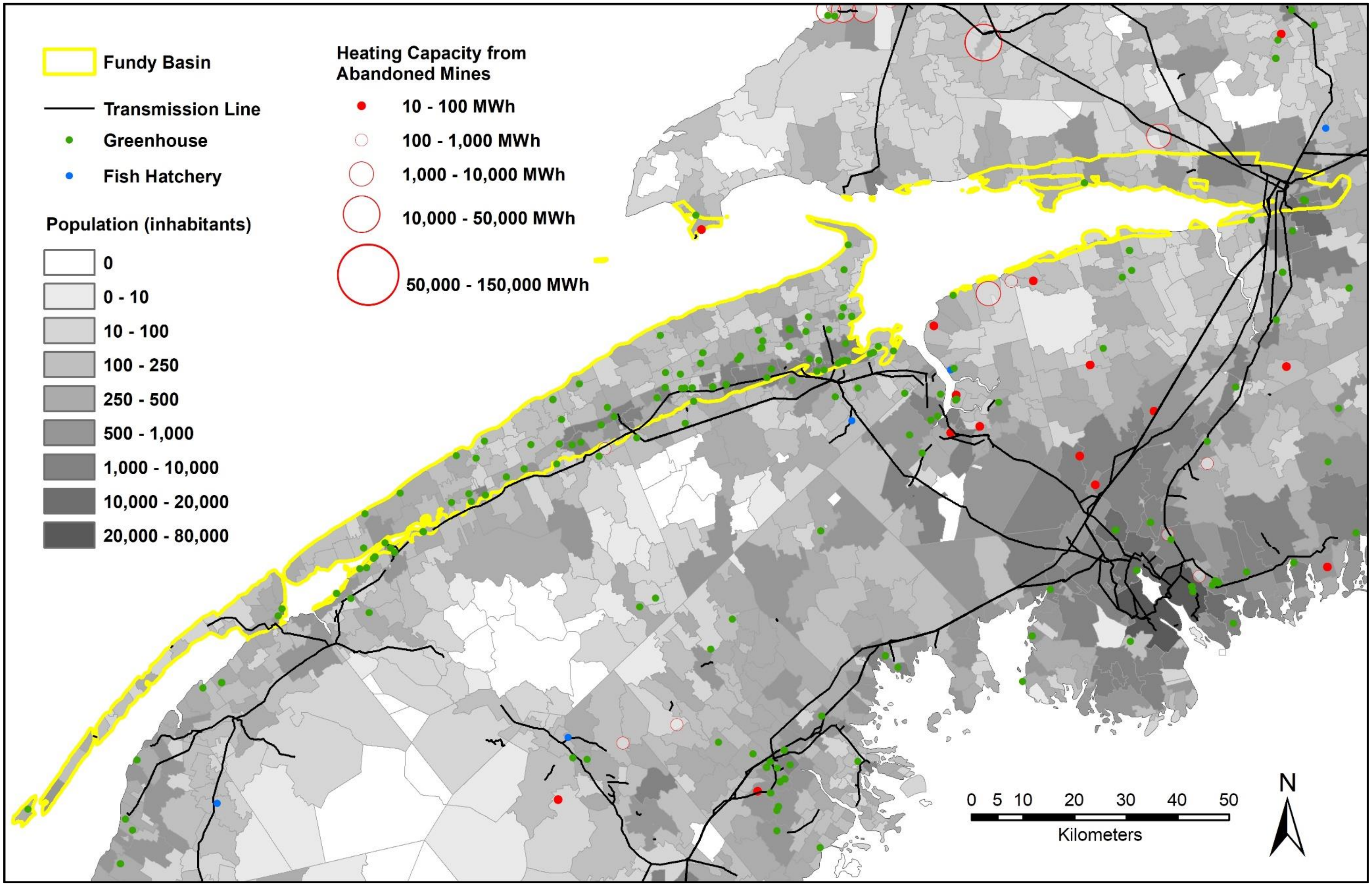

Figure 7.17. Outline of the potential for heating capacity from abandoned mines for the Sydney Basin. Cartographic background: NSDEM (2020) and Government of Nova Scotia (2020).

7.11 Meguma terrane

Underground temperatures and the subsurface geometry of the Meguma terrane are poorly understood. The available data confirm a geothermal potential for electricity generation, direct-use of heat and geothermal energy from abandoned mines. Results from the evaluation are summarized in **Table 7.1** and illustrated on **Figure 7.18**.

An aquifer must be created by means of EGS or deep BHE before the metamorphic rocks that compose the terrane can be considered for electricity generation or direct-use of heat. Subsurface geometry is not a critical parameter in this case.

7.11.1 Electricity generation

A geothermal gradient of 12.63 °C km^{-1} is calculated based on the few data available to constrain the underground temperatures within the vast extent of the Meguma terrane. Based on this gradient the minimal temperature of 80 °C that is required for electricity generation with EGS is reached at a depth of about 5 km and a temperature of about 110 °C is reached at a depth of 7 km, beyond which electricity generation becomes impractical.

7.11.2 Direct-use of heat

Due to the low geothermal gradient of the area the minimal temperature required for direct-use of heat (20 ºC) with deep BHE is reached at a depth of about 1 km and a temperature of about 64 °C is reached at a depth of 4 km, beyond which direct-use of heat becomes impractical.

7.11.3 Heating and cooling capacity from abandoned mines

The total heating and cooling capacities from abandoned mines in the Meguma terrane amount to 4,378 and 1,281 MWh, respectively. It consists mostly of gold mines with individual heating capacities not exceeding 900 MWh.

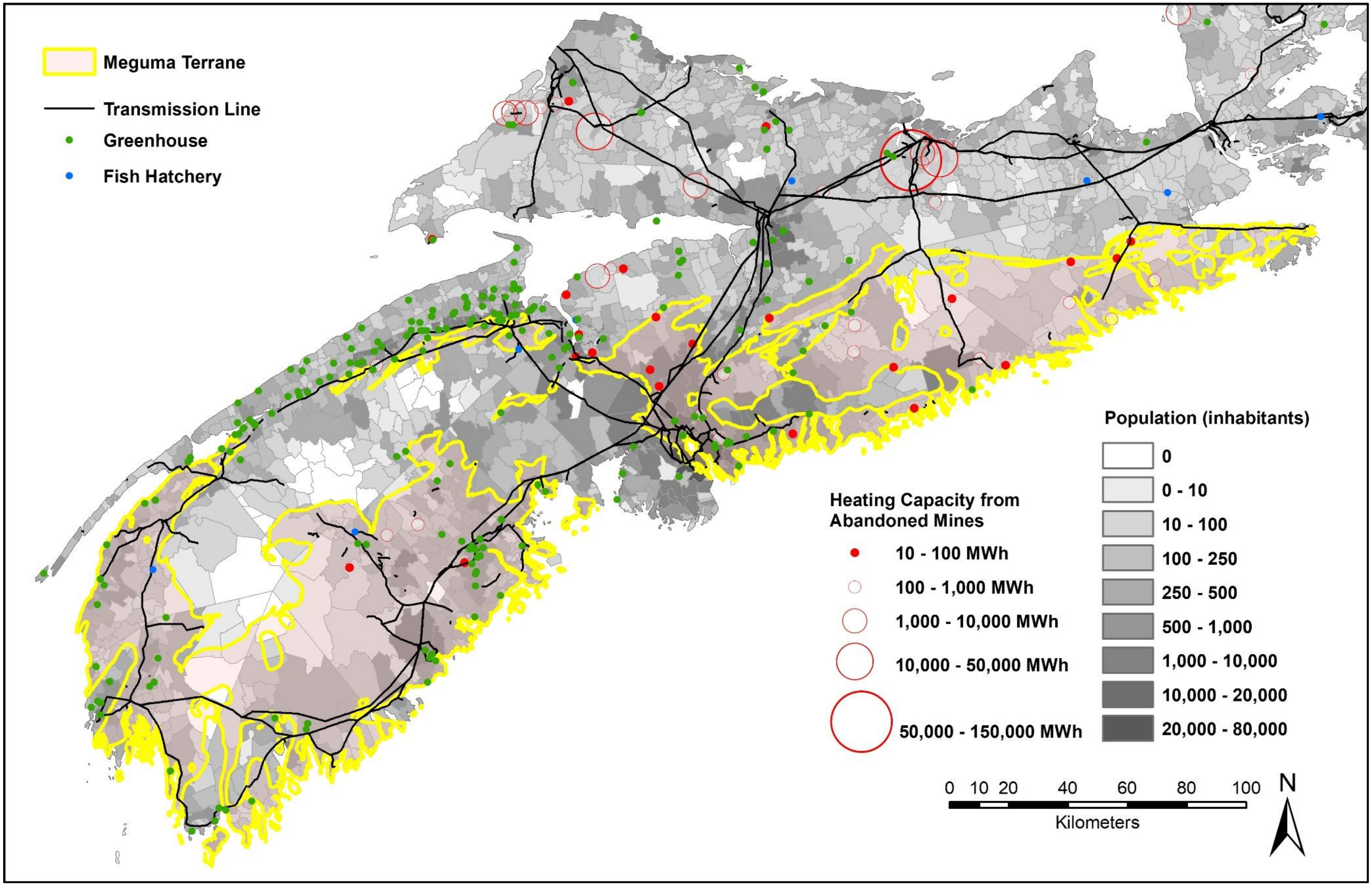

Figure 7.18. Outline of the potential for heating capacity from abandoned mines for the Meguma terrane. Cartographic background: NSDNR (2006) and Government of Nova Scotia (2020).

7.12 Devonian intrusives

Underground temperatures and the subsurface geometry of the Devonian intrusives are poorly understood. The available data are sufficient to confirm a geothermal potential for electricity generation and direct-use of heat. There is no potential for geothermal energy from abandoned mines in this area. Results from the evaluation are summarized in **Table 7.1** and illustrated on **Figure 7.19**.

An aquifer must be created by means of EGS or deep BHE before the magmatic rocks that compose the intrusives can be theoretically considered for electricity generation or direct-use of heat. Subsurface geometry is not a critical parameter in this case.

7.12.1 Electricity generation

The intrusives are not homogeneous and differing concentrations of radioactive minerals may result in different geothermal gradients, a variability that cannot be assessed based on the minimal temperature data currently available. Thus, two contrasted geothermal gradients are obtained from the available data: 17.92 and 41.86 °C km^{-1}.

In the first case, the minimum temperature required for electricity generation with EGS (80 ºC) is reached at a depth of about 3.7 km and a temperature of about 145 °C is reached at a depth of 7 km, whereas for the second gradient, these values are about 1.7 km depth and 310 °C, respectively.

7.12.2 Direct-use of heat

In areas corresponding to the lower geothermal gradient the minimal temperature required for direct-use of heat with deep BHE is reached at a depth of about 800 m and a temperature of about 85 °C is reached at a depth of 4 km, beyond which direct-use of heat becomes impractical. In areas corresponding to the higher geothermal gradient, these values are about 350 m and 180 °C, respectively.

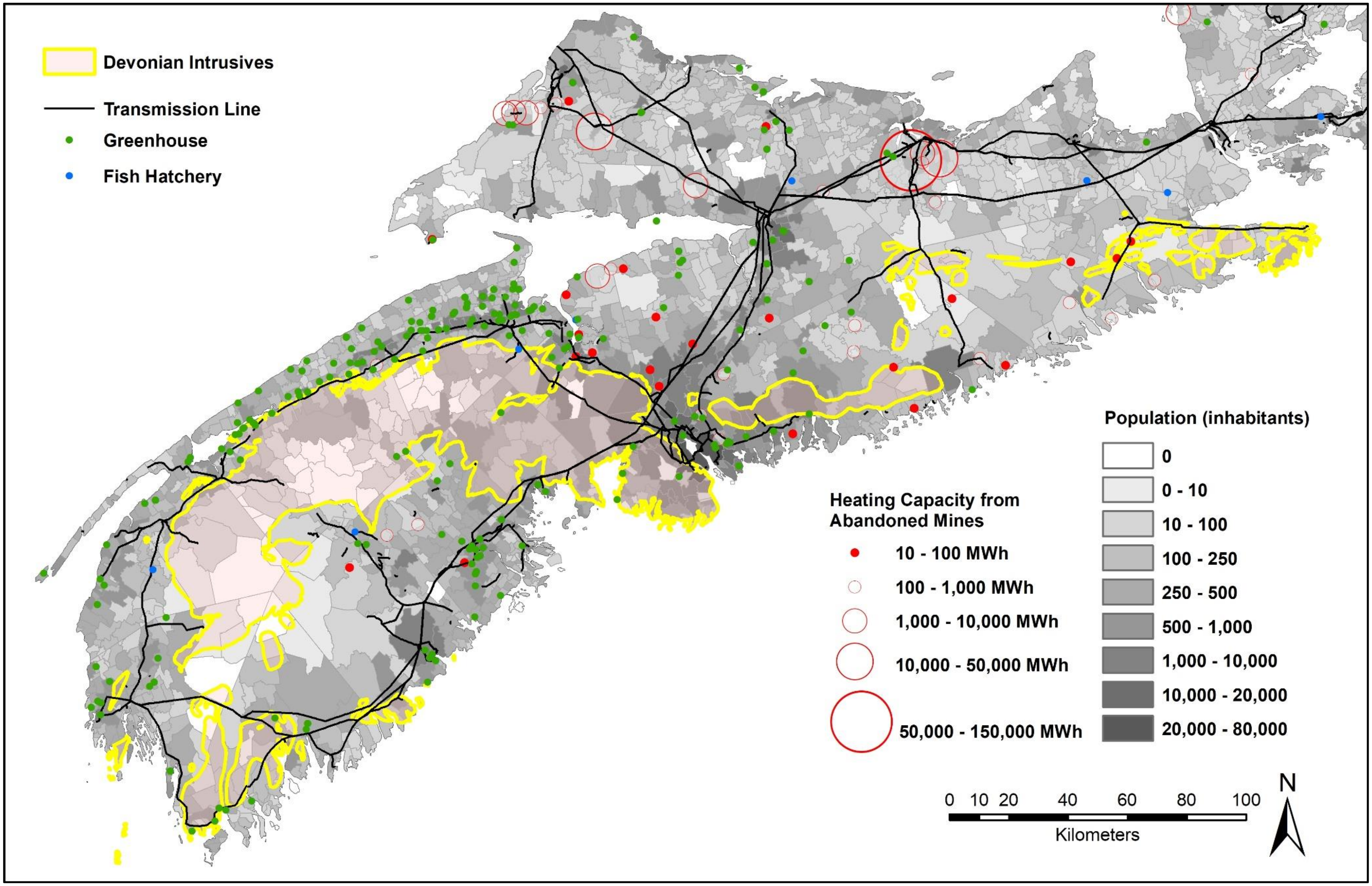

Figure 7.19. Outline of the potential for heating capacity from abandoned mines for the Devonian intrusives. Cartographic background: NSDNR (2006) and Government of Nova Scotia (2020).

7.13 Other areas

The geothermal potential for electricity generation and direct-use of heat in other areas could not be evaluated due to the complete lack of underground temperatures. These areas include the Musquodoboit, St. Mary's and Parrsboro-Kemptown sedimentary basins and the pre-Carboniferous magmatic, metamorphic and sedimentary rocks located mostly north of the Cobequid-Chedabucto Fault.

The potential for geothermal energy from abandoned mines is marginal or absent in the case of the three sedimentary basins listed above. For the pre-Carboniferous rocks, the total heating and cooling capacities amount respectively to 4,998 and 1,465 MWh. This potential is dominated by an underground iron mine in Colchester County (55%) and an underground zinc mine in Richmond County (23%), the remainder corresponding mostly to scattered open-pit mines and small underground iron mines. Results from the evaluation are summarized in **Table 7.1**.

7.14 Comparison with operational analogues

Evaluation of Nova Scotia's geothermal resources for electricity generation and for direct-use of heat was undertaken with the possibilities for long-term development in mind. Thus, electricity generation potential was evaluated down to 7 km depth while known operational geothermal power plants and experimental projects around the world do not exceed 5.5 km depth, as indicated in **Section 2**. Likewise, examples of direct-use of heat around the world do not exceed 3 km depth. **Figure 7.20** illustrates the potential for electricity generation and direct-use of heat based on these current economical thresholds.

The combined heating and cooling capacity from abandoned mines is shown on **Figure 7.21**. Examples of operational systems around the World show that the extent of the heated/cooled area varies considerably across the projects, from single buildings to urban areas of over 125,000 m^2 and can provide a wide range of energy capacity (30 – 30,000 MWh). It thus appears that no matter the volumes involved, an abandoned mine always shows sufficient potential to be exploited, as long as the mine and end-user are spatially close to each other. So, a geothermal heat pump system can be specifically designed such that it can supply the end user requirements while maintaining a sustainable geothermal system over the long term.

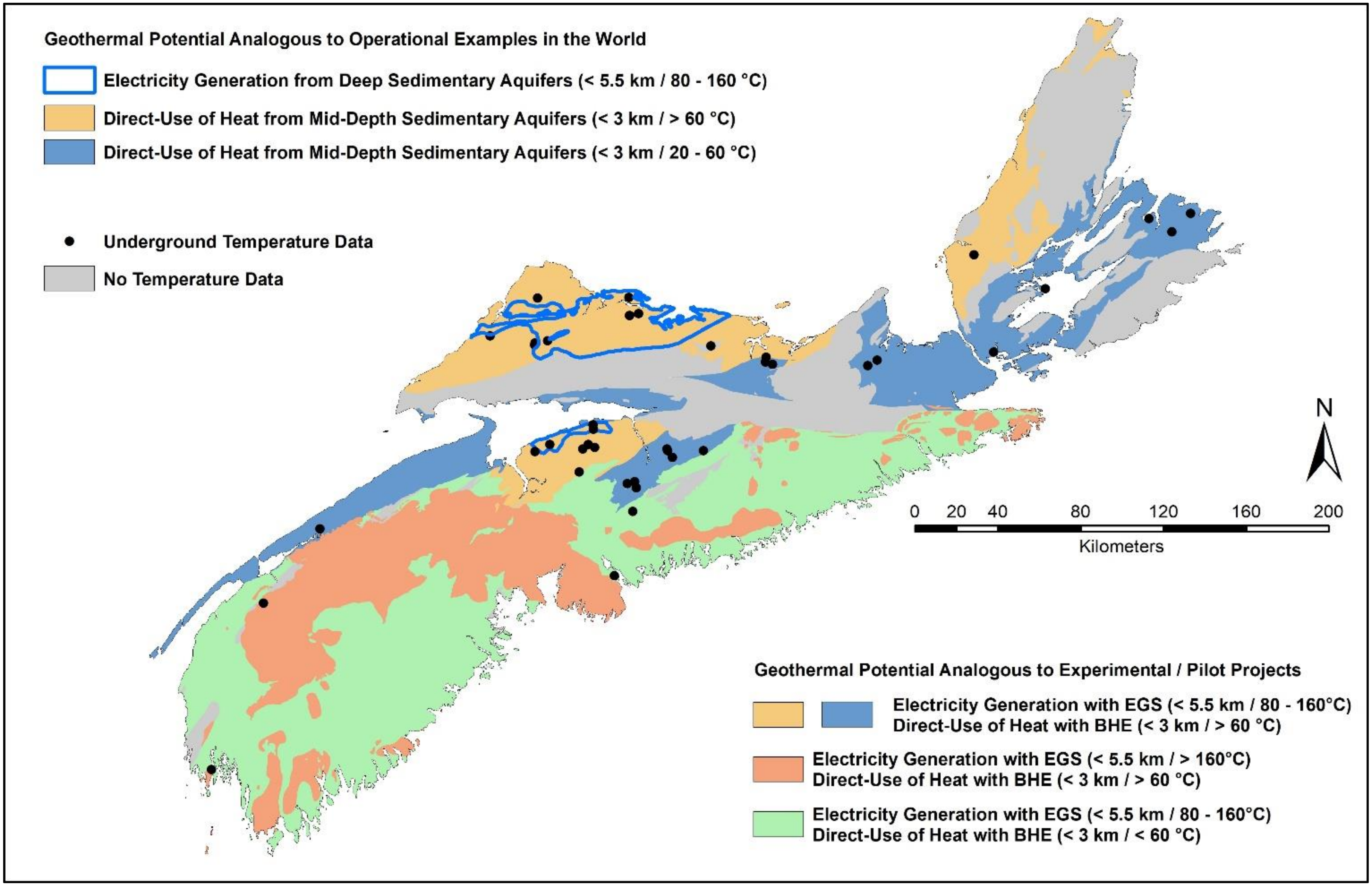

Figure 7.20. Distribution of the potential in Nova Scotia for electricity generation and direct-use of heat, based on similar operational examples around the World.

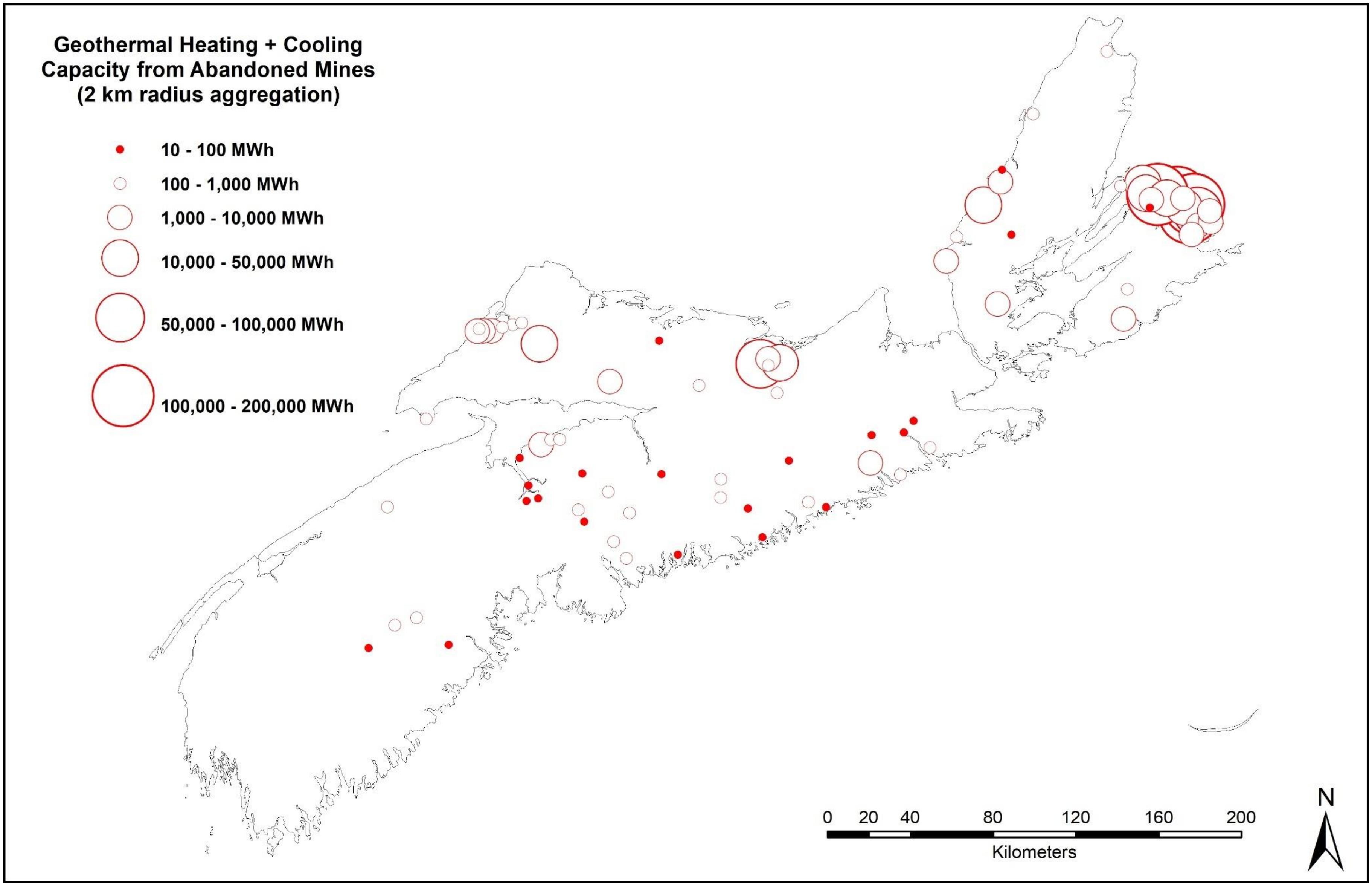

Figure 7.21. Total geothermal energy generation capacity in Nova Scotia from abandoned mines for heating and cooling combined purposes. Mines within a radius of 2 km from each other have been aggregated for clarity purposes.

7.15 References

ADEME, 2020. Coûts des énergies renouvelables et de récupération en France, données 2019. Agence de la transition écologique, Angers, 100 p. https://www.ademe.fr/couts-energies-renouvelables-recuperation-france

Canada Energy regulator, 2019. Canada's Energy Future 2019: Energy Supply and Demand Projections to 2040. https://www.cer-rec.gc.ca/en/data-analysis/canada-energy-future/2019/index.html

Government of Nova Scotia, 2020. Nova Scotia Civic Address File; Nova Scotia Topographic Database. Geographic Data Directory files. https://nsgi.novascotia.ca/gdd/

Hydro-Québec, 2017. Renewable energy option: Deep geothermal energy. Bibliothèque et Archives nationales du Québec, 2016G451A, 9 p. https://www.hydroquebec.com/data/developpement-durable/pdf/file-geothermal.pdf

IRENA, 2017. Geothermal Power Technology Brief. International Renewable Energy Agency, Abu Dhabi, 28 p. https://www.irena.org/publications/2017/Aug/Geothermal-power-Technology-brief

Joint Research Centre, 2018. Cost development of low carbon energy technologies: Scenario-based cost trajectories to 2050, 2017 edition. Luxembourg, 77 p. https://doi.org/10.2760/490059

NSDNR, 2006. Geological map of the province of Nova Scotia, Scale 1:500 000, Compiled by J. D. Keppie, 2000. Digital Version of Nova Scotia Department of Natural Resources Map ME 2000-1. DP ME 43, Version 2.

NSDEM, 2020. Digital contours of sedimentary basins. Nova Scotia Department of Energy and Mines, unpublished data.

Nova Scoria Power, 2020. Tariffs. April 21, 2020. Halifax, 124 p. https://www.nspower.ca/about-us/electricity/rates-tariffs

8. RECOMMENDATIONS

8.1 Knowledge gaps

8.1.1 Sedimentary basin

8.1.1.1 Temperature

Most of the geothermal gradients calculated in this report for depths greater than 1,000 m were determined from temperatures measured in petroleum wells, and that were not at equilibrium. The correction that was applied by the methods of Harrison et al. (1983) or Blackwell et al. (2010) proved to be the most practical with the available data (see **Section 5.1.1.1**), but did not achieve a complete restoration of the temperatures to the point of equilibrium. The consequence is that the corrected temperatures used to calculate the geothermal gradients may be slightly underestimated below 2,000 m and slightly overestimated beyond this depth. Outside the sedimentary basins, the temperatures cannot be corrected other than to account for the paleoclimatic effect.

Also, the geothermal gradient calculated at a regional scale may not be representative of a specific location that has been selected to develop its geothermal potential. For example, local effects due to the circulation of hydrothermal fluids along fault conduits, or simply due to the thickening of the sedimentary basin in a graben, can result in a locally higher geothermal gradient compared to the surrounding area. The Stellarton Basin is an example where both cases can occur at the same place, with a higher gradient at depths shallower than 1,000 m and a lower gradient beyond that depth. On the other hand, the Fundy Basin lacks temperature data to the point that only speculative scenarios can be considered to constrain its geothermal gradient. In the case of the Meguma terrane and the Devonian intrusives in the southern part of the province, only very few (and inadequate) temperature data are available so that the calculated gradients are likely not representative of the whole area and local anomalies can exist.

8.1.1.2 Subsurface geometry

In the sedimentary basins, a good understanding of the subsurface geometry is important so as to accurately know the depth of the aquifers, their regional extent and limits, the presence of possible fault conduits for deep-seated hydrothermal fluids, and the overall thickness of sediments. All these parameters impact the location and the prospectivity of geothermal areas.

The subsurface of the Cumberland and Kennetcook basins is well constrained, thanks to numerous well penetrations and extensive seismic coverage. The understanding of the geometry of the other basins, on the other hand, is much more limited and sometimes only constrained by indirect, offshore data, as it is the case for the Fundy Basin. In these cases, the evaluation of the geothermal gradient has been limited to localized areas where some well data were available. In the case of the Fundy Basin, assumptions have been made based on regional data. Even in well-defined areas, uncertainties remain at the edges of the subsurface model. For example, the outline of the area prospective for electricity generation in the Kennetcook Basin may be modified if additional data were obtained to complete the subsurface data along the northern margin of the basin.

8.1.1.3 Aquifers

The characteristics of an aquifer control the flow capacity of the geothermal system. Sandstones with sufficient permeabilities and large volumes of pores have a higher potential for direct-use of heat and electricity generation than tight formations such as siltstones, shales and magmatic of metamorphic rocks. While the lack of permeability of the latter two examples is obvious, the aquifer properties of most sedimentary rocks can vary significantly and must be carefully analysed before the geothermal potential can be fully appreciated.

In the absence of producing oil or natural gas reservoirs onshore Nova Scotia, little data is available to determine the properties of the potential aquifers. Even in sedimentary basins where the geothermal gradient and the subsurface are reasonably well constrained, the properties of the potential aquifers remain the biggest unknown to evaluate their geothermal potential. Throughout **Sections 6** and **7**, the aquifers evaluated are always referred to as "potential aquifers".

8.1.2 Meguma terrane and the Devonian intrusives

8.1.2.1 Temperature

Only two temperature readings for the Meguma terrane and two temperature readings for the Devonian intrusives were recorded in our compilation. In the case of Meguma terrane, the depths of these data are rather shallow (333 and 607 m). For the Devonian intrusives, one temperature measurement was recorded at a depth of 1,450 m but has a low level of confidence because it was not recorded at equilibrium.

Considering the large spatial extent of these two geological assemblages, as well as their great diversity of mineralogical composition, the availability of temperature data is far too limited to permit a proper evaluation of the potential aquifers with any level of confidence.

8.1.2.2 Radiogenic elements content

The geothermal potential of magmatic rocks such as the Devonian intrusives can be attractive due to the presence of radioactive elements (thorium, potassium, and uranium), which produce heat by radioactive decay. Known as radiogenic resources, they are usually found among granitic intrusions. The lithological distinction is important, because the chemical elements Th, K and U generally reach concentrations that might have geothermal significance only in granite *sensu stricto*. Concentrations of these elements are typically too low in petrologically similar but less geochemically evolved rock types like granodiorites and diorites. This localized heating increases the geothermal gradient, providing warmer temperatures at economical drilling depths, and are called High Heat Production (HHP). However, rocks with a low thermal conductivity, typically below 2.5 W/mK, is needed to trap the heat below the surface creating a thermal blanket effect and ensuring the geothermal gradient remains high.

Leslie (1982, 1983) report some analyses of radioactive element contents in Nova Scotia granitoid rocks and Leslie (1985) mentions further analyses, without providing the results. Additional information may be found in the mining exploration reports.

8.1.2.3 Subsurface geometry

The evidence for assessing the geothermal potential for the Meguma terrane and the Devonian intrusives prospects is far from adequate. Most significantly, knowledge of the distribution of granitic intrusions with high radiogenic elements content is limited to those that are currently at outcrops and for which appropriate geochemical data exist. We need therefore to improve our understanding of the distribution of exposed and buried intrusions containing high heat production rocks.

8.1.3 Abandoned mines

8.1.3.1 Water temperature

Assumptions were made to generalize geothermal potential interpretations across all mines since data on mine depths were partial or missing. Indeed, Arkay (2000) assigned a depth for most underground metallic and industrial mineral mines, but none for underground coal mines. Therefore, in order to provide a more consistent assessment between these two types of mines, a generalized depth for underground coal mines (500 m) and underground metallic and industrial mineral mines (250 m) was assumed. These depths were then used to estimate the average water temperature assuming a uniform geothermal gradient of 20 °C km^{-1}.

Indeed, based on data compiled by Arkay (2000), we found that the largest metallic and industrial mineral mines averaged around 250 m in depth, which was the basis for this choice. However, it is important to note that the two largest underground metallic and industrial mineral mines are 523 and 26 m deep (Walton-Magnet Cove and Malagash mines). The heating potential is thus underestimated by 100% for the first case and overestimated by 50% for the second. Conversely, the cooling potential would be overestimated by 200% and underestimated by 25%, respectively. However, the overall potential combining heating and cooling provides a reasonable estimate.

For coal mines, given that the volume of ore extracted was higher than for metallic and industrial mineral mines and that the depth was twice as much, the average water temperature was 12 °C. In comparison, the Springhill mine is 1.2 km deep and the mine water is pumped at 18 °C. Therefore, in some cases the assessment will remain conservative, but it should be noted that the Springhill case is most likely the optimal scenario.

8.1.3.2 Mine working geometry

Several assumptions were made to overcome the geometry factor in the calculation of the geothermal energy potential of abandoned mines. The most noteworthy are the percentage of backfilling of the galleries after the mine closure as well as the rate of contribution of the rock in the calculation of the heat balance. The backfilling was assumed to be 75% for all underground mines, but it is considered to be a conservative estimation because it is quite possible that this ratio is lower or even non-existent for old mines, which can increase the volume of water in place proportionally. In this case, the geothermal potential, whether for heating or cooling, can also be proportionally increased. For the rate of contribution of the rock, it was set 25 times more than water in the calculation of the heat balance of underground mines. This depends greatly on the geometry of the underground galleries, their diameter, whether they are more or less distributed at depth, etc. Therefore, the geothermal potential of underground mines can be improved or reduced by a factor of 2 depending on this geometry. For open-pit mines, the rock contribution factor was increased by 25% and remains a modest factor.

8.1.3.3 Water chemistry

This parameter was not considered at all in the evaluation of the overall heat balance of the mines. It is, however, important during geothermal operations in order to configure the ground-source heat pump system in an optimal way to anticipate the risks of scaling and corrosion. It is therefore very useful information to collect in subsequent phases of the potential assessment when looking at a specific site, but is less important in a regional assessment such as the present study.

8.2 Key priorities for de-risking the geothermal potential in Nova Scotia

Based on the analysis provided in this report, further work deserves to be carried out with priority in order to increase the level of knowledge on geothermal resources in specific regions. Prioritized work items can be achieved simultaneously or separately without any precise order, as they concern specific regions with different issues. Tasks can be selected according to the local needs and economic opportunities.

8.2.1 Perform equilibrium temperature measurements in old mining and petroleum wells

To this end, an inventory of the condition of all mining and oil and gas drilling that have been abandoned or are currently suspended must be completed, especially those deeper than 300 m where additional temperature data can be beneficial. Then, it can be possible to acquire equilibrium temperature profiles, which are crucial to reduce uncertainties when quantifying the geothermal potential of a specific region and even of the province, since this type of data was found not available at depths greater than 300 m. In addition, this can add missing information in areas where there is little or no data, especially in the Meguma terrane and the Devonian intrusives.

8.2.2 Building a 3D temperature model for the Cumberland and Windsor-Kennetcook basins

These two basins are the most interesting to develop a first pilot project in the province for geothermal direct-use and even electricity generation because they are the most advanced in terms of subsurface understanding. However, before selecting an exact location to implement a pilot project, identification of deep aquifer zones with anomalously high temperature is imperative to define drilling targets. Given that these two sedimentary basins are the ones for which the subsurface geometry is best known, thanks to the large coverage of available seismic data, 3D temperature and geological models should be developed to help identifying the drilling targets

8.2.3 Drilling a stratigraphic borehole in the Fundy Basin

This sedimentary basin contains the largest number of users of agricultural greenhouses and deserves further attention since there are many unknowns in the subsurface geology. These uncertainties can be partly resolved by drilling a stratigraphic borehole. Since the top of the basement is not deep, in the order of one kilometer, a drilling that will intersect the entire sedimentary column of the basin can provide valuable information on the aquifer properties of these geological units for a modest financial cost. Of course, this well could be used to acquire geophysical logs and temperature profiles and even do a production test in the most permeable geological units.

8.2.4 Conduct geophysical surveys to determine the basement depth of the Stellarton Basin

One of the highest geothermal gradients evaluated in this report is attributed to the Stellarton Basin. Unfortunately, a comprehensive evaluation of the geothermal potential of this basin is not currently possible due to the lack of subsurface data. First, the available information from the wells drilled in the basin didn’t identify any potential aquifers, mainly because the wells did not reach sufficient depths. Secondly, as the depth of the basement below the sedimentary sequence is not known, it is therefore difficult to anticipate the presence or lack of aquifers at interesting depths to consider further investigation. Because it is less expensive and easier to carry out, gravimetric surveys could be undertaken first.

8.2.5 Evaluate the long-term sustainability of the geothermal resource of the Springhill mine

Several factors, including an increase in energy costs, advances in heat pump technology to enable provision of high temperature process heating, a focus on greenhouse gas reduction at every level of government, and the availability of various sources of infrastructure funding, suggest it is an excellent time to market Springhill's industrial park as an attractive location for energy-intensive industries (EfficiencyOne, 2017). Further geothermal development at Springhill would benefit from an evaluation of resource sustainability based on a groundwater and heat transfer model to simulate long term system operation. This would allow to fully develop and accurately estimate the total geothermal resource from a mining site with an opportunity to calibrate models based on operational data. Since there are no examples in the world from which it is possible to benchmark with reliability, it is necessary to provide tools to ensure the best practices of the resource to prevent it from being jeopardized by the concentration of too many users. This would therefore demonstrate the potential economic benefit of the efficient use of this resource to potential commercial entities in the specific context of Nova Scotia, which has several other mines that could be subject to geothermal systems development such as Springhill.

8.3 Steps towards a geothermal pilot project in Nova Scotia

Regardless of the amount of data available, the level of knowledge remains low for any region of Nova Scotia, mostly because no equilibrium temperature profiles have been recorded at great depths. Consequently, some fundamental work is mandatory for each of these regions before moving to the pilot project stage. Thus, depending on the economic interest and opportunities on a specific area of Nova Scotia, the development of its geothermal potential should go through the following steps.

8.3.1 Sedimentary basin

8.3.1.1 Short-term

- Sample outcropping geological units and available drill cores from oil and gas exploration wells for laboratory analysis of their physical and thermal properties (ex. Geothermal Open Laboratory at the INRS). In this way, a thermo-hydraulic stratigraphy can be defined for each of the sedimentary basins (ex. Bédard et al., 2017).
- Using the analytical results, the calculation of heat flow in sedimentary basins can be refined, which will allow the development of 1D to 3D geological temperature models depending on the data available (Gascuel et al., 2020; Bédard et al., 2020).
- Study the porosity and permeability of the geological units using available geophysical well logs and drill cores in order to get a better estimate of the extent of permeable zones.
- Build a 3D geological model of sedimentary basins to better constrain their geometry and geothermal potential.

8.3.1.2 Medium-term

- Develop numerical reservoir models to simulate the operation of geothermal systems, which can be carried out through graduate student research projects.
- Improve the subsurface control by gravity and seismic geophysical investigations in areas with less information (e.g. Stellarton and Fundy sedimentary basins).

- Evaluate the impact on the geothermal gradient in areas with non-uniform salt deposits (different thermal conductivity) or underlain with granitic intrusives (presence of radiogenic elements).
- For areas with no aquifer potential, consider regulatory and social acceptability possibilities for EGS stimulation techniques.
- Implement numerical simulations to evaluate the extractable geothermal energy with deep borehole heat exchangers (BHE) or in reusing abandoned oil and gas wells by circulating a fluid into a closed-loop system for extracting heat.

8.3.1.3 Long-term

- Drill an exploratory well to measure the geothermal gradient at equilibrium with geophysical probes and collect cores of the geological units in order to evaluate the heat flow accurately.

8.3.2 Meguma terrane and the Devonian intrusives

8.3.2.1 Short-term

- Compile radiogenic elements data for all the granite intrusions to identify all intrusions that have HHP character at outcrops. Evaluate thermal conductivity of outcrop samples with laboratory methods to determine if heat generating and insulating rock can coexist. A program of systematic surface sampling and geochemical analysis to augment the existing dataset would provide a complete dataset for granites across Nova Scotia.
- Characterize the fracture network in exposed intrusions. A study of fracture patterns in exposed granites can provide an indication of the fracture architecture that will be encountered in geothermal reservoirs developed in buried intrusions.
- Conduct research to identify whether some of the exposed intrusions that do not have high radiogenic content character had this character in now-eroded portions of the intrusion, or may have it in buried portions. This can help to constrain the true areal distribution of granite intrusions with HHP character, and to establish whether buried HHP granite intrusions may exist in parts of Nova Scotia beyond those in which they currently crop out. This can be addressed by:
    - developing a fuller understanding of how and why HHP granite forms;
    - establishing the typical position and proportion of HHP rocks in intrusions;
    - identifying a geochemical "fingerprint" that can be used in intrusions lacking HHP character at outcrops, to point to the presence of HHP rocks in eroded or concealed portions of the intrusion. A detailed study of intrusions in Nova Scotia and elsewhere can help address these issues, drawing on the vast body of published and unpublished granite literature, and gathering new data where necessary.

8.3.2.2 Medium-term

- In onshore areas, reinterpret existing regional geophysical data and 3D geological models using modern methodologies and up-to-date knowledge of the surface and subsurface geology to identify possible buried granite intrusions.
- In offshore areas, use geophysical survey data, if available, to identify buried intrusions and intrusions exposed on the sea floor. This would help to constrain the true areal distribution of granite intrusions.

- Monitor technological developments in the EGS and Deep BHE pilot projects.

8.3.2.3 Long-term

- Conduct a program of deep drilling. Ultimately, one or more deep boreholes will have to be drilled if the potential for exploiting deep geothermal energy is to be evaluated fully. There are no reliable zones of unusually high heat flow and probably no deep boreholes with temperature data in intrusions in Nova Scotia (with the noticeable exception of the borehole MRRD-01, see **Appendix 4.1**), so finding an accessible deep geothermal resource will require a dedicated exploration programme. Initially, our ability to identify and quantify geothermal energy prospects will depend on gathering thermal data at the surface and in shallow boreholes, and on building geological 3D models from surface-based and remote sensing surveys. However, at some point a drilling programme will be needed to provide measured and observed, factual data. To provide a clear indication of the deep geothermal regime, a 500-1,000 m diamond exploration drilling would be sufficient to determine if the anomaly really exists and decide if it would be worthwhile to go further before spending significant amounts of money on drilling deeper than 3 km.

8.3.3 Abandoned mines

8.3.3.1 Short-term

- Compile available chemistry data and, where needed, sample water to calculate saturation indices to assess corrosion and scale potential.
- Acquire temperature profiles, in both summer and winter, of the most promising sites using existing facilities and accessible shafts or wells to evaluate a more accurate geothermal gradient and properly assess changes in water temperature over the operation of a system.
- Sample the rock surrounding the mine and analyze its thermal properties.
- Refine heat balance calculations to assess geothermal potential using mine plans for geometry and backfilling of mine workings (ex. Comeau et al., 2019).

8.3.3.2 Medium-term

- Develop numerical reservoir models utilizing existing information to develop a detailed 3D model of the mine workings. In this way, it will be possible to accurately quantify geothermal resources, to simulate the operation of geothermal systems in order to assess the technical feasibility of installing an open loop system with geothermal heat pumps, perhaps in combination with other forms of energy. This work can be carried out through graduate student projects (ex. Raymond and Therrien, 2014; Alvarado et al., 2019).

8.3.3.3 Long-term

- Conduct a mine water pumping pilot project to develop an energy system for a specific operation using detailed energy needs data, to better simulate the available resource over time.

8.4 Governance and regulatory issues on geothermal

During the last decade, the use of geothermal energy resources in urban areas has experienced an unprecedented development growth. However, the intensive market development experienced by this technology entails different responsibilities towards the long-term technical and environmental sustainability in order to maintain this positive trend. In this perspective, García-Gil et al. (2020) present a geothermal energy management framework structure and a governance model agreed among 13 European Geological Surveys, providing a roadmap for the different levels of management development, adaptable to any urban scale, and independent of the hydrogeological conditions and the level of development of shallow geothermal energy technology implementation. This synthesis provides a very good baseline to improve regulations to ensure the sustainable use of flooded mines in Nova Scotia.

Geothermal systems are developed in several phases. As illustrated in **Figure 8.1**, a simplified way to classify the different steps of a deep geothermal project is as follows:

1) exploration;
2) resource development;
3) construction;
4) commissioning and operation.

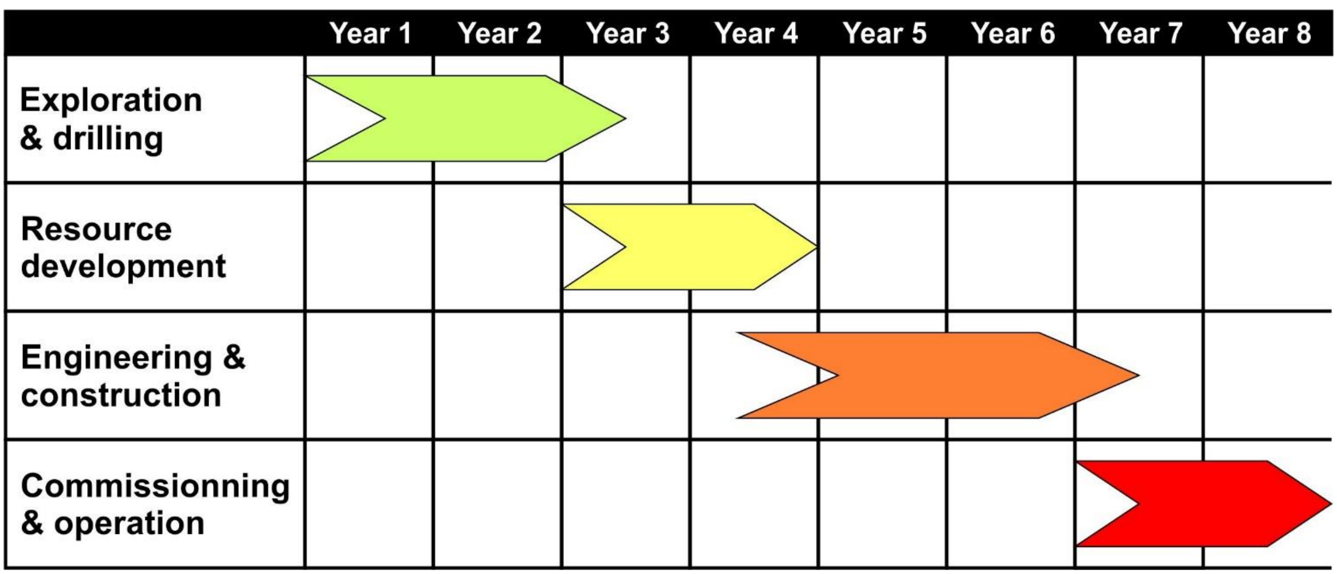

Figure 8.1. Development phases of a deep geothermal project.

Each of these phases requires one or more authorizations and the compliance with a range of national and local rules. The whole set of rules should be as transparent and balanced as possible in order to ensure, simultaneously, the sustainable use of the resource, confidence in the technology, and investment security. Several studies have assessed the most relevant regulatory issues impacting the geothermal sector, which can be classified as follows:

- definition, classification, and resource ownership;
- licencing and authorizations;
- sustainability;
- spatial planning and access to the grid;
- state of play and evolution of national incentives.

Dumas (2019) provides an analysis for each item and introduces the complex and evolving policy and regulatory framework relevant to geothermal energy in Europe. The analysis covers both shallow and deep geothermal technologies producing electrical power, heat, cold and hot water, focusing on the European Union (EU) legislation and its implementation.

Moutenet and Malo (2014) conducted a study to identify the framework needed for the establishment of regulations in Québec concerning the research and operation of future deep geothermal sites. There are currently no legal or regulatory provisions governing the research and exploitation of deep geothermal resources in Québec. This is not the case in British Columbia (Canada), California (USA), France or Queensland (Australia). These jurisdictions have all the legal instruments necessary to take advantage of geothermal resources for electricity production. Overall, the same theme can be found in these four jurisdictions studied. Deep geothermal resources belong to the government and anyone wishing to conduct research to identify deep geothermal resources must obtain authorization from the competent authority to conduct such research within a defined perimeter. Similarly, those who wish to exploit geothermal resources must hold a mineral title granting them the right to exploit specific geothermal deposits. These four jurisdictions can provide interesting examples to help further define a regulatory framework for Nova Scotia's deep geothermal resources.

8.5 References

Alvarado, E., Raymond, J., Comeau, F.-A., Labrecque, D., 2019. Évaluation du potentiel géothermique de la mine Éléonore. INRS, Centre Eau Terre Environnement, Québec, Rapport de recherche R1869, 21 p. http://espace.inrs.ca/9664/

Arkay, K., 2000. Geothermal energy from abandoned mines: A methodology for an inventory, and inventory data for abandoned mines in Quebec and Nova Scotia. Geological Survey Open File 3825, 388 p. https://doi.org/10.4095/211648

Bédard, K., Comeau, F.-A., Millet, E., Raymond, J., Malo, M., Gloaguen, E., 2016. Évaluation des ressources géothermiques du bassin des Basses-Terres du Saint-Laurent. INRS, Centre Eau Terre Environnement, Québec, Rapport de recherche R1659, 100 p. http://espace.inrs.ca/4845/

Bédard, K., Comeau, F.A., Raymond, J., Gloaguen, E., Malo, M. 2020. Deep geothermal resource assessment of the St. Lawrence Lowlands sedimentary basin (Québec) based on 3D regional geological modelling. Geomechanics and Geophysics for Geo-Energy and Geo-Resources volume 6: 46. https://doi.org/10.1007/s40948-020-00170-0

Blackwell, D., Richards, M., Stepp, P., 2010. Texas Geothermal Assessment for the I35 Corridor East - Final report. SMU Geothermal Laboratory, Southern Methodist University, 78 p.

Comeau, F.-A., Raymond, J. et Ngoyo Mandemvo, D.D., 2019. Évaluation du potentiel géothermique des mines désaffectées de Société Asbestos limitée à Thetford Mines. INRS, Centre Eau Terre Environnement, Québec, Rapport de recherche R1856, 63 p.

Dumas P., 2019. Policy and Regulatory Aspects of Geothermal Energy: A European Perspective. In: Manzella A., Allansdottir A., Pellizzone A. (eds) Geothermal Energy and Society. Lecture Notes in Energy 67:19-38. https://doi.org/10.1007/978-3-319-78286-7_2

EfficiencyOne, 2017. Springhill Geothermal Energy Use Study. Prepared for Cumberland Energy Authority. 61 p.

García-Gil, A., Goetz, G., Kłonowski, M.R., Borovic, S., Boone, D.P., Abesser, C., Janza, m., Herms, i., Petitclerc, e., Erlström, m., Holecek, j., Hunter, t., Vandeweijer, V.P., Cernak, R., Mejías, M.M., Epting, J., 2020. Governance of shallow geothermal energy resources. Energy Policy 138:111283. https://doi.org/10.1016/j.enpol.2020.111283

Gascuel, V., Bédard, K., Comeau, F.-A., Raymond, J., Malo, M., 2020. Geothermal resource assessment of remote sedimentary basins with sparse data: lessons learned from Anticosti Island, Canada. Geothermal Energy 8:3. https://doi.org/10.1186/s40517-020-0156-1

Harrison, W.E., Luza, K.V., Prater, M.L., Reddr, R.J., 1983. Geothermal resource assessment in Oklahoma. Oklahoma Geological Survey, Special Paper 83-1, 42 p.

Leslie, J.A., 1982. Investigation of geothermal energy resources - Atlantic Provinces. Energy, Mines and Resources Canada, Earth Physics Branch Open File 82-8, 119 p.

Leslie, J.A., 1983. Investigation of geothermal energy resources - Atlantic Provinces. Energy, Mines and Resources Canada, Earth Physics Branch Open File 83-20, 37 p.

Leslie, J.A., 1985. Investigation of geothermal energy resources - Atlantic Provinces. Energy, Mines and Resources Canada, Earth Physics Branch Open File 85-8, 64 p.

Moutenet, J.-P. and Malo, M., 2014. Encadrement juridique de la géothermie profonde en Colombie-Britannique, en Californie, en France, et en Australie. INRS, Centre Eau Terre Environnement, Québec, Rapport de recherche R1508, 33 p.

Raymond, J., Therrien, R., 2014. Optimizing the design of a geothermal district heating and cooling system located at a flooded mine in Canada. Hydrogeology Journal 22: 217–231. https://doi.org/10.1007/s10040-013-1063-3

APPENDIX I – UNDERGROUND TEMPERATURES OBTAINED FROM LITERATURE

AMST: Annual Mean Surface Temperature
TEMP.: Temperature, as indicated in the original reference

Chevron-Irving Malagawatch 2	**BASIN:**	Central Cape Breton		**SITE:**	Malgawatch	
	AMST (°C)	**EASTING**	**NORTHING**	**DEPTH (m)**	**TEMP. (°C)**	**EQUILIBRIUM**
	6.2	661 435	5 081 707	611.0	17.0	No
	SOURCE(S):	Leslie (1982)			**CONFIDENCE:**	POOR
	COMMENT:	Compiled from NSDME, one measurement, 17 °C at 611 m, no other information.				

Dalhousie	**TERRANE**	Meguma		**SITE:**	Halifax	
	AMST (°C)	**EASTING**	**NORTHING**	**DEPTH (m)**	**TEMP. (°C)**	**EQUILIBRIUM**
	7.5	453 209	4 943 130	333.5	11.7	Yes
	SOURCE(S):	Jessop et al. (2005); Leslie (1981); Jessop (1968)			**CONFIDENCE:**	VERY GOOD
	COMMENT:					

Dow Chemical DCPR-11	**BASIN:**	Central Cape Breton		**SITE:**	Port Richmond	
	AMST (°C)	**EASTING**	**NORTHING**	**DEPTH (m)**	**TEMP. (°C)**	**EQUILIBRIUM**
	6.2	636 479	5 051 096	1,210.0	32.8	No
	SOURCE(S):	Leslie (1981)			**CONFIDENCE:**	POOR
	COMMENT:	Compiled from NSDME, one measurement, 32.8 °C at 1,210 m, no other information.				

EPB No. 18	**HOST ROCK**	Carboniferous granite		**SITE:**	Wedgeport	
	AMST (°C)	**EASTING**	**NORTHING**	**DEPTH (m)**	**TEMP. (°C)**	**EQUILIBRIUM**
	7.2	258 505	4 849 592	480.0	15.8	Yes
	SOURCE(S):	Jessop et al. (2005); Drury et al. (1987); Leslie (1985)			**CONFIDENCE:**	VERY GOOD
	COMMENT:					

Getty No. 1	**BASIN:**	Fundy		**SITE:**	Belleisle	
	AMST (°C)	**EASTING**	**NORTHING**	**DEPTH (m)**	**TEMP. (°C)**	**EQUILIBRIUM**
	7,2	311 009	4 964 623	138,7	11,0	Yes
	SOURCE(S):	Jessop et al. (2005); Leslie (1981)			**CONFIDENCE:**	NONE
	COMMENT:	The level of confidence is NONE because the well is shallower than 300 m.				

Getty No. 10	**BASIN:**	Fundy		**SITE:**	Dempsey Corner	
	AMST (°C)	**EASTING**	**NORTHING**	**DEPTH (m)**	**TEMP. (°C)**	**EQUILIBRIUM**
	7.0	354 395	4 993 502	152.7	10.7	Yes
	SOURCE(S):	Jessop et al. (2005); Leslie (1981)			**CONFIDENCE:**	NONE
	COMMENT:	The level of confidence is NONE because the well is shallower than 300 m.				

Getty No. 3	**BASIN:**	Fundy		**SITE:**	Belleisle	
	AMST (°C)	**EASTING**	**NORTHING**	**DEPTH (m)**	**TEMP. (°C)**	**EQUILIBRIUM**
	7.2	311 042	4 965 734	151.2	10.6	Yes
	SOURCE(S):	Jessop et al. (2005); Leslie (1981)			**CONFIDENCE:**	**NONE**
	COMMENT:	The level of confidence is NONE because the well is shallower than 300 m.				

Getty No. 4	**BASIN:**	Fundy		**SITE:**	Belleisle	
	AMST (°C)	**EASTING**	**NORTHING**	**DEPTH (m)**	**TEMP. (°C)**	**EQUILIBRIUM**
	7.2	311 042	4 965 734	54.9	8.1	Yes
	SOURCE(S):	Jessop et al. (2005); Leslie (1981)			**CONFIDENCE:**	**NONE**
	COMMENT:	The level of confidence is NONE because the well is shallower than 300 m.				

Lacana Mining No. 4	**BASIN:**	Cumberland		**SITE:**	Pugwash	
	AMST (°C)	**EASTING**	**NORTHING**	**DEPTH (m)**	**TEMP. (°C)**	**EQUILIBRIUM**
	6.5	442 545	5 077 648	52.1	8.0	Yes
	SOURCE(S):	Jessop et al. (2005); Leslie (1981)			**CONFIDENCE:**	**NONE**
	COMMENT:	The level of confidence is NONE because the well is shallower than 300 m.				

MRRD-01	**HOST ROCK**	Devonian granite		**SITE:**	Wallace Lake	
	AMST (°C)	**EASTING**	**NORTHING**	**DEPTH (m)**	**TEMP. (°C)**	**EQUILIBRIUM**
	7.3	283 728	4 929 897	1,450.0	68.0	No
	SOURCE(S):	Jessop et al. (2005); Chatterjee and Dostal (2002)			**CONFIDENCE:**	**POOR**
	COMMENT:	Chatterjee and Dostal (2002) mention a temperature of 68 °C at 1,450 m, but the original data are not available.				

Noval E-12	**BASIN:**	Western Cape Breton		**SITE:**	Inverness	
	AMST (°C)	**EASTING**	**NORTHING**	**DEPTH (m)**	**TEMP. (°C)**	**EQUILIBRIUM**
	6.1	630 293	5 122 102	76.2	8.7	Yes
	SOURCE(S):	Jessop et al. (2005); Leslie (1982)			**CONFIDENCE:**	**NONE**
	COMMENT:	The level of confidence is NONE because the well is shallower than 300 m.				

Noval E-23	**BASIN:**	Cumberland		**SITE:**	Maccan	
	AMST (°C)	**EASTING**	**NORTHING**	**DEPTH (m)**	**TEMP. (°C)**	**EQUILIBRIUM**
	6.1	402 740	5 064 809	221.0	9.7	Yes
	SOURCE(S):	Jessop et al. (2005); Leslie (1982)			**CONFIDENCE:**	**NONE**
	COMMENT:	The level of confidence is NONE because the well is shallower than 300 m.				

Noval E-24	**BASIN:**	Stellarton		**SITE:**	Stellarton	
	AMST (°C)	**EASTING**	**NORTHING**	**DEPTH (m)**	**TEMP. (°C)**	**EQUILIBRIUM**
	6.5	525 764	5 042 993	91.4	9.9	Yes
	SOURCE(S):	Jessop et al. (2005); Drury et al. (1987); Leslie (1982)			**CONFIDENCE:**	**NONE**
	COMMENT:	The level of confidence is NONE because the well is shallower than 300 m.				

Noval E-25	**BASIN:**	Stellarton		**SITE:**	New Glasgow	
	AMST (°C)	**EASTING**	**NORTHING**	**DEPTH (m)**	**TEMP. (°C)**	**EQUILIBRIUM**
	6.4	531 229	5 043 018	281.9	15.1	Yes
	SOURCE(S):	Jessop et al. (2005); Drury et al. (1987); Leslie (1982)			**CONFIDENCE:**	**NONE**
	COMMENT:	The level of confidence is NONE because the well is shallower than 300 m.				

Noval E-26	**BASIN:**	Stellarton		**SITE:**	New Glasgow	
	AMST (°C)	**EASTING**	**NORTHING**	**DEPTH (m)**	**TEMP. (°C)**	**EQUILIBRIUM**
	6.5	526 530	5 046 330	182.9	10.2	Yes
	SOURCE(S):	Jessop et al. (2005); Drury et al. (1987); Leslie (1982)			**CONFIDENCE:**	**NONE**
	COMMENT:	The level of confidence is NONE because the well is shallower than 300 m.				

Noval E-5	**BASIN:**	Stellarton		**SITE:**	Stellarton	
	AMST (°C)	**EASTING**	**NORTHING**	**DEPTH (m)**	**TEMP. (°C)**	**EQUILIBRIUM**
	6.4	534 339	5 045 257	83.8	8.5	Yes
	SOURCE(S):	Jessop et al. (2005); Drury et al. (1987); Leslie (1983)			**CONFIDENCE:**	**NONE**
	COMMENT:	The level of confidence is NONE because the well is shallower than 300 m.				

Noval E-6	**BASIN:**	Stellarton		**SITE:**	Stellarton	
	AMST (°C)	**EASTING**	**NORTHING**	**DEPTH (m)**	**TEMP. (°C)**	**EQUILIBRIUM**
	6.5	528 056	5 054 113	289.6	15.5	Yes
	SOURCE(S):	Jessop et al. (2005); Drury et al. (1987); Leslie (1983)			**CONFIDENCE:**	**NONE**
	COMMENT:	The level of confidence is NONE because the well is shallower than 300 m.				

Noval E-8	**BASIN:**	Stellarton		**SITE:**	Westville	
	AMST (°C)	**EASTING**	**NORTHING**	**DEPTH (m)**	**TEMP. (°C)**	**EQUILIBRIUM**
	6.5	523 417	5 044 095	63.4	7.6	Yes
	SOURCE(S):	Jessop et al. (2005); Drury et al. (1987); Leslie (1982)			**CONFIDENCE:**	**NONE**
	COMMENT:	The level of confidence is NONE because the well is shallower than 300 m.				

<table>
<tr><td rowspan="5">Noval P-6</td><td>BASIN:</td><td colspan="2">Stellarton</td><td>SITE:</td><td colspan="2">Stellarton</td></tr>
<tr><td>AMST (°C)
6.4</td><td>EASTING
528 096</td><td>NORTHING
5 045 225</td><td>DEPTH (m)
335.4</td><td>TEMP. (°C)
16.2</td><td>EQUILIBRIUM
Yes</td></tr>
<tr><td>SOURCE(S):</td><td colspan="3">Jessop et al. (2005); Drury et al. (1987); Leslie (1983)</td><td>CONFIDENCE:</td><td>VERY GOOD</td></tr>
<tr><td>COMMENT:</td><td colspan="5">Jessop et al. (2005) refer to Drury et al. (1987) but the later do not mention this well. Leslie (1983) provides the temperature profile.</td></tr>
</table>

<table>
<tr><td rowspan="5">NSDM Oldham</td><td>TERRANE</td><td colspan="2">Meguma</td><td>SITE:</td><td colspan="2">Oldham</td></tr>
<tr><td>AMST (°C)
6.6</td><td>EASTING
462 116</td><td>NORTHING
4 974 176</td><td>DEPTH (m)
607.5</td><td>TEMP. (°C)
14.3</td><td>EQUILIBRIUM
Yes</td></tr>
<tr><td>SOURCE(S):</td><td colspan="3">Jessop et al. (2005); Leslie (1981); Jessop and Judge (1971)</td><td>CONFIDENCE:</td><td>VERY GOOD</td></tr>
<tr><td>COMMENT:</td><td colspan="5"></td></tr>
</table>

<table>
<tr><td rowspan="5">NSDME 84-1</td><td>BASIN:</td><td colspan="2">Windsor-Kennetcook</td><td>SITE:</td><td colspan="2">West Gore</td></tr>
<tr><td>AMST (°C)
6.5</td><td>EASTING
436 260</td><td>NORTHING
4 993 267</td><td>DEPTH (m)
605.0</td><td>TEMP. (°C)
20.8</td><td>EQUILIBRIUM
Yes</td></tr>
<tr><td>SOURCE(S):</td><td colspan="3">Jessop et al. (2005); Drury et al. (1987); Leslie (1985)</td><td>CONFIDENCE:</td><td>VERY GOOD</td></tr>
<tr><td>COMMENT:</td><td colspan="5">Point #425 of Drury et al. (1987). Drury et al. (1987) estimate the gradient at 23.5 mK/m. Leslie (1985) provides the temperature profile.</td></tr>
</table>

<table>
<tr><td rowspan="5">NSDME Glen Rd 83-1</td><td>BASIN:</td><td colspan="2">Antigonish</td><td>SITE:</td><td colspan="2">Glen Road</td></tr>
<tr><td>AMST (°C)
6.1</td><td>EASTING
575 716</td><td>NORTHING
5 044 509</td><td>DEPTH (m)
590.0</td><td>TEMP. (°C)
18.4</td><td>EQUILIBRIUM
Yes</td></tr>
<tr><td>SOURCE(S):</td><td colspan="3">Jessop et al. (2005); Drury et al. (1987); Leslie (1984)</td><td>CONFIDENCE:</td><td>VERY GOOD</td></tr>
<tr><td>COMMENT:</td><td colspan="5">Point #422 of Drury et al. (1987). Drury et al. estimate the gradient at 22.6 mK/m. Leslie (1984) provides the temperature profile.</td></tr>
</table>

<table>
<tr><td rowspan="5">NSDME P-54</td><td>BASIN:</td><td colspan="2">Stellarton</td><td>SITE:</td><td colspan="2">New Glasgow</td></tr>
<tr><td>AMST (°C)
6.5</td><td>EASTING
526 521</td><td>NORTHING
5 048 552</td><td>DEPTH (m)
950.0</td><td>TEMP. (°C)
28.1</td><td>EQUILIBRIUM
Yes</td></tr>
<tr><td>SOURCE(S):</td><td colspan="3">Jessop et al. (2005); Drury et al. (1987); Leslie (1984)</td><td>CONFIDENCE:</td><td>VERY GOOD</td></tr>
<tr><td>COMMENT:</td><td colspan="5">Jessop et al. (2005) refer to Drury et al. (1987) but the latter do not mention this well. Leslie (1984) provides the temperature profile.</td></tr>
</table>

<table>
<tr><td rowspan="5">NSDME Pt. Edward 83-1</td><td>BASIN:</td><td colspan="2">Sydney</td><td>SITE:</td><td colspan="2">Point Edward</td></tr>
<tr><td>AMST (°C)</td><td>EASTING</td><td>NORTHING</td><td>DEPTH (m)</td><td>TEMP. (°C)</td><td>EQUILIBRIUM</td></tr>
<tr><td>6.1</td><td>711 549</td><td>5 115 475</td><td>750.0</td><td>18.7</td><td>Yes</td></tr>
<tr><td>SOURCE(S):</td><td colspan="3">Jessop et al. (2005); Drury et al. (1987); Leslie (1984)</td><td>CONFIDENCE:</td><td>VERY GOOD</td></tr>
<tr><td>COMMENT:</td><td colspan="5">Point #423 of Drury et al. (1987). Drury et al. (1987) estimate the gradient at 16.8 mK/m. Leslie (1984) provides the temperature profile.</td></tr>
</table>

<table>
<tr><td rowspan="5">NSDME SS-8</td><td>BASIN:</td><td colspan="2">Cumberland</td><td>SITE:</td><td colspan="2">Salt Springs (Springhill)</td></tr>
<tr><td>AMST (°C)</td><td>EASTING</td><td>NORTHING</td><td>DEPTH (m)</td><td>TEMP. (°C)</td><td>EQUILIBRIUM</td></tr>
<tr><td>6.3</td><td>421 344</td><td>5 058 990</td><td>210.0</td><td>11.3</td><td>Yes</td></tr>
<tr><td>SOURCE(S):</td><td colspan="3">Jessop et al. (2005); Leslie (1985)</td><td>CONFIDENCE:</td><td>NONE</td></tr>
<tr><td>COMMENT:</td><td colspan="5">The level of confidence is NONE because the well is shallower than 300 m.</td></tr>
</table>

<table>
<tr><td rowspan="5">NSDME Sydney Basin Project</td><td>BASIN:</td><td colspan="2">Sydney</td><td>SITE:</td><td colspan="2">Sydney</td></tr>
<tr><td>AMST (°C)</td><td>EASTING</td><td>NORTHING</td><td>DEPTH (m)</td><td>TEMP. (°C)</td><td>EQUILIBRIUM</td></tr>
<tr><td>5.9</td><td>722 599</td><td>5 109 191</td><td>884.1</td><td>20.5</td><td>Yes</td></tr>
<tr><td>SOURCE(S):</td><td colspan="3">Jessop et al. (2005); Drury et al. (1987); Leslie (1983)</td><td>CONFIDENCE:</td><td>VERY GOOD</td></tr>
<tr><td>COMMENT:</td><td colspan="5">Jessop et al. (2005) refer to Drury et al. (1987) but the later do not mention this well. Leslie (1983) provides the temperature profile.</td></tr>
</table>

<table>
<tr><td rowspan="5">P-84</td><td>BASIN:</td><td colspan="2">Sydney</td><td>SITE:</td><td colspan="2">Petroleum well P-84</td></tr>
<tr><td>AMST (°C)</td><td>EASTING</td><td>NORTHING</td><td>DEPTH (m)</td><td>TEMP. (°C)</td><td>EQUILIBRIUM</td></tr>
<tr><td>--</td><td>736 786</td><td>5 114 736</td><td>--</td><td>--</td><td>No</td></tr>
<tr><td>SOURCE(S):</td><td colspan="3">Hacquebard and Donaldson (1970)</td><td>CONFIDENCE:</td><td>POOR</td></tr>
<tr><td>COMMENT:</td><td colspan="5">No temperature or depth available. Hacquebard and Donaldson (1970) deduced a geothermal gradient of 21.7 °C from the rank of coal. The Birch Grove well mentioned in the reference likely corresponds to the well P-84.</td></tr>
</table>

<table>
<tr><td rowspan="5">Phalen Mine</td><td>BASIN:</td><td colspan="2">Sydney</td><td>SITE:</td><td colspan="2">Phalen Mine</td></tr>
<tr><td>AMST (°C)</td><td>EASTING</td><td>NORTHING</td><td>DEPTH (m)</td><td>TEMP. (°C)</td><td>EQUILIBRIUM</td></tr>
<tr><td>--</td><td>726 551</td><td>5 125 373</td><td>--</td><td>--</td><td>Yes</td></tr>
<tr><td>SOURCE(S):</td><td colspan="3">Young (1997)</td><td>CONFIDENCE:</td><td>POOR</td></tr>
<tr><td>COMMENT:</td><td colspan="5">No temperature or depth provided. The coordinates correspond to the mine location, not of the actual measurements. Young (1997) reports that a geothermal gradient of 22.8 °C has been estimated for the Phalen coal seam from boreholes drilled 8-10 m into four coal faces of the Phalen mine and from an exploratory drill hole on the bottom of three slopes. At each test site, a long plastic probe fitted with a calibrated thermistor and wire cable was inserted into the bottom of each hole. Each was then filled with water to insulate the probe and packing was placed in the collar of the hole to prevent ventilation air from entering. The probe was left in the test hole for 24 hours to reach temperature equilibrium and read the following day.</td></tr>
</table>

<table>
<tr><td rowspan="6">Suncor AP83-0372</td><td>BASIN:</td><td colspan="2">Stellarton</td><td>SITE:</td><td colspan="2">Stellarton</td></tr>
<tr><td>AMST (°C)</td><td>EASTING</td><td>NORTHING</td><td>DEPTH (m)</td><td>TEMP. (°C)</td><td>EQUILIBRIUM</td></tr>
<tr><td>6.4</td><td>529 657</td><td>5 045 233</td><td>740.0</td><td>26.1</td><td>Yes</td></tr>
<tr><td>SOURCE(S):</td><td colspan="3">Jessop et al. (2005); Drury et al. (1987); Leslie (1984)</td><td>CONFIDENCE:</td><td>VERY GOOD</td></tr>
<tr><td>COMMENT:</td><td colspan="5">Point #402 of Drury et al. (1987). Leslie (1984) provides the temperature profile. Drury et al. (1987) indicate: Data from several holes at site #402. Holes shallower than 400 m indicated gradients up to 32 mK/m considerably higher than those usually found in the region. One hole logged to 750 m intersected a shear zone at 480 m, with mudstones above and sandstones below. The gradient in this hole changes from 32 mK/m above the zone to 14 mK/m below it. The change in conductivity associated with the lithological break is insufficient to account for the change in gradient. It is likely that the shear zone is a temperature control boundary caused by the upward flow of water from some greater depth.</td></tr>
</table>

<table>
<tr><td rowspan="5">Unnamed</td><td>BASIN:</td><td colspan="2">Antigonish</td><td>SITE:</td><td colspan="2">Antigonish</td></tr>
<tr><td>AMST (°C)</td><td>EASTING</td><td>NORTHING</td><td>DEPTH (m)</td><td>TEMP. (°C)</td><td>EQUILIBRIUM</td></tr>
<tr><td>6.1</td><td>571 877</td><td>5 038 908</td><td>151.9</td><td>9.1</td><td>Yes</td></tr>
<tr><td>SOURCE(S):</td><td colspan="3">Jessop et al. (2005)</td><td>CONFIDENCE:</td><td>NONE</td></tr>
<tr><td>COMMENT:</td><td colspan="5">The level of confidence is NONE because the well is shallower than 300 m.</td></tr>
</table>

<table>
<tr><td rowspan="5">Wallace</td><td>BASIN:</td><td colspan="2">Cumberland</td><td>SITE:</td><td colspan="2">Wallace Station</td></tr>
<tr><td>AMST (°C)</td><td>EASTING</td><td>NORTHING</td><td>DEPTH (m)</td><td>TEMP. (°C)</td><td>EQUILIBRIUM</td></tr>
<tr><td>6.3</td><td>465 018</td><td>5 069 703</td><td>311.8</td><td>11.7</td><td>Yes</td></tr>
<tr><td>SOURCE(S):</td><td colspan="3">Jessop et al. (2005); Leslie (1981); Jessop and Judge (1971)</td><td>CONFIDENCE:</td><td>VERY GOOD</td></tr>
<tr><td>COMMENT:</td><td colspan="5">The oldest reference is Jessop and Judge (1971) but this source doesn't mention the well. Leslie (1981) provides the temperature profile and indicates the source as "Earth Physics Branch".</td></tr>
</table>

APPENDIX II – UNDERGROUND TEMPERATURES OBTAINED FROM PETROLEUM WELLS

BHT: Bottom Hole Temperature, as reported in the log considered
AMST: Annual Mean Surface Temperature
KBG: Elevation of the Kelly bushing or rotary table and the ground level
Max T: Maximum Temperature, as reported in the log considered
MD: Total Measured Depth of the well or of a log
SOURCES: 1: Open File 2017-09 (Bianco, 2017); 2: Nova Scotia Department of Energy and Mines, archived data
TSC: Time Since the mud Circulation has stopped, before the logging tool reaches the bottom
TVD: True Vertical Depth of the well or of a log. When empty: no deviation survey available

P-1 TO P-82: NO TEMPERATURE DATA (WELLS DRILLED BETWEEN 1869 AND 1960)

P-83	**DRILLED:**	1963	**NAME:**	Pacific Fox Harbour C-96-V		
	SOURCE(S):	1 and 2	**BASIN:**	Cumberland		
	AMST (°C)	**EASTING**	**NORTHING**	**KBG (m)**	**MD (m)**	**TVD (m)**
	6.3	460 216	5 077 394	3.8	3,003.2	
	LOG #	**MD (m)**	**TVD (m)**	**Max T (°C)**	**BHT (°C)**	**TSC (hrs)**
	1	2,984.6		50.0		16.0
	2	2,984.6		50.0	50.0	24.0
	SELECTION:	50 °C at 2,984.6 m after 24 hrs			**CONFIDENCE:**	GOOD
	COMMENT:	LOG # 2 has the longest TSC.				

P-84	**DRILLED:**	1968	**NAME:**	Birch Grove #1		
	SOURCE(S):	1 and 2	**BASIN:**	Sydney		
	AMST (°C)	**EASTING**	**NORTHING**	**KBG (m)**	**MD (m)**	**TVD (m)**
	5.9	736 786	5 114 736	3.2	1,343.6	1,343.2
	LOG #	**MD (m)**	**TVD (m)**	**Max T (°C)**	**BHT (°C)**	**TSC (hrs)**
	1	1,341.7	1,341.3	48.9		6.0
	2	1,341.4	1,341.0	48.9		10.0
	3	1,342.0	1,341.6	48.9	48.9	4.0
	4	1,341.7	1,341.3	48.9	48.9	6.0
	5	1,342.0	1,341.6	48.9	48.9	8.0
	SELECTION:	48.9 °C at 1,341 m after 10 hrs			**CONFIDENCE:**	NONE
	COMMENT:	The temperature reported in the logs (120 °F) seems to be a temperature by default, not an actual measurement.				

P-85	**DRILLED:**	1972	**NAME:**	Wallace Station #1		
	SOURCE(S):	2	**BASIN:**	Cumberland		
	AMST (°C)	**EASTING**	**NORTHING**	**KBG (m)**	**MD (m)**	**TVD (m)**
	6.2	460 527	5 068 720	5.7	4,536.0	
	LOG #	**MD (m)**	**TVD (m)**	**Max T (°C)**	**BHT (°C)**	**TSC (hrs)**
	1	2,501.2			73.9	1.5
	2	3,745.1			72.8	
	3	4,262.3			87.8	21.5
	4	4,523.8			88.3	14.5
	5	2,507.3		75.6	66.7	15.0
	6	3,650.9			71.1	120.0
	7	4,262.9			89.4	
	8	4,536.3		91.7	91.7	60.0
	9	2,488.7			72.2	16.0
	10	4,261.1			89.4	25.5
	11	4,524.8			86.7	18.0
	SELECTION:	88.3 °C at 4,523.8 m after 14.5 hrs			**CONFIDENCE:**	GOOD
		91.7 °C at 4,536.3 m after 60 hrs			**CONFIDENCE:**	GOOD
		86.7 °C at 4,524.8 m after 18 hrs			**CONFIDENCE:**	GOOD
	COMMENT:	LOGS # 4-8-11 are the deepest.				

P-86	**DRILLED:**	1972	**NAME:**	Hastings #1		
	SOURCE(S):	1	**BASIN:**	Cumberland		
	AMST (°C)	**EASTING**	**NORTHING**	**KBG (m)**	**MD (m)**	**TVD (m)**
	6.3	416 100	5 077 186	5.2	2,939.5	2,938.2
	LOG #	**MD (m)**	**TVD (m)**	**Max T (°C)**	**BHT (°C)**	**TSC (hrs)**
	1	616.9	616.8	51.1		10.0
	2	616.3	616.2	50.0		8.0
	3	2,934.3	2,933.0	52.2		21.8
	SELECTION:	52.2 °C at 2,933 m after 21.8 hrs			**CONFIDENCE:**	GOOD
	COMMENT:	LOG # 3 is the deepest.				

P-87	**DRILLED:**	1975	**NAME:**	Noel #1		
	SOURCE(S):	1	**BASIN:**	Windsor-Kennetcook		
	AMST (°C)	**EASTING**	**NORTHING**	**KBG (m)**	**MD (m)**	**TVD (m)**
	6.5	444 714	5 006 806	9.9	1,448.4	1,446.9
	LOG #	**MD (m)**	**TVD (m)**	**Max T (°C)**	**BHT (°C)**	**TSC (hrs)**
	1	395.0	394.8	32.2		2.5
	SELECTION:	32.2 °C at 1,448.4 m after 2.5 hrs			**CONFIDENCE:**	POOR
	COMMENT:	Selected depth corresponds to deepest measurement in log file.				

P-88 AND P-89: NO TEMPERATURE DATA

P-90	**DRILLED:**	1979	**NAME:**	Bras d'Or #1		
	SOURCE(S):	1	**BASIN:**	Central Cape Breton		
	AMST (°C)	**EASTING**	**NORTHING**	**KBG (m)**	**MD (m)**	**TVD (m)**
	6.2	654 839	5 082 103	3.7	216.0	215.9
	LOG #	**MD (m)**	**TVD (m)**	**Max T (°C)**	**BHT (°C)**	**TSC (hrs)**
	1	214.3	214.2	19.0		10.3
	2	216.0	215.9	19.0		17.0
	3	215.0	214.9	20.0		14.0
	SELECTION:	19 °C at 215.94 m after 17 hrs			**CONFIDENCE:**	**NONE**
	COMMENT:	Well is too shallow.				

P-91	**DRILLED:**	1979	**NAME:**	Bras d'Or #2		
	SOURCE(S):	1	**BASIN:**	Central Cape Breton		
	AMST (°C)	**EASTING**	**NORTHING**	**KBG (m)**	**MD (m)**	**TVD (m)**
	6.2	655 150	5 082 574	3.7	375.0	
	LOG #	**MD (m)**	**TVD (m)**	**Max T (°C)**	**BHT (°C)**	**TSC (hrs)**
	1	369.0		15.6		3.0
	2	370.0		18.6		8.5
	3	369.2		16.0		5.5
	SELECTION:	18.6 °C at 370 m after 8.5 hrs			**CONFIDENCE:**	**NONE**
	COMMENT:	Well is too shallow.				

P-92	**DRILLED:**	1979	**NAME:**	Malagawatch #1		
	SOURCE(S):	1	**BASIN:**	Central Cape Breton		
	AMST (°C)	**EASTING**	**NORTHING**	**KBG (m)**	**MD (m)**	**TVD (m)**
	6.2	661 369	5 081 497	4.97	948.0	
	LOG #	**MD (m)**	**TVD (m)**	**Max T (°C)**	**BHT (°C)**	**TSC (hrs)**
	1	559.0		23.0		6.0
	2	560.0		23.0		10.0
	3	944.0		30.0		19.0
	4	940.0		23.0		13.0
	SELECTION:	23 °C at 944 m after 19 hrs			**CONFIDENCE:**	**POOR**
	COMMENT:	Uncertainty on Max T = 23 or 30 °C in LOGS # 3 and 4. Selection of 23 °C to get a sensible gradient comparable to P-98 in Western Cape Breton Basin; Selection of LOG #3 for deepest MD and longest TSC.				

P-93						
	DRILLED:	1981	**NAME:**	Scotsburn #2		
	SOURCE(S):	1	**BASIN:**	Cumberland		
	AMST (°C)	**EASTING**	**NORTHING**	**KBG (m)**	**MD (m)**	**TVD (m)**
	6.4	499 814	5 053 997	6.56	2,638.0	2,636.4
	LOG #	**MD (m)**	**TVD (m)**	**Max T (°C)**	**BHT (°C)**	**TSC (hrs)**
	1	1,086.0	1,085.9	44.6		3.5
	SELECTION:	44.6 °C at 2,636.4 m after 3.5 hrs			CONFIDENCE:	**GOOD**
	COMMENT:	Selected depth corresponds to deepest measurement in log file.				

P-94 TO P-97: NO TEMPERATURE DATA

P-98						
	DRILLED:	1988	**NAME:**	Irving Chevron Mull River #1		
	SOURCE(S):	1	**BASIN:**	Western Cape Breton		
	AMST (°C)	**EASTING**	**NORTHING**	**KBG (m)**	**MD (m)**	**TVD (m)**
	6.2	626 989	5 098 111	3.3	1,502.0	
	LOG #	**MD (m)**	**TVD (m)**	**Max T (°C)**	**BHT (°C)**	**TSC (hrs)**
	1	280.0		31.0		4.3
	SELECTION:	31 °C at 1,499.2 m after 4.3 hrs			**CONFIDENCE:**	**GOOD**
	COMMENT:	Selected depth corresponds to deepest measurement in log file.				

P-99 AND P-100: NO TEMPERATURE DATA

P-101						
	DRILLED:	1994	**NAME:**	River Hebert REI-B2-1		
	SOURCE(S):	1	**BASIN:**	Cumberland		
	AMST (°C)	**EASTING**	**NORTHING**	**KBG (m)**	**MD (m)**	**TVD (m)**
	6.4	393 129	5 058 940	2.9	1,305.0	
	LOG #	**MD (m)**	**TVD (m)**	**Max T (°C)**	**BHT (°C)**	**TSC (hrs)**
	1	1,301.0		34.5		12.0
	SELECTION:	34.5 °C at 1,301 m after 12 hrs			**CONFIDENCE:**	**GOOD**
	COMMENT:					

P-102: NO TEMPERATURE DATA

P-103						
	DRILLED:	1994	**NAME:**	Newville Lake REI-B3-3		
	SOURCE(S):	1	**BASIN:**	Cumberland		
	AMST (°C)	**EASTING**	**NORTHING**	**KBG (m)**	**MD (m)**	**TVD (m)**
	6.4	394 568	5 045 349	3	828.0	
	LOG #	**MD (m)**	**TVD (m)**	**Max T (°C)**	**BHT (°C)**	**TSC (hrs)**
	1	719.0		31.0		4.0
	SELECTION:	31 °C at 828 m after 4 hrs			**CONFIDENCE:**	**POOR**
	COMMENT:	Uncertainty on the depth (log MD or well MD). Arbitrary choice of well MD to get a sensible gradient consistent with the other wells in the area.				

P-104	**DRILLED:**	1994	**NAME:**	Springhill/Athol REI-B1-4		
	SOURCE(S):	1	**BASIN:**	Cumberland		
	AMST (°C)	**EASTING**	**NORTHING**	**KBG (m)**	**MD (m)**	**TVD (m)**
	6.3	414 717	5 054 459	3	1,220.0	
	LOG #	**MD (m)**	**TVD (m)**	**Max T (°C)**	**BHT (°C)**	**TSC (hrs)**
	1	1,198.0		38.0		4.0
	SELECTION:	38 °C at 1,198 m after 4 hrs			**CONFIDENCE:**	GOOD
	COMMENT:					

P-105: NO TEMPERATURE DATA

P-106	**DRILLED:**	1996	**NAME:**	Heather REI-SB-P2		
	SOURCE(S):	1	**BASIN:**	Stellarton		
	AMST (°C)	**EASTING**	**NORTHING**	**KBG (m)**	**MD (m)**	**TVD (m)**
	6.5	526 202	5 046 322	3.68	1,328.0	1,308.7
	LOG #	**MD (m)**	**TVD (m)**	**Max T (°C)**	**BHT (°C)**	**TSC (hrs)**
	1	840.0	832.7	27.0		11.0
	2	1,322.0	1,302.7	40.0		
	3	1,321.0	1,301.7	40.0		
	SELECTION:	27 °C at 832.7 m after 11 hrs			**CONFIDENCE:**	GOOD
	COMMENT:	LOG # 1 is shallower but has a TSC and a more reliable Max T.				

P-107	**DRILLED:**	1996	**NAME:**	Highland Mall REI-SB-P3		
	SOURCE(S):	1 and 2	**BASIN:**	Stellarton		
	AMST (°C)	**EASTING**	**NORTHING**	**KBG (m)**	**MD (m)**	**TVD (m)**
	6.5	526 248	5 047 394	3.65	723.0	718.2
	LOG #	**MD (m)**	**TVD (m)**	**Max T (°C)**	**BHT (°C)**	**TSC (hrs)**
	1	481.3	479.5	32.0		4.0
	2	722.5	717.6	38.0		4.0
	SELECTION:	38 °C at 717.6 m after 4 hrs			**CONFIDENCE:**	GOOD
	COMMENT:	LOG # 2 is the deepest.				

P-108	**DRILLED:**	1999	**NAME:**	Alton 99-1		
	SOURCE(S):	1	**BASIN:**	Shubenacadie		
	AMST (°C)	**EASTING**	**NORTHING**	**KBG (m)**	**MD (m)**	**TVD (m)**
	6.3	478 677	5 004 321	4	1,282.0	
	LOG #	**MD (m)**	**TVD (m)**	**Max T (°C)**	**BHT (°C)**	**TSC (hrs)**
	1	850.7		30.0		7.0
	SELECTION:	30 °C at 1,275 m after 7 hrs			**CONFIDENCE:**	GOOD
	COMMENT:	Selected depth corresponds to deepest measurement in log file.				

P-109 AND P-110: NO TEMPERATURE DATA

P-111						
	DRILLED:	2001	**NAME:**	Coolbrook		
	SOURCE(S):	2	**BASIN:**	Windsor-Kennetcook		
	AMST (°C)	**EASTING**	**NORTHING**	**KBG (m)**	**MD (m)**	**TVD (m)**
	6.5	437 911	5 004 325	3.2	1,349.0	
	LOG #	**MD (m)**	**TVD (m)**	**Max T (°C)**	**BHT (°C)**	**TSC (hrs)**
	1	1,351.0			38.0	
	SELECTION:	38 °C at 1,351 m			**CONFIDENCE:**	GOOD
	COMMENT:					

P-112: NO TEMPERATURE DATA

P-113						
	DRILLED:	2001	**NAME:**	EOG Cloverdale #1		
	SOURCE(S):	1	**BASIN:**	Shubenacadie		
	AMST (°C)	**EASTING**	**NORTHING**	**KBG (m)**	**MD (m)**	**TVD (m)**
	6.4	481 271	5 000 252	4.29	923.0	
	LOG #	**MD (m)**	**TVD (m)**	**Max T (°C)**	**BHT (°C)**	**TSC (hrs)**
	1	921.7		20.0	20.0	9.8
	2	658.2		54.0	35.0	
	SELECTION:	20 °C at 921.7 m after 9.8 hrs			**CONFIDENCE:**	GOOD
	COMMENT:	LOG # 2 is too shallow and has inconsistent temperatures.				

P-114						
	DRILLED:	2001	**NAME:**	Devon Cheverie #1		
	SOURCE(S):	1	**BASIN:**	Windsor-Kennetcook		
	AMST (°C)	**EASTING**	**NORTHING**	**KBG (m)**	**MD (m)**	**TVD (m)**
	6.8	414 879	5 003 098	3.2	1,394.0	
	LOG #	**MD (m)**	**TVD (m)**	**Max T (°C)**	**BHT (°C)**	**TSC (hrs)**
	1	1,999.0		34.0		7.8
	SELECTION:	34 °C at 1,205.9 m after 7.8 hrs			**CONFIDENCE:**	GOOD
	COMMENT:	Selected depth corresponds to total depth of intermediate hole section.				

P-115						
	DRILLED:	2002	**NAME:**	ECA 400-2		
	SOURCE(S):	2	**BASIN:**	Stellarton		
	AMST (°C)	**EASTING**	**NORTHING**	**KBG (m)**	**MD (m)**	**TVD (m)**
	6.4	529 967	5 046 825	4.3	912.0	
	LOG #	**MD (m)**	**TVD (m)**	**Max T (°C)**	**BHT (°C)**	**TSC (hrs)**
	1	846.0		39.0		6.7
	SELECTION:	39 °C at 846 m after 6.7 hrs			**CONFIDENCE:**	GOOD
	COMMENT:	Shallow log MD is explained by sloughing that prevented from logging to well MD.				

P-116						
	DRILLED:	2003	**NAME:**	UPCI Beech Hill #1		
	SOURCE(S):	1	**BASIN:**	Antigonish		
	AMST (°C)	**EASTING**	**NORTHING**	**KBG (m)**	**MD (m)**	**TVD (m)**
	6.1	580 145	5 047 154	5.3	1,044.5	1,037.3
	LOG #	**MD (m)**	**TVD (m)**	**Max T (°C)**	**BHT (°C)**	**TSC (hrs)**
	1	1,043.0	1,035.9	60.0	33.0	7.0
	2	1,044.0	1,036.8	60.0	60.0	7.0
	3	1,044.0	1,036.8	60.0	33.0	7.0
	SELECTION:	33 °C at 1,036.8 m after 7 hrs			**CONFIDENCE:**	GOOD
	COMMENT:	BHT in LOG # 3 is confirmed by a temperature log.				

P-117						
	DRILLED:	2003	**NAME:**	Cogmagun #1		
	SOURCE(S):	1	**BASIN:**	Windsor-Kennetcook		
	AMST (°C)	**EASTING**	**NORTHING**	**KBG (m)**	**MD (m)**	**TVD (m)**
	6.8	417 948	4 992 648	5.5	495.74	484.8
	LOG #	**MD (m)**	**TVD (m)**	**Max T (°C)**	**BHT (°C)**	**TSC (hrs)**
	1	493.0	482.1		40.0	5.5
	2	490.0	479.1	24.2	24.2	6.3
	SELECTION:	24.2 °C at 479.1 m after 6.25 hrs			**CONFIDENCE:**	NONE
	COMMENT:	Well is too shallow.				

P-118: NO TEMPERATURE DATA

P-119						
	DRILLED:	2005	**NAME:**	Barney's Brook #1		
	SOURCE(S):	1	**BASIN:**	Shubenacadie		
	AMST (°C)	**EASTING**	**NORTHING**	**KBG (m)**	**MD (m)**	**TVD (m)**
	6.5	463 060	4 988 515	4.06	749.0	748.3
	LOG #	**MD (m)**	**TVD (m)**	**Max T (°C)**	**BHT (°C)**	**TSC (hrs)**
	1	745.6	744.8			4.0
	2	298.0	298.0	13.0	25.0	
	3	747.3	747.6	27.0		13.8
	SELECTION:	27 °C at 747.6 m after 13.8 hrs			**CONFIDENCE:**	GOOD
	COMMENT:	LOG # 3 is the deepest and most complete.				

P-120	**DRILLED:**	2005	**NAME:**	Hardwoodlands #1		
	SOURCE(S):	1	**BASIN:**	Shubenacadie		
	AMST (°C)	**EASTING**	**NORTHING**	**KBG (m)**	**MD (m)**	**TVD (m)**
	6.5	459 530	4 987 591	4.06	835.0	833.7
	LOG #	**MD (m)**	**TVD (m)**	**Max T (°C)**	**BHT (°C)**	**TSC (hrs)**
	1	745.6	744.6	27.0	27.0	4.9
	2	832.5	831.2	24.0	23.0	9.0
	3	832.5	831.2	24.0	24.0	9.0
	4	298.0	298.0		25.0	
	SELECTION:	23 °C at 831.2 m after 9 hrs			CONFIDENCE:	**GOOD**
	COMMENT:	BHT in LOG # 2 is confirmed by a temperature log.				

P-121	**DRILLED:**	2005	**NAME:**	Milford Station #1		
	SOURCE(S):	1	**BASIN:**	Shubenacadie		
	AMST (°C)	**EASTING**	**NORTHING**	**KBG (m)**	**MD (m)**	**TVD (m)**
	6.5	463 819	4 985 585	4	870.0	
	LOG #	**MD (m)**	**TVD (m)**	**Max T (°C)**	**BHT (°C)**	**TSC (hrs)**
	1	869.5		25.0	25.0	9.5
	SELECTION:	25 °C at 869.5 m after 9.5 hrs			**CONFIDENCE:**	**GOOD**
	COMMENT:					

P-122	**DRILLED:**	2006	**NAME:**	Coal Mine Brook #3		
	SOURCE(S):	1	**BASIN:**	Cumberland		
	AMST (°C)	**EASTING**	**NORTHING**	**KBG (m)**	**MD (m)**	**TVD (m)**
	6.3	414 934	5 055 401	4.1	1,687.6	1,270.1
	LOG #	**MD (m)**	**TVD (m)**	**Max T (°C)**	**BHT (°C)**	**TSC (hrs)**
	1	923.7	923.7	30.0	30.0	13.0
	2	899.5	899.4	30.0	30.0	15.5
	3	899.5	899.4	30.0	30.0	17.5
	SELECTION:	30 °C at 923.7 m after 13 hrs			**CONFIDENCE:**	**GOOD**
	COMMENT:	Well MD and TVD correspond to the horizontal leg; BHT of LOG # 1 is confirmed by a temperature log.				

P-123	**DRILLED:**	2006	**NAME:**	Priestville #4		
	SOURCE(S):	2	**BASIN:**	Stellarton		
	AMST (°C)	**EASTING**	**NORTHING**	**KBG (m)**	**MD (m)**	**TVD (m)**
	6.4	529 971	5 046 944	4.3	759.0	757.6
	LOG #	**MD (m)**	**TVD (m)**	**Max T (°C)**	**BHT (°C)**	**TSC (hrs)**
	1	750.0	748.6	30.0	30.0	7.0
	SELECTION:	30 °C at 748.6 m after 7 hrs			**CONFIDENCE:**	**GOOD**
	COMMENT:					

P-124	**DRILLED:**	2006	**NAME:**	Coal Mine Brook #12		
	SOURCE(S):	2	**BASIN:**	Cumberland		
	AMST (°C)	**EASTING**	**NORTHING**	**KBG (m)**	**MD (m)**	**TVD (m)**
	6.3	414 889	5 054 831	4.3	1,638.4	1,040.2
	LOG #	**MD (m)**	**TVD (m)**	**Max T (°C)**	**BHT (°C)**	**TSC (hrs)**
	1	1,138.5	905.1	30.0		7.3
	SELECTION:	30 °C at 905.1 m after 7.3 hrs			**CONFIDENCE:**	GOOD
	COMMENT:	Well MD and TVD correspond to the horizontal leg.				

P-125: NO TEMPERATURE DATA

P-126	**DRILLED:**	2007	**NAME:**	Kennetcook #1		
	SOURCE(S):	2	**BASIN:**	Windsor-Kennetcook		
	AMST (°C)	**EASTING**	**NORTHING**	**KBG (m)**	**MD (m)**	**TVD (m)**
	6.5	443 757	5 005 132	4.5	1,385.0	
	LOG #	**MD (m)**	**TVD (m)**	**Max T (°C)**	**BHT (°C)**	**TSC (hrs)**
	1	1,357.3		35.0		7.4
	2	1,357.3		35.0		12.7
	3	1,342.0		35.0		13.2
	SELECTION:	35 °C at 1,342 m after 13.2 hrs			**CONFIDENCE:**	GOOD
	COMMENT:	LOG # 3 is selected because TSC is the longest.				

P-127 AND P-128: NO TEMPERATURE DATA

P-129	**DRILLED:**	2007	**NAME:**	Kennetcook #2		
	SOURCE(S):	1	**BASIN:**	Windsor-Kennetcook		
	AMST (°C)	**EASTING**	**NORTHING**	**KBG (m)**	**MD (m)**	**TVD (m)**
	6.5	440 571	5 006 503	4.5	1,935.0	1,920.0
	LOG #	**MD (m)**	**TVD (m)**	**Max T (°C)**	**BHT (°C)**	**TSC (hrs)**
	1	1,920.0	1 905.0	42.0	42.0	15.7
	2	1,935.0	1 920.0	42.0	42.0	7.6
	3	1,935.0	1 920.0		50.0	
	SELECTION:	42 °C at 1,905 m after 15.7 hrs			**CONFIDENCE:**	GOOD
	COMMENT:	LOG # 1 is selected because TSC is the longest.				

P-130	**DRILLED:**	2008	**NAME:**	N-14-A/11-E-5		
	SOURCE(S):	1	**BASIN:**	Windsor-Kennetcook		
	AMST (°C)	**EASTING**	**NORTHING**	**KBG (m)**	**MD (m)**	**TVD (m)**
	6.5	443 038	5 013 820	4.68	2,617.9	2,615.9
	LOG #	**MD (m)**	**TVD (m)**	**Max T (°C)**	**BHT (°C)**	**TSC (hrs)**
	1	2,608.4	2,606.5	55.7	55.7	10.0
	2	2,603.7	2,601.8	55.7	55.7	10.0
	SELECTION:	55.7 °C at 2,606.5 m after 10 hrs			**CONFIDENCE:**	GOOD
	COMMENT:					

P-131: NO TEMPERATURE DATA

P-132	**DRILLED:**	2008	**NAME:**	O-61-C/11-E-4		
	SOURCE(S):	1	**BASIN:**	Windsor-Kennetcook		
	AMST (°C)	**EASTING**	**NORTHING**	**KBG (m)**	**MD (m)**	**TVD (m)**
	6.6	422 123	5 006 480	4.5	2,955.0	2,954.8
	LOG #	**MD (m)**	**TVD (m)**	**Max T (°C)**	**BHT (°C)**	**TSC (hrs)**
	1	2,951.0	2,950.8	61.3	61.3	17.5
	SELECTION:	61.3 °C at 2,950.8 m after 17.5 hrs			**CONFIDENCE:**	GOOD
	COMMENT:					

P-133	**DRILLED:**	2008	**NAME:**	E-38-A/11-E-5		
	SOURCE(S):	1	BASIN:	Windsor-Kennetcook		
	AMST (°C)	**EASTING**	**NORTHING**	**KBG (m)**	**MD (m)**	**TVD (m)**
	6.4	443 001	5 015 963	5	1,726.0	
	LOG #	**MD (m)**	**TVD (m)**	**Max T (°C)**	**BHT (°C)**	**TSC (hrs)**
	1	1,494.0		40.0		8.0
	SELECTION:	40 °C at 1,494 m after 8 hrs			**CONFIDENCE:**	GOOD
	COMMENT:	Shallow log MD is explained by sloughing that prevented from logging to well MD.				

P-134	**DRILLED:**	2010	**NAME:**	ECE-11-01		
	SOURCE(S):	2	**BASIN:**	Stellarton		
	AMST (°C)	**EASTING**	**NORTHING**	**KBG (m)**	**MD (m)**	**TVD (m)**
	6.4	529 976	5 045 865	0	678.0	
	LOG #	**MD (m)**	**TVD (m)**	**Max T (°C)**	**BHT (°C)**	**TSC (hrs)**
	1	673.6			29.4	
	SELECTION:	29.4 °C at 673.6 m			**CONFIDENCE:**	GOOD
	COMMENT:					

P-135	**DRILLED:**	2012	**NAME:**	Eastrock Lauren #1 F-25-D/11-E-2		
	SOURCE(S):	2	**BASIN:**	Cumberland		
	AMST (°C)	**EASTING**	**NORTHING**	**KBG (m)**	**MD (m)**	**TVD (m)**
	6.4	420 980	5 056 480	4	946.0	944.3
	LOG #	**MD (m)**	**TVD (m)**	**Max T (°C)**	**BHT (°C)**	**TSC (hrs)**
	1	944.0	942.3	52.0	52.0	
	SELECTION:	21.5 °C at 886.4 m			**CONFIDENCE:**	GOOD
	COMMENT:	Selection comes from a temperature log.				

P-136	**DRILLED:**	2012	**NAME:**	Forent Alton #1 E-49-C/11-E-03		
	SOURCE(S):	1 and 2	**BASIN:**	Shubenacadie		
	AMST (°C)	**EASTING**	**NORTHING**	**KBG (m)**	**MD (m)**	**TVD (m)**
	6.4	479 037	5 003 558	4.12	996.0	
	LOG #	**MD (m)**	**TVD (m)**	**Max T (°C)**	**BHT (°C)**	**TSC (hrs)**
	1	995.0		23.0	22.0	
	2	995.5			22.0	
	3	940.0			22.0	
	SELECTION:	22 °C at 995.5 m			**CONFIDENCE:**	GOOD
	COMMENT:	LOG # 2 is deepest and BHT is confirmed by a temperature log.				

P-137	**DRILLED:**	2012	**NAME:**	Forent South Branch #1 K-70-D/11-E-03		
	SOURCE(S):	2	**BASIN:**	Shubenacadie		
	AMST (°C)	**EASTING**	**NORTHING**	**KBG (m)**	**MD (m)**	**TVD (m)**
	6.3	496 239	5 003 587	4.13	784.0	783.8
	LOG #	**MD (m)**	**TVD (m)**	**Max T (°C)**	**BHT (°C)**	**TSC (hrs)**
	1	765.0	764.8	25.2	30.0	2.7
	SELECTION:	25.2 °C at 764.8 m after 2.7 hrs			**CONFIDENCE:**	GOOD
	COMMENT:	Max T appears more reliable than BHT.				

P-138	**DRILLED:**	2013	**NAME:**	ECE-13-P1		
	SOURCE(S):	1 and 2	BASIN:	Stellarton		
	AMST (°C)	**EASTING**	**NORTHING**	**KBG (m)**	**MD (m)**	**TVD (m)**
	6.4	530 080	5 045 980	4.4	700.0	699.9
	LOG #	**MD (m)**	**TVD (m)**	**Max T (°C)**	**BHT (°C)**	**TSC (hrs)**
	1	600.8	600.7		25.0	
	2	702.9	702.8		25.0	
	3	698.6	698.5	29.0	29.0	4.0
	SELECTION:	29 °C at 698.5 m after 4 hrs			**CONFIDENCE:**	GOOD
	COMMENT:	LOG # 1 is shallower, LOG # 2 has an inconsistent BHT.				

P-139: NO TEMPERATURE DATA

<table>
<tr><td rowspan="9">CCS1</td><td>DRILLED:</td><td>2014</td><td>NAME:</td><td colspan="3">CCSNS#1</td></tr>
<tr><td>SOURCE(S):</td><td>1 and 2</td><td>BASIN:</td><td colspan="3">Sydney</td></tr>
<tr><td>AMST (°C)
5.9</td><td>EASTING
731 648</td><td>NORTHING
5 118 046</td><td>KBG (m)
4.4</td><td>MD (m)
1,527.0</td><td>TVD (m)</td></tr>
<tr><td>LOG #</td><td>MD (m)</td><td>TVD (m)</td><td>Max T (°C)</td><td>BHT (°C)</td><td>TSC (hrs)</td></tr>
<tr><td>1</td><td>1,533.4</td><td></td><td>36.0</td><td>65.0</td><td>13.3</td></tr>
<tr><td>2</td><td>1,527.6</td><td></td><td>36.0</td><td></td><td>13.3</td></tr>
<tr><td>3</td><td>1,524.0</td><td></td><td>36.0</td><td></td><td>17.6</td></tr>
<tr><td>SELECTION:</td><td colspan="3">36 °C at 1,524 m after 17.6 hrs</td><td>CONFIDENCE:</td><td>GOOD</td></tr>
<tr><td>COMMENT:</td><td colspan="5">LOG # 3 has the longest TSC and Max T is confirmed by a temperature log.</td></tr>
</table>

Offshore wells

F-24	**DRILLED:**	1976	**NAME:**	North Sydney F-24		
	SOURCE(S):	2	**BASIN:**	Sydney - Offshore		
	AMST (°C)	**EASTING**	**NORTHING**	**KBG (m)**	**MD (m)**	**TVD (m)**
	4.0	284 470	5 159 721	89.6	1,706.9	
	LOG #	**MD (m)**	**TVD (m)**	**Max T (°C)**	**BHT (°C)**	**TSC (hrs)**
	1	758.0			37.7	
	2	1,082.0			46.1	
	3	1,691.0			42.2	
	4	1,701.7			42.2	
	5	1,702.0			47.7	
	6	1,702.0			48.8	15.0
	7	1,702.0			48.8	
	8	1,702.3			47.2	
	9	1,702.6			44.4	
	10	1,702.6			44.4	
	11	1,702.6			44.4	
	SELECTION:	48.8 °C at 1,702 m after 15 hrs			**CONFIDENCE:**	GOOD
	COMMENT:	LOG # 6 is the most complete.				

N-37	**DRILLED:**	1975	**NAME:**	Chinampas N-37		
	SOURCE(S):	2	**BASIN:**	Fundy - Offshore		
	AMST (°C)	**EASTING**	**NORTHING**	**KBG (m)**	**MD (m)**	**TVD (m)**
	4.0	690 191	4 979 971	83.21	2,587.0	
	LOG #	**MD (m)**	**TVD (m)**	**Max T (°C)**	**BHT (°C)**	**TSC (hrs)**
	1	861.0			60.0	
	2	1,625.6			56.0	
	3	2,586.0			50.0	
	4	2,586.0			51.0	
	5	2,586.0			55.0	
	SELECTION:	55 °C at 2,586 m			**CONFIDENCE:**	GOOD
	COMMENT:	LOG # 5 has the warmer BHT of the deepest logs.				

APPENDIX III – DATA COMPILED FOR THE ABANDONED MINES

UG: Underground mine. OP: Open-pit mine.

Name	Type	Commodity	Arkay Site #	Community	County	Operating Period	Depth (m)	Total Production (tonnes)	Heating Capacity (MWh)	Cooling Capacity (MWh)	Northing	Easting
Acadia Colliery	UG	Coal	NS-C182	Westville	Pictou	1867-1920		11,562,000	17,403	5,085	5 045 099	522 457
Acadia No.1	UG	Coal	NS-C177	Stellarton	Pictou	1920-1925		241,000	363	127	5 045 611	525 060
Acadia No.2	UG	Coal	NS-C178	Thorburn	Pictou	1920-1921		48,000	72	26	5 044 914	534 879
Acadia No.3	UG	Coal	NS-C179	Thorburn	Pictou	1920-1939		1,377,000	2,073	670	5 045 650	534 658
Acadia No.7	UG	Coal	NS-C181	Stellarton	Pictou	1936-1947		568,000	855	297	5 045 989	524 060
Albion	UG	Coal	NS-C183	Stellarton	Pictou	1867-1942		7,455,000	11,221	3,279	5 045 759	525 237
Allan	UG	Coal	NS-C184	Stellarton	Pictou	1908-1951		4,758,000	7,162	2,093	5 046 640	526 780
Anglo	UG	Coal	NS-C213	New Campbellton	Victoria	1867-1924		158,000	238	84	5 131 172	697 852
Arseneau	UG	Coal	NS-C96	River Hebert	Cumberland	1941-1942		11,000	17	6	5 061 070	391 812
Atlantic	UG	Coal	NS-C69	Bras d'Or	Cape Breton	1957-1959		21,000	32	11	5 125 931	709 676
Atlantic Barite Company Bass River Prospect	OP	Barite		Upper bass River (Hoegs Corner)	Colchester	1984-1984		2,816	< 1	< 1	5 034 557	439 594
Bass River of Five Islands	UG	Barite	21H/08-04(I)	Five Islands	Colchester	1866-1876		3,000	5	2	5 032 552	418 332
Bayview	UG	Coal	NS-C98	Joggins	Cumberland	1923		23,000	35	12	5 060 979	390 450
Bayview No.8	UG	Coal	NS-C99	Joggins	Cumberland	1939-1961		1,898,000	2,857	835	5 061 740	388 217
Beaton	UG	Coal	NS-C155	Inverness	Inverness	1952-1954		500	1	< 1	5 121 240	631 781
Beaver	UG	Coal	NS-C38	Morrison Road	Cape Breton	1950-1961		165,000	248	87	5 107 548	730 478
Beaver Dam Gold District	UG	Gold	11E/02-01	Beaver Lake	Halifax	1889-1931	30	3,000	5	2	4 990 298	522 256
Beech Grove	UG	Coal	NS-C100	River Hebert	Cumberland	1922		7,000	11	4	5 060 928	390 084
Beech Hill	UG	Coal	NS-C101	River Hebert	Cumberland	1940-1943		14,000	21	8	5 061 021	391 654
Black Diamond	UG	Coal	NS-C185	Westville	Pictou	1888-1891		99,000	149	53	5 045 544	522 007
Black Diamond	UG	Coal	NS-C102	Maccan River	Cumberland	1911-1915		11,000	17	6	5 062 974	398 900
Black Diamond	UG	Coal	NS-C39	Sydney Mines	Cape Breton	1938-1940		4,000	6	2	5 124 186	711 241
Blockhouse	UG	Coal	NS-C1	Port Morien	Cape Breton	1868-1888		1,060,000	1,596	539	5 114 424	742 248
Blockhouse Gold District	UG	Gold	21A/08-06	Blockhouse	Lunenburg		91	6,000	9	3	4 921 375	386 826
Boston	UG	Coal	NS-C103	River Hebert	Cumberland	1924-1929		42,000	63	22	5 061 387	394 498

Name	Type	Commodity	Arkay Site #	Community	County	Operating Period	Depth (m)	Total Production (tonnes)	Heating Capacity (MWh)	Cooling Capacity (MWh)	Northing	Easting
Boularderie	UG	Coal	NS-C70	Little Bras d'Or Bridge	Cape Breton	1931		500	1	< 1	5 127 103	708 428
Bras d'Or No.5	UG	Coal	NS-C71	Bras d'Or	Cape Breton	1943-1946		20,000	30	11	5 126 346	709 542
Bridgeport	UG	Coal	NS-C2	Bridgeport	Cape Breton	1884-1892		79,000	119	42	5 120 939	729 704
Bridgeville Iron District	UG	Iron	11E/07-05	Bridgeville	Pictou	1828-1904		170,000	256	75	5 031 259	531 879
Broad Cove	UG	Coal	NS-C156	Inverness	Inverness	1887-1905		394,000	593	207	5 121 916	631 711
Brogan Mining Company Ltd. Little Pond Surface Mine	OP	Coal		Little Pond	Cape Breton	1999-2003		100,000	4	6	5 129 175	710 605
Brogan Mining Company Ltd. Sullivan Creek Surface Mine	OP	Coal		Florence (Sullivan Creek)	Cape Breton	1993-1998		60,000	2	3	5 127 310	710 310
Brookfield	UG	Gold	11E/06-04	Upper Brookfield	Colchester	1889	36	40,000	60	18	4 918 719	347 287
Brookfield Gold District	UG	Gold	21A/07-04	North Brookfield	Queens	1886-1928	38	97,000	146	43	4 919 712	347 246
Broughton	UG	Coal	NS-C3	Broughton	Cape Breton	1914-1915		51,000	77	27	5 107 664	732 881
Caledonia	UG	Coal	NS-C4	Glace Bay	Cape Breton	1864-1892		1,391,000	2,094	669	5 118 878	734 977
Cameron	UG	Coal	NS-C158	Inverness	Inverness	1962-1963		600	1	< 1	5 122 266	631 796
Campbell No.1 and 2	UG	Coal	NS-C157	Inverness	Inverness	1944-1961		86,000	129	46	5 122 247	631 547
Canada Cement Lafarge Ltd. Brookfield Quarry	OP	Gypsum		Brookfield	Hants	1983-1986		23,841	1	1	5 010 567	479 839
Cap d'Or	UG	Copper	21H/07-02	East Advocate	Cumberland	1901-1907	254	57,000	86	25	5 018 715	362 328
Cape Breton Development Corporation Alder Point Surface Mine	OP	Coal		Adler Point	Cape Breton	1974-1974		100,000	4	6	5 132 300	709 530
Cape Breton Development Corporation Lingan Colliery	UG	Coal		New Waterford	Cape Breton	till 1992		20,367,000	30,655	8,958	5 125 887	726 452
Cape Breton Development Corporation Phalen Colliery	UG	Coal		New Waterford	Cape Breton	till 2000		18,156,000	27,327	7,985	5 125 373	726 551
Cape Breton Development Corporation Prince Mine	UG	Coal		Point Aconi	Cape Breton	till 2001		22,384,000	33,691	9,845	5 132 956	707 392
Cape Crushing Company Ltd. Halfway Road Surface Mine	OP	Coal		Sydney Mines (Halfway Road)	Cape Breton	2003-2004		16,500	1	1	5 124 200	711 680

Name	Type	Commodity	Arkay Site #	Community	County	Operating Period	Depth (m)	Total Production (tonnes)	Heating Capacity (MWh)	Cooling Capacity (MWh)	Northing	Easting
Cape Crushing Company Ltd. Merritt Point Surface Mine	OP	Coal		Adler Point	Cape Breton	1991-2005		300,000	11	17	5 131 174	710 000
Caribou Gold District	UG	Gold	11E/02-04	Caribou Gold Mines	Halifax	1867-1947	305	168,000	253	74	4 989 702	504 797
Carter	UG	Coal	NS-C104	Maccan	Cumberland	1922-1927		29,000	44	15	5 062 795	398 470
Casey	UG	Coal	NS-C105	Joggins	Cumberland	1923		4,000	6	2	5 060 959	388 563
Central Rawdon	UG	Gold	11E/04-06	Rawdon	Hants	1888-1939	123	5,000	8	2	4 989 133	433 778
Chestico	UG	Coal	NS-C153	Port Hood	Inverness	1959-1966		152,000	229	81	5 095 204	613 687
Chignecto	UG	Coal	NS-C106	Maccan	Cumberland	1867-1948		328,000	494	173	5 064 907	404 614
Chimney Corner	UG	Coal	NS-C159	Chimney Corner	Inverness	1867-1952		12,000	18	6	5 139 108	640 614
Clyde/Ontario	UG	Coal	NS-C5	Port Caledonia	Cape Breton	1863-1892		216,000	325	114	5 119 011	738 995
Coastal	UG	Coal	NS-C72	Point Aconi	Cape Breton	1918-1922		18,000	27	10	5 132 044	708 743
Cochrane	UG	Coal	NS-C107	River Hebert	Cumberland	1951-1960		215,000	324	114	5 061 774	392 380
Cochrane Hill Gold District	UG	Gold	11E/01-07	Crows Nest	Guysborough	1869-1935	69	11,000	17	5	5 011 083	577 589
Colonial Colliery	UG	Coal	NS-C40	North Sydney	Cape Breton	1907-1958		3,033,000	4,565	1,334	5 126 607	709 003
Colonial No.1	UG	Coal	NS-C74	Bras d’Or	Cape Breton	1909-1958		2,310,000	3,477	1,016	5 126 578	708 545
Colonial No.2	UG	Coal	NS-C41	North Sydney	Cape Breton	1909-1924		257,000	387	136	5 123 839	711 822
Colonial No.3	UG	Coal	NS-C75	Bras d’Or	Cape Breton	1918		300	1	< 1	5 124 001	711 861
Colonial No.4	UG	Coal	NS-C76	Bras d’Or	Cape Breton	1920-1924		347,000	522	183	5 126 607	709 003
Colonial No.5	UG	Coal	NS-C77	Florence	Cape Breton	1920-1923		10,000	15	5	5 126 346	709 542
Connecticut Adamant Gypsum Co. Foul Meadows Quarry	OP	Gypsum		Kempt Shore	Hants	1915-1945		189,982	7	10	4 999 057	408 113
Coolen	UG	Coal	NS-C92	Belmont	Colchester	1925		200	< 1	< 1	5 033 986	470 524
Country Harbour	UG	Gold	11F/04-03	Country Harbour Mines	Guysborough	1868-1951	44	26,000	39	11	5 012 289	593 183
Cow Bay Gold District	UG	Gold	11D/11-01	Cow Bay	Halifax	1896-1905	46	1,000	2	1	4 941 019	463 417
Coxheath	UG	Copper	11K/01-01	Beechmont	Cape Breton	1875-1928	603	3,000	5	2	5 107 246	704 240
Curragh Resources Inc. Westray Mine	UG	Coal		Plymouth	Pictou	till 1992		255,000	384	135	5 044 535	527 593
Delta Coal Incorporated Chignecto Surface Mine	OP	Coal		Chignecto	Cumberland	1997-1997		5,000	< 1	< 1	5 065 100	407 455

Name	Type	Commodity	Arkay Site #	Community	County	Operating Period	Depth (m)	Total Production (tonnes)	Heating Capacity (MWh)	Cooling Capacity (MWh)	Northing	Easting
Dominion Colliery	UG	Coal	NS-C7	Glace Bay	Cape Breton	1893-1922		78,332,000	117,901	34,452	5 118 962	731 422
Dominion No. 1/1A	UG	Coal	NS-C43	Dominion	Cape Breton	1907-1927		6,611,000	9,951	2,908	5 121 807	730 112
Dominion No. 10	UG	Coal	NS-C45	Reserve Mines	Cape Breton	1910-1942		5,335,000	8,030	2,346	5 119 192	730 093
Dominion No. 14	UG	Coal	NS-C46	New Waterford	Cape Breton	1909-1932		4,745,000	7,142	2,087	5 125 909	725 387
Dominion No. 15	UG	Coal	NS-C47	New Waterford	Cape Breton	1910-1925		1,239,000	1,865	620	5 125 482	725 441
Dominion No. 1B	UG	Coal	NS-C10	Bridgeport	Cape Breton	1924-1955		15,844,000	23,848	6,968	5 123 004	733 031
Dominion No.11	UG	Coal	NS-C18	Glace Bay	Cape Breton	1913-1949		6,568,000	9,886	2,889	5 117 938	733 919
Dominion No.16	UG	Coal	NS-C48	New Waterford	Cape Breton	1911-1962		16,770,000	25,241	7,376	5 125 652	723 753
Dominion No.17	UG	Coal	NS-C79	New Victoria	Cape Breton	1914-1921		33,000	50	18	5 125 842	720 502
Dominion No.2	UG	Coal	NS-C11	Glace Bay	Cape Breton	1911-1949		18,331,000	27,591	8,062	5 121 705	734 347
Dominion No.21	UG	Coal	NS-C19	Birch Grove	Cape Breton	1911-1925		1,166,000	1,755	591	5 112 016	734 486
Dominion No.22	UG	Coal	NS-C20	Birch Grove	Cape Breton	1912-1930		2,124,000	3,197	934	5 112 079	736 723
Dominion No.24	UG	Coal	NS-C21	Glace Bay	Cape Breton	1920-1953		5,252,000	7,905	2,310	5 117 964	735 519
Dominion No.25	UG	Coal	NS-C49	Gardiner Mines	Cape Breton	1942-1959		2,023,000	3,045	890	5 120 357	726 813
Dominion No.3	UG	Coal	NS-C12	Glace Bay	Cape Breton	1910-1924		626,000	942	326	5 118 539	732 839
Dominion No.4	UG	Coal	NS-C13	Glace Bay	Cape Breton	1910-1961		18,066,000	27,192	7,946	5 118 878	734 977
Dominion No.5	UG	Coal	NS-C44	Reserve Mines	Cape Breton	1910-1939		2,272,000	3,420	999	5 119 280	730 112
Dominion No.6	UG	Coal	NS-C14	Donkin	Cape Breton	1910-1930		2,869,000	4,318	1,262	5 119 187	741 339
Dominion No.7	UG	Coal	NS-C15	Glace Bay	Cape Breton	1910-1925		1,171,000	1,763	591	5 122 298	734 857
Dominion No.8	UG	Coal	NS-C16	Bridgeport	Cape Breton	1910-1914		546,000	822	286	5 121 726	731 945
Dominion No.9	UG	Coal	NS-C17	Glace Bay	Cape Breton	1910-1925		3,013,000	4,535	1,325	5 121 705	734 347
Dominion Steel & Coal Corporation Chegoggin Point Silica Quarry	OP	Silica		Pembroke (Chegoggin Point)	Yarmouth	1890-1963		100,000	4	6	4 861 347	245 487
Dominion/Devco No. 20	UG	Coal	NS-C8	Glace Bay	Cape Breton	1939-1971		15,898,000	23,929	6,992	5 121 705	734 347
Dominion/Devco No. 26	UG	Coal	NS-C9	Bridgeport	Cape Breton	1944-1985		24,634,000	37,078	10,834	5 123 004	733 031
Dominion/Devco No.12	UG	Coal	NS-C42	New Waterford	Cape Breton	1908-1971		28,073,000	42,254	12,347	5 126 196	723 690
Dominion/Devco No.18	UG	Coal	NS-C78	New Victoria	Cape Breton	1938-1966		6,688,000	10,066	2,942	5 125 693	722 007
Domtar Construction Materials Ltd. Nappan Quarry	OP	Gypsum		Nappan	Cumberland	1907-1962		181,469	7	10	5 070 925	403 495

Name	Type	Commodity	Arkay Site #	Community	County	Operating Period	Depth (m)	Total Production (tonnes)	Heating Capacity (MWh)	Cooling Capacity (MWh)	Northing	Easting
East Lake Ainslie	UG	Barite	11K/03-01(I)	Trout River	Inverness	1916-1938		7,000	11	3	5 107 790	645 034
Eastern	UG	Coal	NS-C108	Maccan	Cumberland	1909-1919		15,000	23	8	5 064 106	402 784
Ecum Secum Gold District	UG	Gold	11D/16-04	Ecum Secum	Halifax	1881-1907	52	3,000	5	2	4 979 877	564 328
Elderbank Silica Mining & Exploration (Atlantic Silica Ltd.) Open Cut	OP	Silica		Elderbank	Halifax	1966-1974		5,600	< 1	< 1	4 978 571	485 166
Emery	UG	Coal	NS-C22	Reserve	Cape Breton	1872-1878		28,000	42	15	5 118 497	730 357
Erinville	UG	Iron	11F/05-17	East Erinville	Guysborough	1870-1901	15	4,000	6	2	5 026 517	599 682
Evans	UG	Coal	NS-C160	St. Rose	Inverness	1946-1976		680,000	1,024	354	5 133 167	639 889
Evans Coal Mines Ltd. Colliery	UG	Coal		St.Rose	Inverness	till 1992		1,233,000	1,856	620	5 133 167	639 889
Fenwick	UG	Coal	NS-C109	Hoeg Road	Cumberland	1917-1929		32,000	48	17	5 065 044	409 184
Fifteen Mile Stream Gold District	UG	Gold	11E/02-10	Lochaber Mines	Halifax	1867-1941	61	45,000	68	20	4 998 693	537 570
Filor	UG	Coal	NS-C110	River Hebert	Cumberland	1951-1955		32,000	48	17	5 061 965	395 372
Forest Hill	UG	Gold	11F/05-12	Forest Hill	Guysborough	1895-1956	23	51,000	77	22	5 017 902	597 802
Four Star	UG	Coal	NS-C23	Broughton	Cape Breton	1950-1969		1,400,000	2,107	664	5 107 717	733 751
Franklin	UG	Coal	NS-C80	Florence	Cape Breton	1885-1957		1,274,000	1,918	630	5 126 167	710 225
Fundy Mines	UG	Coal	NS-C111	Joggins	Cumberland	1903-1934		133,000	200	71	5 062 085	388 703
Fundy No.6	UG	Coal	NS-C112	Joggins	Cumberland	1929-1930		8,000	12	4	5 062 082	389 041
Gardiner	UG	Coal	NS-C50	New Waterford	Cape Breton	1868- 1892		94,000	142	50	5 120 403	727 403
Gays River	UG	Gold	11E/03-09	Gays River	Halifax	1975-1981	91	12,000	18	5	4 991 740	475 517
Gays River Gold District	UG	Gold	11E/03-06	Coldstream	Cochester	1869-1880		14,000	21	6	4 991 865	475 787
Georgia Pacific Corporation River Denys Quarry	OP	Gypsum		River Denys (Big Brook)	Inverness	1962-1990		19,515,236	734	1,071	5 074 252	638 510
German/Marsh	UG	Coal	NS-C188	New Glasgow	Pictou	1867-1909		282,000	425	149	5 045 930	532 394
Glace Bay	UG	Coal	NS-C24	Glace Bay	Cape Breton	1863-1892		1,265,000	1,904	630	5 120 314	735 152
Gold River Gold District	UG	Gold	21A/09-03	Chester Basin	Lunenburg			3,000	5	2	4 936 454	394 318
Goldenville Gold District	UG	Gold	11E/01-01	Goldenville	Guysborough	1862-1942	183	540,000	813	238	4 997 390	577 096
Gowrie	UG	Coal	NS-C25	Port Morien	Cape Breton	1863-1892		1,751,000	2,636	770	5 112 938	741 290
Gowrie and Blockhouse	UG	Coal	NS-C26	Port Morien	Cape Breton	1901-1907		183,000	275	97	5 112 938	741 290
Grant's Quarry	OP	Gypsum		Summerville	Hants	1872-1884		38,958	2	2	4 994 613	407 059

Name	Type	Commodity	Arkay Site #	Community	County	Operating Period	Depth (m)	Total Production (tonnes)	Heating Capacity (MWh)	Cooling Capacity (MWh)	Northing	Easting
Great Northern	UG	Coal	NS-C113	Chignecto	Cumberland	1910		800	1	< 1	5 065 197	405 182
Green Crow	UG	Coal	NS-C114	Joggins	Cumberland	1935		600	1	< 1	5 061 730	388 752
Greener	UG	Coal	NS-C51	Sydney Mines	Cape Breton	1896-1963		623,000	938	325	5 123 328	713 864
Greenwood Colliery	UG	Coal	NS-C191	Greenwood	Pictou	1918-1966		821,000	1,236	423	5 046 259	532 585
Greenwood No.1	UG	Coal	NS-C189	Thorburn	Pictou	1926-1930		153,000	230	81	5 044 610	533 985
Greenwood No.2	UG	Coal	NS-C190	Greenwood	Pictou	1926-1966		293,000	441	154	5 044 736	532 328
Gypsum, Lime and Alabastine (Canada) Co. Herring Cove Quarry	OP	Gypsum		Long Hill (Baddeck Bay)	Victoria	1874-1941		260,075	10	14	5 110 599	677 764
H.C. Higginson Clough Quarry	OP	Gypsum		Lennox	Richmond	1872-1895		11,255	< 1	1	5 049 396	653 525
Harbourside	UG	Coal	NS-C52	North Sydney	Cape Breton	1928-1933		44,000	66	23	5 120 758	712 012
Harrigan Cove Gold District	UG	Gold	11D/16-03	Harrigan Cove	Halifax	1872-1916	15	12,000	18	5	4 976 256	555 558
Hiawatha	UG	Coal	NS-C27	False Bay	Cape Breton	1920-1921		5,000	8	3	5 107 060	742 103
Hillcrest	UG	Coal	NS-C115	Joggins	Cumberland	1941-1942		119,000	179	63	5 061 729	389 772
Hillcrest	UG	Coal	NS-C192		Pictou	1936		600	1	< 1	5 046 351	536 399
Ingonish Gypsum Company Ltd. Ingonish Beach Quarry	OP	Gypsum		Ingonish Beach	Victoria	1924-1928		265,176	10	15	5 168 340	698 860
Intercolonial/Drummond Mines	UG	Coal	NS-C196	Westville	Pictou	1867-1976		13,930,000	20,967	6,127	5 044 199	523 018
Intercolonial/Drummond No.1	UG	Coal	NS-C193	Westville	Pictou	1923-1969		2,441,000	3,674	1,074	5 044 199	523 018
Intercolonial/Drummond No.2	UG	Coal	NS-C194	Westville	Pictou	1923-1984		3,527,000	5,309	1,551	5 044 199	523 018
Intercolonial/Drummond No.5	UG	Coal	NS-C195	Westville	Pictou	1920-1945		589,000	887	308	5 045 099	522 457
International	UG	Coal	NS-C28	Bridgeport	Cape Breton	1863-1892		1,594,000	2,399	725	5 121 726	731 945
International Diatomite Industries Ltd. (Scotia Diatom Products) Factory Bog Mine	OP	Diatomaceous Earth		Little River (Tiddville)	Digby	1917-1955		5,556	< 1	< 1	4 924 600	248 332
Inverness (No.1 and 4)	UG	Coal	NS-C161	Inverness	Inverness	1903-1951		6,292,000	9,470	2,767	5 122 156	632 427
Iona Gypsum Products Company Ltd. Grass Cove Quarry	OP	Gypsum		Iona (Grass Cove)	Victoria	1914-1930		88,479	3	5	5 094 595	669 250
Isaac's Harbour	UG	Gold	11F/04-04	Goldboro	Guysborough	1861-1941	79	49,000	74	22	5 003 227	607 007

Name	Type	Commodity	Arkay Site #	Community	County	Operating Period	Depth (m)	Total Production (tonnes)	Heating Capacity (MWh)	Cooling Capacity (MWh)	Northing	Easting
J & W King 3061831 Nova Scotia Limited Greenhills Surface Mine	OP	Coal		Florence	Cape Breton	2005-2010		75,000	3	4	5 126 850	711 250
Jack Pit	UG	Coal	NS-C54	Sydney Mines	Cape Breton	1920		3,000	5	2	5 123 345	713 809
Joggins	UG	Coal	NS-C116	Joggins	Cumberland	1867-1966		2,842,000	4,278	1,250	5 061 076	387 049
Jubilee	UG	Coal	NS-C117	River Hebert	Cumberland	1897-1951		15,000	23	8	5 062 510	397 169
Jubilee No.6	UG	Coal	NS-C55	Sydney Mines	Cape Breton	1913-1924		*595,000*	896	311	5 124 805	713 127
Kemptville	UG	Gold	21A/04-03	Kemptville	Yarmouth	1885-1938	84	3,000	5	2	4 881 507	271 796
Killag Gold District	UG	Gold	11E/02-02	Marinette	Halifax	1889-1951	38	3,000	5	2	4 985 232	530 002
Kimberly	UG	Coal	NS-C118	River Hebert	Cumberland	1936		2,000	3	1	5 061 585	392 242
Lake Catcha Gold District	UG	Gold	11D/11-04	West Petpeswick	Halifax	1887-1942		23,000	35	10	4 953 238	483 899
Last Chance	UG	Coal	NS-C56	Gannon Road	Cape Breton	1935-1936		8,000	12	4	5 124 070	711 760
Lawler	UG	Coal	NS-C212	Glengarry	Richmond	1929-1938		3,000	5	2	5 082 533	693 318
Leipsigate Gold District	UG	Gold	21A/07-01	Conquerall	Lunenburg	1883-1908	182	34,000	51	15	4 909 758	373 263
Linacy	UG	Coal	NS-C197	Stellarton	Pictou	1960-1963		3,000	5	2	5 047 690	528 963
Lingan (old)	UG	Coal	NS-C57	Lingan	Cape Breton	1863-1886		659,000	992	343	5 125 225	728 036
Lloyd Cove No.7	UG	Coal	NS-C82	Alder Point	Cape Breton	1947-1956		274,000	412	145	5 129 512	710 422
Lodestone Limited Bass River Magnetite Pit	OP	Iron		Upper Bass River (Hoegs Corner)	Colchester	1988-1988		2,000	< 1	< 1	5 034 915	439 020
Londonderry Iron District	UG	Iron	11E/05-07	Londonderry	Colchester	1849-1908	48	1,814,000	2,730	798	5 036 815	451 200
Lorway	UG	Coal	NS-C29	Reserve Mines	Cape Breton	1869-1872		2,000	3	1	5 117 590	729 150
Low Point	UG	Coal	NS-C83	Low Point	Cape Breton	1925		100	< 1	< 1	5 125 181	718 779
Mabou	UG	Coal	NS-C162	Mabou	Inverness	1887-1951		62,000	93	33	5 108 376	618 373
MacBean/Vale	UG	Coal	NS-C198	Thorburn	Pictou	1867-1971		4,700,000	7,074	2,067	5 045 531	535 174
Maccan/Lawson	UG	Coal	NS-C120	Maccan Station	Cumberland	1867-1940		84,000	126	45	5 063 422	400 855
MacDonald No.1	UG	Coal	NS-C163	Inverness	Inverness	1943-1952		141,000	212	75	5 121 718	631 389
MacDonald No.2	UG	Coal	NS-C164	Inverness	Inverness	1948-1957		1,500	2	1	5 122 380	631 164
MacDonald No.3	UG	Coal	NS-C165	Inverness	Inverness	1948-1959		118,000	178	63	5 121 587	630 622
MacDonald No.5	UG	Coal	NS-C166	Inverness	Inverness	1952-1957		9,000	14	5	5 122 266	631 796
MacDougal	UG	Coal	NS-C58	Gannon Road	Cape Breton	1935-1939		17,000	26	9	5 123 525	712 329

Name	Type	Commodity	Arkay Site #	Community	County	Operating Period	Depth (m)	Total Production (tonnes)	Heating Capacity (MWh)	Cooling Capacity (MWh)	Northing	Easting
MacGregor/Albion	UG	Coal	NS-C199	Stellarton	Pictou	1912-1957		2,941,000	4,427	1,294	5 045 759	525 237
Manganese Mines	UG	Manganese	11E/06-17	Manganese Mines	Colchester	1880-1905	21	2,000	3	1	5 029 150	487 367
Maple Leaf Mines	UG	Coal	NS-C121	Joggins	Cumberland	1920-1943		896,000	1,349	459	5 060 912	390 412
Maple Leaf No.4	UG	Coal	NS-C122	Joggins	Cumberland	1929-1939		551,000	829	289	5 060 965	390 992
Maple Leaf No.5	UG	Coal	NS-C123	Joggins	Cumberland	1920-1943		11,000	17	6	5 060 937	390 560
Maritime Gypsum Company Cove Quarry at Cheverie	OP	Gypsum		Cheverie	Hants	1870-1915		864,721	33	48	5 000 772	407 446
Marsh	UG	Coal	NS-C124	River Hebert	Cumberland	1920-1929		86,000	129	46	5 061 545	393 582
McLellan	UG	Coal	NS-C170	Inverness	Inverness	1943-1957		31,000	47	17	5 121 978	631 873
Merigomish	UG	Coal	NS-C201	Merigomish	Pictou	1868-1869		100	< 1	< 1	5 046 288	531 883
Milford No.1/Acadia No.4	UG	Coal	NS-C203	Coalburn	Pictou	1920-1941		244,000	367	129	5 046 308	532 325
Milford No.2/Acadia No.6	UG	Coal	NS-C204	Coalburn	Pictou	1838-1947		184,000	277	97	5 046 701	531 740
Milford/Acadia	UG	Coal	NS-C202	Coalbum	Pictou	1916-1947		622,000	936	325	5 046 701	531 740
Milner	UG	Coal	NS-C125	River Hebert	Cumberland	1883-1935		25,000	38	13	5 061 736	391 532
Minudie	UG	Coal	NS-C126	Minudie	Cumberland	1880-1916		557,000	838	292	5 061 596	392 470
Montague Gold District	UG	Gold	11D/12-01	Montague Gold Mines	Halifax	1865-1939	152	122,000	184	54	4 951 406	459 002
Montreal and New Glasgow	UG	Coal	NS-C205	Coal Brook	Pictou	1868		200	< 1	< 1	5 047 806	526 651
Moose River Gold District	UG	Gold	11D/15-03	Moose River	Halifax	1870-1939	44	139,000	209	61	4 980 804	504 487
Mooseland Gold District	UG	Gold	11D/15-04	Mooseland	Halifax	1863-1914	12	8,000	12	4	4 975 620	517 880
Mount Uniacke Gold District	UG	Gold	11D/13-04	Lewis Mills	Hants	1865-1941	102	54,000	81	24	4 974 790	435 847
National	UG	Coal	NS-C127	River Hebert	Cumberland	1922-1925		9,000	14	5	5 062 046	389 749
National Gypsum (Canada) Co. Ltd. Great Northern Mining & Railway Company Quarry	OP	Gypsum		Cheticamp (Belle Marche)	Inverness	1906-1939		1,521,757	57	84	5 165 950	655 615
National Gypsum (Canada) Co. Ltd. Half Mile Quarry at Dingwall	OP	Gypsum		Dingwall	Victoria	1933-1954		9,671,315	364	531	5 196 167	691 255
National Gypsum Canada Co. Ltd. Fry's Mountain Quarry	OP	Gypsum		Walton	Hants	1950-1967		1,969,998	74	108	5 008 752	426 805
National Gypsum Canada Co. Ltd. South Mountain Quarry	OP	Gypsum		Walton	Hants	1816-1952		2,968,714	112	163	5 008 707	422 551

Name	Type	Commodity	Arkay Site #	Community	County	Operating Period	Depth (m)	Total Production (tonnes)	Heating Capacity (MWh)	Cooling Capacity (MWh)	Northing	Easting
Newark Plaster Company Ottawa Brook Quarry	OP	Gypsum		Ottawa Brook	Victoria	1907-1927		178,043	7	10	5 089 450	659 190
Newport Plaster Mining & Manufacturing Company Avondale (Tunnel) Quarry	OP	Gypsum		Avondale (Newport Landing)	Hants	1892-1922		661,333	25	36	4 986 613	411 795
Nictaux-Torbrook	UG	Iron	21A/14-03	Torbrook	Annapolis	1825-1913	107	144,000	217	63	4 976 769	344 239
Nictaux-Torbrook Iron District	UG	Iron	21A/15-01	Nictaux Falls	Annapolis	1825-1913	152	181,000	272	80	4 975 464	343 214
No.1	UG	Coal	NS-C128	Springhill	Cumberland	1873-1970		3,052,000	4,594	1,342	5 056 098	417 123
No.2	UG	Coal	NS-C129	Springhill	Cumberland	1915-1966		10,822,000	16,289	4,760	5 055 160	416 946
No.3	UG	Coal	NS-C130	Springhill	Cumberland	1915-1968		258,000	388	136	5 055 261	416 771
No.4	UG	Coal	NS-C131	Springhill	Cumberland	1934-1970		3,509,000	5,282	1,543	5 055 121	416 962
No.6	UG	Coal	NS-C132	Springhill	Cumberland	1920-1937		1,376,000	2,071	675	5 056 660	417 459
No.7	UG	Coal	NS-C133	Springhill	Cumberland	1920-1934		925,000	1,392	473	5 056 591	417 429
Noel Plaster Company O'Brien Quarry	OP	Gypsum		Noel Lake	Hants	1907-1913		16,000	1	1	5 012 625	440 610
North Atlantic	UG	Coal	NS-C32	Port Morien	Cape Breton	1907-1912		248,000	373	131	5 113 215	741 300
North Sydney/Indian Cove	UG	Coal	NS-C59	North Sydney	Cape Breton	1859-1919		116,000	175	62	5 123 328	713 864
Northern/Scotia	UG	Coal	NS-C134	Maccan	Cumberland	1872-1936		49,000	74	26	5 065 295	405 582
Nova Construction Company Ltd. Novaco Point Aconi Surface Mine	OP	Coal		Point Aconi	Cape Breton	1980-1985		900,000	34	49	5 131 640	706 920
Nova Scotia	UG	Coal	NS-C207	Middle River	Pictou	1867-1878		308,000	464	162	5 045 544	522 007
Nova Scotia Coal and Gypsum (Gypsum, Lime and Alabastine Canada Ltd.) Company South Quarry	OP	Gypsum		Mabou Harbour	Inverness	1877-1933		75,127	3	4	5 104 945	618 796
Oldham Gold District	UG	Gold	11D/14-03	Oldham	Halifax	1862-1943	488	107,000	161	47	4 973 336	460 588
Oliver (French River)	UG	Copper	11E/11-02	Oliver	Colchester	1866-1900		19,000	29	8	5 056 626	474 922
Pellow Quarry	OP	Gypsum		Windsor	Hants	?-1871		150,000	6	8	4 982 458	410 069
Pioneer Coal Limited Airport Swamp Surface Mine	OP	Coal		Reserve Mines	Cape Breton	1986-1992		700,000	26	38	5 117 280	730 370

Name	Type	Commodity	Arkay Site #	Community	County	Operating Period	Depth (m)	Total Production (tonnes)	Heating Capacity (MWh)	Cooling Capacity (MWh)	Northing	Easting
Pioneer Coal Limited Westville Surface Mine	OP	Coal		Westville	Pictou	1984-1994		1,200,000	45	66	5 044 730	522 602
Pleasant River Gold District	UG	Gold	21A/07-05	Colpton	Lunenburg	1889-1913	38	463,000	697	204	4 922 671	357 589
Port Hood	UG	Coal	NS-C154	Port Hood	Inverness	1875-1958		818,000	1,231	423	5 095 010	613 745
Prospect	UG	Coal	NS-C60	Sydney Mines	Cape Breton	1928-1931		8,000	12	4	5 124 540	711 517
Renfrew Gold District	UG	Gold	11E/04-09	Renfrew	Hants	1862-1958	152	60,000	90	26	4 983 492	450 222
Reserve	UG	Coal	NS-C33	Reserve Mines	Cape Breton	1871-1892		1,421,000	2,139	662	5 118 497	730 357
Richmond	UG	Coal	NS-C209	Port Malcolm	Richmond	1868-1908		2,000	3	1	5 052 708	634 140
River Hebert/Cochrane	UG	Coal	NS-C135	River Hebert	Cumberland	1960-1980		706,000	1,063	366	5 061 525	393 122
Riversdale	UG	Coal	NS-C95	Kemptown	Colchester	1920-1932		331,000	498	174	5 034 812	494 137
Riverside	UG	Coal	NS-C136	River Hebert	Cumberland	1926-1951		98,000	148	52	5 061 546	392 764
Rosebank No.1	UG	Coal	NS-C172	Inverness	Inverness	1943-1946		5,000	8	3	5 121 790	631 415
Rosebank No.2	UG	Coal	NS-C173	Inverness	Inverness	1947-1957		89,000	134	47	5 122 163	632 385
Rosebank No.3	UG	Coal	NS-C174	Inverness	Inverness	1956-1961		42,000	63	22	5 122 626	632 012
Rosebank No.5	UG	Coal	NS-C175	Inverness	Inverness	1955-1957		19,000	29	10	5 122 402	632 286
Ross and Tabor	UG	Coal	NS-C137	Springhill	Cumberland	1960		50	< 1	< 1	5 054 239	416 899
Salmon River Gold District	UG	Gold	11D/16-01	Barkhouse Settlement	Halifax	1881-1942	79	107,000	161	47	4 978 575	546 982
Schooner Pond	UG	Coal	NS-C34	Donkin	Cape Breton	1872-1874		17,000	26	9	5 118 941	742 931
Scotia No.7/Alexander	UG	Coal	NS-C86	Alder Point	Cape Breton	1921-1925		94,000	142	50	5 128 961	710 629
Seaman	UG	Coal	NS-C138	River Hebert	Cumberland	1877		500	1	< 1	5 065 105	411 886
Seashore	UG	Coal	NS-C139	Joggins	Cumberland	1934-1943		113,000	170	60	5 062 125	387 827
Silver Lake	UG	Coal	NS-C61	Morrison Road	Cape Breton	1934-1935		3,000	5	2	5 107 778	728 603
Silver Mine (Yava)	UG	Lead	11F/16-25	Silver Mine	Cape Breton	circa 1911	12	212,000	319	93	5 081 409	701 038
Skyerock Minerals Ltd. Skye Mountain Magnetite Prospect	OP	Iron		Iron Mines (Whycocomagh)	Inverness	1990-1990		200	< 1	< 1	5 092 150	640 567
South Head/Cow Bay	UG	Coal	NS-C35	Port Morien	Cape Breton	1868-1877		6,000	9	3	5 113 084	746 716
South Maitland Quarry	OP	Gypsum		South Maitland	Hants	1872-1879		18,010	1	1	5 012 721	463 452
South Uniacke Gold District	UG	Gold	11D/13-03	South Uniacke	Halifax and Hants	1888-1948	123	11,000	17	5	4 969 152	438 810
St. George	UG	Coal	NS-C141	St. George	Cumberland	1920-1921		34,000	51	18	5 065 049	408 799

Name	Type	Commodity	Arkay Site #	Community	County	Operating Period	Depth (m)	Total Production (tonnes)	Heating Capacity (MWh)	Cooling Capacity (MWh)	Northing	Easting
Sterling (No.3 Mine)	UG	Coal	NS-C142	River Hebert	Cumberland	1917-1923		88,000	133	47	5 061 474	391 442
Stirling	UG	Zinc	11F/09-01	Stirling	Richmond	1906-1956	357	783,000	1,179	344	5 066 961	699 343
Strathcona Mines	UG	Coal	NS-C146	River Hebert	Cumberland	1895-1947		731,000	1,100	379	5 061 800	394 167
Strathcona No 1	UG	Coal	NS-C143	River Hebert	Cumberland	1924-1928		29,000	44	15	5 061 800	394 167
Strathcona No.2	UG	Coal	NS-C144	River Hebert	Cumberland	1922-1947		547,000	823	287	5 061 605	394 037
Strathcona No.3	UG	Coal	NS-C145	River Hebert	Cumberland	1930-1931		15,000	23	8	5 061 710	394 557
Sullivan	UG	Coal	NS-C87	Sydney Mines	Cape Breton	1940-1946		75,000	113	40	5 124 576	711 885
Sullivan/Indian Cove	UG	Coal	NS-C62	Sydney Mines	Cape Breton	1934-1940		57,000	86	30	5 124 576	711 885
Sydney Mines Colliery	UG	Coal	NS-C63	Sydney Mines	Cape Breton	1863-1962		38,882,000	58,523	17,101	5 126 370	714 757
Sydney No. 4/Scotia	UG	Coal	NS-C91	Sydney Mines	Cape Breton	1908-1921		895,000	1,347	460	5 127 711	709 409
Sydney No.1/Princess	UG	Coal	NS-C88	Sydney Mines	Cape Breton	1908-1975		18,753,000	28,226	8,248	5 126 060	715 125
Sydney No.2/Lloyd Cove	UG	Coal	NS-C89	Sydney Mines	Cape Breton	1907-1916		461,000	694	242	5 126 370	714 757
Sydney No.3/Florence	UG	Coal	NS-C90	Florence	Cape Breton	1908-1961		11,999,000	18,060	5,277	5 126 728	711 579
Sydney No.5/Queen	UG	Coal	NS-C64	Sydney Mines	Cape Breton	1908-1916		818,000	1,231	423	5 125 550	714 049
Tangier	UG	Gold	11D/15-01	Tangier	Halifax	1862-1937	183	46,000	69	20	4 961 781	524 775
Tennycape Mines	UG	Manganese	11E/05-19	Tennycape	Hants	1862-1918	50	4,000	6	2	5 011 555	429 745
Thomas Brogan & Sons Construction Ltd. Point Aconi Surface Mine	OP	Coal		Point Aconi	Cape Breton	1976-1993		1,000,000	38	55	5 133 728	707 896
Thomas Brogan & Sons Construction Ltd. Toronto Road Surface Mine	OP	Coal		Little Bras d'Or (Toronto Road)	Cape Breton	1995-1999		100,000	4	6	5 128 300	709 680
Thompson	UG	Coal	NS-C65	Sydney Mines	Cape Breton	1938-1940		7,000	11	4	5 124 474	711 580
Thorburn Mining Ltd. McBean Surface Mine	OP	Coal		Thorburn	Pictou	1995-2000		150,000	6	8	5 045 170	534 950
Tidewater	UG	Coal	NS-C210	Whiteside	Richmond	1928		800	1	< 1	5 050 405	643 751
Tijer	UG	Coal	NS-C176	Mabou	Inverness	1961-1964		900	1	1	5 108 378	618 437
Tom Pit	UG	Coal	NS-C66	Sydney Mines	Cape Breton	1920-1942		681,000	1,025	354	5 123 720	712 714
Tomson	UG	Coal	NS-C67	Sydney Mines	Cape Breton	1940-1962		422,000	635	222	5 124 474	711 580
Trestle Brook	UG	Coal	NS-C147	Joggins	Cumberland	1925-1928		3,000	5	2	5 062 059	389 585
Upper Seal Harbour Gold District	UG	Gold	11F/04-06	Goldboro	Guysborough	1892-1927	232	400,000	602	176	5 006 559	604 950

Name	Type	Commodity	Arkay Site #	Community	County	Operating Period	Depth (m)	Total Production (tonnes)	Heating Capacity (MWh)	Cooling Capacity (MWh)	Northing	Easting
Victoria	UG	Coal	NS-C68	Victoria Mines	Cape Breton	1867-1893		827,000	1,245	426	5 125 080	718 540
Victoria Gypsum Mining & Manufacturing Company Goose Cove Quarry	OP	Gypsum		St. Ann's (Goose Cove)	Victoria	1884-1916		176,382	7	10	5 125 538	681 233
Victoria Mines	UG	Coal	NS-C151	River Hebert	Cumberland	1867-1941		1,013,000	1,525	517	5 061 048	392 197
Victoria No.1	UG	Coal	NS-C148	River Hebert	Cumberland	1921-1930		127,000	191	67	5 061 092	392 192
Victoria No.2	UG	Coal	NS-C149	River Hebert	Cumberland	1915-1930		182,000	274	96	5 061 122	392 148
Victoria No.4	UG	Coal	NS-C150	River Hebert	Cumberland	1931-1941		505,000	760	265	5 061 224	393 743
Waddell	UG	Coal	NS-C152	River Hebert	Cumberland	1943-1952		2,000	3	1	5 060 978	390 235
Wadden	UG	Coal	NS-C208	Westville	Pictou	1946-1953		16,000	24	9	5 045 099	522 457
Walton-Magnet Cove Mine	UG	Lead	21H/01-08	Pembroke	Hants	1940-1970	523	3,900,000	5,870	1,715	5 006 287	418 040
Waverley Gold District	UG	Gold	11D/13-02	Waverley	Halifax	1862-1938	152	152,000	229	67	4 959 505	452 903
West Gore Antimony Mine	UG	Antimony	11E/04-01	West Gore	Hants	1884-1917	259	31,000	47	14	4 992 464	437 822
Whiteburn	UG	Gold	21A/06-01	Caledonia	Queens	1885-1941	61	10,000	15	4	4 908 136	334 479
Windsor Plaster Company Ltd. Martock Quarry	OP	Gypsum		Three Mile Plains	Hants	1870-1949		696,048	26	38	4 979 250	410 750
Windsor Plaster Company Ltd. Mosher Quarry	OP	Gypsum		Gypsum Mines (St. Croix)	Hants	1892-1941		572,110	22	31	4 980 504	416 366
Wine Harbour	UG	Gold	11F/04-02	Sonora	Guysborough	1862-1939		76,000	114	33	4 991 800	591 448

APPENDIX IV – GEOTHERMAL GRADIENTS CALCULATED FOR THE SEDIMENTARY BASINS

AMST: Annual Mean Surface Temperature
UGG: Uncorrected Geothermal Gradient derived from temperatures measured at equilibrium (°C km^{-1})
CGG: Corrected Geothermal Gradient (°C km^{-1})
DDTM: Depth of the Deepest Temperature Measurement
All well depths are True Vertical Depths

SUB-BASIN	Cumberland NE		**BASIN**	Cumberland	
USAGE	**WELL**	**DEPTH (m)**	**UGG (°C km^{-1})**	**CGG (°C km^{-1})**	**CONFIDENCE**
< 1,000 m	Wallace	311.80	17.29		VERY GOOD
< 1,000 m	P-135	886.41	17.11		GOOD
> 1,000 m	P-93	2,636.37		20.35	GOOD
> 1,000 m	P-86	2,933.04		21.45	GOOD
> 1,000 m	P-83	2,984.60		20.40	GOOD
> 1,000 m	P-85	4,528.31		22.52	GOOD
17.2 °C km^{-1} ± 0.09 at 599.11 m (n=2) and > 1,000 m: 21.18 °C km^{-1} ± 1.08 (n=4)					
DDTM: 4528 m		**AMST:** 6.3 °C		**CONFIDENCE:** GOOD	
EXPECTED TEMPERATURE AT SET DEPTH:		**500 m:**	14.9 °C ± 0.04	**4,000 m:**	90.32 °C ± 4.34
		1,000 m:	27.48 °C ± 1.08	**4,500 m:**	101.33 °C ± 4.88
		1,500 m:	38.07 °C ± 1.63	**5,000 m:**	112.3 °C ± 5.42
		2,000 m:	48.66 °C ± 2.17	**5,500 m:**	123.23 °C ± 5.97
		2,500 m:	59.25 °C ± 2.71	**6,000 m:**	134.13 °C ± 6.51
		3,000 m:	69.84 °C ± 3.25	**6,500 m:**	145.02 °C ± 7.05
		3,500 m:	79.26 °C ± 3.8	**7,000 m:**	155.89 °C ± 7.59
EXPECTED DEPTH AT SET TEMPERATURE:		**20 °C:**	690 m ± 29	**100 °C:**	4,416 m ± 223
		40 °C:	1,622 m ± 78	**120 °C:**	5,348 m ± 271
		60 °C:	2,553 m ± 126	**140 °C:**	6,280 m ± 320
		80 °C:	3,485 m ± 175	**160 °C:**	7,211 m ± 368
COMMENT:					

SUB-BASIN	Cumberland SW		BASIN	Cumberland	
USAGE	**WELL**	**DEPTH (m)**	**UGG (°C km^{-1})**	**CGG (°C km^{-1})**	**CONFIDENCE**
Rejected	P-103	828.00	29.82		POOR
< 1,000 m	P-124	905.05	26.31		GOOD
< 1,000 m	P-122	923.65	25.77		GOOD
> 1,000 m	P-104	1,198.00		28.18	GOOD
> 1,000 m	P-101	1,301.00		24.15	GOOD
26.33 °C km^{-1} ± 0.27 at 914.35 m (n=2) and > 1,000 m: 26.17 °C km^{-1} ± 2.01 (n=2)					
DDTM: 1301 m		**AMST:** 6.3 °C		**CONFIDENCE:** GOOD	

EXPECTED TEMPERATURE AT SET DEPTH:	**500 m:**	19.47 °C ± 0.13	**4,000 m:**	115.12 °C ± 8.05
	1,000 m:	32.47 °C ± 2.01	**4,500 m:**	129.34 °C ± 9.06
	1,500 m:	43.58 °C ± 3.02	**5,000 m:**	143.53 °C ± 10.06
	2,000 m:	57.74 °C ± 4.02	**5,500 m:**	157.67 °C ± 11.07
	2,500 m:	72.11 °C ± 5.03	**6,000 m:**	171.79 °C ± 12.07
	3,000 m:	86.5 °C ± 6.04	**6,500 m:**	185.89 °C ± 13.08
	3,500 m:	100.84 °C ± 7.04	**7,000 m:**	199.98 °C ± 14.09
EXPECTED DEPTH AT SET TEMPERATURE:	**20 °C:**	607 m ± 36	**100 °C:**	3,455 m ± 246
	40 °C:	1,319 m ± 89	**120 °C:**	4,167 m ± 299
	60 °C:	2,031 m ± 141	**140 °C:**	4,879 m ± 351
	80 °C:	2,743 m ± 194	**160 °C:**	5,591 m ± 403
COMMENT:				

SUB-BASIN	Stellarton		**BASIN**	Cumberland	
USAGE	**WELL**	**DEPTH (m)**	**UGG (°C km^{-1})**	**CGG (°C km^{-1})**	**CONFIDENCE**
Rejected	Noval P-6	335.40	29.34		GOOD
Rejected	P-134	673.61	34.14		GOOD
Rejected	P-138	698.49	32.56		GOOD
Rejected	P-107	717.57	44.12		GOOD
< 1,000 m	Suncor AP83-0372	740.00	26.65		VERY GOOD
Rejected	P-123	748.61	31.71		GOOD
Rejected	P-106	832.68	24.73		GOOD
Rejected	P-115	846.00	38.73		GOOD
> 1,000 m	NSDME P-54	950.00	22.68		VERY GOOD
> 1,000 m	P-106	1,302.71		28.30	GOOD
26.65 °C km^{-1} ± 1.34 at 740 m (n=1) and > 1,000 m: 25.49 °C km^{-1} ± 2.81 (n=2)					
DDTM:	1303 m	**AMST:**	6.45 °C	**CONFIDENCE:**	**GOOD**
EXPECTED TEMPERATURE AT SET DEPTH:		**500 m:**	20.45 °C ± 0.67	**4,000 m:**	113.13 °C ± 11.24
		1,000 m:	31.94 °C ± 2.81	**4,500 m:**	127.08 °C ± 12.64
		1,500 m:	42.99 °C ± 4.21	**5,000 m:**	140.98 °C ± 14.05
		2,000 m:	56.88 °C ± 5.62	**5,500 m:**	154.85 °C ± 15.45
		2,500 m:	70.96 °C ± 7.02	**6,000 m:**	168.69 °C ± 16.86
		3,000 m:	85.07 °C ± 8.43	**6,500 m:**	182.51 °C ± 18.26
		3,500 m:	99.13 °C ± 9.83	**7,000 m:**	196.31 °C ± 19.66
EXPECTED DEPTH AT SET TEMPERATURE:		**20 °C:**	603 m ± 56	**100 °C:**	3,514 m ± 361
		40 °C:	1,330 m ± 132	**120 °C:**	4,241 m ± 437
		60 °C:	2,058 m ± 208	**140 °C:**	4,969 m ± 513
		80 °C:	2,786 m ± 285	**160 °C:**	5,697 m ± 589

COMMENT: The geothermal gradient < 1,000 m has been estimated using only the well Suncor AP83-0372 because it is derived from a temperature at equilibrium, contrary to the other data points. The estimation of the geothermal gradient > 1,000 m includes the well NSDME P-54 despite its depth (950 m) because a temperature at the equilibrium was also available for this well. NOTE: Drury et al. (1987) indicate that in the case of the well Suncor AP83-0372, a higher geothermal gradient is documented above a shear zone at 480 m. The results presented here are representative of the area, not of this specific case.

SUB-BASIN	Windsor-Kennetcook		BASIN	Windsor	
USAGE	**WELL**	**DEPTH (m)**	**UGG (°C km^{-1})**	**CGG (°C km^{-1})**	**CONFIDENCE**
Rejected	P-117	479.10	36.74		NONE
< 1,000 m	NSDME 84-1	605.00	23.60		VERY GOOD
> 1,000 m	P-114	1,205.90		24.34	GOOD
> 1,000 m	P-126	1,342.00		24.10	GOOD
> 1,000 m	P-111	1,351.00		26.23	GOOD
Rejected	P-87	1,448.40		21.30	POOR
> 1,000 m	P-133	1,494.00		26.26	GOOD
> 1,000 m	P-129	1,905.02		23.81	GOOD
> 1,000 m	P-130	2,606.45		24.73	GOOD
> 1,000 m	P-132	2,950.80		24.32	GOOD
23.6 °C km^{-1} ± 0 at 605 m (n=1) and > 1,000 m: 24.34 °C km^{-1} ± 0.95 (n=7)					
DDTM: 2951 m		**AMST:**	6.5 °C	**CONFIDENCE:**	GOOD
EXPECTED TEMPERATURE AT SET DEPTH:		**500 m:**	18.3 °C ± 0	**4,000 m:**	106.93 °C ± 3.79
		1,000 m:	30.84 °C ± 0.95	**4,500 m:**	120.12 °C ± 4.27
		1,500 m:	40.58 °C ± 1.42	**5,000 m:**	133.26 °C ± 4.74
		2,000 m:	53.7 °C ± 1.9	**5,500 m:**	146.37 °C ± 5.22
		2,500 m:	67.03 °C ± 2.37	**6,000 m:**	159.46 °C ± 5.69
		3,000 m:	80.38 °C ± 2.85	**6,500 m:**	172.52 °C ± 6.17
		3,500 m:	93.69 °C ± 3.32	**7,000 m:**	185.57 °C ± 6.64
EXPECTED DEPTH AT SET TEMPERATURE:		**20 °C:**	650 m ± 19	**100 °C:**	3,726 m ± 135
		40 °C:	1,419 m ± 48	**120 °C:**	4,495 m ± 164
		60 °C:	2,188 m ± 77	**140 °C:**	5,264 m ± 192
		80 °C:	2,957 m ± 106	**160 °C:**	6,033 m ± 221
COMMENT:					

SUB-BASIN	Shubenacadie		BASIN	Windsor	
USAGE	WELL	DEPTH (m)	UGG (°C km^{-1})	CGG (°C km^{-1})	CONFIDENCE
< 1,000 m	P-119	747.56	27.57		GOOD
< 1,000 m	P-137	764.75	24.84		GOOD
< 1,000 m	P-120	831.21	19.95		GOOD
< 1,000 m	P-121	869.50	21.37		GOOD
< 1,000 m	P-113	921.70	14.82		GOOD
< 1,000 m	P-136	995.50	15.74		GOOD
> 1,000 m	P-108	1,275.00		20.95	GOOD
20.66 °C km^{-1} ± 4.99 at 850.36 m (n=6) and > 1,000 m: 20.95 °C km^{-1} ± 0 (n=1)					
DDTM: 1275 m		**AMST:**	6.4 °C	**CONFIDENCE:**	**GOOD**
EXPECTED TEMPERATURE AT SET DEPTH:		**500 m:**	16.73 °C ± 2.5	**4,000 m:**	94.22 °C ± 0
		1,000 m:	27.35 °C ± 0	**4,500 m:**	105.83 °C ± 0
		1,500 m:	35.8 °C ± 0	**5,000 m:**	117.38 °C ± 0
		2,000 m:	47.34 °C ± 0	**5,500 m:**	128.91 °C ± 0
		2,500 m:	59.08 °C ± 0	**6,000 m:**	140.41 °C ± 0
		3,000 m:	70.85 °C ± 0	**6,500 m:**	151.88 °C ± 0
		3,500 m:	82.57 °C ± 0	**7,000 m:**	163.35 °C ± 0
EXPECTED DEPTH AT SET TEMPERATURE:		**20 °C:**	744 m	**100 °C:**	4,245 m
		40 °C:	1,619 m	**120 °C:**	5,120 m
		60 °C:	2,494 m	**140 °C:**	5,995 m
		80 °C:	3,370 m	**160 °C:**	6,870 m
COMMENT:					

<table>
<tr><td>SUB-BASIN</td><td colspan="2">Antigonish</td><td>BASIN</td><td colspan="2">Cape Breton</td></tr>
<tr><td>USAGE</td><td>WELL</td><td>DEPTH (m)</td><td>UGG (°C km^{-1})</td><td><b>CGG (°C km^{-1})</td><td>CONFIDENCE</td></tr>
<tr><td>< 1,000 m</td><td>NSDME Glen Rd 83-1</td><td>590.00</td><td>20.86</td><td></td><td>VERY GOOD</td></tr>
<tr><td>> 1,000 m</td><td>P-116</td><td>1,036.84</td><td>26.08</td><td></td><td>GOOD</td></tr>
<tr><td colspan="6">20.86 °C km^{-1} ± 0 at 590 m (n=1) and > 1,000 m: 26.08 °C km^{-1} ± 0 (n=1)</td></tr>
<tr><td>DDTM:</td><td>1037 m</td><td>AMST:</td><td>6.1 °C</td><td>CONFIDENCE:</td><td>GOOD</td></tr>
<tr><td colspan="2" rowspan="7">EXPECTED TEMPERATURE AT SET DEPTH:</td><td>500 m:</td><td>16.53 °C ± 0</td><td>4,000 m:</td><td>115.51 °C ± 0</td></tr>
<tr><td>1,000 m:</td><td>32.18 °C ± 0</td><td>4,500 m:</td><td>129.79 °C ± 0</td></tr>
<tr><td>1,500 m:</td><td>43.73 °C ± 0</td><td>5,000 m:</td><td>144.02 °C ± 0</td></tr>
<tr><td>2,000 m:</td><td>57.95 °C ± 0</td><td>5,500 m:</td><td>158.21 °C ± 0</td></tr>
<tr><td>2,500 m:</td><td>72.36 °C ± 0</td><td>6,000 m:</td><td>172.38 °C ± 0</td></tr>
<tr><td>3,000 m:</td><td>86.8 °C ± 0</td><td>6,500 m:</td><td>186.53 °C ± 0</td></tr>
<tr><td>3,500 m:</td><td>101.18 °C ± 0</td><td>7,000 m:</td><td>200.66 °C ± 0</td></tr>
<tr><td colspan="2" rowspan="4">EXPECTED DEPTH AT SET TEMPERATURE:</td><td>20 °C:</td><td>633 m</td><td>100 °C:</td><td>3,453 m</td></tr>
<tr><td>40 °C:</td><td>1,338 m</td><td>120 °C:</td><td>4,158 m</td></tr>
<tr><td>60 °C:</td><td>2,043 m</td><td>140 °C:</td><td>4,863 m</td></tr>
<tr><td>80 °C:</td><td>2,748 m</td><td>160 °C:</td><td>5,568 m</td></tr>
<tr><td colspan="6">COMMENT:</td></tr>
</table>

SUB-BASIN	Western Cape Breton		**BASIN**	Cape Breton	
USAGE < / > 1,000 m	**WELL** P-98	**DEPTH (m)** 1,499.20	**UGG (°C km^{-1})**	**CGG (°C km^{-1})** 20.30	**CONFIDENCE** GOOD
20.3 °C km^{-1} ± 0 (n=1)					
DDTM:	1499 m	**AMST:**	6.2 °C	**CONFIDENCE:**	**GOOD**
EXPECTED TEMPERATURE AT SET DEPTH:		**500 m:**	16.35 °C ± 0	**4,000 m:**	90.47 °C ± 0
		1,000 m:	26.5 °C ± 0	**4,500 m:**	101.64 °C ± 0
		1,500 m:	34.22 °C ± 0	**5,000 m:**	112.77 °C ± 0
		2,000 m:	45.33 °C ± 0	**5,500 m:**	123.86 °C ± 0
		2,500 m:	56.63 °C ± 0	**6,000 m:**	134.92 °C ± 0
		3,000 m:	67.97 °C ± 0	**6,500 m:**	145.96 °C ± 0
		3,500 m:	79.25 °C ± 0	**7,000 m:**	156.99 °C ± 0
EXPECTED DEPTH AT SET TEMPERATURE:		**20 °C:**	780 m	**100 °C:**	4,424 m
		40 °C:	1,691 m	**120 °C:**	5,335 m
		60 °C:	2,602 m	**140 °C:**	6,246 m
		80 °C:	3,513 m	**160 °C:**	7,157 m
COMMENT:	In the absence of well data shallower than 1,000 m, the gradient < 1,000 m is inferred from the gradient > 1,000 m.				

SUB-BASIN	Central Cape Breton		BASIN	Cape Breton	
USAGE	**WELL**	**DEPTH (m)**	**UGG (°C km^{-1})**	**CGG (°C km^{-1})**	**CONFIDENCE**
Rejected	P-91	370.00	33.85		NONE
< 1,000 m	Chevron-Irving Malagawatch 2	611.00	17.68		POOR
< 1,000 m	P-92	944.00	17.89		POOR
> 1,000 m	Dow Chemical DCPR-11	1,210.00		23.77	POOR
17.78 °C km^{-1} ± 0.11 at 777.5 m (n=2) and > 1,000 m: 23.77 °C km^{-1} ± 0 (n=1)					
DDTM: 1210 m		**AMST:**	6.2 °C	**CONFIDENCE:**	POOR

EXPECTED TEMPERATURE AT SET DEPTH:	**500 m:**	15.09 °C ± 0.05	**4,000 m:**	105.62 °C ± 0
	1,000 m:	29.97 °C ± 0	**4,500 m:**	118.66 °C ± 0
	1,500 m:	39.97 °C ± 0	**5,000 m:**	131.67 °C ± 0
	2,000 m:	52.96 °C ± 0	**5,500 m:**	144.63 °C ± 0
	2,500 m:	66.15 °C ± 0	**6,000 m:**	157.58 °C ± 0
	3,000 m:	79.35 °C ± 0	**6,500 m:**	170.5 °C ± 0
	3,500 m:	92.52 °C ± 0	**7,000 m:**	183.4 °C ± 0
EXPECTED DEPTH AT SET TEMPERATURE:	**20 °C:**	695 m	**100 °C:**	3,783 m
	40 °C:	1,467 m	**120 °C:**	4,555 m
	60 °C:	2,239 m	**140 °C:**	5,327 m
	80 °C:	3,011 m	**160 °C:**	6,099 m
COMMENT:	The geothermal gradient for this sub-basin is constrained by data that have a poor level of confidence.			

SUB-BASIN	Sydney		BASIN	Sydney	
USAGE	**WELL**	**DEPTH (m)**	**UGG (°C km^{-1})**	**CGG (°C km^{-1})**	**CONFIDENCE**
Rejected	Phalen Mine		22.80		POOR
< 1,000 m	NSDME Pt. Edward 83-1	750.00	16.97		VERY GOOD
< 1,000 m	NSDME Sydney Basin Project	884.10	16.48		VERY GOOD
Rejected	P-84	1,341.03		34.93	NONE
Rejected	P-84		21.70		POOR
> 1,000 m	CCS1	1,524.00		23.65	GOOD
16.73 °C km^{-1} ± 0.25 at 817.05 m (n=2) and > 1,000 m: 23.65 °C km^{-1} ± 0 (n=1)					
DDTM: 1524 m		**AMST:**	5.93 °C	**CONFIDENCE:**	GOOD
EXPECTED TEMPERATURE AT SET DEPTH:		**500 m:**	14.3 °C ± 0.12	**4,000 m:**	103.49 °C ± 0
		1,000 m:	29.58 °C ± 0	**4,500 m:**	116.32 °C ± 0
		1,500 m:	41.98 °C ± 0	**5,000 m:**	129.1 °C ± 0
		2,000 m:	51.7 °C ± 0	**5,500 m:**	141.85 °C ± 0
		2,500 m:	64.67 °C ± 0	**6,000 m:**	154.57 °C ± 0
		3,000 m:	77.66 °C ± 0	**6,500 m:**	167.28 °C ± 0
		3,500 m:	90.6 °C ± 0	**7,000 m:**	179.97 °C ± 0
EXPECTED DEPTH AT SET TEMPERATURE:		**20 °C:**	697 m	**100 °C:**	3,854 m
		40 °C:	1,487 m	**120 °C:**	4,643 m
		60 °C:	2,276 m	**140 °C:**	5,433 m
		80 °C:	3,065 m	**160 °C:**	6,222 m
COMMENT:	For P-84, the first value has been calculated from the log data, the second comes from Hacquebard and Donaldson (1970).				

SUB-BASIN	Fundy		**BASIN**	Fundy	
USAGE	**WELL**	**DEPTH (m)**	**UGG (°C km^{-1})**	**CGG (°C km^{-1})**	**CONFIDENCE**
< 1,000 m	Low Scenario	1,000.00	20.00		SPECULATIVE
< 1,000 m	Getty No. 1	138.70	27.54		NONE
< 1,000 m	Getty No. 3	151.20	22.22		NONE
Rejected	Getty No. 4	54.90	16.21		NONE
< 1,000 m	Getty No. 10	152.70	24.17		NONE
< 1,000 m	High Scenario	1,000.00	30.00		SPECULATIVE
20 °C km^{-1} – 24.64 °C km^{-1} ± 2.66 at 147.53 m (n=3) – 30 °C km^{-1}					
DDTM:	148 m	**AMST:**	7.13 °C	**CONFIDENCE:**	**NONE or SPECUL.**
EXPECTED TEMPERATURE AT SET DEPTH:		**500 m:**	16.27 °C ± 0 18.52 °C ± 1.33 21.27 °C ± 0	**4,000 m:**	87.19 °C ± 0 105.7 °C ± 10.64 127.19 °C ± 0
		1,000 m:	25.33 °C ± 0 29.91 °C ± 2.66 35.33 °C ± 0	**4,500 m:**	97.53 °C ± 0 118.36 °C ± 11.97 142.53 °C ± 0
		1,500 m:	35.11 °C ± 0 42.01 °C ± 3.99 50.11 °C ± 0	**5,000 m:**	107.82 °C ± 0 130.97 °C ± 13.3 157.82 °C ± 0
		2,000 m:	45.39 °C ± 0 54.61 °C ± 5.32 65.39 °C ± 0	**5,500 m:**	118.07 °C ± 0 143.55 °C ± 14.63 173.07 °C ± 0
		2,500 m:	55.86 °C ± 0 67.4 °C ± 6.65 80.86 °C ± 0	**6,000 m:**	128.3 °C ± 0 156.1 °C ± 15.96 188.3 °C ± 0
		3,000 m:	66.36 °C ± 0 80.22 °C ± 7.98 96.36 °C ± 0	**6,500 m:**	138.51 °C ± 0 168.63 °C ± 17.29 203.51 °C ± 0
		3,500 m:	76.81 °C ± 0 92.99 °C ± 9.31 111.81 °C ± 0	**7,000 m:**	148.71 °C ± 0 181.14 °C ± 18.62 218.71 °C ± 0
EXPECTED DEPTH AT SET TEMPERATURE:		**20 °C:**	755 m 604 m 521 m	**100 °C:**	4,339 m 3,778 m 2,996 m
		40 °C:	1,651 m 1,398 m 1,140 m	**120 °C:**	5,235 m 4,571 m 3,615 m
		60 °C:	2,547 m 2,191 m 1,759 m	**140 °C:**	6,131 m 5,365 m 4,234 m
		80 °C:	3,443 m 2,985 m 2,378 m	**160 °C:**	7,027 m 6,158 m 4,853 m
COMMENT:	In the absence of deep temperature measurements, low and high scenarios are evaluated for geothermal gradients of 20 and 30 °C. The range is supported by the available temperature data at the equilibrium, but these measurements are too shallow to be used with any level of confidence.				

Terrane	Meguma		**Age**	Cambro-Ordovician	
USAGE	**WELL**	**DEPTH (m)**	**UGG (°C km^{-1})**	**CGG (°C km^{-1})**	**CONFIDENCE**
< / > 1,000 m	Dalhousie	333.50	12.59		VERY GOOD
< / > 1,000 m	NSDM Oldham	607.50	12.67		VERY GOOD
12.63 °C km^{-1} ± 0.04 at 470.5 m (n=2)					
DDTM:	608 m	**AMST:**	7.05 °C	**CONFIDENCE:**	POOR
EXPECTED TEMPERATURE AT SET DEPTH:		**500 m:**	12.4 °C ± 0.02	**4,000 m:**	63.68 °C ± 0.16
		1,000 m:	18.66 °C ± 0.04	**4,500 m:**	71.21 °C ± 0.18
		1,500 m:	25.64 °C ± 0.06	**5,000 m:**	78.69 °C ± 0.2
		2,000 m:	33.1 °C ± 0.08	**5,500 m:**	86.14 °C ± 0.22
		2,500 m:	40.77 °C ± 0.1	**6,000 m:**	93.57 °C ± 0.24
		3,000 m:	48.46 °C ± 0.12	**6,500 m:**	100.97 °C ± 0.26
		3,500 m:	56.1 °C ± 0.14	**7,000 m:**	108.36 °C ± 0.28
EXPECTED DEPTH AT SET TEMPERATURE:		**20 °C:**	1,086 m	**100 °C:**	6,436 m
		40 °C:	2,423 m	**120 °C:**	7,774 m
		60 °C:	3,761 m	**140 °C:**	9,111 m
		80 °C:	5,098 m	**160 °C:**	10,449 m
COMMENT:	In the absence of well data deeper than 1,000 m, the gradient > 1,000 m is inferred from the shallow temperature data. The level of confidence is POOR because of the lack of deep temperature data.				

Intrusive rocks			Age	Devonian	
USAGE	**WELL**	**DEPTH (m)**	**UGG (°C km^{-1})**	**CGG (°C km^{-1})**	**CONFIDENCE**
Low Scenario	EPB No. 18	480.00	17.92		VERY GOOD
High Scenario	MRRD-01	1,450.00	41.86		POOR
17.92 °C km^{-1} ± 0 at 480 m (n=1) – 41.86 °C km^{-1} ± 0 at 1,450 m (n=1)					
DDTM:	**1 450 m**	**AMST:**	7.25 °C	**CONFIDENCE:**	POOR
EXPECTED TEMPERATURE AT SET DEPTH:		**500 m:**	16.16 °C ± 0 28.23 °C ± 0	**4,000 m:**	84.99 °C ± 0 178.01 °C ± 0
		1,000 m:	24.08 °C ± 0 49.16 °C ± 0	**4,500 m:**	95.16 °C ± 0 199.99 °C ± 0
		1,500 m:	33.7 °C ± 0 70.09 °C ± 0	**5,000 m:**	105.29 °C ± 0 221.91 °C ± 0
		2,000 m:	43.82 °C ± 0 89.65 °C ± 0	**5,500 m:**	115.39 °C ± 0 243.81 °C ± 0
		2,500 m:	54.13 °C ± 0 111.76 °C ± 0	**6,000 m:**	125.46 °C ± 0 265.68 °C ± 0
		3,000 m:	64.47 °C ± 0 133.9 °C ± 0	**6,500 m:**	135.51 °C ± 0 287.53 °C ± 0
		3,500 m:	74.76 °C ± 0 155.99 °C ± 0	**7,000 m:**	145.54 °C ± 0 309.36 °C ± 0
EXPECTED DEPTH AT SET TEMPERATURE:		**20 °C:**	784 m 356 m	**100 °C:**	4,746 m 2,197 m
		40 °C:	1,774 m 8 7 m	**120 °C:**	5,736 m 2,657 m
		60 °C:	2,765 m 1,277 m	**140 °C:**	6,727 m 3,117 m
		80 °C:	3,755 m 1,737 m	**160 °C:**	7,717 m 3,577 m
COMMENT:	The level of confidence is POOR because a wide range of temperatures is considered and the upper-end of the range has a POOR level of confidence.				